Differentiation and transplantation of mouse embryonic stem cell-derived cone photoreceptor precursors

Kamil Kruczek

A thesis submitted for the degree of

Doctor of Philosophy

2016

Division of Biosciences

Department of Cell and Developmental Biology

University College London

I, Kamil Kruczek confirm that the work presented in this thesis is my own. Where information has been derived from other sources, I confirm that this has been indicated in the thesis.

Abstract:

Daytime vision is highly dependent on cone photoreceptors and retinal degenerations resulting in their death are a leading cause of blindness. A promising treatment strategy is the replacement of lost cones by cell therapy. Here we characterise cone differentiation in retinae derived from suspension cultures of mouse embryonic stem cells (mESCs). Similar to *in vivo* development, a temporal pattern of progenitor marker expression is followed by the differentiation of early thyroid hormone receptor β2-positive cone precursors and at later stages of culture, photoreceptors exhibiting cone-specific phototransduction-related proteins. We also established that the Notch pathway limits cone genesis, whilst retinoic acid signalling regulates their maturation comparable to their actions *in vivo*. Importantly, mESC-derived cones can be isolated in large numbers and transplanted into the adult mouse retina. Following transplantation, these cells show the capacity to survive and express mature markers. Together, this work identifies a robust renewable source of transplantable cone precursors for daylight vision repair studies.

Table of contents:

Tables, figures and diagrams:

Acknowledgements:

I would like to thank Dr Robin Ali for creating the opportunity to undertake my doctoral project in his group and his interest and support during my studies. I am particularly grateful to Dr Emma West for critical comments and help in preparation of this manuscript and Dr Anai Gonzalez-Cordero for input and supervision throughout the project. Additionally, I'd like to mention Dr Anastasios Georgiadis, who helped with molecular cloning, Dr Alexander Smith, who provided continued feedback on the design of the experiments, Dr Jane Sowden with whom I had many constructive discussions about the progress of the project and Mrs Yanai Duran, who performed most subretinal injections and helped with animal work.

Finally, I'd like to thank my parents, Jolanta and Janusz, for their love and support of my interest in science, without which I couldn't have started this work.

I. Introduction

I.I. Retina within the mammalian eye

Vision is a key sense that allows an organism to gather information about the surrounding environment and has evolved independently in several groups of organisms (Lamb, 2013). Eyes evolved as an organ mediating the first steps in vision namely light detection and initial visual signal processing. Despite diverse habitats and varied eye morphology, a common mechanism underlying vision is absorption of light quanta by the use of visual pigments (Larhammar et al., 2009). These biomolecules change their conformation following absorption of light triggering downstream signalling. Visual pigments and associated signalling molecules are expressed in specialised sensory cells called photoreceptors (Larhammar et al., 2009). Photoreceptors in vertebrate species are located in neural retina tissue within the eye. This tissue contains not only the light-detecting photoreceptors but also neurons involved in the first steps of processing the visual stimuli and projection neurons, which extend axons passing the visual information to the brain. Other tissues in the eye play a supporting role or focus the light onto the retina (Lamb, 2009, 2013; Palczewski, 2012; Sung and Chuang, 2010).

I.I.I. Structure of the mammalian eye

The mammalian eye is formed of three layers with different basic functions (Diagram I.I):

- external layer (fibrous tunic or *tunica fibrosa oculi*) consisting of the cornea and sclera;
- intermediate layer (vascular tunic or *tunica vasculosa oculi*) is a vascularized middle compartment consisting of the iris, ciliary body and choroid;
- internal layer (nervous tunic or *tunica nervosa oculi*) which includes the retina the sensory tissue within the eye (Hoon et al., 2014).

The external layer made by the cornea and sclera provides a barrier separating the eye from the external environment, maintains the shape of the eye and protects from trauma. Sclera is a resilient layer of connective tissue composed of collagen and elastin giving the eye its form. The front of the eye is covered by the cornea (Diagram I.I), which is a transparent multi-layered tissue allowing passage of light into the eye acting as a fixed lens (DelMonte and Kim, 2011). The intermediate layer composed of the iris,

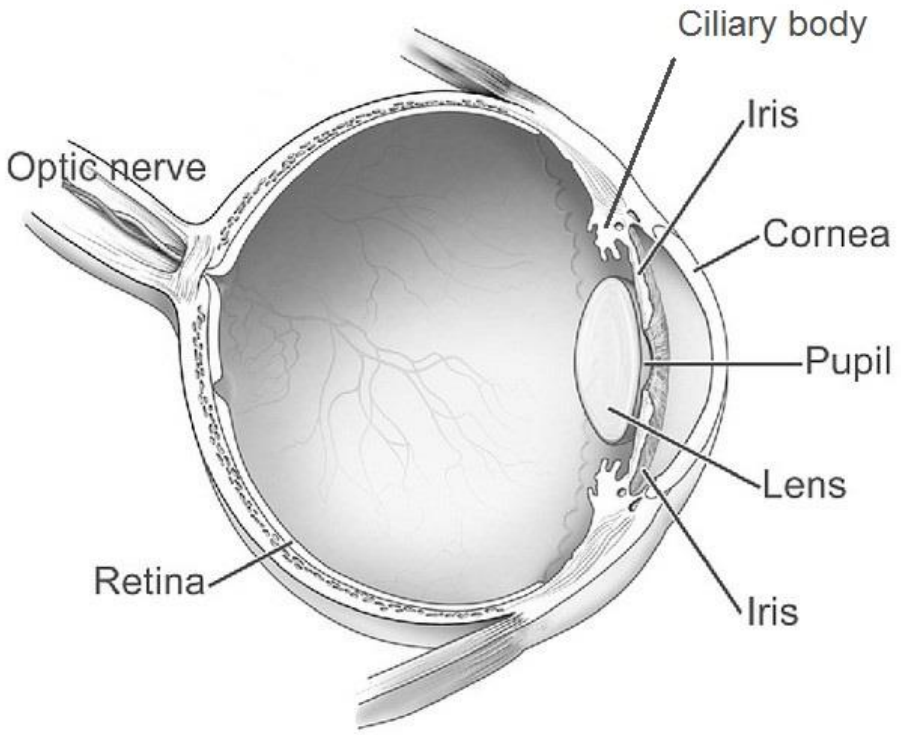

Diagram I.I. Structure of the mammalian eye

The overall structure of the eye is well conserved in most mammalian species. The organ is composed of three layers, which perform distinct functions. The external layer consisting of sclera and the *cornea* creates a barrier from the external environment and provides structural support. The intermediate layer provides supportive roles for the inner sensory part of the eye, which is the retina. The intermediate layer consists of the *iris*, ciliary body and the vascular network of the choroid. Papillary muscles of the *iris* regulate the size of the *pupil* and therefore the amount of light passing to the retina. In addition to the cornea, which acts as a fixed lens, there is a *lens* behind the iris that is adjusted to focus through the action of ciliary muscles. The retina is the light-sensitive layer that extracts and performs initial processing of visual information, which is passed on to the brain via the optic nerve.

Graphic:

https://commons.wikimedia.org/wiki/File:Human_eye_diagram-sagittal_view-NEI.jpg

used under a Creative Commons License.

ciliary body (Diagram I.I) and the choroid surrounds the eye globe from the pupil to the optic nerve. Papillary muscles in the iris regulate the size of the pupil and thus the amount of light passing to the retina. The ciliary body secures the lens in its position and via the ciliary muscle to adjust its shape to focus on farther or closer objects in the process of accommodation. Moreover, the ciliary body releases aqueous humor which provides nutrients and oxygen to the avascular lens and cornea. The choroid is a network of capillaries, arterioles and venules that together with larger vessels oxygenate and provide nutrition to the retina. Additionally, pigmentation of the choroid absorbs stray light preventing internal reflection that would disturb creation of an accurate visual image in the retina. The inner layer of the eye is formed by the neural retina (Diagram I.II and I.II) and retinal pigmented epithelium (RPE; Diagram I.II). The neural retina is the light-sensitive part of the eye, whilst the RPE plays a supporting role. These tissues are closely apposed through extracellular proteins in the subretinal space that divides the two. The retinal layers create three fluid-filled cavities within the eye, the anterior chamber between the cornea and the iris, the posterior chamber between the iris and the lens and the vitreous chamber between the lens and the retina (Campbell et al., 2014; DelMonte and Kim, 2011; Hoon et al., 2014; Lamb, 2013).

I.II. Structure and function of the neural retina

I.II.I. Cellular organization of the retina

The vertebrate retina is composed of six types of neurons and one glial cell type in a laminar organization (Diagram I.II). The neuronal cell types are two types of *photoreceptor cells*: *cone photoreceptors* and *rod photoreceptors*, which are located furthest from the front of the eye; three types of retinal *interneurons*: *bipolar* cells, *horizontal* cells and *amacrine* cells; one type of *projection* neuron called the retinal *ganglion cell* and one type of *glial* cells called *Müller glia* (Bassett and Wallace, 2012). The cell somas are organized into three nuclear layers, photoreceptors, the sensory neurons, which detect light stimuli, are located in *outer nuclear layer*, at the scleral side of retina, interneurons have their cell bodies within *inner nuclear layer*, between somas of interneurons reside nuclei of Müller glia, which extend processes that span the whole retina; ganglion cells somas compose a separate nuclear layer located on the vitreal side of the retina. Photoreceptors extend apical processes beyond the outer nuclear layer forming outer segments that contain visual pigments required for light detection. Outer segments contact retinal pigment epithelium, which has important roles in the recycling of visual pigments as well as preventing back scatter of light due

to the dark pigmentation absorbing stray light. Retinal cells make all their synaptic connections in two *synaptic* layers called *inner* and *outer plexiform layers* which are located between the ganglion cell layer and inner nuclear layer and the inner nuclear layer and outer nuclear layer, respectively. Ganglion cells extend axons that are organised into the optic nerve that projects to the visual centres in the brain (Hoon et al., 2014; Swaroop et al., 2010; Diagram I.II).

In certain species of reptiles, birds and in primates including humans, a central region of the retina that lies on the visual axis of the eye, specialises to mediate high-acuity vision (Lamb, 2009). This region is called the fovea and exhibits characteristic features such as displacement of cell bodies other than those of photoreceptors, which are only cones in this location (Diagram I.II.). These cone cells are the thinnest and longest in the retina. Displacement of other cell types allows for more direct passage of light to the cone segments, whilst tight packing of cone photoreceptors in this area is necessary to provide high visual acuity. In humans the central area is composed of approximately 10 000 cones and is 0.3 mm in diameter (Lamb, 2013).

I.II.I.I. Retinal neuron types

As discussed above there are six major classes of retinal neurons and one type of glial cells (Diagram I.II.) that make up the cellular composition of the retina (Bassett and Wallace, 2012).

I.II.I.II. Photoreceptors

Photoreceptor cells are divided based on characteristic morphologies and functional properties into two types: cone photoreceptors and rod photoreceptors, mediating daylight and night vision respectively (Swaroop et al., 2010). Additionally, cone cells are responsible for central high-acuity vision as well as colour discrimination. Rod photoreceptors constitute the majority of photoreceptors in most mammalian species (95% in humans and over 97% in mice). Cone photoreceptors are a minor population in mice (<3%) and humans (around 5% of photoreceptors; Mustafi et al., 2009). Photopigments concentrated in photoreceptor outer segments enable light detection, through absorption of light quanta leading to conformational changes in these proteins triggering downstream signalling events (Palczewski, 2012; Sung and Chuang, 2010). Most vertebrates possess one type of rod photoreceptor containing the photopigment rhodopsin and multiple types of cone photoreceptors expressing colour opsins with peak sensitivities in different parts of the visual spectrum (Lamb, 2009, 2013; Larhammar et al., 2009). In mice two types of colour opsins are expressed: blue opsin and red-green opsin, many mouse cone cells co-express both types of cone opsins (Applebury et al., 2000), while in humans three types of cone opsins (blue, green and

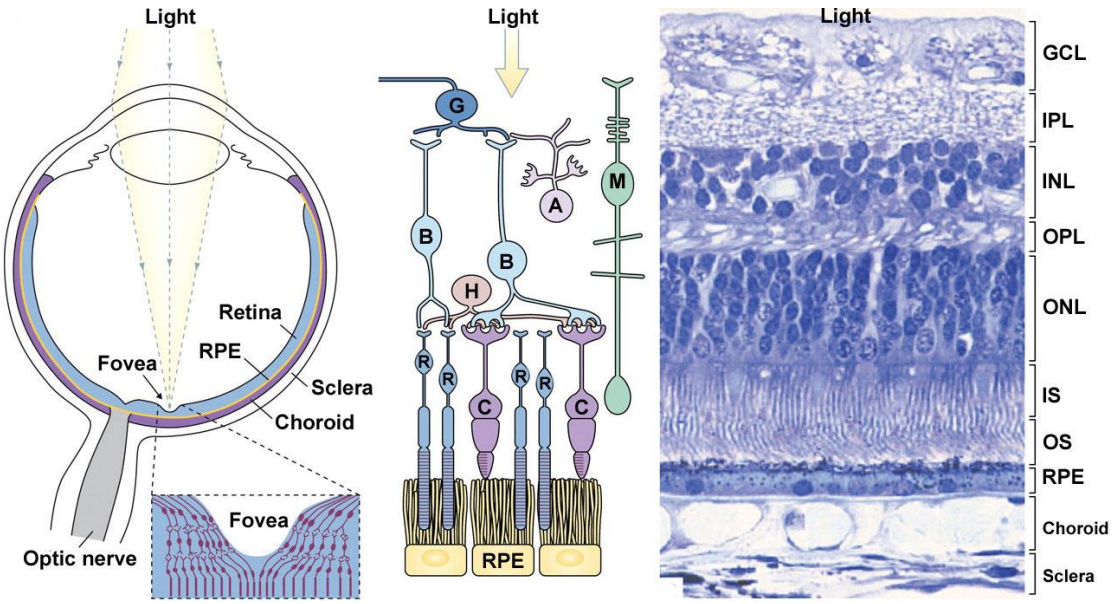

Diagram I.II. Histology of the eye and retina.

Light entering the eye is focused on the light-sensitive retina. Many diurnal species possess a central region enabling high visual acuity such as the primate fovea containing predominantly cone photoreceptors and showing displacement of the overlying retinal neurons (**left panel**). There are seven cell types in the mammalian retina, six types of neurons and one glial cell type. Cone (C) and rod (R) photoreceptors are the primary sensory neurons of the retina. Photoreceptors synapse to interneurons including bipolar cells (B) and horizontal cells (H). An additional interneuron type is the amacrine cell (A). Interneurons contact retinal ganglion cells (G), which are the projection neurons of the retina. Photoreceptor function is supported by retinal pigment epithelium (RPE) (**middle panel**). Retinal neurons are organised into three nuclear layers: ganglion cell layer (GCL), inner nuclear layer (INL), in which interneuron and Müller glia nuclei are located, and outer nuclear layer, where photoreceptor nuclei reside (ONL). Between the nuclear layers two synaptic layers are located, the inner plexiform layer (IPL) and outer plexiform layer (OPL). Photoreceptors extend distal structures inner (IS) and outer segments (OS) responsible for light detection towards the RPE cells (RPE). Underneath the RPE there is a vascular layer of the choroid surrounded by sclera (**right panel**). Light passes from ganglion cells, through the interneurons to the photoreceptors.

Graphic:

Hill, M.A. (2016) **Embryology** *Eye and retina cartoon.jpg*. Retrieved April 3, 2016, from https://embryology.med.unsw.edu.au/embryology/index.php/File:Eye_and_retina_cartoon.jpg used under a Creative Commons License.

red) are exclusively expressed. Light absorption leads, through downstream signal transduction, to the hyperpolarization of the photoreceptor and reduces glutamate neurotransmitter release, detected by retinal interneurons (Sung and Chuang, 2010).

The two types of photoreceptors differ not only in terms of their morphological features but also their distribution within the eye (Lamb, 2013). As mentioned before the central region in some species is specialised to form a fovea, important for daytime vision. This part of the retina is composed nearly exclusively of cone photoreceptors tightly-packed into a hexagonal array. Red and green opsin expressing cones dominate the primate fovea, whilst blue opsin expressing cones are rare in this region. Blue opsin expressing cells, making up around 5% of primate cones are located more peripherally in the retina. The rodent retina lacks a fovea, and in mice the majority of cones co-express blue and red-green opsin (Applebury et al., 2000). Gradients of expression of these do exist though with blue opsin being more abundant in the inferior (ventral) retina, whilst an opposing gradient of red-green opsin is observed (expression increasing towards superior/dorsal retina (Lukáts et al., 2005).

I.II.I.III. Bipolar cells

Bipolar cells are the output neurons for photoreceptor cells receiving signals through synapses on their dendrites in the outer plexiform layer and extending axons with terminals in the inner plexiform layer. Multiple types of bipolar cell subtypes have been identified in the vertebrate retina, one subtype receives exclusively input from rod photoreceptors, whilst the rest receive cone inputs. Rod bipolar cells make synaptic contacts with between 15-50 rod cells depending on the location within the retina, the more peripheral the more the cells they receive input from. Cone bipolar cells can either connect to a single cone or to several cones depending on their subtype. Bipolar cells mediating ON and OFF responses have axons segregated into different depths of the inner plexiform layer (Hoon et al., 2014).

I.II.I.IV. Horizontal cells

Horizontal cells are retinal interneurons connecting through synapses on processes confined to the outer plexiform layer, allowing them to mediate lateral interactions within this synaptic zone. In most vertebrates, horizontal cells form two morphologically distinct classes receiving input from either rods or cones, in many mammals rods provide input onto horizontal cells axon terminals, whilst synapses with cones are formed on horizontal cell dendritic branches (Hoon et al., 2014).

I.II.I.V. Amacrine cells

Amacrine cells show a diverse set of morphologies with processes branching within the inner plexiform layer. These processes do not include typical axons, though some

of them might have axon-like properties, such as elongated morphology and function as an output process of the cell. Based on their morphologies they are broadly divided into diffuse and stratified. Diffuse amacrine cells have their processes distributed fairly uniformly across the thickness of the inner plexiform layer, whilst stratified amacrine cells show branches extending in one or several levels within the synaptic layer. Amacrine cells can be further morphologically classified based on the extent of branching into narrow- and wide-field (Hoon et al., 2014; Sung and Chuang, 2010).

I.II.I.VI. Ganglion cells

Ganglion cells are the projection neurons of the retina, their axons extend along the margin of the retina, cluster together at the optic disc to form the optic nerve, which passes visual information to the brain. Similarly to amacrine cells, ganglion cells exhibit varied morphologies with many cells showing stratification of their dendritic branches. Also the extent of the processes varies with some ganglion cells in the central retina receiving input from as little as one cone bipolar cell (Hoon et al., 2014).

I.II.I.VII. Müller glia

Müller cells are the principal type of glial cells in the retina performing neuron-supporting functions similar to those of astrocytes and oligodendrocytes in the brain. Müller cells are a type of radial glia that span the whole depth of the retina. Their nuclei are located in the inner nuclear layer among interneurons. Junctions formed between photoreceptor inner segments and elongated apical Müller cell processes create the outer limiting membrane, a barrier separating retinal neurons somas from the subretinal space (Hoon et al., 2014).

I.II.II. Cell biology of vision

I.II.II.I. Structure of photoreceptors

To perform their function in generating visual information photoreceptors developed specialized subcellular structures (Diagram I.III.). Four morphological regions can be distinguished in vertebrate photoreceptors: (1) outer segments containing visual pigments; (2) inner segments in which much of the biosynthetic and metabolic processes occur; (3) cell soma with the nucleus and (4) an axon ending in synaptic terminals in the outer plexiform layer. Outer segments are structures developed as a specialisation of photoreceptor cilia to concentrate visual pigments and phototransduction proteins. The ultrastructure of outer segments is best studied in rod photoreceptors (Mustafi et al., 2009; Palczewski, 2012; Sung and Chuang, 2010).

I.II.II.I.I.Rod outer segments

Rod outer segments are approximately 24 µm in length and 1.4 µm in diameter and have a cylindrically shaped membrane sac containing around a thousand flat lammelar discs stacked perpendicularly to the proximal-distal axis of the cell (Palczewski, 2012). In the rod cell disc membranes are separate from the plasma membrane, however, macromolecular complexes bridging adjacent disc and disc rims to the plasma membrane can be observed using high resolution electron microscopy (Nickell et al., 2007). In rods the majority of disc protein is the visual pigment rhodopsin, which constitutes up to 95% of disc protein. Rhodopsin molecules in the disc are arranged in a crystal-like lattice (Nickell et al., 2007). Outer segments, when viewed along the longitudinal section shows asymmetric organisation resembling a hair comb, the spine of which is the ciliary stalk. Axonemal microtubules run along the stalk, ending around halfway into the outer segment in a rod cell. The microtubule structures are anchored in the basal body at the distal end of the inner segment. Rod axonemal microtubules are organised into nine dublets arranged concentrically lacking a central pair of microtubules characteristic of motile cilia (9+0 organisation). This subcellular organisation allows the identification of outer segments as modified primary cilia. Primary cilia are thin protrusions, 3-6 µm in length, present on the majority of eukaryotic cells involved in sensing extracellular signals. Reminiscent of primary cilia the connecting cilium forms the only physical bridge connecting the outer to the inner segment (Mustafi et al., 2009; Palczewski, 2012; Sung and Chuang, 2010).

I.II.II.I.II. Cone outer segments

Cone outer segments also show lamellar stacks of membrane folds, however, these differ from the rod counterparts in several ways. Firstly, discs in cones are plasma membrane evaginations, which retain connection to the cilium stalk, therefore in cones discs form a continuous membrane system. Within the cilium, axonemal microtubules extend along the full length of the segment. Moreover, the disc rim in cones is incomplete and its formation is thought to be a gradual, slow process arising from the cilium. In addition, cone outer segments show a characteristic tapered conical appearance, which is believed to stem from membrane loss at their distal tip. This open disc outer segment morphology results in a much greater surface area for rapid exchange of substances between cell exterior and the interior cytoplasm of this type of photoreceptor that might be important for chromophore uptake for pigment regeneration and fast calcium dynamics during light adaptation (Mustafi et al., 2009).

In both cones and rods outer segments form a separate cell compartment connected to the rest of the cell through a narrow connecting cilium linking it to the *inner segment*.

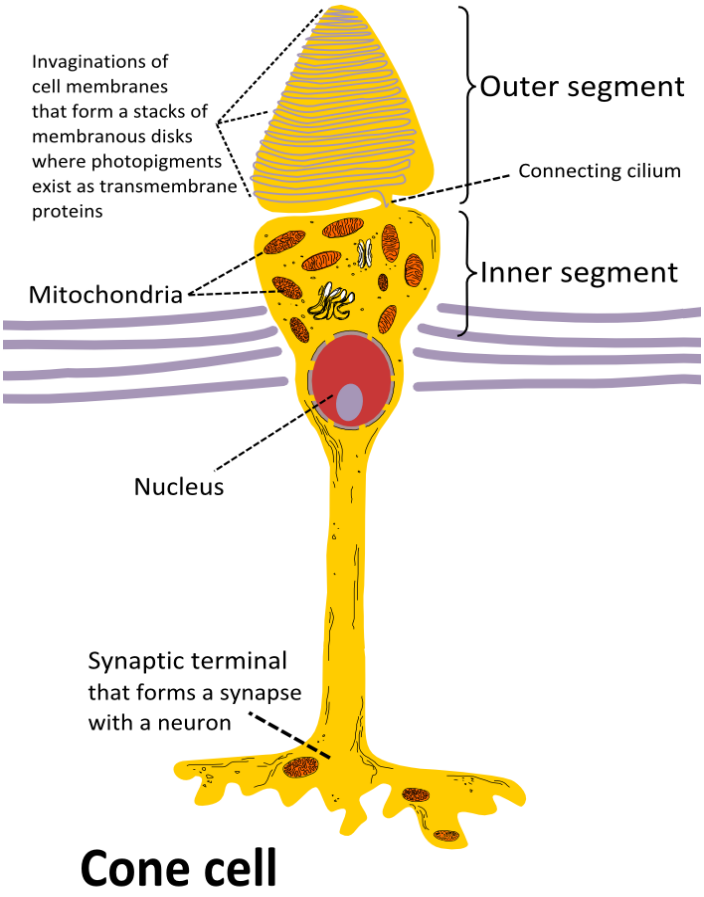

Diagram I.III. Structure of the cone photoreceptor.

Cone photoreceptors display specialised features allowing their function as light sensory neurons. The apical process of the cone cell forms an inner and outer segment. The inner segment contains mitochondria and is a site of biogenesis. The outer segment contains phototransduction proteins including the visual pigments concentrated in stacks of membrane discs. The outer segment is isolated from the rest of the cell and linked through a connecting cilium. The basal process of the cone cell forms synaptic terminals with retinal interneurons.

The inner segment of photoreceptors is where biosynthesis, metabolism and endocytosis occur most. Photoreceptors are highly active metabolically and the demand for energy is answered by numerous mitochondria concentrated in this domain (Sung and Chuang, 2010).

I.II.II.I.III. Cell soma

The inner segment extends from the *cell soma*. The soma contains little cytoplasm which surrounds a centrally located nucleus. Nuclei of rod photoreceptors in nocturnal animals exhibit a highly specialised architecture differing from most eukaryotic cells. A great majority of interphase cells in eukaryotes possess nuclei in which condensed chromatin, termed heterochromatin, lies in the periphery in close proximity to the nuclear membrane, whereas loose euchromatin is located centrally. This architecture is inverted in rods of nocturnal species with clustered heterochromatin occupying the centre of the nucleus (Solovei et al., 2009). This specialised architecture arises from remodelling of the conventional nuclear architecture in post-mitotic rod precursors, depending on the action of rod-specifying transcription factor Nrl (Mears et al., 2001), and is only fully developed between the third and fourth post-natal week in mice (Solovei et al., 2009). Cone photoreceptors show typical nuclear organisation with several clusters of heterochromatin centrally in their nucleus (Mustafi et al., 2009; Solovei et al., 2009).

I.II.II.I.IV. Synaptic terminals

From the soma a basal photoreceptor axon extends ending in *synaptic terminals* in the outer plexiform layer (Hoon et al., 2014). Cone and rod synapses are atypical and developed to fulfil the requirements of visual signal detection. Photoreceptors, with other sensory neurons, differ from the majority of central nervous system neurons in that rather than using action potentials to transmit information, these cells employ graded continuous release of neurotransmitter. To achieve prolonged neurotransmitter release sensory neurons of the visual and auditory systems possess a specialised type of synapse called a *ribbon synapse* (Matthews and Fuchs, 2010). On an ultrastructural level this type of synapse appears as an electron-dense plate docked at a right angle in close proximity to the terminal plasma membrane. The ribbon structure is attached to the pre-synaptic plasma membrane via a structure called arciform density. The ribbon itself is approximately 200 nm into the cytoplasm and can vary considerably in length depending on the cell type. Large numbers of synaptic vesicles are tethered through fine filaments to the ribbon at regular intervals and do not touch each other. Vesicles at the base of the ribbon are in very close proximity to the presynaptic plasma membrane and called ‘docked’, these can be released very fast in response to

membrane depolarization, whilst vesicles associated with the ribbon further into the cytoplasm can be released readily, but at slower kinetics. These pools of synaptic vesicles that can be swiftly exocytosed into the synaptic cleft are an important mechanism underlying sustained neurotransmitter release from sensory neuron synapses (Matthews and Fuchs, 2010; Mercer and Thoreson, 2011; Sung and Chuang, 2010).

I.II.II.II. Phototransduction.

Visual information, passed on as neurotransmitter release patterns, is generated through a series of biochemical reactions following light absorption in photoreceptor outer segments termed the phototransduction cascade (Maeda and Palczewski, 2013; Palczewski, 2012; Diagram I.IV.). This process can be divided into three general steps:

(1) *Photoactivation*. Upon absorption of a quantum of light 11-*cis*-retinal, the chromophore bound to both cone and rod opsins undergoes isomerisation to the all-*trans*-retinal triggering a conformational change in the protein part of the visual pigment molecule. This conformational change in the opsin molecule triggers binding to a G protein called transducin to initiate downstream signalling. Binding of opsin to transducin results in exchange of GDP for GTP, which activates the α-subunit of transducin. This subunit dissociates from the complex and activates a membrane-associated phosphodiesterase (PDE) through removal of its two regulatory γ-subunits. Activated PDE catalyses the hydrolysis of cyclic guanosine monophosphate (cGMP) lowering its intracellular levels. cGMP levels regulate the conductance of photoreceptor plasma membrane through interaction with cation channels. In the dark cGMP concentrations are high and cations flow into the photoreceptor. When light is absorbed PDE lowers cGMP concentration through its hydrolysis, what results in channel closure and subsequently hyperpolarization of the photoreceptor.

(2) *Reduction in neurotransmitter release*. Hyperpolarization of the photoreceptor plasma membrane blocks the excitatory neurotransmitter glutamate release. Decrease in glutamate release is sensed at the level of outer plexiform layer synapses by retinal interneurons and interpreted as light detection.

(3) *Recovery*. In the final step, photoreceptors recover phototransduction components through a series of quenching and termination reactions of the activated phototransduction proteins allowing return to the basal dark-adapted state (Maeda and Palczewski, 2013).

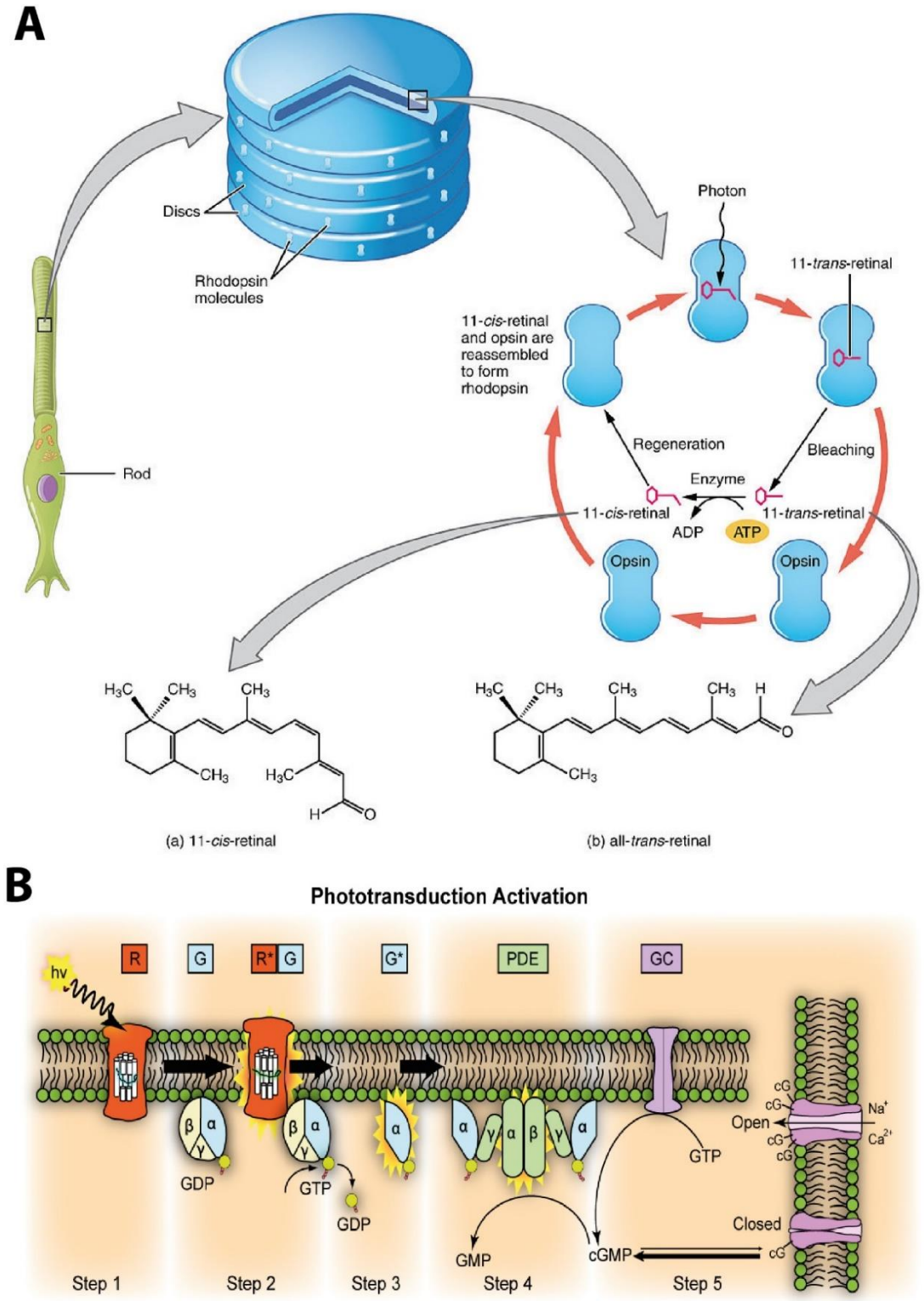

Diagram I.IV. Phototransduction cascade.

(**A**) Visual pigments are concentrated in the outer segments of rod or cone photoreceptors in membranous disc stacks. Opsin, which act as the light-detecting biomolecules are transmembrane proteins containing a covalently-attached

chromophore 11-*cis* retinal. Photon absorption triggers isomerisation of 11-*cis* to 11-*trans* retinal. This photoisomerisation triggers downstream signalling known as the phototransduction cascade. Following photon absorption isomerised visual pigment needs to be recycled in a series of biochemical reactions called the visual cycle. (**B**) Phototransduction begins with photon absorption by opsin (Step 1). Visual pigment activated in this way associates with transducin, triggering exchange of GDP for GTP in the α subunit of transducin (Step 2). The GTP-bound α subunit dissociates (Step 3) and binds to the inhibitory γ subunit of phosphodiesterase, activating its enzymatic activity (Step 4). Activated phosphodiesterase hydrolyses cyclic GMP, which lowers its intracellular concentration. Reduction in cytosolic concentration of cyclic GMP causes closure of cyclic GMP-gated Na^+ and Ca^{2+} channels (Step 5), which in turn affects neurotransmitter release from synaptic terminals.

I.II.II.III. The visual cycle

All known visual pigments contain as their photoreceptive chromophore 11-*cis*-retinal, a derivative of vitamin A coupled to an opsin protein via a Schiff base (Lamb, 2009). Retinal has a highly favourable chemical structure for light detection containing a conjugated system of 5-6 carbon-carbon double bonds whose interaction with the opsin allows absorption of light quanta with energies lower than those absorbed by cell components (i.e. proteins, nucleic acids) and not within the range that would result in excessive thermal activation of the receptor cell. Absorption range of retinal defines therefore the visible range of electromagnetic radiation. Moreover, stemming from the molecular structure is the potential for *cis*-*trans* photoisomerization enabling the photopigment to remain in an active state for a limited time before quenching. Lastly, the reactivity of retinal's aldehyde group allows it to be linked through this chemical moiety to opsin proteins, in which after photoisomerization it can induce conformational changes triggering downstream signalling. However, there are also several downsides to the use of retinal as a base of vision: (1) the aldehyde group is highly reactive and needs protection from accidental oxidation; (2) the retinoids are poorly soluble in water and require association with carrier proteins in water-based solutions; (3) the subcellular localization of retinoids needs to be controlled to avoid adverse reactions (Maeda and Palczewski, 2013; Palczewski, 2012; Sung and Chuang, 2010).

After a photon of light is absorbed by the photopigment 11-*cis*-retinal isomerises to the all-*trans* form and the visual pigment converts to a signalling form called *metaII*. In invertebrates this form absorbs another quantum of light and isomerises back to 11-*cis* conformation. Vertebrate opsins, however, evolved for increased sensitivity and are unstable in *metaII* with all-*trans*-retinal being released from the protein. This creates a requirement for regeneration of the photopigment (Diagram I.V.). Regeneration of 11-*cis*-retinal is localised outside the photoreceptor cell in adjacent cell types (Palczewski, 2012; Sung and Chuang, 2010). Despite the similarities in visual pigment activation in cones and rods, the two cell types diverged in their physiologies and are believed to utilise different pathways for pigment regeneration (Wang and Kefalov, 2011).

I.II.II.III.I. Rod visual cycle

Diagram I.V. shows schematically the rod visual cycle. Photons of light that reach rod outer segments isomerize 11-*cis*-retinal of rhodopsin into the all-*trans* isoform creating an activated photoproduct called meta-rhodopsin II, which initiates downstream signalling (Diagram I.IV.). The Schiff base bond coupling all-*trans*-retinal to rhodopsin hydrolyses and all-*trans*-retinal is released mostly to the cytoplasmic leaflet of rod outer segment disc membrane. All-*trans*-retinal is then reduced by all-*trans*-retinol

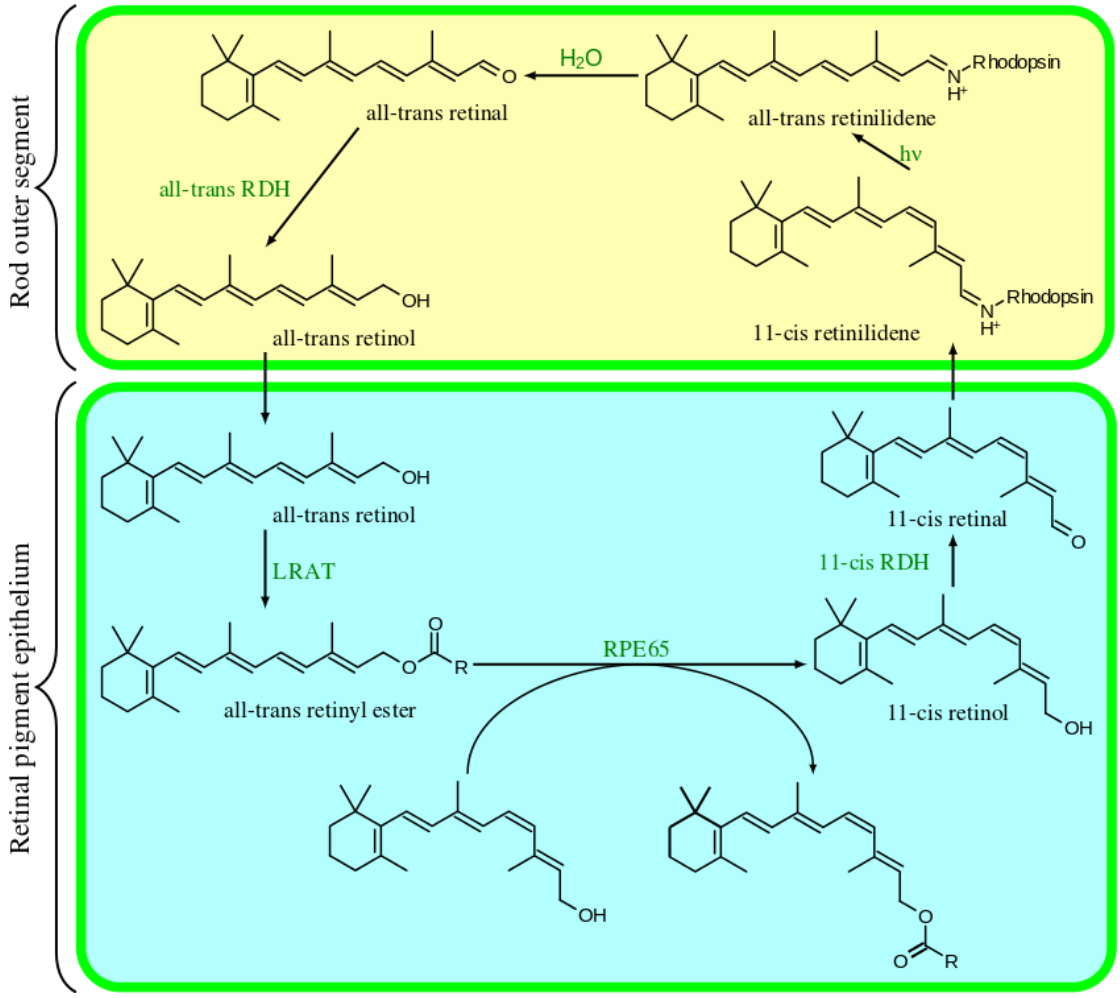

Diagram I.V. The visual cycle.

Photon absorption by 11-*cis* retinal bound to Rhodopsin leads to its isomerisation to all-*trans* retinal (upper right corner). Subsequently, all-*trans* retinal is released from the opsin protein and undergoes reduction by all-*trans*-retinol dehydrogenases present in rod outer and inner segments to all-*trans*-retinol (upper left corner). All-*trans*-retinol is trafficked to the retinal pigmented epithelium cells, where it is esterified by lecithin:retinol acyltransferase (LRAT) to retinol esters (lower left part). Isomerohydrolase of the visual cycle RPE65 uses retinyl esters as substrates for the isomerasation reaction yielding the 11-*cis* isoform bound to cellular retinal binding protein (CRALBP). 11-*cis*-retinol dehydrogenases then oxidise 11-*cis*-retinol is to 11-*cis*-retinal (lower right part). 11-*cis*-retinal is released from CRALBP and associates with IRBP to be trafficked extracellularly to the rod outer segments completing the cycle following binding to *apo*-rhodopsin.

Graphic:

By Krishnavedala - CC BY-SA 4.0,

https://commons.wikimedia.org/w/index.php?curid=39504470

dehydrogenases present in rod outer and inner segments to all-*trans*-retinol. All-*trans*-retinol is trafficked out of the rod photoreceptor cell through the extracellular compartment between outer segment and RPE cells in the subretinal space bound to interphotoreceptor retinoid-binding protein (IRBP). It is subsequently taken up by the RPE cells in which it is esterified by lecithin:retinol acyltransferase (LRAT) and these retinol esters can be stored in the RPE in specialised organelles called retinosomes. All-*trans*-retinol (vitamin A) can also enter the cycle by uptake from the bloodstream through the scavenger receptor stimulated by retinoic acid 6 (STRA6) present on RPE cells. RPE65 enzyme is the isomerohydrolase of the visual cycle using retinyl esters as substrates for isomerasation reaction producing the 11-*cis* isoform bound to cellular retinal binding protein (CRALBP). 11-*cis*-retinol is then oxidised to 11-*cis*-retinal by 11-*cis*-retinol dehydrogenases. 11-*cis*-retinal is released from CRALBP and associated with IRBP trafficked extracellularly to the rod outer segments completing the cycle when binding to *apo*-rhodopsin (Maeda and Palczewski, 2013).

I.II.II.III.II. Cone visual cycle

Cones differ from rods in many physiological properties including possibly the way they recycle photopigment to sustain fast responses in high light illumination. As in rods, 11-*cis*-retinal after photon absorption isomerises into the all-*trans* conformation activating the phototransduction cascade. All-*trans*-retinal dissociates from opsin and is reduced in cones into all-*trans*-retinol. However, all-*trans*-retinol from cones is trafficked to Müller cells (it is not yet clear if instead or in addition to RPE cells). In the Müller cells all-*trans*-retinol is isomerised into 11-cis-retinol in a two-step reaction involving esterification with palmitoyl-coenzyme A and with likely participation of CRALBP as retinoid binding protein. 11-*cis*-retinol ester is hydrolysed and 11-*cis*-retinol released from Müller cells for uptake in cones. Once in cones, it is oxidised to 11-*cis*-retinal, which binds to *apo*-cone opsin to form the visual pigment. For 11-*cis*-retinol oxidation NADP is used, therefore in cones and oxidation/reduction cycle exists in which NADPH is utilised by all-*trans*-retinol dehydrogenase for all-*trans*-retinal reduction, whilst NADP generated in this reduction serves in oxidation of 11-cis-retinol for pigment regeneration. It is hypothesised that this set of reactions is the biochemical basis for the fast pigment regeneration in cone photoreceptors (Parker et al., 2011; Wang and Kefalov, 2011).

I.II.II.IV. Disc renewal

Photoreceptors throughout the life of an animal are exposed to intense illumination in the presence of high oxygen levels and toxic retinoid derivatives, which together generate free radical species leading to accumulation of oxidative damage in the

photoreceptor outer segments. Unless countered by protective biochemical mechanisms and continuous renewal of photoreceptor cells, this would inevitably lead to rapid retinal degeneration and loss of function. Since photoreceptors are post-mitotic neurons that do not proliferate themselves nor are renewed from tissue-residing stem cells in adult animals, mechanisms other than replacement by new cells generated from divisions had to be employed to maintain photoreceptor outer segment function. Continuous shedding of distal photoreceptor discs provides a way of replenishing damaged outer segment components (Palczewski, 2012). Classical experiments in the 1960s by Young and colleagues (Young, 1967, 1968) by use of pulse-labelling and autoradiography showed that newly-made proteins containing a radioactive label first appear as a band at the basal proximal part of the rod outer segment and are progressively displaced towards the distal tip of the outer segment before later disappearing after detection in the RPE. Complete rod outer segment renewal takes around 10 days in higher vertebrates (LaVail, 1973). Removal of shed outer segment discs is possible due to the phagocytic activity of RPE cells (LaVail, 1983). Microvilli of RPE cells surround the distal half of rod photoreceptor outer segments and take part in the engulfment of distal outer segment tips, these cells also extend long tubular apical processes that reach and ensheath the tips of cone segments. Following ingestion by the RPE shed segment components are encircled by plasma membrane to form a phagosome. To this structure endosomes and lysosomes fuse, some mediating recycling of components such as unsaturated lipids and retinoids for use in the biosynthesis of new discs (Bok, 1993). Activity of Mer tyrosine kinase, mutations in which are linked to human retinitis pigmentosa, is required for the phagocytic activity of RPE and efficient breakdown of phagosome contents (Gal et al., 2000). These renewal events occur in a circadian manner with cone discs shed mostly after dark and rod distal tips in the morning (Bok, 1993).

With respect to cone outer segment renewal specifically, the actual turnover rate has not been determined to date, however, autoradiographic and kinetic data are suggestive of a slower turnover rate as compared to rod photoreceptors. This slower replenishment rate is in fact more typical of turnover rates for intracellular components in other cell types pointing to a specialised enhanced renewal mechanism for rod cells. These analyses suggest as well that cone outer segments may contain a higher proportion of older pigment molecules than those of rods, what might not be detrimental to their function given that these cells evolved to signal detection of hundreds to millions of photons, but nevertheless, may pose a limit to cone sensitivity (Mustafi et al., 2009).

I.II.II.V. Biosynthesis of new outer segment discs

In order to balance out the apical loss of segment disks, photoreceptor cells need to continuously synthesize and target new disk membranes for addition at the base of the outer segment. Mechanisms regulating this membrane genesis and fidelity of outer segment trafficking are only just being elucidated (Sung and Chuang, 2010). Studies in rod photoreceptors lead researchers to postulate a model of basal disks generation through repeated fusion of specialized vesicles carrying the photopigment rhodopsin as their major cargo. These rhodopsin vesicles incorporate also syntaxin 3 and a protein called Smad anchor for receptor activation (SARA) with these three components physically interacting with each other. Presence of SARA on the surface of those vesicles allows fusion with nascent basal disks in a SNARE and phosphatidylinositol 3-phosphate mediated mechanism (Chuang et al., 2007). Besides vesicle transport, targeting of single structural and functional protein components of disks is of importance. Study of retinitis pigmentosa causing mutation in rhodopsin leading to the loss of the last five aminoacids of its cytoplasmic C-terminal tail revealed a highly conserved across species VXPX motif essential for correct rhodopsin localization (Sung and Tai, 1999). Previously mentioned SARA protein facilitates rhodopsin trafficking through recognition of this motif among other interacting proteins. Most other major outer segment components seem to use different targeting mechanisms since similar motifs have not been found in their peptide sequence. A common strategy could be “hitching a ride” by interaction with rhodopsin or rhodopsin vesicles abundant in rods. Additionally, high affinity interactions might drive translocation as in the case of activated photopigment recruiting arrestin upon illumination (Sung and Chuang, 2010). All the proteins destined for the outer segment need to pass through the connecting cilium. Molecular mechanisms that govern transport through this compartment have yet to be elucidated in detail. However, two hypothesis regarding rhodopsin transport were put forward. The first proposes that rhodopsin vesicles fuse to the cilium membrane at the apical part of the inner segment then the membrane components are moved through the connecting cilium by a mechanism called intraflagellar transport dependent on the action of kinesin motor proteins to then be recovered via endocytosis at the base of the outer segment (Sedmak and Wolfrum, 2010). The second mechanism postulates that rhodopsin vesicles are channelled through the cilium along the axonemal microtubules in the cilium shaft and is supported by electron microscopy observations of small vesicles in the connecting cilium of photoreceptors. Modes of transport in cone cells are largely avenues for future interrogation (Sung and Chuang, 2010).

I.III. Retinal development

I.III.I. Early eye development

I.III.I.I. Morphogenesis of the early eye

Eyes are specialised extensions of brain tissue and are specified early in embryonic development alongside other major parts of the nervous system (Zagozewski et al., 2014). Nervous system development starts with neural induction when within ectoderm, one the three germ layers in the early embryo, cells lying along the dorsal midline of the embryo are directed to commit to neural lineage. These cells heighten becoming columnar neuroepithelium form a so-called neural plate along anterior-posterior axis of the embryo, which then invaginates to form a neural tube from which the central nervous system develops. The anterior part of the neural tube forms three vesicles that give rise to the brain regions. The most anterior vesicle called prosencephalon (forebrain) is the site where a subset of cells committed to subsequently form the eye tissue are located (Chow and Lang, 2001). This group of cells defined at the molecular level by expression of specific transcription factors (see following sections) can be identified before neural tube formation in the anterior neural plate at the late gastrula stage. Interactions with and signals from surrounding tissues lead to the eye field splitting into two bilateral optic vesicles (Kim and Kim, 2012). Optic vesicles start as symmetrical bilateral evaginations slowly expanding through the mesenchyme until they reach the surface ectoderm. In the mouse embryo optic vesicles can be discerned from around embryonic day 8.5 (Chow and Lang, 2001). Contact with the surface ectoderm triggers a series of structural changes in the vesicles, the proximal-distal part starts to invaginate and the vesicle becomes a two-layered optic cup in which the outer layer differentiates into RPE cells whilst the inner part becomes neural retina (Kim and Kim, 2012). The hinge regions subsequently develop into the anterior structures of the eye, the ciliary body and iris. As the cup invaginates the surface ectoderm forms a pit that becomes the lens placode and lens vesicle as it further folds, invaginates and separates from the overlying ectoderm. The ventral part of the vesicle narrows into the optic fissure that after closure forms the optic nerve. The requirement for the overlying tissue and lens in neural retina specification is still a matter of debate. It appears that early contact with the pre-lens ectoderm specifies the neuroepithelium to become neural retina (via FGF signalling, see following sections), since later removal of the lens placode or lens does not affect neural retina specification (Chow and Lang, 2001). Recent milestone studies using mouse and human pluripotent stem cells directed towards retinal differentiation

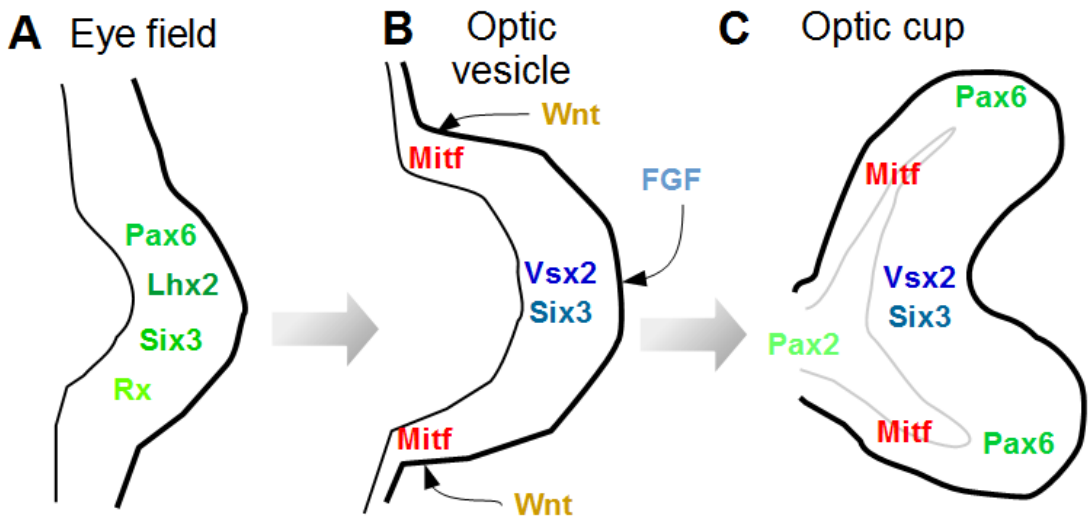

Diagram I.VI. Early eye development.

(**A**) Eye development commences with the specification of the eye field in the anterior neuroepithelium. The eye field is delineated by expression of a set of specific transcription factors including LIM homeobox protein 2 (Lhx2), Paired box protein 6 (Pax6), Retinal homeobox protein (Rx) and SIX homeobox protein 3 (Six3). The eye field subsequently undergoes evagination forming an optic vesicle. (**B)** The optic vesicle becomes divided into the proximal and distal domains through activity of Wnts and FGFs, respectively. The proximal domain becomes the presumptive RPE expressing Microphthalmia-associated transcription factor (Mitf), whereas the distal part becomes the prospective neural retina upregulating Visual system homeobox protein 2 (Vsx2). (**C**) The evaginating optic vesicle folds forming a bi-layered optic cup and the division into RPE and neural retina becomes apparent. The outside shell of the cup is the rigid RPE, whilst the internal part is the more flexible neural retina. Distal optic cup expresses Pax6, whereas the optic stalk is marked by expression of Paired box protein 2 (Pax2).

demonstrated self-formation of optic vesicles, which subsequently folded into optic cups without any overlying surface ectoderm, highlighting strong self-assembly potential for this structure and the importance of self-autonomous regulators in the morphogenetic process (Eiraku et al., 2011; Meyer et al., 2009).

I.III.I.II. Genetic regulators of eye morphogenesis

Recent observations on the self-organisation potential of optic tissues stresses the role of intrinsic genetic regulators of this process (Eiraku et al., 2011; Meyer et al., 2009). A gene-regulatory network for eye assembly commences at the eye field stage (Diagram I.VI.). In the anterior neural plate expression of a set of transcription factors, best studied in *Xenopus laevis*, defines the commitment to differentiate into eye tissue and therefore delineates the eye field (Zagozewski et al., 2014). Hence, these transcription factors that include *Rx1/Rax*, *Pax6*, *Six3*, *Lhx2*, *Tll/Tlx*, *Optx2/Six6* and *ET/Tbx3*, are termed the *eye field transcription factors*. What distinguishes eye field transcription factors is their necessity for eye development, since loss of either *Rax*, *Pax6, Six3* and *Lhx2* leads to absence or eye abnormalities (Carl et al., 2002; Mathers et al., 1997; Porter et al., 1997; Zagozewski et al., 2014). Moreover, mis-expression of these transcription factors alone, as in case of *Pax6* or *Rx1*, or in a mix is sufficient for induction of ectopic eyes (Chow et al., 1999; reviewed in Zuber et al., 2003). In addition to eye field transcription factors, the forebrain specification factor *Otx2* plays an important permissive role for eye field transcription factor expression without directly inducing them (Matsuo et al., 1995; Zagozewski et al., 2014).

Establishment of the midline in the embryo leads to eye field division into two lateral components that will give rise to two identical eyes. In this process sonic hedgehog (Shh) signalling plays a crucial role. Inactivation of Shh leads to failure of midline formation and development of a single eye (cyclopia). Expression of Shh in the forming forebrain is regulated by one of the eye field transcription factors *Six3*, which binds to an enhancer sequence upstream of Shh gene to stimulate its transcription (Chiang et al., 1996).

Subsequent to the bisection of the eye field, optic vesicles form and begin to evaginate from the ventral forebrain towards overlying surface ectoderm (Chow and Lang, 2001). Homeodomain transcription factor Rax is necessary for eye field establishment and consecutive outgrowth of optic vesicles (Mathers et al., 1997). Loss of Rax in zebrafish, frog, mouse and human leads in anophthalmia (Zagozewski et al., 2014). Rax expression if found initially throughout the entire anterior neural plate prior to, from E10.5, becoming restricted to the optic vesicle and ventral diencephalon (Mathers et al., 1997). In zebrafish eyes the lateral outgrowth of optic vesicles results from

migration of Rx3-positive progenitor in the lateral direction and *Rx3 null* mutants show clustering of optic progenitors around the embryo midline (Rembold et al., 2006).

During evagination the optic vesicle undergoes both proximal-distal as well as dorsal-ventral patterning specifying regions of the future eye (Kim and Kim, 2012). Shh signalling plays a role in setting both of these axes (Sasagawa et al., 2002). The ventral domain of the eye is set up by the activity of homeodomain transcription factors Vax1 and Vax2. Expression of these transcription factors is triggered by Shh and lost in absence of Shh. At E9.5 Vax1 and Vax2 localize to the boundary of the prospective optic stalk and neural retina. Following optic vesicle invagination Vax1 is found in the optic stalk, whilst Vax2 becomes confined to the ventral neural retina. Genetic ablation of both *Vax1* and *Vax2* results in a dorsalized eye phenotype with neural retina expanding ventrally at the expense of the optic stalk. In *Vax1/2*$^{-/-}$ eyes expression of Pax2, which marks the optic stalk is severely reduced and an increase in Pax6 observed highlighting the role of Pax6 in establishing the ventral domain of the neural retina (Take-uchi et al., 2003). Dorsal optic vesicle is marked by expression of the transcription factor Tbx5 induced by bone morphogenetic protein 4 (BMP4; (Behesti et al., 2006; Sasagawa et al., 2002). Tbx5 represses Vax expression in this part of the optic vesicle thereby delineating dorsal versus ventral domains in the vesicle. In addition, for the upregulation of both Vax genes as well as Tbx5 activity of the LIM homeodomain transcription factor Lhx2 is necessary. Loss of Lhx2 results in an arrest in the transition from the optic vesicle to the optic cup with the lack of Vax and Tbx5 expression in the arrested vesicles (Yun et al., 2009). With respect to the proximal-distal specification, this is regulated by expression of Pax2, marking the proximal optic stalk, and Pax6, which is a marker of the distal optic cup, with inputs from Shh signalling (Sasagawa et al., 2002). These two transcription factors repress each other's expression to create the boundary between the optic stalk and the optic cup (Zagozewski et al., 2014).

Alongside the patterning in the proximal-distal and dorsal-ventral axes, also division into neural retina and RPE takes place. As mentioned above, once the evaginating optic vesicle reaches the surface ectoderm, invagination is triggered to form a cup structure with the neural retina on the inside surrounded by the RPE as the outer layer. Neural retina can be traced to the distal/ventral part of the optic vesicle (Fuhrmann, 2010). The distal optic vesicle receives TGFβ signalling triggering the induction of the basic helix-loop-helix transcription factor, Mitf, and the homeodomain transcription factor Otx2 and these two regulators are drivers of RPE specification. Both factors activate expression of RPE-specific genes and their loss of function leads to formation

of ectopic neural retina at the expense of RPE (Fuhrmann et al., 2000). Following contact with surface ectoderm of the distal/ventral optic vesicle, expression of the paired-like homeodomain transcription factor Vsx2 is induced. Vsx2 (formerly Chx10) is the earliest known marker of the prospective neural retina with expression commencing as early as E9.5 in the mouse and which acts to repress Mitf expression to allow neural retina differentiation (Liu et al., 1994). Interestingly, this division seems to occur independent of the action of Pax6, a master regulator transcription factor for eye development. Genetic ablation of *Pax6* leads to failure of optic cup formation, however, in the optic vesicles of *Pax6*$^{-/-}$ embryos division into Vsx2-positive and Mitf-positive regions remains (Fuhrmann, 2010). Another eye field transcription factor becomes involved in this process, namely Six3, which is required for neural retina but not RPE differentiation (Liu et al., 2010). Despite these regulatory actions at early stages, the neuroepithelium of the optic vesicle exhibits a significant level of developmental plasticity with early neural retinal progenitors being able to produce RPE and early RPE able to convert into neural retina (Kuwahara et al., 2015).

I.III.I.III. Role of soluble factors in early eye morphogenesis

In addition to the cell-autonomous actions of transcription factors, important regulatory roles can be ascribed to soluble molecules in the course of eye morphogenesis (Chow and Lang, 2001; Diagram I.VI.). Early in embryonic development, graded Wnt signalling is critical for establishment of the anterior-posterior axis of the developing brain with high levels of Wnts promoting posterior fates (Kiecker and Niehrs, 2001). Restricted Wnt signalling is therefore permissive for eye field specification (Zuber et al., 2003). For the eye field to split into two lateral prospective optic vesicles, Shh signalling is essential. Shh loss in prechordal mesoderm leads to failure in the formation of the ventral midline and splitting the eye field resulting in cyclopia (Chiang et al., 1996). Furthermore, Shh plays a role also in the optic vesicles patterning inducing Pax2 expression in the proximal optic stalk and Vax gene expression in the ventral optic vesicle (Geng et al., 2008). Retinoic acid, produced by Raldh2 and Raldh3 enzymes has also been implicated in contributing to the establishment of the ventral identity in the optic vesicle (Alfano et al., 2011; McCaffrery et al., 1993; Mic et al., 2000). The dorsal part of the vesicle on the other hand receives BMP signalling of the TGFβ superfamily, mainly through BMP4, which induces the dorsal marker Tbx5 (Behesti et al., 2006). The subsequent cup formation, division and differentiation into RPE and neural retina is regulated by TGFβ, Wnt and fibroblast growth factor (FGF) signalling. Activin A, a member of the TGFβ protein superfamily secreted from extraocular mesenchyme, was found to trigger Mitf expression in the prospective RPE

(Kim and Kim, 2012). In collaboration with TGFβ signalling, Wnt signalling is essential for acquisition and maintenance of the RPE fate. Depletion of β-catenin at the optic cup stage leads to Mitf and Otx2 loss and transdifferentiation into neural retina (Westenskow et al., 2009). Conversely, for development into neural retina FGF signalling is required (Kim and Kim, 2012; Kuwahara et al., 2015; Pittack et al., 1997). Surface ectoderm secretes FGFs, which trigger differentiation of the optic vesicle neuroepithelium, in contact with the ectoderm, into neural retina. Optic vesicles depleted of surface ectoderm do not develop neural retina, a phenotype rescued by addition of FGFs. Moreover, optic vesicles cultured in isolation *in vitro* in the presence of FGF2 develop into neural retina only, whilst blocking FGF signalling with neutralizing antibodies prevents neural retina differentiation (Pittack et al., 1997). These insights into the role of soluble molecules involved in eye development not only broadened our understanding of the developmental biology of the eye, but have also greatly facilitated the development of retinal differentiation protocols in recent years.

I.III.II. Regulation of retinal neurogenesis.

I.III.II.I. Overview of histogenesis in the retina

Retinal neurons are generated from a pool of retinal progenitor cells over a prolonged period of tissue formation and maturation (reviewed in Swaroop et al., 2010). The six neuron classes and Müller glial cells are generated in an evolutionary conserved temporal birth order, which might reflect their appearance in the course of evolution (reviewed in Cepko, 2014). Thus differentiating cell types emerge in partially overlapping waves of genesis, starting with retinal ganglion cells, shortly followed by cone photoreceptors, horizontal cells, the majority of amacrine cells and a minority of rod photoreceptors followed by a later phase in which the majority of rod photoreceptors, the remainder of amacrine cells, bipolar cells and Müller glia are born (reviewed in Bassett and Wallace, 2012). Retinal progenitor cells from which these neurons arise were found in early lineage studies to be multipotent, giving rise to clones of a wide range of sizes and compositions (reviewed in Cepko, 2014). Even so, through experiments in which progenitors from one stage were removed and placed into an earlier or later environment, it has been shown that at any stage of development retinal progenitors are limited in the set of progeny they can generate (Watanabe and Raff, 1990). Hence, it is currently proposed that progenitors pass through temporal competence states in which certain types of progeny are made as retinal development unfolds.

I.III.II.II. Maintenance and multipotency of retinal progenitors

Before the onset of retinal neurogenesis retinal progenitor cells (RPCs) need to acquire the competence to undergo the sequential production of all retinal cell types. This competence appears to heavily depend on the ratio of two transcription factors: Sox2 and Pax6 (reviewed in Xiang, 2013). Mutations in the paired type transcription factor Pax6 underlie ocular phenotypes such as anophthalmia, microphthalmia and aniridia in both mouse and human (Glaser et al., 1994). Genetic removal of Pax6 expression from RPCs results in loss of all retinal cell types apart from GABAergic amacrine cells highlighting its role in conferring RPC multipotency (Marquardt et al., 2001). Pax6 exerts its effects on multipotency by acting on neurogenic basic helix-loop-helix and homeodomain transcription factors that determine commitment to particular fates. In addition, it is highly expressed in the anterior structures of the eye, the iris and ciliary body, and required for their differentiation. The HMG box transcription factor Sox2 also plays a key role in RPCs maintenance and multipotency. Similarly to Pax6, loss of Sox2 leads to loss of neurogenic potential and a fate switch to ciliary pigmented epithelium associated with an increase in Pax6 expression. This phenotype can be partially rescued by inactivation of a single Pax6 allele (Matsushima et al., 2011). Therefore it appears that a balance of activities of those two transcription factors is required for proper retinal morphogenesis, supported by observations that both of these transcriptional regulators show phenotypes sensitive to gene dosage (Glaser et al., 1994; Marquardt et al., 2001; Matsushima et al., 2011; Taranova et al., 2006). In addition, activity of Vsx2 is required for competence to form the neural retina. Vsx2 prevents transdifferentiation into retinal pigmented epithelium by repressing RPE fate driver Mitf (Rowan et al., 2004).

I.III.II.III. Role of Notch signalling in retinal neurogenesis

Genetic inactivation of *Sox2* leads to the loss of neural retina genesis potential through the loss of neurogenic transcription factors and Notch1 expression (Taranova et al., 2006), highlighting the requirement for Notch signalling in retinal neurogenesis. Notch signalling plays important roles in the regulation of neurogenesis in both vertebrates and invertebrates (Lewis, 1996). Targeted disruption of the *Notch1* gene during retinal development revealed its function in maintaining the cycling pool of retinal progenitors as well as involvement in cell fate specification (Jadhav, 2006; Yaron, 2006). Loss of Notch1 activity leads to reduction in the size of retina. This is due to a decrease in proliferation and premature neurogenesis (Jadhav, 2006; Nelson et al., 2007; Yaron, 2006). Following Notch downregulation a set of pro-neural genes becomes upregulated including *Neurogenin2* (*Ngn2*), *Neurod1*, *Mash1* and *Atoh7,* whereas genes associated with cell cycle progression such as *CyclinD1* become downregulated

(Jadhav, 2006; Nelson et al., 2007). Surprisingly, genetic ablation of *Notch1* at early stages of retinogenesis leads to nearly uniform acquisition of cone cell fate by the newly generated neurons (Jadhav, 2006; Yaron, 2006). At neonatal stages its genetic inactivation results in adoption of rod fate (Jadhav, 2006). Therefore, despite the competence of progenitors to generate a set of different neuronal fates at each stage of retinogenesis, loss of signalling from Notch1 receptor leads to nearly exclusive adoption of the photoreceptor fate (Jadhav, 2006; Nelson et al., 2007; Yaron, 2006). Activity of the Notch3 receptor, which is also expressed in the mammalian retina was found to limit the production of retinal ganglion cells through downstream effector Hes1 (Riesenberg et al., 2009), suggesting that a combination of a particular Notch receptor with downstream signalling molecules likely determines cell fate decisions in the retina. Notch signalling can be separated into two types: canonical and non-canonical. In the canonical pathway binding of Notch ligands triggers cleavage of the transmembrane Notch receptor with subsequent release of its intracellular domain mediated by the proteolytic activity of presenilin/γ-secretase (reviewed in Martinez Arias et al., 2002). Potent pharmacological inhibitors targeting γ-secretase were developed and one them DAPT became widely adopted in biological research. Treatment of chick and mouse developing retinae was found to phenocopy effects of *Notch1* genetic deletion and provided insights into kinetics of developmental processes involved. Pharmacological block of Notch signalling for longer than 6 hours was found to lead to irreversible initiation of the differentiation programme similarly leading to an increase in cone markers when performed early in retinogenesis (Nelson et al., 2007). Altogether, Notch signalling was found to play a crucial role in maintenance of retinal progenitors by preventing precocious neurogenesis.

I.III.II.IV. Differentiation of retinal neurons

Signals that trigger retinal neurogenesis with commitment and differentiation towards one of the six neuronal and one glial type are not spread uniformly across the eye and in most species exhibit a central to peripheral gradient with the central retina being less proliferative and differentiating earlier than the peripheral domain. Neurogenesis is dependent on expression of combinations of fate-determining transcription factors, most of which fall into either the homeobox or basic helix-loop-helix (bHLH) families (Bassett and Wallace, 2012; Ohsawa and Kageyama, 2008; Swaroop et al., 2010; Xiang, 2013; Zagozewski et al., 2014).

I.III.II.IV.I. Retinal ganglion cells

Retinal ganglion cells are the projection neurons of the retina sending axons to the visual centres in the brain. Ganglion cells are the earlier born and first neuronal type

to differentiate as early as E10.5 in the mouse. The bHLH transcription factor, Atoh7 (formerly Math5), plays a crucial role in specifying ganglion cell fate. Genetic ablation of *Atoh7* results in the loss of all ganglion cells and lack of optic nerve development. Downstream of Atoh7 in the ganglion cell specification pathway lies the POU-domain transcription factor Brn3b. Brn3b is necessary for ganglion cell survival and its removal leads to loss of the majority of ganglion cells due to apoptotic death. Similarly, Dlx homeodomain transcription factors Dlx1 and Dlx2 are required for survival of late born ganglion cells with their loss resulting in excessive apoptosis of this subpopulation.

I.III.II.IV.II. Horizontal cells

Horizontal cells play important roles in information processing at the level of outer plexiform layer through lateral interactions with photoreceptor and bipolar cells. Horizontal cells are an early-born retinal cell type. The forkhead/winged helix transcription factor Foxn4 is a key determinant of horizontal cell fate and its loss leads to a complete absence of horizontal cells in the retina. Expression of both Onecut1 and Ptf1a directs differentiation of Foxn4-positive progenitors into horizontal cells, as expression of Foxn4 with Ptf1a alone leads to adoption of amacrine cell fate, highlighting the necessary role of Onecut1 for horizontal cell genesis. Downstream of Onecut1 and Ptf1a, homeobox transcription factors Prox1 and Lhx1 (Lim1) play important roles in terminal differentiation and migration of horizontal cells into appropriate laminar position.

I.III.II.IV.III. Amacrine cells

Amacrine interneurons form synaptic contacts in the inner plexiform layer to mediate interactions between bipolar cells and ganglion cells. Amacrine cells share many fate determinants with horizontal cells, namely, they also require Foxn4 and Ptf1a expression for differentiation. Concomitant action of two bHLH transcription factors Math3 and NeuroD is also a necessary step in amacrine fate specification with complete loss of amacrine cells following genetic removal of both of these factors.

I.III.II.IV.IV. Bipolar cells

Bipolar interneurons carry signals from photoreceptors to ganglion cells, the projection neurons of the retina, and also interact laterally with horizontal and amacrine cells. There are multiple subtypes of bipolar cells showing unique gene expression patterns, however, several key fate determinants have been identified for this cell type. In addition to its role in progenitor divisions, Vsx2 is an essential factor for bipolar cell development and Vsx2 mutants show a pronounced reduction in the number of bipolar cells. Moreover, combined loss of Math3 and Mash1 results in complete absence of

bipolar cells showing a requirement for these two factors in determining bipolar cell fate.

I.III.II.IV.V. Müller glia

Müller cells are the only glial type of the retina and play important supportive roles for the tissue with processes spanning the whole thickness of the retina. Müller glia are mostly the last cell type to be generated during retinogenesis and they share many differentiation regulators with retinal progenitor cells. The Notch pathway and its downstream targets bHLH transcription factors Hes1 and Hes5 have been implicated in Müller glia differentiation. Genetic knockout of *Notch1*, *Hes1* and *Hes5* leads to diminished numbers of Müller cells, whilst overexpression of these promote Müller glia differentiation. In addition, reduction in expression of the SRY-related HMG box transcription factors Sox2, Sox8 and Sox9 likewise leads to impaired Müller glia differentiation, suggestive of their contribution to this process. In the case of both Notch-Hes and Sox gene downregulation increased numbers of rods are generated, pointing to a rod versus Müller glia cell fate choice occurring in late retinal progenitors.

I.III.II.V. Photoreceptor specification

Genesis of photoreceptor cells in mammals occurs over a long time window and is a multi-step process. From the division of a competent progenitor weeks or months pass, depending on the species, until functional maturation is completed. Several steps can be identified, first, multipotent retinal progenitors (RPCs) undergo divisions, second, these RPCs undergo restriction of their competence, third, commitment to photoreceptor cell fate is initiated during or soon after RPC terminal mitosis, then photoreceptor-specific genes, related to processes such as phototransduction (Diagram I.VII.), become expressed and, finally, axons grow and form synaptic connections and outer segments biogenesis occurs (Bassett and Wallace, 2012; Livesey and Cepko, 2001; Swaroop et al., 2010). In mice, the eyes of newborn pups remain closed for nearly two weeks as photoreceptor maturation is not complete at birth. Cone genesis commences at around E11 and is largely complete before birth with S opsin being expressed from late embryonic stages (E18). With respect to rod photoreceptors, the peak of their genesis is in the neonatal period and rhodopsin expression commences in the first few days after birth (detectable from around P2). M opsin expression in cones lags behind that of S opsin and is initiated from P6. In human retinal development all photoreceptors are generated before birth. In contrast to the rodent retina, the human retina shows pronounced differences in the degree of maturation between the cental and peripheral domains. First cones appear around foetal week (Fwk) 8, whereas rods are born from Fwk 10. All cellular layers can be

identified in the fovea region by Fwk 11. As early as Fwk 12 S opsin transcripts can be detected. Subsequently, from Fwk 15 M opsin and Rhodopsin transcription begins. At Fwk 15, concomitantly with the visual pigments expression outer segment biogenesis commences (Hendrickson et al., 2008; O'Brien et al., 2003; Xiao and Hendrickson, 2000). With maturation functional synaptic connections with bipolar and horizontal cells are formed, outer segments elaborate and come in close apposition with the RPE cells and phototransduction starts (reviewed in Swaroop et al., 2010).

Early events in photoreceptor lineage specification are poorly understood. As discussed above, downregulation of signalling downstream of Notch1 receptor is an essential step to induce generation of photoreceptor progeny from RPCs (Jadhav, 2006, Yaron et al., 2006; Nelson et al., 2007; Riesenberg et al., 2009). More recently, the role of signalling through Notch1 was also examined in newly post-mitotic cells. Profiling of single cells transitioning from a progenitor to a differentiated state revealed some of the molecular effectors downstream of Notch1 receptor. Inhibitor of DNA binding factors Id1 and Id3 were found to be required for the generation of Müller glial cells, whereas Notch-regulated Ankyrin Repeat Protein expression drove commitment to the rod fate (Mizeracka et al., 2013). Both genetic ablation as well pharmacological inhibition of Notch signalling demonstrated reduction of downstream transcriptional effectors Hes1 and Hes5, which in turn repress pro-neural basic helix-loop-helix (bHLH) transcription factors. Indeed gene expression analysis showed that a panel of these genes including *Neurogenin2* (*Ngn2*), *Neurod1*, *Mash1* and *Atoh7* became upregulated (Jadhav, 2006; Nelson et al., 2007; Yaron, 2006). These pro-neural bHLH have redundant and poorly defined roles in photoreceptor development with likely combinatorial or transient functions at this stage (Swaroop et al., 2010).

Better characterized are the later steps in post-mitotic photoreceptor precursor differentiation and these again require sequential combinatorial action of several transcriptional regulators to establish a rod or cone fate (Swaroop et al., 2010; Diagram I.VII.). An essential role in the first stages of photoreceptor lineage induction is played by the paired-type homeodomain transcription factor Otx2, a homolog of the *Drosophila* orthodenticle (Otd), which is required for the formation of anterior brain, eye and antenna in the fly. Otx2 is expressed by many cell types in the brain and in the eye by photoreceptors, bipolar cells and RPE, with expression commencing during terminal mitosis of a progenitor or shortly thereafter (Beby and Lamonerie, 2013). Genetic ablation of Otx2 in mouse retinal progenitor cells leads to almost complete loss of cone and rod photoreceptors, horizontal and bipolar cells (Nishida et al., 2003). Otx2 performs its role in photoreceptor specification through participation in gene regulatory networks

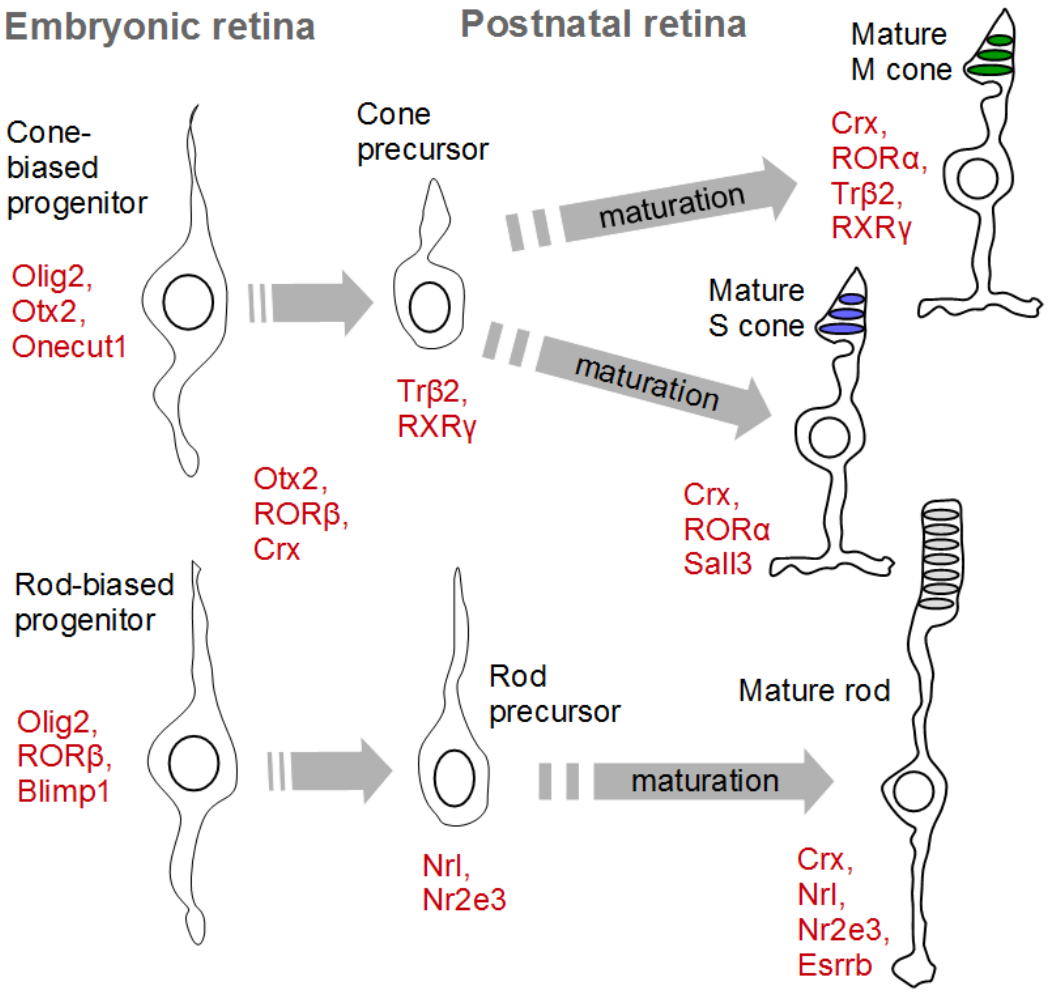

Diagram I.VII. Transcriptional control of photoreceptor differentiation.

Photoreceptor precursors are generated from multipotent retinal progenitors. Progenitors biased towards generation of photoreceptors show expression of specific molecular markers, specifically progenitors dedicated to generation of cone cells express Olig2, Otx2 and Onecut1. Following divisions of retinal progenitors the newly born photoreceptor precursors express early markers of photoreceptor lineage commitment such as Crx for both photoreceptor types, Trβ2 and RXRγ for cone precursors and Nrl with Nr2e3 for rod precursors. Some of these regulators are also essential for maturation of the precursors alongside additional molecules including Sall3 in S cone development and Esrrb in maintenance of mature rod cells.

leading to establishing commitment to these fates. In progenitors competent for cone and horizontal cell fates it collectively binds with Onecut1 transcription factor to regulatory sequences in the locus of an early cone marker *Thrb2*, stimulating transcription of the gene (Emerson et al., 2013). In the progenitors that generate rod and bipolar cells at neonatal stages, Otx2 participates in the induction of Blimp1 expression. This transcriptional regulator creates a direct negative feedback loop downregulating expression of Otx2 and Vsx2/Chx10, high levels of which promote bipolar differentiation, as well as leading to its own repression (Wang et al., 2014). Therefore, Otx2 provides a necessary but not sufficient signal to induce commitment to cone or rod cell fate.

The orphan nuclear receptor RORβ is expressed in all cellular layers of the retina and in the pineal gland and is required for several aspects of photoreceptor development (reviewed in Swaroop et al., 2010). Two isoforms of RORβ are expressed in the developing retina. RORβ1 is detected in progenitor cells, photoreceptor precursors and in other cell types across different retinal layers, whereas RORβ2 isoform is found in rod precursors (Fu et al., 2014). Both isoforms contribute to establish the commitment to the rod fate through induction of the rod-specific determinant Nrl. In *Rorb*$^{-/-}$ mice expression of Nrl and many other rod-specific genes is abolished (Jia et al., 2009). Aside from induction of Nrl, RORβ participates in induction of the gene regulatory network determining dual fate choice between rod and bipolar cells by cooperating with Otx2 in the induction of Blimp1 expression (Wang et al., 2014). In rod precursors Nrl, once its transcription is activated by RORβ, acts on the specific promoter of the RORβ2 isoform, its own inducer gene, stimulating its transcription in a positive feedback loop (Fu et al., 2014). This mechanism is thought to strengthen the commitment to rod fate. Both RORβ isoforms appear to participate in the establishment of the correct ratio of cones versus rods since deletion of each single isoform results in 2-3 fold increase in the proportion of cones (Fu et al., 2014), whereas no rods are formed in the full knockout (Jia et al., 2009). In cone precursor development RORβ is required for induction of both S opsin and M opsin photopigments, demonstrated by developmental delay in expression of S opsin and a reduction in M opsin in the *Rorb*$^{-/-}$ mice (Jia et al., 2009). An additional role in both photoreceptor types is the requirement for RORβ in outer segment biogenesis. S cone-like cells in the *Rorb*$^{-/-}$ mice generated as a result of loss of rods exhibit primitive morphology and improperly formed outer segments, which correspondingly showing deficits in functionality (Jia et al., 2009). Therefore, similarly to Otx2, RORβ is a necessary but not sufficient factor in the photoreceptor differentiation gene regulatory network.

In photoreceptor precursors Otx2 induces expression of another member of the Otx homeodomain family – the cone-rod homeobox transcription factor (Crx) (Furukawa et al., 1997). Otx2 binds to the *Crx* promoter region *in vivo* and genetic deletion of *Otx2* abolishes *Crx* expression (Nishida et al., 2003). Crx is expressed early in post-mitotic precursors for both rod and cone cells, being one of the first markers of commitment to this lineage (Muranishi et al., 2010). Crx expression becomes detectable from as early as E12.5 in the mouse correlating with the genesis of the first cone precursors and peaks at around P5 corresponding to initiation of rod differentiation (Furukawa et al., 1997; Muranishi et al., 2010). The major role of Crx in the developing photoreceptors is to facilitate transcriptional activation of a wide array of photoreceptor-specific genes (Livesey et al., 2000). This activity of Crx is mediated via cooperation with a number of transcriptional regulators including rod-determinants Nrl (Neural Retina Leucine Zipper) and Nr2e3 (nuclear receptor subfamily 2, group E, member 3) to stimulate *Rhodopsin* and other rod-specific gene expression, ROR family nuclear receptors, general transcription factors, transcription co-activators CBP and p300 and chromatin remodelling complexes (Hennig et al., 2008). Consistent with the importance of Crx in the induction of gene expression required for photoreceptor development and function, outer segments do not form and activity of photoreceptors in $Crx^{-/-}$ mice is lost resulting in blindness and progressive retinal degeneration (Furukawa et al., 1997). In accordance Crx mutations in humans underlie inherited retinal diseases including cone-rod dystrophy, retinitis pigmentosa and Leber's congenital amaurosis (Freund et al., 1998). In conclusion, Crx is a key enhancer in activation of genes essential for photoreceptor development and maturation.

Downstream of RORβ in the photoreceptor differentiation pathway lies the basic-leucine zipper Maf family transcription factor Nrl (Swaroop et al., 1992) a key inducer of rod fate (Mears et al., 2001). Nrl is highly expressed in the retina, lens, regions of the brain and pineal gland (Swaroop et al., 1992). Onset of Nrl expression correlates with the birth of the first rods around E12.5-E14.5 and the gene is expressed during or early after exit from progenitor terminal mitosis (Akimoto et al., 2006). Genetic ablation of Nrl leads to complete loss of rod photoreceptors (Mears et al., 2001). The resulting retina in $Nrl^{-/-}$ mice is composed of S cone-like cells that do not express any rod genes, show uncondensed chromatin and poorly formed short outer segments. Additionally, retinal morphology is disrupted with formation of whorls and rosettes and subsequent degeneration at adult stages (Mears et al., 2001). Forced expression of Onecut1, an early regulator of cone and horizontal lineage specification was found to lead to generation of immature cones at the expense of rods most likely through inhibition of

Nrl (Emerson et al., 2013). Conversely, misexpression of Nrl from early stages in all prospective photoreceptors using the *Crx* promoter led to loss of the mature cone cell phenotype, however using S opsin promoter to drive Nrl expression in a *Nrl*$^{-/-}$ background resulted in hybrid cells that expressed both S opsin as well as Rhodopsin (Oh et al., 2007). Moreover, inducible deletion of *Nrl* at various stages of development has shown that conversion of rods into the S cone-like phenotype is only possible during a limited developmental time window delineated by acquisition of epigenetic marks stabilising mature phenotypes (Montana et al., 2013). Therefore, it appears that Nrl is a key transcriptional regulator involved in a binary fate choice between cone and rod precursor fates that occurs early in the process of photoreceptor specification.

To consolidate the commitment to the rod fate Nrl induces expression of the nuclear receptor Nr2e3. This molecule was identified through homology to the *Drosophila* tailless (Tlx, Nr2e1) nuclear receptor and is also an orphan nuclear receptor meaning that a physiological ligand for it has not been identified. Nr2e3 expression is detected from E18 in the developing retina, peaks at a time of rod precursor cell differentiation and is maintained at a lower level in adulthood, localized to the rod photoreceptors (Kobayashi et al., 1999). In mice a naturally occurring mutation in *Nr2e3* gene was identified, whereby an L1 retrotransposon insertion disrupts Nr2e3 mRNA splicing leading to a 380 bp deletion in the coding region that prevents Nr2e3 protein production (Chen et al., 2006). These *rd7* mice show abnormal retinal histology with formation of rosettes followed by slow retinal degeneration. On the level of electroretinogram (ERG) function of S cones is strongly enhanced, whereas rod function declines as the retina degenerates at later stages (Akhmedov et al., 2000). Indeed, detailed analysis revealed that the number of S opsin expressing cones is increased around 2-3 fold in these mice (Corbo and Cepko, 2005), suggesting that Nr2e3 plays a role in setting the cone to rod ratio. The remaining majority of photoreceptors in the rd7 mice were found to be hybrid cells expressing both cone and rod genes supported by microarray analysis showing widespread de-repression of gene transcription associated with cone photoreceptors (Corbo and Cepko, 2005). Molecular analysis shows that Nr2e3 is a dual transcription regulator that binding with Crx and Nrl stimulates *Rhodopsin* transcription, but represses cone opsins transcription with repressing activity on many other cone-specific genes (Peng et al., 2005). Analysis of the *Nrl*$^{-/-}$ retinae showed that expression of Nr2e3 is abolished in those animals demonstrating that Nr2e3 is a downstream effector of Nrl in the rod specification pathway (Mears et al., 2001). Forced expression of Nr2e3 in a *Nrl*$^{-/-}$ background suppresses cone gene expression and restores expression of some but not all rod genes (Cheng et al., 2006) indicating that

activity of both Nrl and Nr2e3 is required for establishment of a proper rod phenotype. Consistent with observations in mice, mutations in human NR2E3 cause retinal disease characterized by enhanced S cone function, defects in rod function and degeneration leading to blindness at late stages (Haider et al., 2000). Curiously, not only expanded cone population but also cells co-expressing both L/M and S opsins were found in the histopathological sample from an affected individual, an unusual phenotype for human cones (Milam et al., 2002). Altogether, these studies show that Nr2e3 is an important downstream effector of Nrl that cooperates with it to establish the rod phenotype primarily through repression of cone gene expression.

With respect to cone photoreceptor specification, despite identification of several important regulators, a clear pathway remains elusive. A feature of many rod pathway loss of function models is reversion to S opsin-expressing cone-like cells with a moderate 2-3 fold increase in mature-appearing cone photoreceptor cells (Corbo and Cepko, 2005; Fu et al., 2014; Haider et al., 2000; Jia et al., 2009; Kobayashi et al., 1999; Mears et al., 2001; reviewed in Swaroop et al., 2010). Indeed S opsin is the ancestral vertebrate visual pigment (Lamb, 2013; Larhammar et al., 2009). Recent evidence suggests that the transcription factor Onecut1 participates in the binary fate choice between rod and cone precursors by inducing the expression of the early cone marker thyroid hormone receptor β2 (Trβ2). Activity of this factor in the chicken retina is also required to represses a homolog of Nrl, L-Maf. Consistently, forced expression in the mouse results in increased numbers of immature cone precursors and a decrease in rod precursors (Emerson et al., 2013). Transcription factor Sall3 of the Spalt family was found to activate expression of multiple cone genes and particularly play a role in the induction of S, but not M, opsin expression (de Melo et al., 2011). Development of S cones was also found to depend on the expression of DNA methyltransferase 1 (Dnmt1) (Nasonkin et al., 2013). When it comes to M opsin expression thyroid hormone signalling through Trβ2 nuclear receptor is crucial for its induction (Lu et al., 2009; Roberts et al., 2006; discussed further below). Taken together, these data suggest that whilst S opsin is the default visual pigment in mammals the number of mature cone cells is determined by the activity of positive regulators as well as the repressive activity of the rod differentiation pathway inducers.

I.III.II.VI. Determination of cone opsin expression patterns

Whilst there is one type of rod photoreceptors expressing a single photopigment *Rhodopsin*, there are usually at least two types of cone cells in any vertebrate species, that express different types of cone opsins (Lamb, 2013; Larhammar et al., 2009). Therefore an issue related to cone specification is the generation of an appropriate

number and spatial distribution of cones expressing different opsins (Swaroop et al., 2010). The detailed mechanisms guiding opsin patterning in mice have not yet been elucidated, however, intrinsic transcriptional regulators activity combined with external stimuli and spatial location in the tissue was found to be key in this process (Swaroop et al., 2010). Animal studies have identified that two nuclear receptors, that bind external ligands to regulate transcription, are involved in establishing the cone opsin gradient in mice. In a mature mouse retina S opsin exhibits ventral high to dorsal low expression gradient, whilst the opposite is seen for M opsin (Applebury et al., 2000). Thyroid hormone receptor β2 (Trβ2) is crucial for induction of M opsin expression, which is abolished in *Thrb2*$^{-/-}$ mice (Ng et al., 2001). The thyroid hormone triiodothyronine (T3) is the physiological high-affinity ligand for Trβ2 (Ng et al., 2001). Levels of T3 show a rise in the early postnatal retina between P4 and P10 forming a dorsal high-ventral low gradient correlating with the induction of M opsin expression (Roberts et al., 2006). Effects of the rise in T3 on M opsin induction are not observed in a mouse model with a knockin mutation disrupting Trβ2 DNA binding without affecting the ligand recognition domain (Shibusawa et al., 2003) supporting the notion that uniformly distributed Trβ2 receptor determines the gradient of M opsin expression by detecting T3 gradient set across the retina at early postnatal stages. Setting the S opsin gradient on the other hand requires cooperative action of Trβ2 with another nuclear receptor Retinoid-related X receptor γ (RXRγ). In *Thrb2*$^{-/-}$ animals M opsin expression is lost and all cones across the retina express S opsin. Thyroid hormone receptors often act as heterodimers with RXR family nuclear receptors and RXRγ expression was found restricted to cone photoreceptors (and ganglion cells). Similarly to *Thrb2*$^{-/-}$ mice, in *Rxrg*$^{-/-}$ animals all cones throughout the retina express S opsin, however in contrast to the *Thrb2*$^{-/-}$ model, normal M opsin gradient is observed (Roberts et al., 2005). This suggests that homodimers of Trβ2 mediate induction of M opsin in developing cones, whereas heterodimers with RXRγ mediate suppression of S opsin expression.

In addition, bone morphogenetic protein (BMP) and retinoic acid (RA) signalling were also found to be important for establishment of opsin gradients in the mouse. BMP signalling plays a role in establishing the dorso-ventral axis in the developing optic cup and is temporarily active in the dorsal retina at around E11 in mice (Satoh et al., 2009). BMP signalling exerts its effects on opsin patterning through chicken ovalbumin upstream promoter-transcription factors (COUP-TFs) I and II. These transcriptional regulators exhibit dorso-ventral gradients in distribution with COUP-TF I more prominent in the ventral retina whilst COUP-TF II highly expressed in the dorsal part

(Satoh et al., 2009). Expression of both COUP-TFI and COUP-TFII is required for suppression of S-opsin expression in the dorsal part of the retina, but COUP-TFI alone plays a role in suppressing M-opsin expression in the ventral retina (Satoh et al., 2009). Retinoic acid, an important morphogen in development of many tissues, was also implicated in setting the spatial distribution of cone opsins. Transcription factor Vax2 was found to regulate spatial aspects of retinoic acid signalling in the developing retina. Genetic removal of *Vax2* leads to expansion of the retinoic acid free zone into the ventral part of the retina. This correlates with the loss of S opsin expression and ectopic upregulation of M opsin in the ventral retina leading to near loss of M opsin gradient with M opsin expression close to uniform across the retina (Alfano et al., 2011). In summary, proper spatial distribution of cone opsins in mice was found to be dependent on the cooperation of intrinsic transcriptional regulators with gradients of soluble signalling molecules such as thyroid hormone, BMP and retinoic acid.

I.III.III. Models of cell lineage specification in the retina.

The retina is a convenient model to investigate cell lineage being an accessible part of the central nervous system with orderly arranged neuronal and glia types exhibiting characteristic positions and morphologies, facilitating tracing and progeny identification. The wealth of observations initiated by classical studies from late 1970s and the 1980s (Carter-Dawson & LaVail, 1979; Turner & Cepko, 1987) forms the basis and starting point for three interpretations of how to model the differentiation of retinal cell types currently put forward in this field of research (Diagram I.VIII.).

I.III.III.I. Transcriptional dominance model of photoreceptor differentiation

Advances in identification of the molecular regulators controlling commitment to the photoreceptor fate as well as mechanism of specification into photoreceptor types led A. Swaroop, D. Kim and D. Forrest to propose the ‘transcriptional dominance’ hypothesis to explain the process of photoreceptor differentiation (Swaroop et al., 2010). Three major points summarise this model: (1) following initial inductive cues photoreceptors differentiate from a common, generic, early post-mitotic precursor type with a potential to give rise both to cone subtypes as well as a rod; (2) in the absence of specific determinants this generic precursor develops into a blue opsin-expressing cone; (3) differentiation into a particular type of photoreceptor is dependent on abundance and/or activity at any developmental time of a set of transcription factors with different and often opposing effects on acquisition of a specific fate. This model predicts two ‘crossroads’ or ‘transcriptional control boxes’ with binary choice options

and outcome dependent on the activity of fate determinants, first divergence into cone versus rod precursors and then decision to express a particular opsin type for cone precursors. Another prediction is that once appropriate numbers of cone precursors are made the differentiation cues will shift to promote solely rod precursor generation.

The gene regulatory network for photoreceptor specification would present as follows, Otx2 biases progenitors to generate photoreceptors with Blimp1 and RORβ acting to differentiate between the rod photoreceptor and bipolar fate in late Otx2-expressing cells (Wang et al., 2014). Cooperative action of RORβ and Crx leads to initial induction of S opsin (Hennig et al., 2008). RORβ is also an inducer of Nrl expression, which drives differentiation towards rod lineage (Fu et al., 2014). Commitment to this fate is strengthened and stabilized by Nrl-driven expression of RORβ2 isoform (Fu et al., 2014) and activation of Nr2e3, which acts to suppress cone gene expression (Corbo and Cepko, 2005). Unless a 'decisive threshold' of Nrl activity is achieved, the photoreceptor precursor will develop along a default pathway into an S cone (through action of RORβ and Crx). In mouse cone precursors Trβ2 and RXRγ are responsible for cone opsin patterning, by induction of M opsin and suppression of S opsin, respectively (Ng et al., 2001; Roberts et al., 2005). At different stages of differentiation the aforementioned factors compete for dominance in a 'tug of war'-like fashion, the outcome depending of their relative levels and/or activity.

This hypothesis is supported by several lines of evidence, firstly, analysis of molecular evolution of opsins suggests that S opsin is the first photoreceptor pigment to have evolved and species of lampreys, an ancient lineage of vertebrates, were found with photoreceptors morphologically resembling cones but functionally similar to rods, suggesting an ancestral cone-like photoreceptor (Lamb, 2013). Moreover, during embryonic development in many species, which can resemble phylogeny, S opsin is the first photopigment to be expressed (from around E18 in mice) and in a human foetus at 19 weeks of gestation S cones cover 90% of the retina, despite being a minor population in the mature retina. Furthermore S opsin expression expands following deletion of several transcriptional regulators of photoreceptor differentiation: *Trβ2*$^{-/-}$ mice, where M opsin expression is lost, and Nrl and Nr2e3 knockouts, in which all prospective rods express S opsin instead of rhodopsin. In addition in isolated Nrl-expressing early rod S opsin transcripts could be detected as well as infrequent cells staining for both cone and rod markers can be detected in the developing retina (reviewed in Swaroop et al., 2010). However, several aspects of this model can raise criticism. If S cone fate is the default developmental programme for cones, then photoreceptors in animals lacking Nrl should be identical to wild-type S cones.

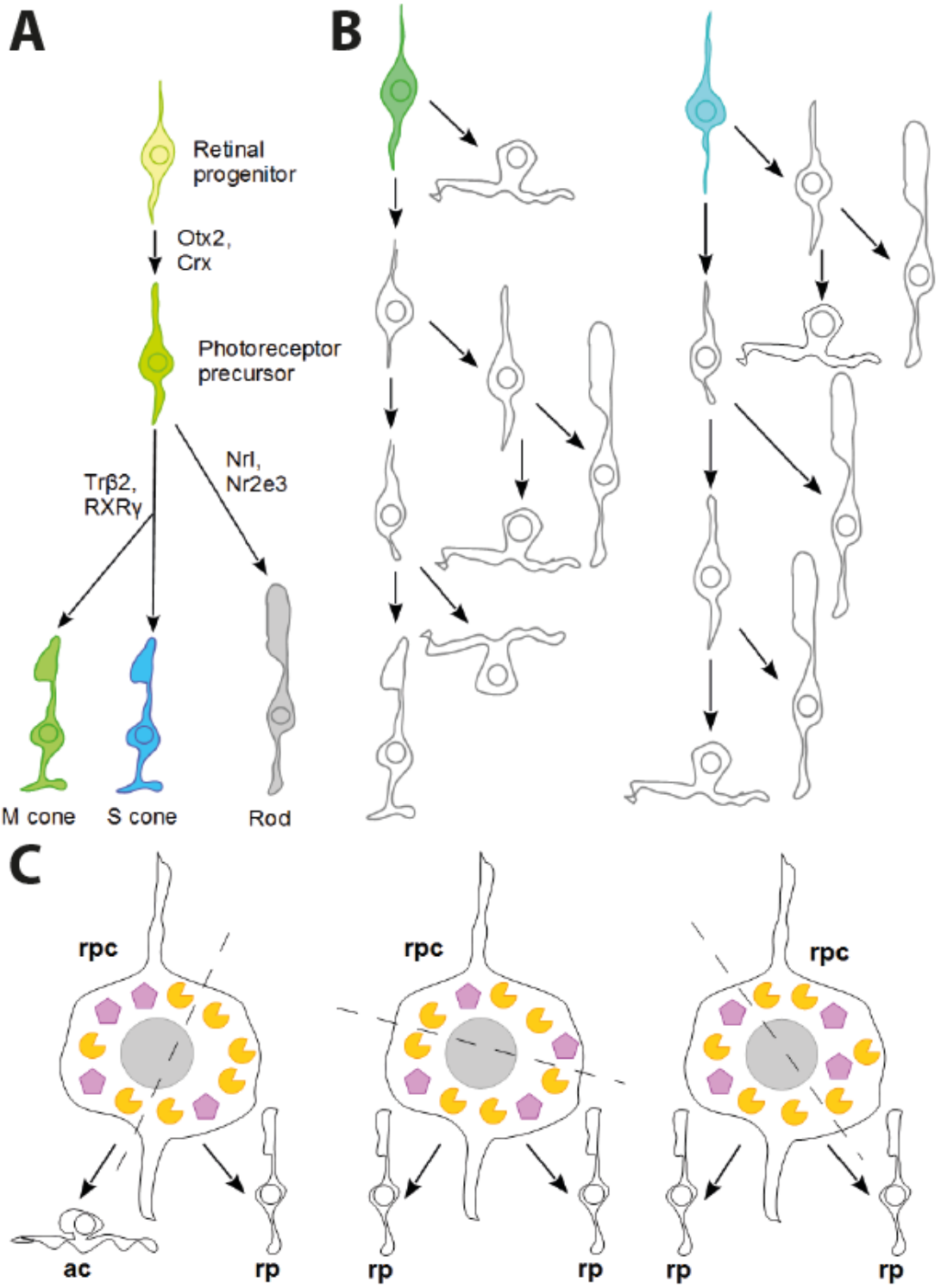

Diagram I.VIII. Models of lineage commitment in the retina.

Most models of retinal differentiation recognize a strong intrinsic programme of retinal development. In model (**A**) photoreceptor specification occurs in a stepwise manner. Poorly understood factors including reduction in Notch signalling trigger progenitor commitment to photoreceptor lineage. This is initially driven by the transcription factor Otx2 and then Crx. A generic photoreceptor precursor follows a defaults S cone differentiation pathway unless otherwise induced. Nrl drives commitment to the rod

fate, whereas in the cone precursors Trβ2 mediates formation of M cones. Another model (**B**) recognises gene expression heterogeneity amongst retinal progenitor cells. It postulates that retinal progenitors express different sets of transcriptional regulators that bias them to generate varied lineages. Stochastic mechanisms can also play a role in cell fate specification in the retina (**C**). Shown here is a progenitor that expresses determinants for rod (orange) or amacrine cell (magenta) fates. Depending on the plane of cell division (in dashed lines), different sets of resulting progeny are formed.

Photoreceptors in *Nrl*$^{-/-}$ mice exhibit shorter outer segments though, raising the possibility that they are a more primitive cell type (Mears et al., 2001). Alternatively, this could arise from disruption of retinal architecture in those mice. Inactivation of Nrl in single cells in the developing retina could distinguish between these two possibilities, but has not been performed to date. Additionally, numbers of typical cones are increased following genetic ablation of single isoforms of RORβ and Nr2e3, suggesting existence of factors promoting this fate in the absence of rod-determining regulators (Corbo and Cepko, 2005; Fu et al., 2014). Lastly, it has been found that deletion of the Spalt family transcription factor Sall3 or DNA methyltransferase 1 (DNMT1) affect only S cone differentiation (de Melo et al., 2011), undermining the notion of S cone differentiation being a default pathway not requiring specific regulators.

I.III.III.II. Intrinsically different progenitors generate specific types of progeny

Classical lineage studies conducted in the retina discovered two characteristics of retinal progenitors: multipotency on a population level, meaning the ability to give rise to all retinal cell types, together with high variability in the size and composition of progeny clones derived from individual RPCs, suggesting diversity in the progenitor population. These studies, however, could not determine whether the diversity of the clones arises from intrinsic differences in the progenitor population or extrinsic factors acting on progenitors or their progeny. Therefore, one could propose two extreme models for cell fate acquisition in the retina, on one hand, uniform intrinsic genetic programme operating in all RPCs to generate all retinal cell types, on the other hand, the environmental cues solely specifying the progeny. Studies in which progenitors were isolated from their environment at a particular stage and then cultured or transplanted into retina at a different developmental stage demonstrated that retinal progenitors at any particular time during development have intrinsically determined ability to only produce the cell types appropriate for the timepoint at which they were removed from the developing retina. This observation argues against the environment being a major determinant of cell identity in the retina. For this reason, any comprehensive model of retinal cell fate specification needs to incorporate an intrinsic genetic programme unfolding over time. Two alternative scenarios are possible in this case, in the first, all progenitors undergo invariant transition through temporary competence states and clone size variation comes from terminal differentiation triggered only in a subset of cells at each given competency state, the other possibility is that progenitors diversify in their gene expression profiles creating cells with increased propensity to produce specific lineages (Cepko, 2014).

Work from her own as well as other groups led C. Cepko to propose that heterogeneity in the expression of molecular determinants of cell fate underlies generation of subsets of RPCs strongly biased to produce very specific progeny. Several lines of evidence appear to support this conclusion. Firstly, advent of methods to globally assess gene expression (also in single cells), enabled examination of temporal patterns of gene expression in the developing retina. Despite the use of multiple approaches, little was found in terms of consistent trends in temporal changes in gene expression in RPCs, suggesting that diversity in those profiles (Trimarchi et al., 2008) either simply stems from biological noise or is a real phenomenon important in the context of retinal development. Moreover, evidence of molecular markers of terminally dividing RPCs has accumulated.

Use of *Cre recombinase driven by a gene specific promoter* enables marking cells with a history of expression of the gene of interest. Such strategy was used to study expression history of two bHLH genes achaete-scute complex homologue 1 (*Ascl1*) and neurogenin 2 (*Ngn2*). In both cases labelling was observed in small clusters or single cells indicating that their expression must have been initiated either in a terminally dividing RPC or postmitotically. Additionally, *Ascl1*-derived clones were depleted in retinal ganglion cells (Brzezinski et al., 2011).

Early retinal lineage studies used gamma retroviruses that could infect any dividing cell. Utilizing mouse genetic technology it is possible to express an *avian retrovirus receptor TVA under the control of a promoter of a specific gene* allowing for infection only dividing cells expressing that gene and subsequent tracing of their progeny also removing the ambiguity of pre-terminal division versus postmitotic expression inherent in Cre fate mapping. This strategy allowed examination of progeny derived from RPCs expressing the bHLH transcription factor Olig2, by infection with avian gamma-retrovirus of knock-in transgenic mice in which *Olig2* promoter drives TVA expression. Infection performed at early stages of development (E13.5-14.5) yielded very small clones of one or two cells indicating that Olig2 is expressed mainly in terminally dividing RPCs. In stark contrast infection with a control virus infecting all RPCs at this stage resulted in large clones averaging 30 cells. Clones obtained from Olig2 expressing RPCs were composed solely of cones and horizontal cells, which are some of the rarest cell types in the mature retina demonstrating a heavy bias in progeny types in this lineage. When infection was performed at neonatal stages clones again showed a skew in the type of progeny, being only composed of rods and amacrine cells and lacking bipolar and Müller cells, which are also generated at these timepoints (Hafler et al., 2012).

Advances in *live imaging techniques in zebrafish* allowed long-term imaging cells expressing fluorescent reporters during retinogenesis. Such a reporter based on cone rod homeobox (*crx*) shows expression in RPCs, cones rods and bipolar cells in the fish. Progenitors that expressed this reporter during terminal divisions made homotypic pairs of cones expressing the same type of cone opsin. Similarly, RPCs expressing a reporter based on zebrafish thyroid hormone receptor beta (*thrb*), a marker of L cones in this species, mostly divided terminally and symmetrically to produce pairs of L opsin expressing cones (Suzuki et al., 2013).

Infection of early chick RPCs with retrovirus yields large dense clones, which are difficult to analyse with respect to cell type composition. However, horizontal cells were found to be separated enabling quantification. Chick retina possesses three types of horizontal cells, H1, H2 and H3 cells that differ in morphological features and connectivity. Surprisingly, it has been observed that clones with just two horizontal cells always contained homotypic pairs of either H1 or H3 cells, but not H2 cells. H2 cells were enriched in clones containing just a single horizontal cell. It is therefore proposed that H1 and H3 are generated in a terminal division of dedicated progenitor, whilst H2 cells likely are siblings with cone cells (see below). A reporter based on a conserved region in the THRB locus was also studied in the chick. As in zebrafish, this reporter was found to be expressed not only in developing cones but also in a subset of RPCs and early in horizontal cells. Retroviral lineage analysis of RPCs in which this genetic element was active showed that their progeny were cones and horizontal cells, again highlighting existence of progenitors expressing a marker of bias in the cell types that they generate (Rompani and Cepko, 2008).

Altogether, these observations demonstrate that whilst retinal progenitors produce clones varying widely in size and exhibit a high degree of heterogeneity in their gene expression patterns, markers of predictable biases towards generation of very specific post-mitotic progeny types can be identified. Furthermore, this suggests that a part of the intrinsic genetic programme of retinal development could be generation of a pool of heterogeneous progenitors, amongst which there will be cells with very specific competences that together on a population level act to create the appropriate cellular diversity of the mature retina.

I.III.III.III. Stochastic model of fate choices in the retina

Given the apparent multipotency of retinal progenitors combined with a highly variable size and composition of generated clones a study from M. Cayouette's laboratory (Gomes et al., 2011) examined if this behaviour could be explained as a stochastic process. In order to investigate this aspect of retinal development, rat retinal

progenitors isolated at E20 and plated *in vitro* at clonal density were used as a model system. Single progenitors were imaged long-term using videomicroscopy and their divisions recorded. Lineage trees were subsequently reconstructed using imaging data combined with immunostaining to determine the final composition of the obtained clones. Several important observations regarding progenitor behaviour were made. Firstly, progenitors seemed to stochastically choose between different modes of division i.e. self-renewing, terminal or asymmetrical generating a progenitor and a differentiating cell. This choice occurs with fixed probability and does not depend on lineage history. Additionally, at the examined developmental stage this ratio did not appear to change over time. It is worth noting, however, that at early stages *in vivo* progenitors only self-renew before starting to produce differentiating ganglion cells from around E13, therefore a relatively fixed ratio may only apply to certain stages of retinogenesis. Secondly, cell cycle times vary considerably with a normal distribution on the population level. Duration of consecutive cycles is uncorrelated. Furthermore, cell cycle time is not predictive of the mode of division or the type of progeny made. Lastly, the birth order of amacrine, rod photoreceptor, bipolar and Müller cells, which are the cell types generated at this stage, within single clones does not strictly reflect the population-wide birth order. Probability of generating a particular cell type was found simply to reflect its abundance in the mature retina. The authors found that, taken together, these observed features of progenitor behaviour is strikingly consistent with a simple stochastic mathematical model in which different modes of division are assigned set probabilities, cell cycles times show log normal distribution around the population mean and cell types are made with probabilities reflecting their abundance in the mature retina. This work implies that the intrinsic genetic programme (soluble factors are unlikely to contribute given isolation of cells at clonal density) mostly defines probabilities of various outcomes with only few seemingly stereotypical lineages found. Cell fate choices are hypothesised to occur just before mitosis for example in the G2 phase of the cycle, since no evidence of correlation between behaviour of cells in consecutive generations in the lineage was observed. The apparent stochasticity can derive from a combination of action of a complex regulatory machinery with heterogeneity in expression profiles related to proliferation and differentiation.

I.III.IV. Retinoic acid signalling and photoreceptor development

I.III.IV.I. Retinoic acid and its mechanism of action

Vitamin A (retinol) has been long known to play a key role in vision. Retinaldehyde, the aldehyde form of vitamin A serves as the chromophore for the visual pigments and is critical for the visual cycle. Early studies examining the deficiency of vitamin A during embryogenesis reported ocular malformations as a typical outcome (McLaren, 1999; Sommer and Vyas, 2012; Warkany and Schraffenberger, 1946). Since phototransduction does not commence until much later it was hypothesised that another metabolite of retinol is involved and subsequent research identified retinoic acid as the primary vitamin A derivative regulating embryonic eye morphogenesis (reviewed in Hyatt and Dowling, 1997).

Retinoic acid is a key morphogen involved in development of anterior-posterior axis of the embryo, outgrowth and patterning of the limb bud and formation and maintenance of skin amongst its many roles (Das et al., 2014; Hyatt and Dowling, 1997). Effects of retinoic acid are mediated by diffusion through plasma membranes and binding to soluble cytoplasmic receptors. These are members of the nuclear receptor superfamily that comprises also steroid hormone, thyroid hormone and vitamin D3 receptors. Nuclear receptors are modular in structure, being composed of several parts with the key ligand-binding domain and the double zinc finger DNA-binding domain. This structure allows coupling hormonal signals directly to induction of transcription of a set of specific genes (Huang et al., 2014; Hyatt and Dowling, 1997). There are several physiologically active forms of retinoic acid that can act as natural ligands for retinoic acid receptors including all-*trans* retinoic acid, all-*trans* 3,4 didehydro retinoic acid, 9-*cis* retinoic acid and 4-oxo retinoic acid. Specific effects of these ligand variants appear to be context dependent. With respect to retinoic acid receptors, two families have been identified. Retinoic acid receptors (RARs) and Retinoid X receptors (RXRs) each come in three isotypes α, β and γ, adding to the control of the diverse biological effects of retinoic acid (Das et al., 2014; Huang et al., 2014; Hyatt and Dowling, 1997). RARs are activated by a range of ligands encompassing all-*trans*, 9-*cis*, 3,4 didehydro and 4-oxo retinoic acid. In contrast, RXRs are only sensitive exclusively to 9-cis retinoic acid. Retinoic acid receptors heterodimerize and bind to specific DNA sequences called Retinoic acid-response elements (RAREs) as RAR/RXR dimers. These

heterodimers were shown to interact with an array of co-activators and co-repressors (Huang et al., 2014).

I.III.IV.II. Expression of retinoic acid signalling components in the developing eye

The all-*trans* form of retinoic acid is biosynthesised from retinol (vitamin A) via retinaldehyde in an irreversible reaction (Hyatt and Dowling, 1997). In mammals three enzymes with aldehyde dehydrogenase activity on retinaldehyde as substrate have been identified, which show dynamic expression patterns and distinct localization in the developing eye (McCaffrery et al., 1993; Mic et al., 2000). RALDH1 (ALDH1A1) enzyme is first observed at E9.5 in the dorsal optic vesicle and remains restricted to dorsal retina throughout life (McCaffrery et al., 1993; Mic et al., 2000). Highest expression of RALDH1 is found in the developing retina with levels significantly dropping postnatally (McCaffrery et al., 1993). RALDH2 (ALDH1A2) enzyme shows a brief burst of expression in the ventral optic pit/ vesicle between E8.5 and E9.5, later being expressed in the RPE cells within the eye (Hyatt and Dowling, 1997; Mic et al., 2000). Finally, the third enzyme, RALDH3 (ALDH1A3) is initially detected in the ventral optic eminence from E8.75, then in the ventral optic vesicle/ cup between E9.5 and E11.5 (Mic et al., 2000). Expression levels of this enzyme decline with development and activity measurements reach noise levels in adult retina (McCaffrery et al., 1993). Retinoic acid in the eye is primarily degraded via the activity of monooxygenase Cytochrome P450 26A1 (Cyp26a1) (Abu-Abed et al., 2002; Alfano et al., 2011; Sakai et al., 2004). This metabolising enzyme shows early onset of expression around E8.5-E9 in the dorsal optic vesicle, followed by high expression in the embryonic retina and subsequent gradual decrease and loss of expression soon after birth (McCaffery et al., 1999; Sakai et al., 2004), exhibiting a similar expression pattern to the synthesising enzymes that decrease in expression or are absent postnatally.

Effects of retinoic acid on target cells are mediated by its receptors. Members of both RAR and RXR families were found to show dynamic expression patterns in development of ocular tissues (Mori et al., 2001). RARα is ubiquitously expressed in the embryonic eye before becoming localized to a subset of interneurons and ganglion cells in the neural retina and the ciliary body postnatally. RARβ, RARγ and RXRα are preferentially localized to periocular mesenchyme throughout development. RXRβ shows ubiquitous expression at all stages. In contrast, RXRγ exhibits a very specific expression pattern. It is found in early post-mitotic developing cone precursors and remains expressed in this cell type throughout adulthood. Additionally, retinal ganglion cells postnatally also express RXRγ (Mori et al., 2001; Roberts et al., 2005). These

stage-specific expression patterns of retinoic acid metabolising enzymes and its receptors during eye development are suggestive of specific roles of retinoic acid in the morphogenesis of this organ.

I.III.IV.III. Retinoic acid and eye morphogenesis

Consistent with the requirement for dietary vitamin A during embryonic development (Warkany and Schraffenberger, 1946), biochemical assays showed high levels of retinoic acid at early stages of retinogenesis decreasing with age. Retinal tissue harvested around E15 is very abundant in retinoic acid, containing 500 nM total retinoic acid, of which 310 nM is all-*trans* retinoic acid. In young adult retina levels are considerably lower with only 140 nM total retinoic acid (90 nM all-*trans* isoform) (McCaffrery et al., 1993). With the progression of retinal morphogenesis expression of enzymes responsible for retinoic acid synthesis dynamically changes (as described in the previous section). At the optic vesicle stage around E9 both RALDH2 and RALDH3 are expressed, whereas from E9.5 RALDH2 is no longer expressed in the optic vesicle and is replaced by RALDH1 (Mic et al., 2000). These two enzymes take up opposite localizations in the developing neural retina with RALDH1 on the dorsal side, whilst RALH3 is confined to the ventral part (McCaffery et al., 1999, 1999; Mic et al., 2000). Ventral enzyme, RALDH3, is much more active generating around 70% of total retinoic acid and producing a dorsal low to ventral high gradient of retinoic acid in the embryonic retina (McCaffrery et al., 1993). Expression of both drops with retinogenesis progression with a sharper decline in the ventral RALDH3 enzyme, activity of which drops below RALDH1 between P4 and P8 (McCaffrery et al., 1993). In summary, retinoic acid levels are very high at the onset of retina morphogenesis, but decline as development proceeds.

Effects of perturbation of retinoic signalling were also examined. Zebrafish embryos were exposed to an excess of retinoic acid at the optic primordia formation stage. This resulted in hyperproliferation of cells in the ventral part of the eye field leading subsequently to formation of a second ventral retina that then separates from the dorsal counterpart (Hyatt et al., 1992). In those duplicated retinae cellular differentiation in the dorsal retina precedes that in the additional ventral organ (Hyatt et al., 1992), suggesting that high levels of retinoic acid promote early ventral retina characteristics. In contrast pharmacological inhibition of the ventral retinal retinoic acid synthesising enzyme using citral resulted in formation of half-eyes lacking ventral retina (Marsh-Armstrong et al., 1994), supporting the notion that retinoic acid is required for ventral retina development. In further support, genetic ablation of RXRα leads to ventral retinal malformations. Heterodimers of RXRα with RARγ are largely

mediating the effects of retinoic acid on morphogenesis of this part of the retina, since inactivation of a single allele of RXRα in an RARγ knockout background phenocopies RXRα deletion effects and the resulting phenotype becomes even more severe when both receptors are deleted (Kastner et al., 1994). Together, these observations demonstrate that retinoic acid signalling regulates morphogenesis of the retina, with the ventral part being particularly dependent on this pathway.

I.III.IV.IV. Retinoic acid and photoreceptor differentiation

Retinoic acid remains generated throughout the period of retinal histogenesis with enzymes responsible for its synthesis and degradation expressed at least until early postnatal development (Hyatt and Dowling, 1997; McCaffery et al., 1999; McCaffrery et al., 1993; Sakai et al., 2004), suggestive of a role also at those later stages. Indeed, perturbation of retinoic acid signalling at the time of photoreceptor maturation revealed its involvement in this process. Application of exogenous all-*trans* retinoic acid to developing zebrafish during the initial stages of photoreceptor development resulted in precocious rod differentiation with increased levels of rhodopsin visual pigment transcripts and better developed rod morphology with longer rod outer segments, particularly in the ventral half of the retina. In contrast the effect of retinoic acid on cone cells was to inhibit their differentiation. Treatment with retinoic acid led to the disappearance of a ventral cone-dominated region adjacent to the optic nerve. Instead of typically prominent cones only miniature cones resembling immature cells at the far retinal periphery were observed at this site following retinoic acid treatment. Expression of both UV and blue cone opsins were diminished in the treated animals. Blocking retinoic acid synthesis at the same stage using citral, a pharmacological inhibitor of the ventral synthesising enzyme, led to a dose-dependent decrease in rhodopsin expression. Neither cone opsins expression nor other cell types were affected by this treatment, indicating some specificity for regulation of rod development (Hyatt et al., 1996). Further research showed altered photoreceptor mosaics in zebrafish treated with exogenous retinoic acid and provided evidence suggesting that the RARαb receptor is partially mediating these effects (Stevens et al., 2011). In accordance with these findings, application of exogenous retinoic acid to cultures established from dissociated embryonic and neonatal rat retinal cells showed a significant induction of rod photoreceptor markers (Kelley et al., 1994; Wallace and Jensen, 1999). There were some discrepancies between these two studies as to whether these increases should be ascribed to biasing progenitors to produce rods or enhancement of marker expression in post-mitotic cells, however the evidence is most consistent with the latter hypothesis. Wallace and Jensen demonstrated that the time

lag between final mitosis and expression of rhodopsin in post-mitotic rod precursors was shortened in retinoic acid-treated samples (Wallace and Jensen, 1999). Induction of rod markers was more pronounced by treatment with 9-*cis* rather than all-*trans* retinoic acid isoform, suggesting that this effect might be mediated by RXR family receptor/s, for which 9-*cis* retinoic acid is the higher affinity ligand (Kelley et al., 1994). Subsequently, retinoic acid has also been found to facilitate rod precursor differentiation from both mouse and primate pluripotent stem cells (Eiraku et al., 2011; Gonzalez-Cordero et al., 2013; Osakada et al., 2008; Zhong et al., 2014). In addition to murine rod precursors, effects of retinoic acid on mouse cone opsin patterning were identified. Dorso-ventral patterning of the retina is regulated by the eye-specific Vax2 homeobox transcription factor. Vax2 exerts its function in part by regulating the expression of retinoic acid-metabolising enzymes Cyp26a1, Cyp26c1 and Raldh3. Loss of Vax2 expression leads to upregulation in retinoic acid-catabolising enzymes Cyp26a1 and Cyp26c1 and downregulation of retinoic acid-synthesising enzyme Raldh3, resulting in ventral expansion of a retinoic acid free zone in the developing retina. Altered retinoic acid levels were associated with loss of S opsin expression and expansion of M opsin into the ventral retina, disrupting its dorsal-high to ventral-low gradient. Opsin gradients were rescued in Vax2 knockouts by *in utero* injections of retinoic acid supplementing the developing eye with this molecule (Alfano et al., 2011). In conclusion, retinoic acid signalling is not only important for early eye development, but also for photoreceptor maturation regulating expression of rod and cone markers and cone opsins patterning across the dorso-ventral axis of the mouse retina.

I.IV. Cell therapy in the retina

I.IV.I. Background

The most common cause of untreatable blindness in developed countries is the loss of light-sensitive photoreceptor cells due to retinal degeneration (Cruess et al., 2008; Owen et al., 2012; Rudnicka et al., 2015). Approximately 1 in 3000 of the population in the UK is affected by inherited retinal dystrophies and around 1 in 10 over the age of 60 is affected by Age-related Macular Degeneration with incidence rising with an ageing population (Owen et al., 2012). Diseases of different etiologies ultimately converge on photoreceptor cell death as the common manifestation (Roosing et al., 2014). Since the few current treatments only limit the progression of the disease there

is a clear need for interventions that would also aim at restoring lost visual function. Given that the loss of vision is a result of the loss of photoreceptor cells, replacement of photoreceptor cells appears a logical treatment strategy (Song and Bharti, 2015). Several features of photoreceptors make them amenable to this approach. Firstly, photoreceptors are afferent neurons that receive no incoming connections, second they are only required to extend a short axon and make a single synaptic connection to reach retinal interneurons in order to contribute to vision. Moreover, the eye in general and in particular the subretinal space, next to which the photoreceptors reside, are accessible by standard surgical procedures facilitating delivery of fresh cells. This accessibility and relative simplicity of organization have also made the retina a model of choice to study neural development and disease. The wealth of knowledge garnered through these studies has allowed the identification of appropriate populations in donor mice for successful transplantation, as well as recreating the developmental niche to obtain equivalent populations from renewable sources (Jayakody et al., 2015). It is these recent developments that make cell therapy in the retina such a promising strategy (Song and Bharti, 2015) and they will be discussed in more detail below.

I.IV.II. Cell replacement strategies

Photoreceptor cells are post-mitotic neurons that in most mammals once lost cannot be replaced to any significant extent by division of tissue residing stem cells. Therefore, several approaches to replace the lost cells have been investigated (reviewed in Jayakody et al., 2015):

1. *Endogenous repair*. This strategy aims to re-activate the developmental mechanisms operating in lower vertebrates that allow them to regenerate the injured or destroyed retina. Pharmacological agents or delivery of transgenes would be used to trigger these repair mechanisms.
2. *Retinal sheets transplantation*. Full or partial-thickness retina is transplanted in an approach similar to whole organ transplants.
3. *Cell suspension transplantation.* This approach uses dissociated and often purified cells that are injected into the eye in the form of a cell suspension.

The first two strategies achieved only limited success and will be only briefly discussed, whilst more attention will be devoted to describing the more promising cell suspension transplantation.

I.IV.II.I. Endogenous repair

Retinogenesis in the mammalian retina is confined to young animals and new retinal neurons cease to be added in adults. In contrast, in fish and amphibians the retina expands continuously through adulthood due to the presence of an active stem cell niche in the peripheral retina generating additional cells as the animal grows (Amato et al., 2004). Furthermore, lower vertebrates possess the capability to regenerate injured retina via multiple populations located in various parts of the eye that can act as stem cells when activated by specific stimuli (Reh and Pittack, 1995). The ciliary margin zone in fish and amphibians is a site of active neurogenesis and can respond to ablation of specific cell types by production of these particular cells. However, whilst retinogenesis continues throughout life, the regeneration capacity of this niche declines with age (Amato et al., 2004). Similarly, the peripheral edge of the retina was found to be a site of cell division and growth in the postnatal chick, mouse and during human retinal development, but in contrast to lower vertebrates it becomes quiescent in adolescence, with proliferation lost in the rat by P14 (Engelhardt et al., 2004). This quiescent niche can be activated by exposure to growth factors and mitogens such as insulin, bFGF and EGF (Bhatia et al., 2009; Zhao et al., 2005). Proliferation markers also appear to be increased in this area in response to retinal degeneration (Jian et al., 2009). Cells with stem cell properties were also identified in the adjacent structure in higher vertebrates, the ciliary body. These have very similar properties to the ciliary margin stem cells, but in both cases, while giving rise to cells expressing early markers of commitment to retinal neuronal lineage, little expression of more mature markers was found and these cells were restricted to the periphery of the eye (Nickerson et al., 2007). Retinal pigmented epithelium (RPE) that performs many functions supporting vision is derived from same neuroepithelial progenitors as the neural retina and as development is completed it becomes post-mitotic. In amphibians retinal regeneration is predominantly mediated by transdifferentiation of RPE into proliferating retinal progenitors that repopulate the lost neural retina (reviewed in Barbosa-Sabanero et al., 2012). Analogously, the embryonic rat RPE cells possess a limited ability to transdifferentiate and regenerate the neural retina, which is lost once the mature pigmented phenotype is acquired (Zhao et al., 2001). The principal support cell type in the neural retina the Müller glia were also found to exhibit some regenerative potential. In contrast to retinal neurons, Müller cells, due to particular features of their metabolism, are very resistant to stresses such as ischemia, anoxia and hypoglycemia, facilitating their survival in injury or degeneration (Silver et al., 1997; Stone, 1999). This characteristic makes Müller cells an attractive target for regenerative strategies. Fish Müller cells divide following injury and express many progenitor markers such as *pax6*,

rx1, *six3*, *vsx2* and *crx*, subsequently generating photoreceptor precursors that migrate into the outer nuclear layer (Bernardos et al., 2007). A seminal study from Dyer and Cepko showed that mammalian Müller cells can also be induced to proliferate by neurotoxic damage (Dyer and Cepko, 2000). Further studies demonstrated that these newly generated cells express the progenitor marker Nestin prior to onset of Protein Kinase C, Neuron-specific Enolase, Recoverin and Rhodopsin expression, which are markers of bipolar neurons and photoreceptors (Ooto et al., 2004). Pharmacological activation of Müller glia division *in vivo* resulted in generation of rare Glutamine Synthetase and Opsin-positive cells that were sufficient to drive visually-induced head-tracking responses in a rat model lacking photoreceptor function (Del Debbio et al., 2010). However, the absolute numbers of cells generated through the mitotic activity of Müller glia is low and it is speculated that these cells might only undergo a single round of division (Ooto et al., 2004). Research in recent years has identified several populations within the mammalian eye that can act as stem cells to mediate retinal regeneration following injury or in degeneration. Although signals and molecular pathways that regulate this process have begun to be elucidated and significant progress has been made in harnessing this regenerative potential, the extent of the repair appears very limited and the ability of newly generated cells to drive significant levels of visual function dubious.

I.IV.II.II. Retinal sheet transplantation

Severe retinal degenerations can lead to nearly complete loss of photoreceptor cells. In such cases, where the outer nuclear layer is virtually absent, transplantation of a whole photoreceptor layer has the potential to treat a large area of the retina by cell replacement. Several groups working in this area demonstrated graft survival, further differentiation *in vivo*, limited connectivity to the endogenous retinal circuitry and some improvements in basic visual responses such as light-dark discrimination (reviewed in Reh, 2016) Moreover, patients that received fetal retinal sheet transplants reported subjective improvements in vision (Seiler and Aramant, 2012). It remains unclear however, whether these are due to the functionality of transplanted cells or trophic support to the host photoreceptors (Reh, 2016; Seiler and Aramant, 2012). In the case of full-thickness transplants that contain inner retinal neurons, it remains unclear how this inclusion affects connectivity and signal processing. Limited success has been achieved so far with partial thickness transplants in which the inner retinal neurons are omitted from the donor graft, as techniques used to this end seem to result in significant trauma to the tissue (Ghosh et al., 1999). The success of sheet transplantation also faces other obstacles, such as the surgical logistics of placing fragile tissue into the

subretinal space so that it lies flat against the host retinal layers which is challenging. In addition, the supply of feotal tissue is scarce. Addressing the latter issue a study by the Takahashi group showed differentiation of retinal sheets from mouse pluripotent stem cells (Assawachananont et al., 2014). These were transplanted into the *Retinal Degeneration 1* (*Rd1*) mouse, a model for rapid and severe photoreceptor degeneration with a near complete loss of the ONL by three weeks of age. Grafts survived, inner and outer segments developed and expression of photoreceptor markers Rhodopsin and Recoverin was observed in the transplanted tissue. Two outcomes with respect to connectivity to the recipient interneurons were observed. When the graft contained donor interneurons, little contact was seen. Processes extending from the graft to the host tissue were much more readily detectable when inner retinal neurons were missing in the graft (Assawachananont et al., 2014). Collectively, these observations show that while retinal sheets offer a high extent of cell replacement several key aspects of this approach need to be optimized to clearly demonstrate that useful vision could be restored using this method.

I.IV.III. Cell suspension transplantation

The most successful approach so far to replace photoreceptors lost due to retinal degeneration has been achieved with dissociated cells from exogenous sources (summarized in Diagram I.IX.). Despite possible changes associated with degeneration in higher order retinal neurons, synaptic connectivity and activity of receptive brain centers, insights from gene therapy and the use of retinal implant devices strongly suggested that restoring at least some level of function is possible when photosensitivity is provided (Bainbridge et al., 2008; Caspi et al., 2009). Before restoration of rod-mediated visual responses could be shown (Pearson et al., 2012), several requirements for successful cell replacement had to be met. Foremost, an appropriate donor population capable of migrating and giving rise to functional photoreceptors following transplantation needed to be identified. These cells were required to successfully connect to retinal interneurons, so that the visual signals detected could be passed on for processing. Furthermore, the delivery methods and quantities of transplanted cells had to be optimised for maximal benefit. Related to this, barriers to engraftment in the recipient environment were identified and tackled. Finally, to have potential for clinical translation, a renewable, ethically acceptable and sufficiently scalable source of donor cells needed to be identified. How these issues have been addressed so far will be discussed in detail below.

I.IV.III.I. Identification of appropriate donor population

Retina is a part of the central nervous system (CNS) and both brain and retina are derivatives of neuroectoderm. Neural progenitors in many parts of the brain are intrinsically capable of migration and differentiation into various classes of neurons. Therefore, many studies have looked at transplantation of neural stem or progenitor cells into the retina. Whilst these cells are capable of migration into multiple retinal layers, they do not develop into mature retinal neurons (Sam et al., 2006; Young et al., 2000). Since this limitation became apparent, many groups tested the potential of retinal cells as a source of donor cells, because these have an intrinsic capacity to yield mature retinal phenotypes. Often these retinal donor cells were either expanded or cultured *in vitro* prior to transplantation. Depending on the protocol used these either differentiated into glia (Yang et al., 2002) or neurons, which were at times found to express photoreceptor markers (Qiu et al., 2005) following transplantation. However, these cells typically remained at the site of transplantation not entering the host outer nuclear layer. Placing isolated retinal progenitors in an immature recipient environment proved more successful. Murine retinal progenitors transplanted into the eyes of neonatal Brazilian opossum showed migration into the recipient retina, albeit not into the outer nuclear layer (Sakaguchi et al., 2005). Nevertheless, this study identified that the early progenitors might only be able to complete their differentiation in an immature recipient environment.

A study from the Ali group investigated further the developmental stage of the donor and recipient population (MacLaren et al., 2006). Retinal cells of a donor mouse ubiquitously expressing GFP isolated at the early postnatal peak of rod genesis were found to migrate into the host photoreceptor layer (and only that layer) and exhibit mature rod photoreceptor morphology following transplantation into age-matched immature recipient eyes. Use of a transgenic line expressing GFP under the control of Nrl, a rod-determining transcription factor expressed soon after terminal division, allowed the identification of the cells with the highest integration capability as immature rods. These post-mitotic rod precursors integrate most readily within a specific time window with highest integration potential between P3 and P10. Cells at this stage were also found to migrate as efficiently into a non-neurogenic adult host retina (MacLaren et al., 2006) and in variable numbers into models of retinal degeneration (Barber et al., 2013). Subsequent studies showed that mature rods can also engraft into the recipient photoreceptor layer, but much less frequently (Gust and Reh, 2011). This observation showed that the appropriate stage of the donor cell population is key to successful engraftment and post-mitotic rod precursors at a stage at which their fate is specified

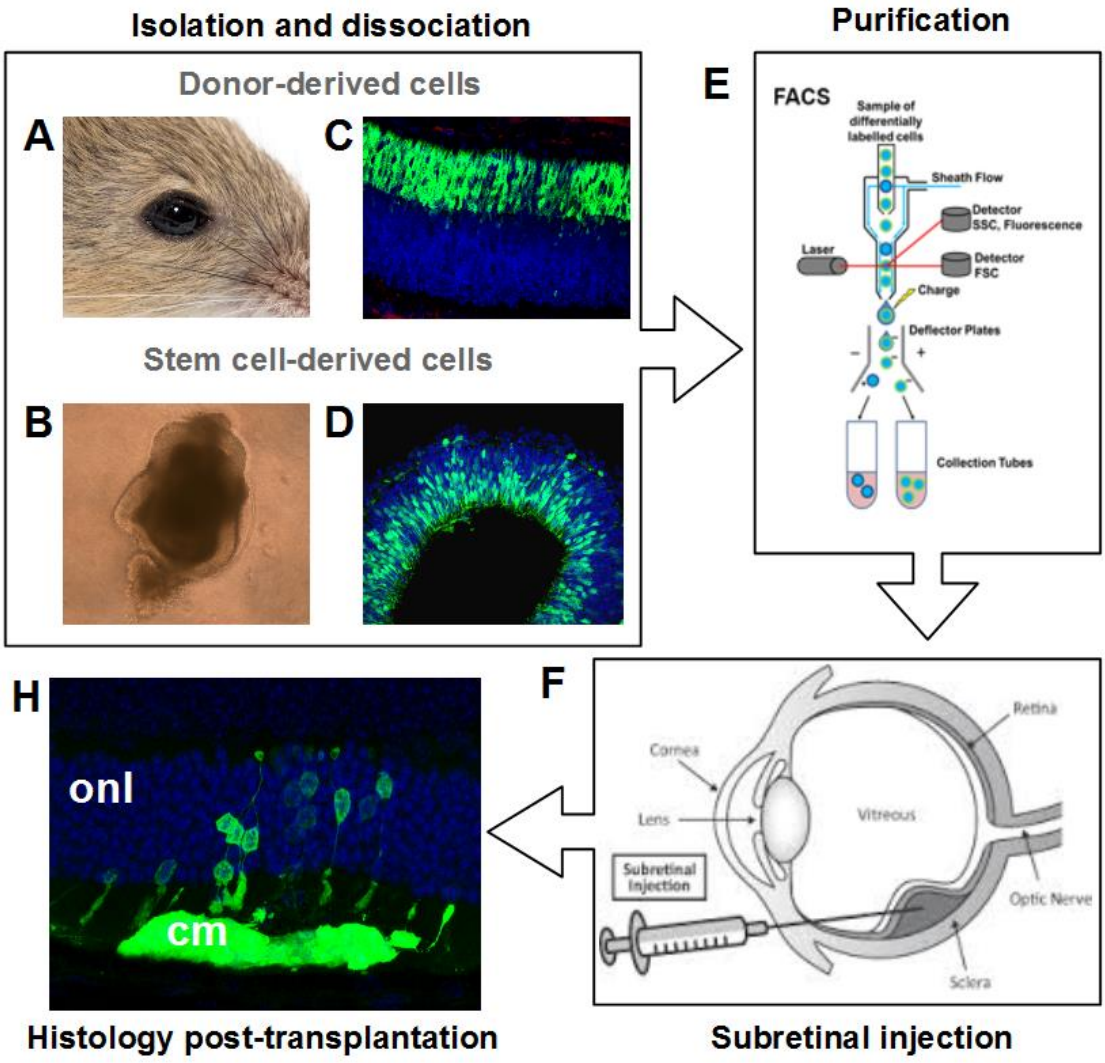

Diagram I.IX. Transplantation of isolated photoreceptor precursors in suspension as a strategy for cell replacement therapy in the retina

Photoreceptor precursors at an appropriate developmental stage can be harvested from eyes of donor mice **(A)** or retinal organoids derived from pluripotent stem cells **(B)**. Most commonly photoreceptor precursors are marked with a fluorescent reporter such as Nrl:GFP in transgenic donor mice **(C)** or Crx:GFP in an mESC line **(D)**. Donor tissue is enzymatically dissociated into suspension, from which required cells are purified by means of fluorescence-activated cell sorting (FACS) **(E)** or magnetic-activated cell sorting (MACS). A single cell suspension of purified donor cells is then injected into the subretinal space of recipient mice **(F)**. Engraftment is usually assessed by histology of treated eyes post-transplantation **(H)**. In a successful outcome a mass of donor cells (cm) is found surviving in the subretinal space and integration of donor photoreceptors into the host outer nuclear layer (onl) is observed.

but they do not yet show mature features such as fully formed outer segments or synapses was optimal.

I.IV.III.II. Functional integration following transplantation

Rod precursors were found to migrate into the recipient outer nuclear layer. However, to call a transplanted cell integrated it has to develop mature morphological features of a photoreceptor, exhibit photoreceptor marker expression and function similarly to a healthy endogenous rod. Closer inspection of the integrated rod precursors showed that these cells developed outer segments staining for proteins associated with phototransduction and extended basal processes terminating in synapses indistinguishable from those of endogenous rods (MacLaren et al., 2006; Pearson et al., 2012). Optimization of the transplantation methodology resulted in substantial increases in the number of integrating cells (20-30 fold), showing that in addition to isolation of a population exhibiting strong engraftment capacity, streamlining the transplantation procedures can make a pronounced difference in the outcome (Pearson et al., 2012). With the number of integrated cells reaching an average of over 16,000 it was possible to determine their functionality. Mice lacking rod transducin (*Gnat1*$^{-/-}$), a model of stationary night blindness, that received transplants of Nrl:GFP rod precursors showed activity recorded in the V1 region of the visual cortex when presented with a low low-light visual stimulus, indicating that the information from the integrated cells is passed on to interneurons and projection neurons and into the brain. Activity of the cells also led to improvements in contrast sensitivity and visual acuity measured by scotopic optokinetic head-tracking responses. Finally, transplantation of rod precursors allowed knockout animals to solve a visually-guided water maze task under dim-light conditions (Pearson et al., 2012). The level of function restored was found to correlate with the number of integrated cells (Pearson et al., 2012) and expression of rod transducin in these cells (Warre-Cornish et al., 2014). Altogether, there is substantial evidence that transplanted dissociated photoreceptor precursors functionally integrate into the adult host retina restoring visual responses.

I.IV.III.III. Impact of recipient retinal environment

Before appropriate donor cells can even attempt to integrate into the host retina, they need to be successfully delivered into the recipient eye in the right quantities. Several issues surrounding this step were examined. The main considerations are the site of injection, reflux of the cell suspension, physical impact of the injection procedure on the recipient retina and the number of cells used (Pearson et al., 2014). There are two standard routes of delivery to the retina, by intravitreal or subretinal injection. Intravitreal injection has the advantages of technical ease and being less invasive.

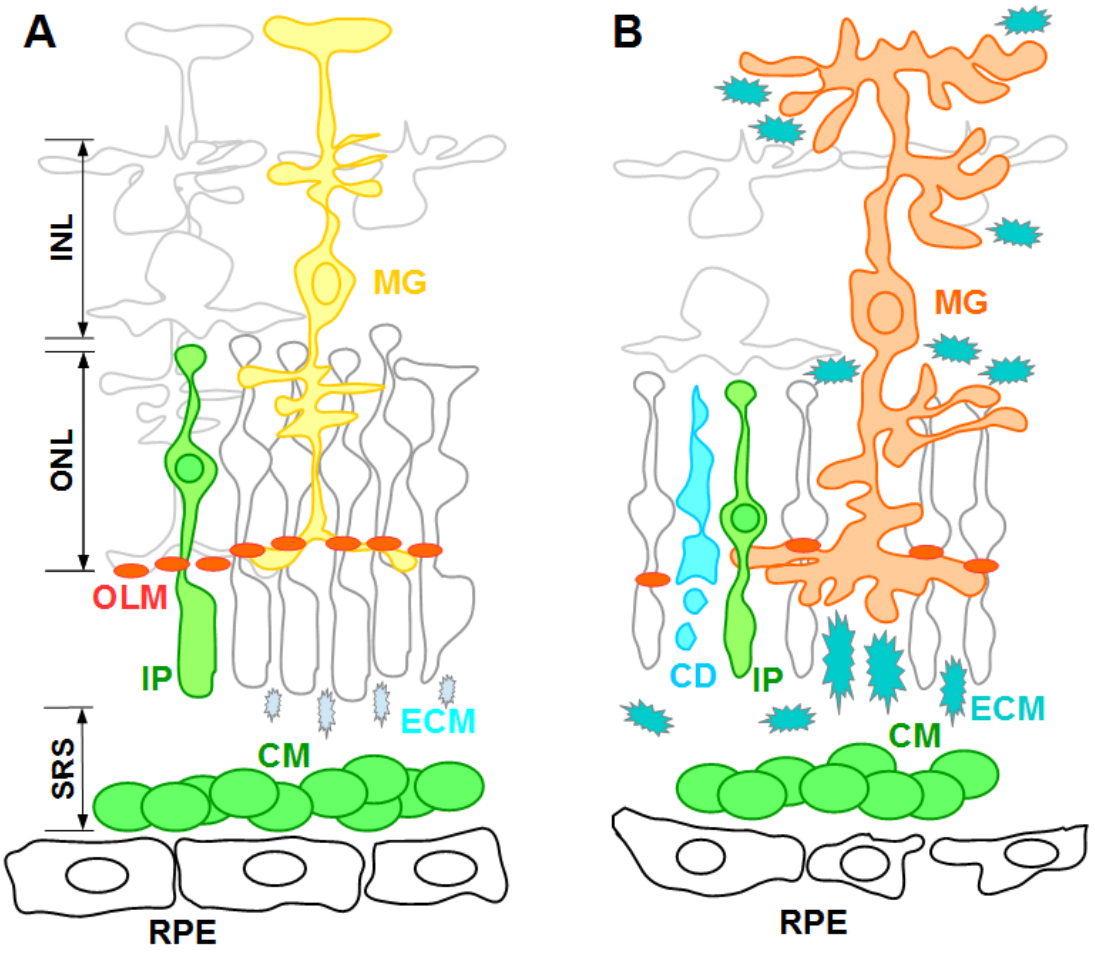

Diagram I.X. Barriers for transplanted photoreceptor precursor integration present in the recipient retinal environment.

Photoreceptor precursors are typically transplanted into the subretinal space (SRS) of healthy wild-type animals **(A)** or models of retinal degeneration **(B),** where the surviving cells form a subretinal cell mass (CM). Following transplantation into a wild-type eye, the photoreceptor precursors have to migrate out of this mass through a layer of extracellular matrix components (ECM, in cyan) called the interphotoreceptor matrix. Once they reach the apical edge of the host outer nuclear layer (ONL), where photoreceptors reside, the migrating cells need to cross the outer limiting membrane (OLM, in red). The OLM is a layer of tight-junction contacts between photoreceptor and Müller glia (MG) apical processes. In a degenerating retina **(B)**, tissue integrity is often compromised due to the death of host photoreceptors (CD, in blue). In response, processes of Müller cells proliferate (MG, in orange) to provide additional support, often ensheathing degenerating photoreceptors. The OLM can be compromised or remodelled in these conditions (in red). Müller cells can also secrete extracellular matrix components (in magenta), that can play either a stimulatory or inhibitory role for photoreceptor precursor integration.

However, the donor cells delivered via this route need to migrate through the dense meshwork of retinal ganglion cells fibers and then cross the inner plexiform layer, full thickness of the interneuron layer and the outer plexiform layer before reaching the photoreceptor layer. Only cells with very high migratory capacity like derivatives of neural stem cells are able to achieve this, but these were not found to yield functional integration (Klassen et al., 2004; Sakaguchi et al., 2005; Sam et al., 2006; Young et al., 2000). The subretinal route is more technically challenging and results in more trauma to the retina. However, it allows the delivery of cells into close proximity of host photoreceptors taking advantage of the natural anatomical cleavage plane between RPE cells and the outer nuclear layer (schematically depicted in Diagram I.IX. and Diagram I.X.). Temporary detachment of the photoreceptor layer from contact with the RPE usually smoothly resolves within a few hours allowing a rapid return to normal vision. In addition, viral vectors for gene replacement in patients have been successfully administered in this way (Bainbridge et al., 2008; Maguire et al., 2008). Another issue related to injection is reflux of the cell suspension. This occurs frequently as the eye is an enclosed pressurized space. In a pig large animal model it has been found that addition of an air bubble can help to prevent this (Klassen et al., 2008), however, addition of air to retinal detachments in the mouse seems to exacerbate immune responses to the transplant (Pearson et al., unpublished observations). It is not surprising that a key consideration is also the number of transplanted cells. It has to be balanced so that maximal integration is achieved without creating too large a mass of cells remaining in the subretinal space, that prevent reattachment and contact between the recipient photoreceptor layer and the RPE, negatively impacting on function (West et al., 2010). In addition to the number of desired cells, their purity is a key factor and techniques allowing the selection of populations which possess high integration capacity, such as FACS, can lead to significant improvements (Pearson et al., 2012).

A recent study from the Ali group was the first to comprehensively examine integration of rod precursors into different models of retinal degeneration (Barber et al., 2013). Rod precursors integrated into rod transducin knockout animals (*Gnat1*$^{-/-}$), a model of stationery night blindness, in numbers similar to those in the wild-type retina and robustly developed outer segments and synapses (Barber et al., 2013; Pearson et al., 2012). In contrast, transplants into the moderately fast degeneration model the Rhodopsin knockout (*Rho*$^{-/-}$) yielded poor morphology with little segment or synapse formation. Surprisingly, transplantation into the Retinal Degeneration 1 (*rd1*) model of rapid degeneration, in which most of outer nuclear layer is lost by 6 weeks of age,

results in robust integration with synaptic connectivity and segment elaboration, though the morphology of integrated cells is poor (Barber et al., 2013; Singh et al., 2013). Therefore, the disease etiology but not severity is the determining factor for transplantation outcome. This work highlights that in addition to the transplantation procedure methodology, specific features of the degenerating retina affect the outcome. The most important factors identified so far are activation of Müller cells in a process of retinal gliosis, composition of the extracellular matrix in the recipient, integrity of the outer limiting membrane and immune responses of the recipient (Pearson et al., 2014; schematically summarized in Diagram I.X.).

I.IV.III.III.I. Retinal gliosis

Glial cells throughout the nervous system respond to injury by proliferation, hypertrophy, upregulation of intermediate filament proteins, such as vimentin or glial acidic fibrillary protein (GFAP), and secretion of extracellular matrix components (Lewis and Fisher, 2003). Two glial cell types reside in the retina, these are Müller cells with cell bodies in inner nuclear layer and processes that extend through the whole thickness of the inner and outer retina (see Diagram I.X.) and astrocytes located at the inner surface of the ganglion cell layer. In the course of retinal degeneration or as a result of injury, Müller cells and astrocytes undergo reactive gliosis (Fisher et al., 1991). Features of this process are hypertrophy with proliferation of processes (graphically depicted in Diagram I.X.; reviewed in Marc et al., 2003) and an increase in intermediate filament components GFAP and vimentin (Fisher et al., 1991). It is believed that upregulation of intermediate filaments provides structural support when tissue integrity is compromised (Marc et al., 2003). Reactive gliosis leads to the formation of a glial scar that can at later stages of degeneration envelope the whole retina forming a physical barrier to the passage of transplanted cells (Pearson et al., 2014). In two disease models, *Prph2*$^{+/\Delta 307}$ and *rd1*, examined by Pearson and colleagues withdrawal of GFAP-positive Müller glial processes at late stages of degeneration correlated with improved integration (Barber et al., 2013), supporting the notion that processes of activated glial cells hinder migration of transplanted cells into the host photoreceptor layer.

I.IV.III.III.II. Deposition of extracellular matrix components

Extracellular matrix (ECM) is a complex network of scaffolding molecules not only providing structural support but also playing a role in processes such as cell signaling and migration. As a result of injury or degeneration the composition of ECM becomes altered (please see Diagram I.X. for a schematic representation) and expression of molecules both inhibiting and supporting cell migration can occur depending on the

context. In particular, proteoglycans, a major ECM component in the brain, were found to have an impact on migration and axon extension. Proteoglycans are formed of a protein core with glycosaminoglycan side chains attached. Of the proteoglycans, chondroitin sulfate proteoglycans (CSPGs) predominate in the neural retina (Inatani and Tanihara, 2002; Inatani et al., 2000). They are important in development for axonal guidance out of the retina (Ichijo, 2004). In the context of degeneration they show upregulation throughout the central nervous system (Inatani et al., 2000) and inhibit axonal regeneration primarily via their glycosaminoglycan side chains (Friedlander et al., 1994). Patterns of CSPG expression vary significantly between different models of retinal degeneration as assessed using broad-spectrum CSPGs antibody CS-56. Qualitative examination suggests an inverse correlation between the intensity of CSPG expression and rod precursor integration following transplantation (Barber et al., 2013). Indeed, the use of a bacterial enzyme chondroitinase ABC to break down the glycosaminoglycan side chains of CSPGs during transplantation significantly increased the number of integrated rod precursors (Barber et al., 2013) highlighting that manipulation of the composition of host ECM components can improve photoreceptor precursor transplantation outcome.

I.IV.III.III.III. Outer limiting membrane integrity

Transplantation of retinal cells into the opossum eye results in donor cell migration into the host retina of juvenile but not adult animals (Sakaguchi et al., 2005), this coincides with maturation of Müller cells, which amongst other functions form an anatomical barrier separating photoreceptor cell bodies from the subretinal space. This barrier is called the outer limiting membrane (OLM) and is formed between the end feet of Müller glia and photoreceptors (graphical representation in Diagram I.X.). Structurally the OLM is composed of adherens junctions consisting of transmembrane cadherin-catenin complexes, mediating cell to cell adhesion forming a diffusional barrier, and cytoplasmic adaptor proteins, including Crb1 and ZO1, responsible for their formation and stabilization. The *Crb1*$^{rd8/rd8}$ mouse harbors a single base deletion in the Crb1 gene that causes fragmentation of the OLM and progressive retinal degeneration (Mehalow et al., 2003). Consistently, mutations in human *CRB1* gene also result in retinal disease (Meuleman et al., 2004). Integration of rod precursors is markedly increased in *Crb1*$^{rd8/rd8}$ mice compared to wild-type recipients (Pearson et al., 2010). The OLM can be indirectly compromised in wild-type recipients through treatment with alpha-aminoadipic acid (AAA), a glial toxin that affects Müller cell function leading to disruption of OLM integrity. This treatment led to a significant increase in the number of integrating transplanted rod photoreceptor precursors (West et al., 2008). Further

evidence supporting the idea that the intact OLM is a barrier to migration of transplanted cells was gathered by knockdown of the adhesion complex adaptor protein ZO1. Transient transcriptional gene silencing by short interfering RNA (siRNA), that reduced ZO1 levels *in vivo*, combined with cell transplantation resulted in an enhanced integration of donor cells in both wild-type and diseased retina (Barber et al., 2013; Pearson et al., 2010). Collectively, these findings show that the OLM is a barrier to the migration of subretinally transplanted cells into the host photoreceptor layer and that a transient reduction in its integrity improves transplantation outcome.

I.IV.III.III.IV. Host immune responses

A common feature of retinal disease is photoreceptor death triggering activation of a resident retinal macrophage population called microglia. In wild-type mice injected with rod precursors the presence of a high number of macrophages in the subretinal space following transplantation is associated with fewer integrated cells (West et al., 2010). It is speculated that the degree of trauma associated with the injection determines the level of macrophage recruitment. It also remains unclear whether macrophages prevent transplanted cells from migrating into the host photoreceptor layer or lead to the destruction of already integrated cells (Pearson et al., 2014). Once integrated, the cells face the challenge of long term survival. As in any other transplantation paradigm, transplant rejection is a major concern. The subretinal space is a partially immune-privileged site meaning that foreign grafts can survive for extended periods without rejection (Jiang and Streilein, 1991). Neonatal retinal grafts placed in genetically matched recipients survive indefinitely, but in non-matched recipients they are slowly rejected (Jiang and Streilein, 1991). With respect to photoreceptor transplantation the immune status of the subretinal space is a key consideration. This site displays two important features of immune-privilege, it protects grafts from rejection and promotes systemic immune deviation to antigens placed in this site. Immune deviation is a form of immune tolerance mediated by antigen-specific T regulatory cells. These are made in the spleen and act to suppress host immune reactions to antigens placed in the anterior chamber of the eye (Wilbanks and Streilein, 1990). Immune deviation is lost with the death of RPE cells or with the disruption of the blood-retinal barrier (Wenkel and Streilein, 1998). Both of these are often compromised in degeneration or injury. The procedure of transplantation can also cause some additional trauma, which should be limited to a necessary minimum. Many different sources of cells are proposed for retinal repair and these differ in their immunological profile. Few studies looked at this aspect, but it appears that cultured cells are less immunogenic, or at least this is true in the case of neural progenitors (Ma and Streilein, 1998). Rod photoreceptor

precursors, capable of functional integration, when transplanted into recipients with partially mismatched haplotypes are subject to a delayed host immune response from around 4 months post transplantation. It is possible though for these cells to survive up to a year provided that these immune responses are modulated (West et al., 2010). As mentioned above, if high numbers of macrophages were found in the subretinal space the number of integrated cells decreased significantly as early as 1 month post transplantation (West et al., 2010). Immunological maturity occurs relatively late in development past the point at which donor or stem cell-derived precursors are harvested. Yet, as these cells functionally integrate they are likely to begin to express molecules able to trigger immune reactions. One strategy to avoid this could be the use of immunosuppressive drugs. This strategy has the drawbacks of the toxicity of these agents and induction of general immunosuppression that increases the risk of infection and cancer (Pearson et al., 2014). Disruption of co-stimulatory pathways required for T lymphocytes activation could present a safer alternative protection strategy (Felix et al., 2010). The use of induced pluripotent stem cells (iPSCs) to derive transplanted cells offers an alternative to avoid mismatched haplotypes. However, even cells derived from iPSCs were found to trigger some immunogenicity when transplanted into syngeneic mice (Zhao et al., 2011). Therefore careful assessment and tools for managing host immune responses will be required for clinical application of cell replacement in the retina.

I.IV.III.IV. Cone photoreceptor replacement

A great majority of studies looking at photoreceptor transplantation so far focused on rod precursors (Pearson, 2014). This is not surprising given that mice, the most commonly used model species in these studies, are nocturnal animals (Solovei et al., 2009) predominantly depending on dim-light vision mediated by rod cells. In contrary, humans are a diurnal species (Solovei et al., 2009) and the most important aspects of our vision depend on the function of cone cells. Cone photoreceptors mediate high acuity vision in daylight and permit colour discrimination. As with rod precursors, there are several challenges to cone photoreceptor replacement. Namely, identification of an appropriate donor population, managing barriers presented by the recipient retinal environment and achieving improvements in visual function.

I.IV.III.IV.I. Donor populations for cone cell replacement

Transplantation of cultured retinal progenitor cells into the subretinal space of *Rho*$^{-/-}$ mice did not yield rod integration, however, one transplanted cell in the outer nuclear layer showed expression of cone opsin (Klassen et al., 2004). Retinal cells derived from human ESCs following intravitreal transplantation migrated into all retinal layers

and cells positive for S opsin exhibiting immature morphology lacking inner and outer segments were found (Lamba et al., 2009). These encouraging observations were followed by the first proper proof-of-principle study showing that replacement of both rods and cones is possible in a degenerating retina (Lakowski et al., 2010). In this study, Crx:GFP transgenic animals were used as donors. This allowed isolation of GFP-positive photoreceptor precursor cells at the peak of cone genesis between E12.5 and E17.5 and at the early postnatal peak of rod birth (P2-3). Photoreceptor precursors integrated much more efficiently (around 10 fold) at the early postnatal stage. However, when rod versus cone identity was identified through immunostaining for the cone marker RXRγ, it became apparent that integrated cone photoreceptors were only found in the embryonic stage donor transplants. These RXRγ-expressing cells showed unambiguous features of mature cone cells, being aligned with the host cone cells at the apical aspect of the photoreceptor layer, showing multiple foci of heterochromatin in their nuclei, short, stubby inner and outer segments as well as basal processes ending in a large pedicle located in the outer plexiform layer. The proportion of integrated cells that showed cone marker expression was found to be very similar to the proportion of cone to rod cells in the recipient retina, being around 1:35 (median of 0.76% in all transplants from E14.5 donors). The absolute numbers of integrated cones were very low with the maximum of 54 cells in the retina transplanted with E17.5 donor cells. These low numbers were in stark contrast to the abundance of cone precursors in the initial donor Crx:GFP population (>60% at every embryonic timepoint) and in the subretinal space following transplantation (over 30% of cells in the subretinal cell masses positive for RXRγ). Therefore the authors concluded that despite the high proportion of cone precursors in the donor population and their survival in the subretinal space after transplantation cone precursors integration capacity is low and the final proportion of cones amongst integrated photoreceptors is likely determined by the ratio of cones to rods in the adult host retina (Lakowski et al., 2010).

Only one other study focused specifically on daylight vision repair. In the work of Ader and colleagues (Santos-Ferreira et al., 2015) authors took advantage of the advances in understanding the gene regulatory networks responsible for photoreceptor specification and mouse genetic technology. They used cells from *Nrl*$^{-/-}$ mice, which lack the expression of Nrl, a key determinant of rod fate resulting in prospective rods turning into cone-like cells expressing S opsin photopigment (Mears et al., 2001). Crossing this knockout model with animals ubiquitously expressing GFP under the actin promoter allowed isolation of fluorescently labelled cone-like cells. Differently to most of the other studies, magnetic-associated cell sorting (MACs) based on the cell

surface marker CD73 that is expressed in wild-type rods and cone-like photoreceptor precursors in *Nrl*$^{-/-}$ animals was utilised to pull out donor cells of interest for transplantation. These cells were isolated at early postnatal stages since their birth peak is equivalent to the peak of rod genesis in the wild-type retina. Integration into the adult wild-type retina was most efficient when the donor population was isolated at P4 and was much higher than that observed for the Crx:GFP embryonic donor population rich in cone precursors in the study of Lakowski et al. with nearly 900 integrated cells found per retina following transplantation. Integrated cells showed typical photoreceptor morphology with development of outer segments and basal processes ending in synaptic terminals. However, these integrated cone-like donor cells exhibited only some features of mature cone cells. They showed multiple heterochromatin foci in the nucleus, well developed inner and outer segments including formed outer segment discs stacks upon ultrastructural analysis but the soma often lied more basally in the tissue than that of endogenous host cones. Moreover, these cells misexpressed S opsin in their somas in contrast to its typical confinement to the outer segment. In addition, synaptic terminals were most often small and round, more reminiscent of the rod spherule than the cone pedicle, however, this could be related to the cells being S cone-like since S opsin-only expressing cells show more slender terminals (Breuninger et al., 2011). Despite the atypical features these integrated cone-like cells were shown to be light sensitive and integrated functionally into recipient circuitry driving bright light-evoked responses measured from retinal ganglion cells using multi electrode arrays (Santos-Ferreira et al., 2015). Collectively, this study showed that cone-like cells could present a donor cell source capable of functional integration for daylight vision repair.

I.IV.III.IV.II. Impact of the recipient environment on cone precursor transplantation

Similar to the observations regarding rod precursor transplants, the recipient retinal environment was found to impact on cone precursor integration. In the study by Sowden and colleagues (Lakowski et al., 2010) integration of Crx:GFP donor photoreceptors at embryonic stages, when cone precursors constitute the majority of the transplanted population, was examined in the wild-type retina and in two models of retinal degeneration the *Crb1*$^{rd8/rd8}$ and *Gucy2e*$^{-/-}$. As mentioned above, the *Crb1*$^{rd8/rd8}$ mice have a single base mutation in the *Crb1* gene resulting in a premature stop codon and dysfunctional protein product. Since Crb1 is an adherens junction adaptor required for outer limiting membrane formation this structure is compromised in this model and retinal degeneration ensues. The second model, *Gucy2e*$^{-/-}$ mice, harbour a targeted deletion in the retinal guanylate cyclase 1 (*RetGC1/Gucy2e*) locus, which results in

cone dysfunction and progressive cone loss. At 3 months of age only around 25% of cones survive in the *Gucy2e*$^{-/-}$ retinae, creating a cone-depleted environment. When transplantation was performed into adult wild-type retina in this study, even though cone precursors constituted a high percentage of the donor population, a high number of mature integrated cones was not observed following transplantation. Donor cells were also transplanted into developing P14 retinas with a similar result. This suggested that the postnatal retinal environment might not be particularly permissive to cone integration. It was noted however, that with the embryonic donor cells the final proportion of integrated cones was close to the ratio of cones to rods in the recipient (around 1:35). With respect to integration into the two degeneration models it was observed that the compromised OLM in the *Crb1*$^{rd8/rd8}$ model did not facilitate higher integration of cone cells from the embryonic Crx:GFP donor population. In contrast, transplants into the cone-depleted environment of the *Gucy2e*$^{-/-}$ recipients yielded a significantly increased proportion of cone cells in the integrated photoreceptor population (1.9% versus 0.15%), although the absolute numbers were still low even in this model (2-28 cells per retina; Lakowski et al., 2010). Altogether, this data set demonstrates that photoreceptor precursors isolated at early stages of retinogenesis when cone precursors predominate yield integrated mature cone cells following transplantation, albeit in low numbers, and the proportion of cones to rods in these transplants appears determined by recipient environment. The ratio of integrated cones to rods is similar to that in the host retina with integration increased in the case of a retina, in which cones are lost due to degeneration.

The study of Ader and colleagues also examined the impact of recipient environment on the integration of cone-like cells. Transplantation was performed into adult wild-type animals, the *cone photoreceptor function loss 1* (*Cpfl1*) mice, that exhibit cone function loss from three weeks of age arising from a spontaneous point mutation in the phosphodiesterase 6C gene (PDE6C), and the *Nrl*$^{-/-}$ model of rodless retina. A trend was observed for increased integration into the *Cpfl1* cone degeneration model although this was not statistically significant (wild type average of 804 cells versus 1359 for *Cpfl1* mutants). Integration into the *Nrl*$^{-/-}$ knockout retina that lacks rods was very strongly enhanced with around a 13 fold increase in the number of integrated cells following transplantation (average of 10,829). Additionally, highly polarised cells extending processes towards the recipient outer nuclear layer were frequently observed in the subretinal space of this host type. Several factors are hypothesised to contribute to this strong enhancement. First, due to the altered outer nuclear layer composition and architecture, with the formation of rosettes and abnormal packing of

photoreceptors, contacts between the photoreceptor layer and the RPE (Mears et al., 2001) are weaker facilitating detachment following subretinal injection, a factor known to promote increased integration (Pearson et al., 2012). Second, the outer limiting membrane is compromised in this model and this again has been shown to promote donor cell migration into the host photoreceptor layer (Barber et al., 2013; reviewed in Jayakody et al., 2015 and Pearson et al., 2014). Finally, the composition of the host photoreceptor environment could also impact on integration. Authors also examined the survival and recruitment of host immune cells following cone-like cell transplantation. The number of integrated cells was found to decline over time with similar kinetics in both wild-type as well as *Cpfl1* degenerating retinae, similar to previous observations for rod cells (West et al., 2010). Activation of host immune responses were examined by immunostaining for CD68-positive monocytes and macrophages present in the subretinal space following transplantation into the *Cpfl1* mutant hosts. Increased numbers of these cells was not correlated with poorer integration, contrary to reports examining responses to rod precursor transplantation (West et al., 2010). In conclusion, this study provided evidence that the host retinal environment impacts on cone-like cell integration with both adult retina and a cone degeneration model being permissive to substantial numbers of cone-like cell integration and very robust integration observed in the rodless retina of *Nrl*$^{-/-}$ recipients.

I.IV.IV. Cell sources for retinal cell replacement therapies

Significant achievements in the development of a cell-based therapeutic approach for retinal degenerations have been made using donor cells derived from newborn mice (Pearson, 2014). An important limitation in the clinical translation of these findings is the supply of human tissue at equivalent stages. Moral considerations aside, rarity of miscarriages and abortions at a specific developmental stage and logistics of the harvest and processing of such tissues would likely preclude their wider use in the clinical setting (Jayakody et al., 2015). Therefore, for further development of this approach identification of a robust, renewable and scalable source of cells is key.

Three main sources are proposed for this purpose: (1) isolation and differentiation of ocular stem/progenitor cells into photoreceptor precursors or use of pluripotent stem cells as a source, either (2) embryonic stem cells or (3) induced pluripotent stem cells (iPSCs) (graphically represented in Diagram I.XI). To date limited success was achieved with the use of ocular stem/progenitor cells due to their restricted capacity to

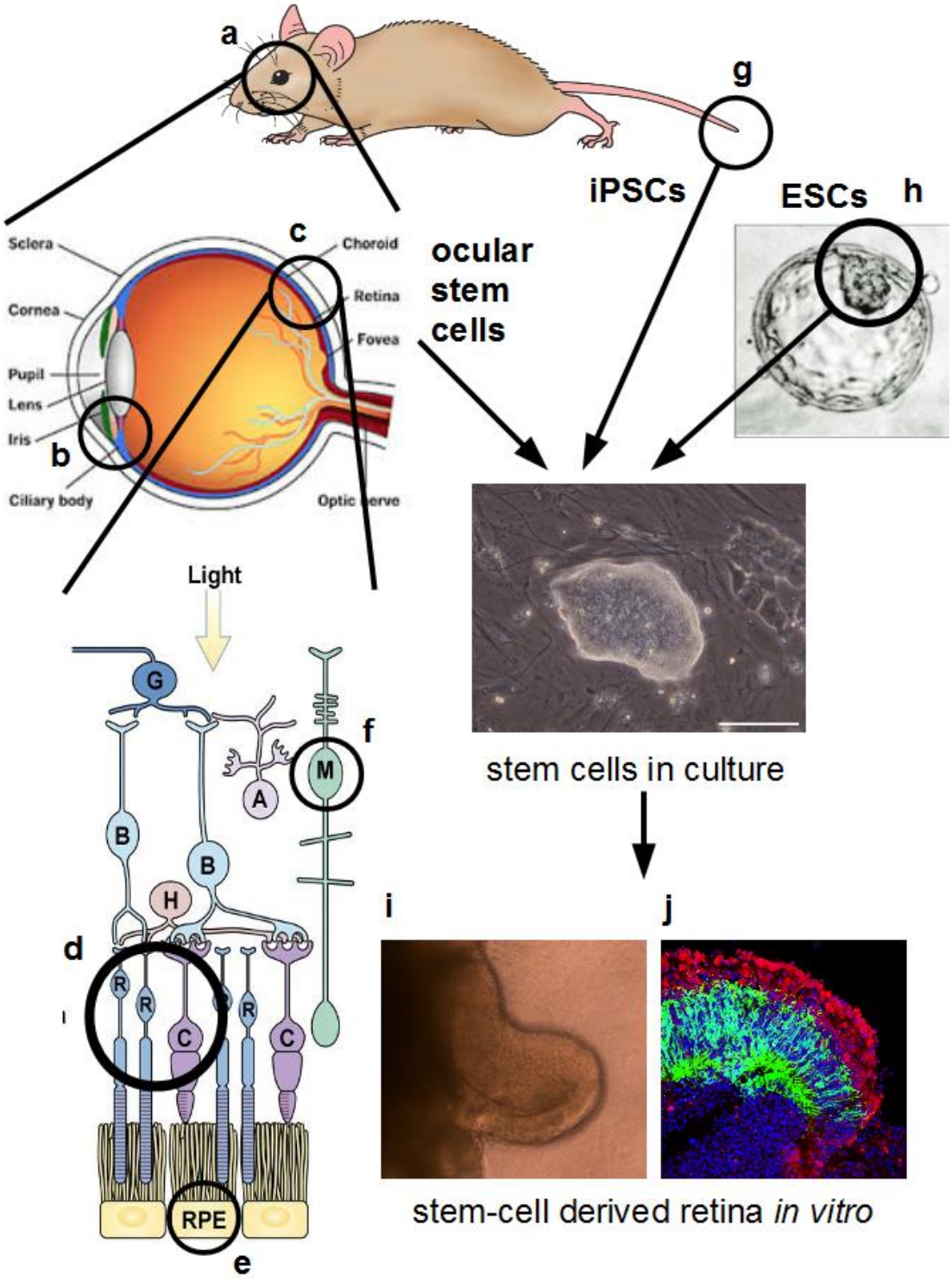

Diagram I.XI. Cell sources for retinal cell therapy

Most research into cell replacement in the retina has focused on using photoreceptor cells **(d)** isolated from the donor mouse retina **(a,c)**. The search for expandable and renewable cell sources has triggered interest in defining the capacity of various stem cells for retinal repair. Pluripotent or multipotent stem cells can be derived from various sources **(a,b,c,g,h)**, including the inner cell mass of the blastocyst **(h)** (embryonic stem cells; ESCs), the adult eye **(a)** (ocular stem cells) or other adult tissues **(g)** (induced

pluripotent stem cells; iPSCs). These ocular stem cells consist of cells of the iris and ciliary body **(b)**, stem cell features can be also be triggered in RPE cells **(e)** and Müller cells **(f)**. All these stem cell populations can be cultured *in vitro* and directed into specific retinal lineages as required, through appropriate culture conditions. Importantly, retinal morphogenesis can be recapitulated in the 3D culture of pluripotent stem cells with the formation of optic cups **(i)** that contain laminated retinal tissue **(j)**. Typically ocular stem cells show a much restricted differentiation capacity compared to ESCs or iPSCs.

Images in i and j – own work.

Rest acquired from:

https://commons.wikimedia.org/

differentiate into photoreceptor phenotypes (Jayakody et al., 2015) and for this reason studies examining this cell source will not be discussed in detail here.

Pluripotent stem cells are considered the most attractive source of cells for retinal cell therapy. Despite the fact that they are not suitable for transplantation in their undifferentiated state, these sources are virtually inexhaustible and technologies for their defined large scale culture are rapidly developing (Carpenter and Rao, 2015).

I.IV.IV.I. Embryonic stem cells

Two independent laboratories in the early 1980s first described the isolation and characterization of embryonic stem cells derived from the inner cell mass of mouse blastocysts (Evans and Kaufman, 1981; Martin, 1981) (also see Diagram I.XI). The authors reported several characteristic properties of these cells. Firstly, mESCs can be maintained *in vitro* in an undifferentiated state for an indefinite period. Secondly, they show the potential to differentiate into cell lineages of all three germ layers – endoderm, mesoderm and ectoderm. Finally, when introduced into the pre-implantation stage embryos, mESCs show the potential to give rise to chimeric animals. Only fifteen years later an equivalent population of cells has been isolated from human embryos (Thomson et al., 1998), which spurred the interest in the use of the newly isolated human embryonic stem cells (hESCs) in regenerative medicine.

I.IV.IV.II. Induced pluripotent stem cells

Reports showing that it is possible to obtain and *in vitro* culture pluripotent stem cells from early mouse (Evans and Kaufman, 1981; Martin, 1981) and human embryos (Thomson et al., 1998) also allowed for study of the biological determinants of the pluripotent state. A study from Takahashi and Yamanaka in 2006 showed that from candidate 24 transcription factors, just four, namely Oct4, Sox2, cMyc and Klf4, are required to reprogram fibroblasts into pluripotent stem cells (Takahashi et al., 2006), which became referred to as induced pluripotent stem cells (iPSCs) (also see Diagram I.XI.). Cells reprogrammed in this way were shown to exhibit many features reminiscent of embryonic stem cells such as similar morphology, virtually unlimited self-renewal capacity and ability to form teratomas when introduced *in vivo* (Takahashi et al., 2006). Subsequent reports confirmed that iPSCs are similar, though not identical, to ESCs on the level of gene expression, miRNA profile and with respect to epigenetic modifications (Wernig et al., 2007). Furthermore, iPSC lines were shown to be capable of giving rise to viable chimeras with germline transmission (Okita et al., 2007; Wernig et al., 2007). From then iPSC technology rapidly evolved and at present there are a variety of approaches enabling the reprogramming of somatic cells into pluripotent stem cells, importantly including integration free methods, such as Sendai virus,

episomal plasmids, recombinant proteins and small molecules (reviewed in the context of retinal cell therapy in Borooah et al., 2013). Historically fibroblasts were most commonly used to derive iPSCs, however a diversity of tissue sources have been used since, including blood cells (Loh et al., 2009), cord blood cells (Giorgetti et al., 2009), keratinocytes (Aasen et al., 2008) and adult neuronal cells (Kim, 2007). Interest in different tissue sources for reprogramming stems from reports describing the existence of partial 'epigenetic memory' remaining in iPSCs following reprogramming, which affects the efficiency of differentiation into specific lineages (Kim et al., 2010). In the context of ocular tissue sources, human foetal RPE cells have been reprogrammed into iPSCs and these iPSCs lines showed enhanced capacity to form RPE when subjected to spontaneous *in vitro* RPE differentiation protocols, compared to other ESC and iPSCs lines (Hu et al., 2010). With respect to photoreceptors, iPSC lines were derived from mouse rod cells (r-iPSCs) and differentiated into retina using a standardized 3D suspension retinal differentiation protocol (Hiler et al., 2015) based on the method described by Sasai and colleagues (Eiraku et al., 2011). Quantification of multiple parameters characterizing the retinae derived from either r-iPSCs or more common sources such as mESCs or fibroblast-derived mouse iPSCs, showed that r-iPSCs significantly outperformed other pluripotent cell lines examined (Hiler et al., 2015). Curiously however, the main deficits observed with sources other than rod photoreceptors were in the presence of inner nuclear layer cells, particularly amacrine cells (Hiler et al., 2015). Comparative epigenetic analysis of fibroblast versus rod-derived iPSC lines showed that DNA methylation patterns and formation of cell-type specific chromatin domains contribute to this phenotype (Hiler et al., 2015). In conclusion, both ESCs and iPSCs are considered promising sources to derive photoreceptor precursors. The success of developing therapeutic approaches will likely depend on the combination of a robust and well-characterized cell source with an efficient differentiation protocol. It is important to note that the multiple stem cell sources show varying propensity for retinal differentiation, determined at least partially by epigenetic state of the cells.

I.IV.IV.III. Directed differentiation and transplantation of mouse embryonic stem cell-derived photoreceptor precursors

I.IV.IV.III.I. Induction of neural specification in mESCs

In the very first two studies describing embryonic stem cells both Evans and Martin have shown that mESCs cultured in suspension as floating aggregates, termed embryoid bodies (EBs) (schematically shown in Diagram II.4 A), exposed to serum spontaneously differentiate into cells of multiple lineages of all the three germ layers

(Evans and Kaufman, 1981; Martin, 1981). In these early studies neuronal cells were not prominent amongst the multitude of cell types (Evans and Kaufman, 1981; Martin, 1981). Subsequently many groups have developed protocols to direct the differentiation of mESCs towards specific lineages, including neuronal cells. The study by Bain and colleagues first showed that EBs formed from mESCs and exposed to retinoic acid develop into neuronal cells expressing markers such as βIII tubulin, neurofilaments and various voltage-gated ion channels (Bain et al., 1995). In this work floating EBs were first induced into neuronal cells in suspension, followed by dissociation and plating for adherent cultures, in which further differentiation occurred. The formation of three-dimensional (3D) aggregates or two-dimensional monolayer cultures remain the two main methods for triggering differentiation of pluripotent stem cell sources into specific lineages. Specificity of this process is achieved through selection of the initial method of EB formation (such as using low-adherent 96-well plates, hanging drop culture, bioreactors etc.), varied media composition with addition of specific soluble factors or serum as well as supplementation with extracellular matrix components (Kurosawa, 2007; Yin et al., 2016). From the very beginning the idea of stepwise induction, whereby cells are alternately cultured as 3D aggregates and in monolayers has been explored (Bain et al., 1995; Kawasaki et al., 2000; Lee et al., 2000; Wichterle et al., 2002; Ying et al., 2003). This principle was utilised to first derive cells of retinal lineage from mESCs (graphically represented in Diagram I.XII.).

I.IV.IV.III.II. Retinal differentiation of mESCs

During development the neural retina is specified through progressive lineage restriction from telencephalic progenitors, through formation of the eye field, optic vesicle, optic cup followed by genesis of all classes of retinal neurons (Bassett and Wallace, 2012; Zagozewski et al., 2014). The first study to show derivation of retinal cells from mESCs used retinoic acid or insulin-transferrin-selenium-fibronectin (ITSFn) with basic fibroblast growth factor (bFGF) to induce initial neural differentiation of mESC aggregates, which were then dissociated and plated onto poly-D-lysine coated dishes for subsequent adherent co-culture with P0 retinal cells on a Millipore membrane (Zhao et al., 2002). This was sufficient to trigger differentiation of BrdU-labelled mESC-derived progenitors into cells expressing early markers of retinal progenitors (Nestin, Pax6, Notch1, Rx) then photoreceptor precursors (NeuroD, Crx, Nrl) and finally infrequent photoreceptor maturation markers (Rhodopsin, Rod arrestin, Rhodopsin kinase, Peripherin2; Zhao et al., 2002), providing an important proof of concept for the feasibility of photoreceptor differentiation from mESCs.

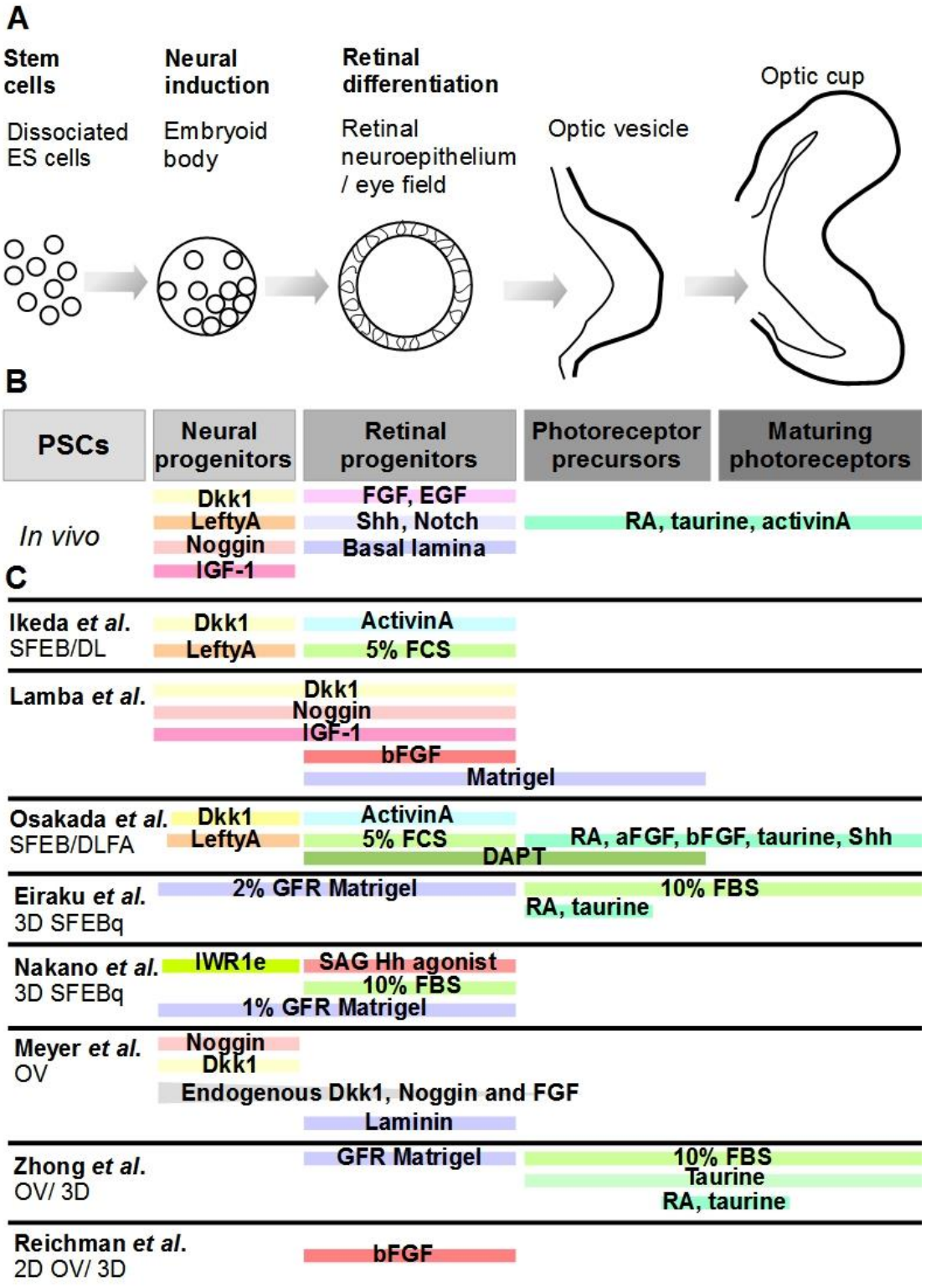

Diagram I.XII. Directed differentiation of retinal tissues from pluripotent stem cells.

Physiologically-relevant retinal tissue can be obtained through the recapitulation of major retinal morphogenesis steps by directed differentiation of pluripotent stem cells **(A)**. In most protocols stem cells are aggregated into an embryoid body which

subsequently undergoes neural induction in appropriate culture conditions. Neural progenitors need to acquire a rostral CNS identity to be able to form eye field-like neuroepithelium. Addition of matrigel is often used to facilitate formation of thick and rigid retinal neuroepithelium. Once an eye field-like domain is specified, three dimensional culture allows evagination of an optic vesicle structure, which folds into a bi-layered optic cup as occurs *in vivo*. Both cell intrinsic genetic programmes as well as input from soluble factors and basement membrane components drive this sequence *in vivo* **(B)**. Many soluble and extracellular matrix components have been utilised in differentiation protocols to date, in an attempt to trigger faithful recapitulation of this sequence of morphogenetic events and their use is schematically represented in **(C)**.

An important step in establishing efficient protocols for mESC differentiation into retinal cells was the development of serum-free floating culture of embryoid body-like aggregates (SFEB). In this neural induction protocol serum was substituted with knockout serum replacement (KSR). After around a week of culture using this method 70% of cells expressed the neural precursor marker Nestin (Watanabe et al., 2005). Furthermore, a similar proportion of cells expressed a GFP reporter based on the neuroectodermal marker Sox1 (Watanabe et al., 2005). In the developing embryo, Wnt signalling is involved in dorsal-ventral patterning, whereas Nodal signalling mediates the establishment of the anterior-posterior axis (Zagozewski et al., 2014). In the absence of 'caudalizing' signals mESCs spontaneously differentiate into rostral-most brain tissues (Kawasaki et al., 2000; Watanabe et al., 2005) consistent with the two-signal model of neural development positing that development of the caudal part of the nervous system requires additional inductive signals (Nieuwkoop and Others, 1952). Through addition of Wnt antagonist and head inducer Dickkopf-1 (Dkk1) and Nodal inhibitor LeftyA for the first 5 days of neural induction, the authors showed enhanced neural differentiation with up to 90% efficiency (Watanabe et al., 2005). Therefore, this work established that regional specification can be effectively guided by timely addition of embryologically-relevant patterning factors.

The SFEB culture system was subsequently further developed to derive retinal tissues (Ikeda et al., 2005). In the rostral Six3-positive CNS tissues co-expression of Rx with Pax6 marks retinal progenitors (reviewed in Zagozewski et al., 2014). The SFEB cultures supplemented with Dkk1 and LeftyA efficiently generated Six3-expressing cells. A screen of developmental regulators, including serum, ActivinA, Shh, Wnt, BMP4, Nodal (without LeftyA), IGF, FGF-1, FGF-2, and FGF antagonists, for the ability to induce Rx+,Pax6+ retinal progenitors revealed that only serum had a strong effect further potentiated by addition of ActivinA (Ikeda et al., 2005; protocol schematically represented in Diagram I.XII. C). This SFEB DLFA (from Dkk1, LeftyA, FCS and ActivinA addition) method yielded around 16% Rx+ retinal progenitors. These progenitors expressed the proliferation marker Ki67 as well as Otx2, but not Nestin or Sox1 (Ikeda et al., 2005) consistent with the *in vivo* expression profile (Bassett and Wallace, 2012; Livesey and Cepko, 2001; Trimarchi et al., 2008). Authors of this study observed that some of the inductive signals for further differentiation of these mESC-derived retinal progenitors towards photoreceptor lineage were either absent or present at insufficient levels since Rhodopsin expression was very infrequent and the number of Rhodopsin-positive cells could be significantly increased through overexpression of Crx. Moreover co-culture with embryonic mouse retinal cells

increased the percentage of cells differentiating to express photoreceptor markers Rhodopsin and Recoverin (Ikeda et al., 2005), further supporting the conclusion that some aspects of the photoreceptor differentiation niche are not fully recapitulated using this method of *in vitro* differentiation.

The search for additional inductive signals required for efficient photoreceptor differentiation was performed in a study from the Sasai and Takahashi laboratories (Osakada et al., 2008). In this work to improve efficiency of differentiation towards retinal lineages the authors used a mESC line in which GFP was knocked into the *Rx* locus. This fluorescent reporter allowed for purification of Rx:GFP+ retinal progenitors on day 9 of differentiation according to the SFEB DLFA method through FACS and subsequent plating for adherent culture on poly-D-lysine/laminin/fibronectin-coated dishes. On day 20 in these purified cultures around 7% of total cells expressed Crx (Osakada et al., 2008), still a relatively low percentage. Significant improvement in the generation of Crx-positive photoreceptor precursors came from inhibiting the Notch pathway that *in vivo* regulates the balance of proliferation to neurogenesis. Addition of DAPT, a pharmacological inhibitor of signalling downstream of Notch receptor, led to significantly increased proportion of cells differentiating into Crx-expressing photoreceptor precursors as well as Pax6+/Islet1+ retinal ganglion cells (Osakada et al., 2008), in accordance with observations in other systems (Jadhav, 2006; Nelson et al., 2007; Riesenberg et al., 2009; Yaron, 2006). In such cultures the proportion of cone photoreceptor precursors generated was high, approximately 11% of both S and M opsin-expressing cells. However, the Rhodopsin-positive cells were infrequent, around 5%. To enhance rod differentiation, effects of a range of relevant soluble regulators were tested. From the examined panel acidic and basic FGFs (aFGF and bFGF), taurine, Sonic hedgehog (Shh) and retinoic acid (RA) were found to further increase the number of Rhodopsin-positive cells. In combination all these molecules triggered Rhodopsin immunoreactivity in over 17% of cells, without significantly increasing the abundance of Crx-positive cells in culture (Osakada et al., 2008, represented schematically in Diagram I.XII. C). Photoreceptor precursors differentiated this way showed expression of a panel of cone and rod maturation markers such as Recoverin, Arrestins (Arr1 and Arr3), Retinol-binding protein (IRBP) and photoreceptor Phosphodiesterases (Pde6c and Pde6b; Osakada et al., 2008). In conclusion, this study marked a significant step towards establishing defined culture conditions for mESC retinal differentiation and identified soluble molecules that stimulate the acquisition of mature rod marker expression.

Reports described so far demonstrated derivation of maturing photoreceptor precursors from mESC in a stepwise manner. In a landmark study from the Sasai laboratory authors went one step further and achieved not only stepwise differentiation but also recapitulation of retinal morphogenesis *in vitro* (Eiraku et al., 2011). Similar to the preceding method embryoid bodies were formed from pluripotent mESCs. In this study these were generated by a modified SFEB method with quick re-aggregation in a very low binding 96-well plate. Round EBs were supplemented with basement membrane components mixture matrigel on day 1 to prompt formation of rigid continuous epithelial structures. Aggregates were next cultured under low growth factor conditions in a serum-free medium (graphically presented in Diagram I.XII. C). This initial neural induction led to expression of Rx-GFP reporter in between 30 to 70% of cells in culture. During the first week of culture this retinal neuroepithelium formed hollowed spheres, which by day 7 formed hemispherical vesicles evaginating from the aggregate. Most remarkably, from day 8 the distal part of these vesicles flattened and then invaginated forming a cup shape. Cells in the proximal part of the vesicle expressed lower levels of Rx and turned on Mitf, a marker of retinal pigmented epithelium, whereas the distal portion remained strongly positive for Rx and expressed additional neural retinal markers Pax6, Six3 and Chx10/Vsx2. The optic cup formed *in vitro* contained the thick invaginated neural retina epithelium in the inner portion surrounded by a rigid outer shell of RPE precursors. Notably, the invagination phenomenon occurred without the overlying surface ectoderm or lens, but was supported by the presence of the RPE (Eiraku et al., 2011), indicating that an intrinsic self-organisation mechanism operates in the developing optic vesicle to drive morphogenesis of the optic cup (Eiraku et al., 2012) and acquisition of neural retina and RPE domains. In the optic cups derived from mESCs, retinal progenitors showed frequent divisions exhibiting interkinetic nuclear migration as seen *in vivo*. These progenitors subsequently generated all the cell types found in the developing retina *in vivo* including rod and in very low frequencies cone photoreceptors. Generation of various neuronal cell types followed the sequence of retinal neurogenesis *in vivo* with cell-birth analysis showing peak of ganglion cells genesis around day 10 in culture followed by rod precursors from day 16 and bipolar cells from day 18. Moreover, addition of Notch inhibitor DAPT to cultures at day 16 triggered increased generation of Crx-expressing photoreceptor cells. On day 24 the isolated mESC-generated neural retina showed clear lamination with an apically located photoreceptor layer, interneuron layer underneath and scattered ganglion cells at the basal side (Eiraku et al., 2011) similar to the organisation of the early post-natal retina. Longer term culture did not show outer segment formation, however in a later study from the Roska group

forced expression of members of the sensory organ-specific microRNA cluster miR-182 and miR-183 induced formation of short outer segments in this system (Busskamp et al., 2014). In conclusion, this report showed nearly complete recapitulation of retinal morphogenesis *in vitro* and opened new possibilities for developing retinal cell therapy.

I.IV.IV.IV. Transplantation of mESC-derived photoreceptor precursors

Studies using photoreceptor precursors derived from donor mice indicated two parameters key for successful transplantation: (1) appropriate donor cell population at the right stage of development and (2) sufficient quantities of donor cells. Only post-mitotic photoreceptor precursors show significant integration capacity, especially when harvested at the early post-natal peak of rod birth (MacLaren et al., 2006; Pearson et al., 2012). Efficient integration also requires a relatively high number of photoreceptors to be placed into the subretinal space of the recipient mouse (200,000 rod precursors was found necessary to observe robust integration; Pearson et al., 2012). These two considerations presented a significant challenge for using mESC-derived photoreceptor precursors in developing cell therapy approaches for retinal degenerations.

The first study to examine the integration capacity of mESC-derived retinal cell types was the report from Takahashi and Sasai groups (Ikeda et al., 2005). In this study differentiation of Rx+/Pax6+ retinal progenitors in SFEB mESC culture was limited and few cells expressed Crx. However, the authors tested the ability of the retinal cells obtained according to this protocol to integrate into donor retinae in organotypic culture. A drop of dissociated mESC-derived retinal differentiation culture was placed on a membrane filter and covered by dissected E17.5 embryonic retina scleral side towards the filter. After 12 days of co-culture an average of over a hundred labelled mESC-derived cells migrated into multiple layers of the explant including the outer nuclear layer, in which around 10% of cells were found. Cells in the photoreceptor layer had characteristic photoreceptor morphology and expressed Rhodopsin (Ikeda et al., 2005). This report therefore provided a proof of concept that mESC derived cells are capable of migration into the host retina and expression of mature markers in that environment.

Development of iPSC technology allowed Tucker and colleagues to derive an iPSC line from an adult dsRed mouse dermal fibroblast biopsy (Tucker et al., 2011). This line was subjected to a retinal differentiation protocol using a cocktail of soluble molecules including Noggin, Dkk-1, IGF-1, bFGF, aFGF and DAPT. These defined culture conditions yielded over a third of total cells expressing Crx at day 33 of differentiation and more than 10% of cells immunoreactive for Rhodopsin. Glutamate

stimulation of these cells evoked intracellular calcium responses characteristic of retinal neuron physiology. Transplantation of whole dissociated cultures led to formation of teratomas in the majority of adult recipient mice likely due to presence of undifferentiated stem cells. Accordingly, depletion of SSEA1-expressing stem cells through magnetic bead-based cell sorting (MACS) prevented teratoma formation. DsRed-positive miPSCs-derived retinal cells were then transplanted into a model of severe retinal degeneration the Rhodopsin knockout (*Rho*$^{-/-}$). Around 16,000 of the 250,000 transplanted cells survived and formed patches of repopulated photoreceptor layer showing expression of mature markers such as Rhodopsin, Recoverin and ROM1. Some dsRed-positive cone opsin-expressing cells were also identified. Basal processes of these cells showed signs of connectivity with inner nuclear layer neurons as determined by staining with the synaptic markers Synaptophysin and Bassoon. Finally, ERG recordings showed signs of increased light-evoked electrical activity with increased b-wave amplitude. It is important to note however, that b-wave derives primarily from interneuron activity and detailed analysis with gene therapy vectors showed that reliable and reproducible recordings can only be obtained from at least 120,000 functional rod photoreceptors in the *Gnat1*$^{-/-}$ model of stationery night blindness (Pearson et al., 2012). Nevertheless, this study demonstrated that mESC-derived cells are capable of survival and maturation following transplantation into a severe retinal degeneration model.

An adaptation of the SFEB DLFA differentiation method further examined the importance of the differentiation niche for generation of integration-competent photoreceptor precursors (West et al., 2012). In order to scale up the differentiation process to suit the transplantation demands, optimal cell density was determined for generation of Rx-GFP+ retinal progenitors in embryoid bodies formed from this mESC line in 96-well plates. From day 10 FACS-purified Rx-GFP+ cells were cultured in adherent 2D conditions on poly-lysine, laminin and fibronectin-coated plates. All major retinal cell types developed in these cultures including Brn3+ retinal ganglion cells, Calbindin+ horizontal neurons, S opsin+ cone cells, Rhodopsin+ rod photoreceptors, PKC+ bipolar cells and GFAP+ Müller glia in a temporal order consistent with their *in vivo* generation. When the sorting of Rx-GFP+ cells step was omitted the efficiency of Crx+ photoreceptor precursors was significantly diminished, suggesting the importance of the retinal differentiation niche. Even with the Rx-GFP-sorted populations levels of *Nrl* expression in these cultures were markedly lower than at comparable stages *in vivo*, despite relatively high transcription of the early photoreceptor marker *Crx* (nearly half of that in P0 retina). Consistently, few cells in

culture expressed an Nrl-RFP reporter. Mixed populations of retinal cells at day 28 in culture labelled with an AAV vector carrying a GFP reporter under the control of the ubiquitously expressed CMV promoter did not give rise to photoreceptor integration when transplanted into adult mice. Collectively, these results highlighted that some critical features of the photoreceptor differentiation niche were missing in this 2D differentiation method.

In 2011 the groundbreaking study from the Sasai laboratory demonstrating recapitulation of optic cup morphogenesis in 3D mESC culture (Eiraku et al., 2011) opened brand new opportunities for the development of cell-based therapies in the retina. Researchers from the Ali group successfully adapted this differentiation protocol to efficiently obtain rod precursors for transplantation by removing the need for manual excision of mESC-derived optic tissues, supplementing maturation medium with retinoic acid and taurine that promote rod differentiation (Hyatt et al., 1996; Kelley et al., 1994; Osakada et al., 2008; Wallace and Jensen, 1999) and developing the protocol for labelling, isolation and purification of mESC-derived rod precursors in large numbers (Gonzalez-Cordero et al., 2013). In this study a thorough examination of rod development in these cultures was performed including microarray analysis comparing mRNA profile of mESC-derived rod precursors with their donor-derived counterparts. These analyses revealed that cultures at d26 are equivalent to P4-6 mouse retinae and that day 36 resembles P10-12 when outer segment biogenesis occurs. Despite expression of outer segment development markers such as Gnat1 and Peripherin2 and presence of mitochondria-filled inner segments and typical photoreceptor cilium structures, no outer segment formation was found *in vitro*. Developing rods were labelled using rAAV2/9 viral vector encoding a *Rhodopsin* promoter driving reporter GFP expression. 200,000 GFP+ cells purified by FACS were transplanted into the *Gnat1*$^{-/-}$ model of retinal degeneration, which allowed the observation of outer segment formation *in vivo* following migration and integration of cells into the host retina. Remarkably approximately 80% of cells found engrafted in the recipient photoreceptor layer showed Gnat1-positive segment formation. This experimental paradigm also excluded the possibility of vector carry-over in the cell preparation, which could lead to false-positive results. Unsorted dissociated cells caused significant false-positive labelling, which was not observed following FACS. In addition to the *Gnat1*$^{-/-}$ model, GFP-positive rods also integrated into the *Rho*$^{-/-}$ and the *Prph2*$^{rd2/rd2}$ knockout models, in each case expressing the missing protein. Furthermore integrated cells showed intracellular calcium responses very similar to endogenous photoreceptors (Gonzalez-Cordero et al., 2013). In summary, this work showed unequivocally that mESCs can

provide a source of appropriately-staged and integration-competent rods that mature to form outer segment structures following transplantation into degenerate retina.

Another variation on the protocol developed by the Sasai laboratory came from the Arsenijevic group (Decembrini et al., 2014). Crx-GFP mESC line was derived and characterized in this study to provide a traceable population of photoreceptor precursors for transplantation. Differentiation of this cell line followed a very similar timecourse as described by Eiraku *et al*., in this case however, culture in hyperoxic conditions better supported healthy differentiation with a lower proportion of active caspase3-positive cells in the high oxygen condition. Synthetically generated Crx-GFP retinae recapitulated reporter expression found *in vivo* (Muranishi et al., 2010; Samson et al., 2009). A minor difference was a high percentage of Crx-GFP and RXRγ-expressing cone precursors, above 10% even at day 23 of differentiation (equivalent to P2-3), contrasting with the low percentages of cones reported in the two previous studies (Eiraku et al., 2011; Gonzalez-Cordero et al., 2013). Crx-GFP photoreceptor precursors were isolated at stages corresponding to early post-natal development using FACS and transplanted into the subretinal space of immune deficient NOD-SCID mice. Numbers of integrated cells were very close to those reported by Gonzalez-Cordero *et al*. suggesting that immune rejection does not pose a major limiting factor in this non-autologous transplant setting. In conclusion, this work further supported the finding that proper recapitulation of retinal morphogenesis is essential for generation of integration-competent photoreceptor precursors.

In summary, stepwise differentiation of mESCs provided a renewable source of retinal cells for the study of photoreceptor replacement. Studies using various protocols highlighted the need for recreating multiple aspects of retinogenesis since truly successful integration of mESC-derived photoreceptor precursors was only obtained when donor cells where isolated from cultures in which optic vesicle and optic cup morphogenesis were recapitulated.

I.IV.IV.V. Retinal differentiation and transplantation of human pluripotent stem cells

In parallel to the developments in differentiation of mESCs into retinal lineages there has been intense investigation into the development of protocols using pluripotent stem cell sources of human origin.

Studies from the Reh group employed the idea of sequential specification to derive retinal cell lineages from human ESCs (Lamba et al., 2006) and to subsequently perform transplantation experiments using these cells (Lamba et al., 2009). Embryoid

bodies formed from hESCs were subjected to neural induction using a combination of Wnt antagonist Dkk-1, BMP antagonist Noggin and IGF-1, which similarly antagonises Wnt activity. During embryogenesis Dkk-1 and Noggin act as neural inducers (Smith and Harland, 1991) and IGF-1 is a head inducing factor. Notably, in *Xenopus* IGF-1 overexpression triggers the generation of ectopic eyes (Richard-Parpaillon et al., 2002). A brief 3 day suspension culture, followed by 3 weeks of differentiation in adherent cultures on poly-D-lysine and matrigel-coated dishes, was used to generate retinal cells (schematically depicted in Diagram I.XII. C). Noteworthy, the same developmental process takes around 10 weeks in the human foetus (O'Brien et al., 2003) and this enhancement could stem from unspecified signalling molecules present in matrigel. After this period around 80% of cells were retinal progenitors as determined by Pax6 and Chx10/Vsx2 immunostaining. Photoreceptor differentiation ensued with around 12% of cells expressing Crx and some cells positive for S cone opsin and Rhodopsin also detected. Co-culture of these hESC-derived progenitors with wild-type mouse retinal explants and explants from *Aipl1*$^{-/-}$ in which photoreceptors are rapidly lost in both cases led to increased photoreceptor differentiation of human cells (Lamba et al., 2006). This differentiation paradigm was also used to examine the transplantation of hESC-derived retinal cells. Delivery using the intravitreal route resulted in migration into recipient retinae only when injection was performed prior to P2. Human cells were found in all retinal layers including the outer nuclear layer, in which reporter-expressing cells positive for Recoverin and S opsin were found. Transplants into adult mice were performed into the subretinal space, where the cells survived for at least 3 weeks without being rejected by the host immune system or forming teratomas. Apparent integration into the photoreceptor layer was observed, however the morphology of the integrated cells resembled that of host photoreceptors. NRL antibody specific for the human protein was used to assess the number of cells differentiating into photoreceptors and their integration. An average of nearly 3,000 cells (~4.5% of all transplanted cells) were NRL+ in the injected eyes, including some located in the outer nuclear layer. Retinal cells derived from this differentiation protocol were transplanted into the *Crx*$^{-/-}$ model of inherited retinal degeneration, where the cells engrafted into the host photoreceptor layer but did not extend outer segments, which are lacking in this model. Noteworthy, Crx expression in donor cells was not confirmed by immunostaining in that location. With only a modest number of cells surviving a small increase in B-wave amplitude in electroretinograms of eyes that received the transplants was reported and the number of remaining cells strongly correlated with the magnitude of the B-wave response amplitude (Lamba et al., 2009). Whilst this study highlighted the possible feasibility of using hESCs as a donor material source for

cell therapy in the retina, a more detailed examination of human photoreceptor precursor transplantation is clearly required.

Since then the focus has shifted towards establishing differentiation protocols that closer resemble the temporal aspects of human retinal development, as well as better defined culture conditions for more clinically-relevant protocols (Borooah et al., 2013). The Gamm group developed a differentiation approach mimicking the timing of human embryonic development without the use of extrinsic signalling factors (Meyer et al., 2009). In this differentiation paradigm floating aggregates of hESCs were left to adhere to laminin-coated plates on which they formed neural rosettes. On day 16 these were manually dissected and subsequently grown as neurospheres. Cells in neurospheres acquired expression of eye field transcription factors Rx, Six3, Six6, Lhx2 and Tll. Forebrain marker Otx2 was also detected. Co-expression of Rx and Pax6, which is characteristic of the eye field appeared in the majority of cells. These neurospheres endogenously expressed Wnt antagonist Dkk-1 and BMP antagonist Noggin and their later differentiation into neural retina required FGF signalling (graphically represented in Diagram I.XII. C). Retinal progenitors that initially expressed Mitf and then switched on Chx10/Vsx2 expression formed in culture between days 20 and 40. Both neural retina and the RPE could be derived from these hESCs cultures with RPE differentiation in adherent conditions and neural retina developing in the suspension culture of neurospheres. Around a fifth of neurospheres showed retinal phenotype with more than half of the cells expressing the early photoreceptor marker Crx at day 80 of differentiation. Some of the Crx-positive cells also expressed later markers such as Recoverin and cone opsin. Importantly, similar differentiation could also be achieved using an iPSC line. Hence, this study showed close stepwise recapitulation of the *in vivo* human retinal histogenesis.

Work from the Sasai and Takahashi groups investigated the use of defined conditions to induce retinal specification in monkey and human ESCs (Osakada et al., 2008). Authors optimized the SFEB method with addition of DKK-1 and LEFTY-A (WNT and NODAL antagonists, respectively) at the initial neural induction stage. In the case of human cells, hESCs were initially dissociated into small clumps, which were subjected to the differentiation in suspension culture for the first 20 days, followed by plating on poly-D-lysine/laminin/fibronectin-coated slides. In these adherent cultures both RPE and neural retina differentiation occurred. 15% of colonies were RX+-PAX6+ indicating the appearance of retinal progenitors. Differentiation of photoreceptors was stimulated by addition of retinoic acid, taurine and N2 supplement for the rest of the culture period (schematic of differentiation protocol in Diagram I.XII. C). More than 10% of cells

became CRX+ by day 120 increasing to nearly 20% by day 170. A relatively high proportion of S- and L/M-opsin-expressing cone precursors were observed (approximately 9% of cells each) and around 5% of cells expressed the rod visual pigment Rhodopsin. Other phototransduction-related genes began to be expressed at these later stages as well. Altogether, these analyses indicate, that it is possible to derive photoreceptor precursors from hESCs using defined culture conditions.

In parallel to their work on inducing mouse optic cup formation in mESC retinal differentiation cultures, the Sasai group applied similar principles to demonstrate that not only step-wise lineage commitment, but also 3D tissue morphogenesis of human retinal tissue can be recapitulated *in vitro* (Nakano et al., 2012). Human ESCs differ in several characteristics from their mouse counterparts and therefore triggering retinal tissue formation was not a trivial task. Firstly, hESCs are prone to dissociation-induced apoptosis, which had to be prevented by use of a ROCK inhibitor Y-27632. Secondly, hESCs did not show high propensity to form retinal neuroepithelia under low-knockout serum concentration conditions used for mESCs differentiation. KSR content in the initial stages of culture had to be increased to 20%, which caused undesired caudalizing effects. This caudalizing activity of KSR was prevented through addition of Wnt inhibitor IWR1-endo (IWR1e). Further retinal differentiation was supported by addition of 10% FBS and treatment with the Hedgehog agonist smoothened agonist (SAG; culture approach depicted in Diagram I.XII. C). This differentiation paradigm showed efficient (70% of cells) generation of RX+ retinal progenitors, which later expressed Chx10 (Vsx2), in contrast RPE differentiation was poor. To achieve balanced formation of both RPE and neural retina, timely treatment with the Wnt agonist CHIR99021 (GSK3b inhibitor) during days 15–18 of culture was required. With this improvement formation of localized, thick retinal neuroepithelia surrounded by MITF+ RPE progenitors was observed, followed by evagination of optic vesicle-like structures, which by day 19-24 formed through invagination of a bi-layered optic cup structure. Human ESC-derived optic cups were much larger than the mouse ones. An important observation regarding later development of these hESC-derived retinae was that the differentiation of cone photoreceptor precursors was much more prominent than in the mouse cultures with colour opsins detected from day 126. Importantly from a clinical application perspective, methods of cryopreservation of hESCs-derived optic tissues were developed and assessed. A vitrification method with pre-treatment in 10% DMSO + 5% ethylene glycol (EG) + 10% sucrose on ice was found to be most effective for NR cryopreservation (Nakano et al., 2012). Taken together, these results showed that self-driven retinal morphogenesis can be triggered in hESCs.

In many species retinogenesis is driven by two populations of progenitors: sequentially lineage restricted progenitors of the neural retina and the stem cell-like progenitors of the ciliary margin zone. Presence of a stem cell niche in the retinal periphery is a matter of ongoing debate in the field due to the difficulty in performing relevant experiments using primary human tissue. Another study from the Sasai group employed hESCs self-organisation potential to generate a ciliary margin-like stem cell niche from hESCs (Kuwahara et al., 2015). Optimization of initial retinal lineage induction was performed using a human ESCs Rx:Venus knock-in line. Aggregates grown in chemically defined culture medium without Matrigel and treated with a low concentration of BMP4 from day 6 showed potent Rx:Venus fluorescence induction. Later differentiation was supported by addition of 10% FBS, retinoic acid and taurine. In these conditions neural retinal differentiation was prominent. To generate neural retina aggregates also containing an RPE domain, cultures were transiently treated with Wnt agonist GSK3 inhibitor CHIR99021 in combination with FGF signalling inhibitor SU5402 between days 18 and 24. This resulted in the formation of a tapered distal neural retinal domain surrounded by RPE cells. This niche expressed markers of the ciliary margin zone such as Aquaporin1, Otx1, Zic1, Rdh10 and the stem cell marker SSEA1. Cells in that region showed high proliferative capacity shown by dilution of nucleotide analogues BrdU and EdU. Addition of these analogues also revealed progressive displacement of postmitotic cells towards the central portion of the hESCs-derived retina. Therefore, hESCs induced towards retinal lineage in a chemically defined fashion can generate a ciliary margin-like stem cell niche.

The remaining challenge in the differentiation of human pluripotent stem cells was the derivation of maturing photoreceptors forming outer segments and showing light-sensitivity. This goal was achieved by researchers from the Canto-Soler group (Zhong et al., 2014). Through modification of the protocol developed by J. Meyer and D. Gamm, optic vesicles showing expression of eye field and later early neural retina markers were obtained from hiPSCs. These vesicles formed cup-shaped structures in adherent cultures on matrigel-coated dishes (see Diagram I.XII. C). Using manual dissection these were detached and further cultured in suspension as neural retinal cups. Neural retina cups at this stage also contained some RPE tissue bundled at the tip, which matured to become highly pigmented in the following culture period. Within the optic cups retinal progenitors were dividing producing retinal neurons and showing interkinetic nuclear migration typical of early retinogenesis. To stimulate survival and maturation of photoreceptor precursors in the isolated floating cups addition of FBS with retinoic acid and taurine was necessary. With such culture conditions it was

possible to maintain the neural retina tissue for extended periods. With time retinogenesis *in vitro* progressed with neurons generated in an order mimicking the conserved sequence of neurogenesis *in vivo*, whereby initial differentiation of retinal ganglion cells (BRN3B+, from week 6) was followed by genesis of photoreceptors (OTX2+, from week 7), amacrine and horizontal cells, up to formation of late born cell types the bipolar cells (VSX2+/MCM2+, from week 18) and finally formation of Müller glia (CRALBP+). Therefore all major retinal cell types were present following around 23-week culture period, with timing of development resembling temporal aspects of human foetal development. The first clear expression of Rhodopsin and S-opsin was detected at week 17, which increased to being observed throughout the prospective photoreceptor layer by week 21. Distal apical processes of developing photoreceptors formed inner segments, connecting cilia and outer segment buds with membrane stacks as determined by electron microscopy. Immunohistochemistry showed expression and localization to distal apical segment-like buds of a panel of phototransduction-related proteins including the GTPase Gta-1, phosphodiesterase PDE6a/b, cation channel subunits CNGA1 and CNGB1 and guanylate cyclase RetGC1. Electrophysiology was employed to test if this expression correlated with light-sensitivity. Perforated patch-clamp recordings determined that out of 13 cells analysed 2 showed appropriate light-evoked response. In summary, this study showed that human iPSCs can provide a source of physiologically-relevant retinal tissue with photoreceptors showing onset of outer segment biogenesis and light responsiveness.

In conclusion, progress with human pluripotent stem cell culture yielded reports showing efficient formation of photoreceptor precursors that mature to the initial stages of functionality and protocols that use defined culture conditions are rapidly improving. Together these advances show promising prospects for clinical development of retinal cell therapy approaches.

II. Methods of molecular biology

II.I. DNA analysis

Table 1 below lists all constructs used in this study.

Table 1. List of DNA constructs

Plasmid name	Promoter/s	Gene/s of interest	Used for
Lenti.CMV.Onecut1.IRES.GFP	CMV, IRES	Onecut1, GFP	Lentiviral vector production
Lenti.CMV.GFP	CMV	GFP	Lentiviral vector production
Lenti.Olig2.GFP	Olig2*p*	GFP	Lentiviral vector production
AAV2/9 cap	ITR	AAV2/9 rep cap	AAV vector production
ShH10 cap	ITR	ShH10 rep cap	AAV vector production
PHGTI	P5	E4, E2a, VA	AAV vector production
pD10.2.1.GFP	2.1*p*	GFP	AAV vector production
pD10.U6.shControl.CBA.RFP	U6, CBA	shControl, RFP	AAV vector production
pD10.U6.shNrl.CBA.RFP	U6, CBA	shNrl, RFP	AAV vector production
pD10.U6.shNr2e3.CBA.RFP	U6, CBA	shNr2e3, RFP	AAV vector production
pD10.Rhop.RFP	Rho*p*	RFP	AAV vector production
Lenti.Nrl	CMV	Nrl	Overexpression
Lenti.Nr2e3	CMV	Nr2e3	Overexpression

II.I.II. Nrl and Nr2e3 knockdown constructs

Artificial miRNAs targeting the coding sequence of mouse *Nrl* and *Nr2e3* genes were designed using siDESIGN software (Dharmacon). Candidates with highest scores and lowest predicted off-target effects were synthesised. Oligonucleotides coding the miRNA cassette were ligated into U6 plasmid designed for miRNA expression. Positive colonies after transformation were checked by restriction digestion (with *Asc*I and *Sna*BI enzymes) and sequencing. Correct clones were used to evaluate knockdown efficiency in 293T cells by qPCR.

Nrl knockdown target sequences and the short hairpin sequences synthesised were as follows:

sh-Nrl-1 target sequence

5’-GATTTGATGAAGTTCGAAA-3’

short hairpin cassette oligonucleotides sequences:

5’ – TTTGGCGAGATTTGATGAAGTTCGAAACTGTGAAGCCACAGATGGGTTTCGA ACTTCATCAAATCCTGCTTTT-3’

and

5’ – CTAGAAAAGCAGGATTTGATGAAGTTCGAAACCCATCTGTGGCTTCACAGTTTCGAACTTCATCAAATCTCGC -3’

sh-Nrl-2 target sequence

5’-GGGTCCTGTCTCTATGGAA-3’

short hairpin cassette oligonucleotides sequences:

5’ – TTTGGCGAGGGTCCTGTCTCTATGGAACTGTGAAGCCACAGATGGGTTCCATAGAGACAGGACCCCTGCTTTT-3’

and

5’ – CTAGAAAAGCAGGGGTCCTGTCTCTATGGAACCCATCTGTGGCTTCACAGTTCCATAGAGACAGGACCCTCGC -3’

Target sequences and miRNA cassette sequences of two candidates that showed substantial reduction of *Nr2e3* levels are as follows:

sh-Nr2e3-1 target sequence

5'-GGACAGCAGCAGTGGGAAA-3',

short hairpin cassette oligonucleotides sequences:

5’-TTTGGCGAGGACAGCAGCAGTGGGAAACTGTGAAGCCACAGATGGGTTTCCCACTGCTGCTGTCCCTGCTTTT-3’

and

5’–CTAGAAAAGCAGGGACAGCAGCAGTGGGAAACCCATCTGTGGCTTC

ACAGTTTCCCACTGCTGCTGTCCTCGC-3’

miR-Nr2e3-3 target sequence
5'-CGCC GAAACTTGTGCTAAA-3'

short hairpin cassette oligonucleotides sequences:
5’TTTGGCGACGCCGAAACTTGTGCTAAACTGTGAAGCCACAGATGGGTTTAGCACAAGTTTCGGCGCTGCTTTT-3’
and
5’-
CTAGAAAAGCAGCGCCGAAACTTGTGCTAAACCCATCTGTGGCTTCACAGTTT
AGCACAAGTTTCGGCGTCGC-3’

sequences forming the hairpin regions are underlined.

II.I.III. Transformation and isolation of plasmids

Alpha-Select Gold (Bioline Ltd., UK) chemically competent cells were used for plasmid transformation. Cells were thawed on ice, subsequently ligation solution was added and incubated on ice for 30 minutes. Next, the sample was heat-shocked for 45 seconds at 42°C in a heat block, then quickly transferred on ice for 2 minutes and diluted in 100 µl of S.O.C. medium (Super Optimal broth with Catabolite repression, Life Technologies Ltd., UK). The sample was then transferred to incubation at 37°C at 225 rpm rotation. This allowed for expression of ampicillin antibiotic resistance gene prior to selection. Samples were spread on selective LB agar plates containing ampicillin. Plates were prepare by diluting 12.5 g of LB broth powder (Luria Bertani, Sigma-Aldrich Ltd., UK) and 7.5 g of bacteriological agar (Sigma-Aldrich Ltd., UK) in 500 ml of distilled water. Ampicillin for antibiotic resistance selection was added at 100 µg/ml (Sigma-Aldrich Ltd., UK). Inoculated plates were incubated overnight at 37°C allowing growth of antibiotic-resistant bacterial colonies.

Following day, single, isolated colonies were picked and bacteria expanded by inoculation of 5 ml of LB broth (Life Technologies Ltd., UK) containing 100 µg/ml ampicillin (Sigma-Aldrich Ltd., UK) and incubation overnight at 37°C. For further analysis, plasmids were recovered using Invitrogen mini-prep kit (Life Technologies Ltd., UK) following manufacturer’s protocol. Large scale preparations were obtained

by adding 50 µl of the 5 ml overnight culture to 500 ml of 5 ml of LB broth (Life Technologies Ltd., UK) containing 100 µg/ml ampicillin (Sigma-Aldrich Ltd., UK). Bacterial cultures were grown overnight at 37°C at 225 rpm rotation. If highly recombinogenic plasmid were used, bacteria were grown at 30°C for 48 hr instead.

II.I.IV. DNA electrophoresis

Electrophoresis was utilized to assess the size of DNA fragments. Gels were prepared from 1 to 2% (w/v) agarose dissolved in TBE buffer (Life Technologies Ltd., UK), depending on the expected fragment sizes. Ethidium bromide (at 0.2 µg/ml) or SafeView dye (at 0.25 µl/ml; NBS Biologicals Ltd., UK) were used to visualize the nucleic acid bands. Loading buffer (5x; Promega Corp., USA) was used to increase sample density for loading onto wells. 1 kb DNA ladder (Promega Corp., USA) was run simultaneously to allow band size comparison. Voltage was set at 180 V. UV transilluminator with a camera was used to photograph gels.

II.I.V. DNA isolation and purification from agarose gels

Fragments required for subsequent ligation were excised from agarose gels and DNA extracted using QIAquick™ Gel Extraction Kit (QIAGEN Ltd., UK) according to manufacturer's instructions. Concentration of the eluted DNA was measured on NanoDrop® ND-1000 spectrophotometer (LabTech Int., UK).

II.I.VI. Ligation reactions

Ligation of DNA fragments extracted from agarose gels was carried out at 15°C overnight in a thermal cycler using T4 DNA ligase (New England Biolabs Inc., USA or Promega Corp., USA) with the supplied buffer. Insert to backbone ratios and quantities were adjusted following manufacturer's guidelines to achieve final volume of 20 µl per reaction. Successfully ligated plasmids were identified following transformation of competent bacteria (as describe above). Ligation was confirmed by appropriate restriction digests. For long term storage of obtained DNA constructs bacterial suspension from overnight culture in LB broth (800 µl) was mixed with glycerol (200 µl; Sigma-Aldrich Ltd., UK) and transferred to -80°C.

II.I.VII. Sequencing

DNA sequences were obtained using Beckman Coulter Cogenics sequencing service (Beckman Coulter Inc., UK).

II.II. Viral vectors

II.II.I. Lentiviral vectors

Lentiviral vectors are engineered wild-type lentiviruses, a group of retroviruses with human immunodeficiency virus (HIV) being the most prominent member. Lentiviruses deliver to infected cells single stranded RNA that is reverse-transcribed into cDNA and then integrated stably into the host genome. In contrast to other groups of retroviruses, lentiviruses can integrate even when the nuclear envelope of the host is intact, stably transducing also non-dividing cells. Second generation HIV-based lentiviral vectors were used in this study. Vector were made using a three plasmid system developed to minimise the risk of emergence of replication competent viral particles. As a packaging helper plasmid pCMV Δ R8.74 (11,921 bp) was used containing sequences of *gag*, *pol*, *tat* and *rev* allowing production of respective viral proteins. Original HIV accessory genes *vpr*, *vif*, *vpu* and *nef* were either rendered inactive or deleted altogether. The construct was engineered for optimised expression and vector production. Lentiviral particles were pseudotyped with vesicular stomatitis virus G (VSV-G) envelope delivered using pMD2.G (5,824 bp) plasmid. The transfer vector either encoded CMV promoter driving GFP expression or CMV promoter driving mouse Onecut1 cDNA sequence followed by internal ribosome entry site (IRES) allowing the expression of a GFP reporter from the same transcript. Transgene expression was boosted by inclusion of a downstream enhancer the woodchuck hepatitis virus posttranscriptional regulatory element (WPRE).

Vectors were produced in HEK 293T cells maintained in DMEM with Glutamax (Thermo-Fisher Scientific Ltd, UK) supplemented with 10% heat-inactivated fetal bovine serum (FBS; Thermo-Fisher Scientific Ltd, UK) and antibiotic-antimycotic solution at 100x dilution (Thermo-Fisher Scientific Ltd, UK). Cells were plated on 150 mm diameter Nunc cell culture dishes (145 mm^2 culture surface; Thermo-Fisher Scientific Ltd, UK). To maintain high transfection efficiency cells were split frequently (three times a week). Around 72 hours prior to transfection, cells were seeded at 2.5 x 10^6 per plate (approximately 1 to 7 split of a confluent plate). Usually 10 plates were seeded for one vector preparation. An hour before transfection medium was aspirated and replaced with 25 ml of fresh pre-warmed medium. Transfection mixture was prepared containing 1300 µl of OPTI-MEM medium (Thermo-Fisher Scientific Ltd, UK) in which 80 µg of total plasmid DNA and 112.5 µg polyethylenimine (PEI; MW 40,000, Polysciences, Germany) were dissolved, giving a PEI to DNA ratio of 2.25 to 1. PEI working solution was used at 2 mg/ml, prepared in water with pH adjusted to 7.4 using

HCl, kept at -20°C before use. Three plasmids encoding transfer gene, envelope and helper sequences were mixed at a molar ratio of 50:17.5:32.5. Transfection mix was incubated at room temperature for 20 minutes to allow formation of DNA-PEI complexes. Following incubation the transfection mix was added drop-wise to the plates. 4-6 hours following transfection medium was removed and changed for 22 ml of fresh pre-warmed medium. Approximately 48 hours later, medium was collected and replaced with the same volume of fresh medium for harvest next day at 72 hours post-transfection. Collected supernatant was centrifuged at 3500 x g for 10 minutes to pellet cell debris and then passed through a 0.45 µm membrane filter (Stericup 500 ml filter unit; Merck Milipore Ltd, UK) and kept on ice for concentration.

Medium harvested from cells at 48 hours post-transfection contained 10^5-10^6 viral particles per ml and in order to concentrate the vector preparation ultracentrifugation was employed. The supernatant with vector particles was transferred into UltraClear 38.5 ml polyallomer ultra-centrifuge tubes (Beckman Coulter, UK) and centrifuged at 23,000 rpm for 1 hour 45 minutes in a Beckman SW 32 Ti rotor (Beckman Coulter, USA), this corresponded to an average relative centrifugal force of 64,965 x g. Following centrifugation, supernatant was decanted and the tube placed upside down on a layer of Whatman paper for 10-15 minutes to remove the remaining liquid. Next, 100 µl of DMEM medium was added to the bottom of the tube and carefully pipetted several times to dislodge and resuspend the viral pellet, top of the tubes was sealed off with parafilm (VWR Ltd, UK) and the tubes were placed on ice and left for around 30 minutes to allow viral particles to dissolve in the medium. After the incubation, medium containing the vector was pipetted up and down several times again to mix and collected from all the tubes, pooled together and aliquoted into 1.5 ml Eppendorf tubes (VWR Ltd, UK) for storage at -80°C. From a typical 10 plate preparation approximately 600 µl of vector solution was obtained containing 10^8-10^9 infectious virus particles per ml. To assess the virus titer serial dilutions of vectors (from 10^3-10^8) were added to 293T cells seeded on a 24-well plate. Transduced cells expressing the GFP reporter were counted in two suitable dilution steps and averaged.

II.II.II. Adenovirus associated viral vectors

Constructs encoding human red-green opsin promoter (2.1 kb fragment) driving green fluorescent protein reporter (Coneopsin.GFP) and bovine rhodopsin promoter driving red fluorescent protein reporter (Rhop.RFP) were available in the laboratory. Expression patterns from both promoters have been previously characterized in the retina (Wang et al., 1992). Coneopsin.GFP promoter vector was courtesy of J. Nathans. Knockdown constructs targeting mouse Nrl and Nr2e3 genes with an RFP

reporter were cloned and amplified as described in previous sections. Plasmid encoding ShH10 capsid was kindly provided by J. Flannery, other capsid and helper plasmids were available in the laboratory.

II.II.III. Recombinant AAV vectors production

Production of recombinant AAV vectors was carried out in HEK 293T cell line transfected with three plasmids encoding construct of interest, viral capsid and helper genes (on pHGTI plasmid). Appropriate plasmids were transfected using polyethyleneimine (PEI) to facilitate DNA uptake. HEK 293T cells were seeded onto 150 mm tissue culture plates (Greiner Bio-One Ltd., UK) at 10^6 cells per plate in DMEM Glutamax® (Life Technologies Ltd., UK) medium containing 10% foetal bovine serum (Life Technologies Ltd., UK) and penicillin, streptomycin and antifungal agent mix (Life Technologies Ltd., UK). The following day cells reached approximately 70% confluency. 20 plates of cells were prepared for a batch of virus. Transfection mixture was prepared using components listed below:

Table 2. Recombinant AAV production

Recombinant AAV production transfection	
Reagent	**Quantity**
DMEM	52.5 ml
Capsid plasmid	100 µg
pHGTI	30 µg
Transfer construct	100 µg
PEI	1.2 ml

Transfection solution was incubated at room temperature for 10 minutes and then 2.7 ml of it was added dropwise onto plates with cells (medium in which cells were growing was not removed at this point). The following day, medium was changed on HEK 293T plates. Cells were after that incubated for 48 hr to allowing production of viral vector particles. After 72 hr from transfection, cells were harvested by scraping off plates by the use of a cell scraper (Greiner Bio-One Ltd., UK). Medium with cells was collected in 50 ml Falcon tubes and spun down at 2000 xg for 5 minutes and resuspended in TD buffer pH 7.4. Release of viral particles from harvested cells and adequate lysis was facilitated by 3 cycles of freezing (in -80°C), thawing (at 37°C) and mixing on a vortex shaker for 5 minutes. This was followed by treating the cell lysate with 50 units of benzonase (Sigma-Aldrich Ltd., UK). This DNase was utilised to remove remaining free plasmid DNA. Cell lysate was subsequently centrifuged at 18000 xg and

supernatant filtered through membrane filters, first 5 µm pores, then 0.45 µm and, finally, 0.22 µm. Viral vector was purified from this supernatant by means of ion exchange fast protein liquid chromatography (FPLC). ÄKTA™ prime or ÄKTA™ pure (GE Healthcare Ltd., UK) FPLC apparatus was used to purify vector particles on anionic sephacryl S300 and a POROS 50HQ columns prior to elution using increasing salt gradient. This yielded approximately 20 mls of eluate which was concentrated on Vivaspin 4 columns (Sartorius AG., Germany) to a final volume of 250 µl. Viral preparation was aliquoted and stored at -80°C until use.

II.II.IV. Viral vectors titration

Concentration of copies of viral genome in ml of vector preparation was determined by quantitative real time PCR (for details please see following sections) using primers specific for viral inverted terminal repeat (ITR). Number of copies of viral genome was determined by comparison of amplification of samples with amplification of standards of known quantity of vector.

II.III. RNA analysis

II.III.I. Total RNA isolation

For extraction of mRNA from cultured cells, ESC-derived differentiated embryoid body aggregates, retinal tissue or FACS isolated cells RNeasy Mini or Micro Kits (QIAGEN Ltd., UK) were employed. RNA isolation was performed according to manufacturer's instructions. Concentration of isolated RNA was determined using spectrophotometry with a NanoDrop® ND-1000 machine (LabTech Int., UK). RNA samples were kept at -80°C.

II.III.II. cDNA synthesis

Synthesis of complementary DNA from RNA templates was performed using QuantiTect® Reverse Transcription Kit (QIAGEN Ltd., UK) following manufacturer's instructions. Per sample, 1 µg of template RNA was diluted to 12 µl, residual genomic DNA was removed by addition of 2 µl of genomic DNA elimination solution (gDNA Wipeout Buffer). This 14 µl sample was incubated at 42°C for removal of gDNA to take place. Subsequently, 1 µl of Quantiscript® reverse transcriptase, 4 µl of RT Buffer and 1 µl of RT Primer Mix (containing both random octamers as well as oligo-dT primers) were pre-mixed and added to each sample. The final volume of 20 µl of sample was then incubated at 42°C for 40 minutes to allow synthesis of DNA strands complementary to the template RNA. Reverse transcriptase was heat inactivated by 3

minute incubation at 95°C. Assuming high efficiency of the reaction, which results in generation of cDNA in 1:1 ration to template RNA, approximately 1 µg of cDNA was therefore made per sample. The cDNA was later stored at -20°C.

II.III.III. Reverse transcription PCR

Total RNA was isolated from samples of interest with RNeasy Mini of Micro Kit (QIAGEN Ltd., UK), reverse transcribed with QuantiTect Reverse Transcription Kit (QIAGEN Ltd., UK). Samples prepared this way was the amplified by PCR with GoTaq Green Hot Start Master Mix (Promega Corp., USA) using gene-specific primers. PCR amplification was set up using 12.5 µl of master mix, 9.5 µl of water, 1 µl each of forward and reverse primers (at 10 µM) and 1 µl of cDNA (at 50 ng/µl). Thermal cycling conditions were as follows:

1. Initial denaturation at 94°C for 2 minutes.
2. Denaturation at 95°C for 30 seconds,
3. Annealing at appropriate temperature depending on primers melting temperatures for 30 seconds,
4. Extension at 72°C for 1 minute, steps 2-4 repeated 35 times;
5. Final extension for 5 minutes at 72°C.

For each pair of primers used, annealing temperature was optimized but running a reaction with a temperature gradient. In every PCR reaction negative control lacking cDNA (replaced by water) was run alongside samples of interest. Results were visualised by agarose gel electrophoresis performed as described previously.

II.III.IV. Quantitative PCR

II.III.IV.I. Relative quantification with real-time PCR

For relative comparison of gene expression, 50 ng of cDNA prepared as described above was loaded per well of 96-well plate (Life Technologies Ltd., UK) mixed with 2x Fast Start TaqMan® Probe Master Mix (Roche Ltd., UK), gene-specific forward and reverse primers at a final 900 nM concentration and an appropriate hydrolysis probe binding to the amplified region at a final concentration of 250 nM (Roche Diagnostics Ltd., UK), all dissolved in DNase and RNase free water up to 20 µl final volume. Each cDNA samples was run in triplicate to obtain accurate measurements. The reactions prepared in this way were then run on an ABI Prism 7900HT Fast Real-time Sequence Detection System (Applied Biosystems Ltd., UK) equipped with SDS 2.2.2 software, provided by the manufacturer, which was used to analyse the amplification results.

From detected amplification curves Ct values were obtained for each sample. Expression levels were normalized to beta actin (*Actb* gene) mRNA levels for each sample to assess relative expression of particular genes in different experimental conditions. Cycling conditions were as follows 40 cycles of 95°C for 30 sec. and 60°C for 1 minute.

II.III.IV.II. Absolute quantification with real-time PCR

To assess the absolute number of transcripts present in each sample, a dilution series of plasmid DNA containing cDNA sequence for a particular mRNA was prepared, ranging from 10^2 to 10^{12} molecules. The number of molecules was calculated given known concentration and size of these plasmids. Amplification of these samples gave a standard curve. Number of molecules in samples was determined based on these standard curves. Water controls were set up for each primer-probe combination. All amplification reactions were prepared as previously described using reagents from Roche Diagnostics, including 2x Fast Start TaqMan® Probe Master Mix and FAM-labelled hydrolysis probes from Roche Universal Probe Library. Primers were designed to include the probe binding regions using online design software on Roche Diagnostics website (www.roche.com). Sequences of gene-specific primers as well as associated hydrolysis probes numbers are listed in Table X. Samples were run on an ABI Prism 7900HT Fast Real-time Sequence Detection System (Applied Biosystems Ltd., UK) as described previously.

Table 3. PCR primer list

Gene-specific primer details				
Gene name	Forward Primer (5'-3')	Reverse Primer (5'-3')	Amplicon size (bp)	Probe number
Actb	aaggccaaccgtgaaaagat	gtggtacgaccagaggcatac	100	56
Arr3	tgtgtttgttcaggagttcaca	aggccctgcttctgacagt	105	71
Calb1	aaggcttttgagttatatgatcagg	ttcttctcacacagatctttcagc	89	42
Cnga3	agaacagaagccaccagacg	cagtcagccagcggtagtaga	92	67
Cngb3	tggacaaagcatatgtctacagagt	cccagtaataaacacaggcgtta	87	02
Crx	ccccaatgtggacctgat	ggctcctggtgaatgtggt	89	64
Cyp26a1	ccggcttcaggctacaga	ggagctctgttgacgattgtt	125	17
Dio2	agcttcctcctagatgcctaca	ccgaggcataattgttacctg	106	47
Dio3	gttggtggtcggagaaggt	cagagcctcagcgagtgaa	93	49
Hes1	gccagctgatataatggagaaaa	ctccatgataggctttgatgact	127	83
Hes5	ccaaggagaaaaaccgactg	cttggagttgggctggtg	128	67
Gnat1	agagctggagaagaagctgaaa	tagtgctcttcccggattca	95	89

Nrl	ttctggttctgacagtgactacg	tgggactgagcagagagagg	77	53
Nr2e3	cagccagcctgtgaggtt	agaagctcaatgcgctcag	81	32
Oc1	ggagttccagcgcatgtc	cgacgttggacgtctgtg	123	64
Olig2	agaccgagccaacaccag	aagctctcgaatgatccttcttt	107	21
Opn1sw	ccccatcatctactgcttcat	gacacgtcagattcgtctgc	93	04
Opn1mw	atcgtgctctgctacctcca	tttctgttgctttgccactg	60	05
Pde6c	tgactgcctgtgacctgtct	ttgcaaccagaagtgctacct	72	09
Raldh1	caccatggatgcttcagaga	actttcccaccattgagtgc	108	40
Raldh3	tttggtggcttcaaaatgtct	acttctgtatattcagccagagca	71	53
Rara	ggagcttggaacctgcac	gaggatgccactcccaga	76	83
Rcvrn	caatgggaccatcagcaaa	cctcaggcttgatcattttga	71	67
Rho	acctggatcatggcgttg	tgccctcagggatgtacc	70	32
Rorb	gctgactgaggaagagattgc	atcagccaggctcggtct	69	82
Rxrg	cagaagtgcctggtcatgg	cctcactctctgctcgctct	82	82
Thrb2	atgcatctatgttggcatgg	gcttggctagcctcttgct	62	42

II.IV. Protein Analysis

II.IV.I. Immunohistochemistry

Tissue from stem cell aggregates or mouse eyes was frozen in OCT embedding matrix (Pyramid Innovation Ltd., UK) and sectioned at 18 µm on a Bright OTF 5000 cryostat (Bright Instruments Ltd., UK). Cryosections were thawed and rehydrated by adding PBS. For certain antibody stainings sections were treated with 1 or 4% paraformaldehyde solution for 10 minutes followed by a wash with PBS. Slides were blocked with a solution of 5% goat or donkey serum, 1% BSA, 0.1% Triton X-100 in PBS for 2 hours at room temperature. This was followed by 5 washes with PBS, after which primary antibodies were added dissolved in 1% BSA, 0.1% Triton X-100 in PBS and incubated overnight at 4°C. List of primary antibodies used in this study can be found in Table X. Following day slides were washed 5 times with PBS, before adding Alexa Fluor®-conjugated secondary antibodies (Life Technologies Ltd., UK) diluted 1:100-1:500 (depending on the primary antibody used) in 1% BSA, 0.1% Triton X-100 in PBS. Slides were incubated with secondary antibodies for 2 hours at room temperature. Subsequently, they were washed 3 times with PBS and nuclei counterstained with 4'-6-diamidino-2-phenylindole (DAPI; Sigma-Aldrich Ltd., UK) and mounted using coverslides and fluorescent microscopy mounting medium (DAKO Ltd., UK).

Table 4. Antibody list

Antigen	Host species	Dilution	Supplier
BrdU	rat	1 in 100	Abcam (ab6326)
Calbindin	rabbit	1 in 300	Millipore (AB1778)
Cleaved caspase 3	rabbit	1 in 50	Abcam (ab2302)
Cone arrestin	rabbit	1 in 250-500	Millipore (AB15282)
Crx	rabbit	1 in 500	Gift from C.Gregory-Evans
GFP	rabbit	1 in 300	Life Technologies (A-21311)
GFP	goat	1 in 300	(FITC-conj.) Abcam ab6662
Gnat2 (Gαt2)	rabbit	1 in 500	Santa Cruz (I-20; sc-390)
Histone H4K20me3	rabbit	1 in 500	Abcam (ab9053)
Ki67	rabbit	1 in 100	Abcam (ab15580)
M opsin	rabbit	1 in 500	Millipore (AB5405)
LaminB	goat	1 in 500	Santa Cruz (C-20; sc-6216)
Olig2	rabbit	1 in 100	Millipore (AB9610)
Onecut1	rabbit	1 in 100	Santa Cruz (H-100; sc-13050)
Otx1/2	rabbit	1 in 200	Abcam (ab21990)
RALDH1 (ALDH1A1)	rabbit	1 in 200	Abcam (ab23375)
RARα	rabbit	1 in 100	Santa Cruz (C-20; sc-551)
Recoverin	rabbit	1 in 500	Chemicon (AB5585)
Rhodopsin	mouse	1 in 1000	Sigma (O4886)
Ribeye (CtBP2)	mouse	1 in 500	BD Biosciences (612044)
RXRγ	rabbit	1 in 100	Santa Cruz (Y-20; sc-555)
RXRγ	rabbit	1 in 100	Abcam (ab15518)
S opsin	goat	1 in 100	Santa Cruz (H-17; sc-14365)
S opsin	rabbit	1 in 250-500	Millipore (AB5407)
Synaptophysin	mouse	1 in 1000	Sigma-Aldrich (S5768)
Trβ2	rabbit	1 in 500	Wako (016-24261)

II.V. Methods of tissue culture

II.V.I. Embryonic stem cell cultures

The table below list all mouse embryonic stem (ES) cell lines used in this study.

Table 5. Stem cell lines used in the study

Embryonic stem cell line	Derived from
E16 CCE	Wild-type 129/Sv mouse strain
Crx::GFP	Crx::GFP mouse transgenic line
Chrnb4::GFP	Chrnb4::GFP mouse transgenic line

II.V.I.I. Maintenance cultures

In order to maintain mouse ES cells in an undifferentiated state, the cells were cultured in the presence of leukemia inhibitory factor (LIF, Millipore Ltd., UK) or, alternatively the '2i' medium containing CHIR99021 and PD03259010, inhibitors of GSK3β and MEK respectively. LIF was used at 1000U/ml, whilst CHIR99021 at 3 μM and PD03259010 at 1 μM. These differentiation inhibitors were added to adherent cultures on tissue culture dishes coated with gelatin. To further avoid spontaneous differentiation, the cells were kept at low (below 30%) confluence and passaged every Monday, Wednesday and Friday. To passage the cells, tissue culture plates were first coated with gelatin by adding 3 ml (per 60 mm plate) or 6 ml (per 100 mm plate) of 0.1% gelatin solution and incubated for 1 hour at 37°C before adding cells. Phosphate-buffered saline pH7.4 (PBS, Life Technologies Ltd., UK), 0.25% trypsin-EDTA solution (Life Technologies Ltd., UK) and maintenance medium were pre-warmed in a water bath at 37°C for around 10 minutes. Culture medium was aspirated from cells and immediately cells were washed with 3 ml (per 60 mm plate) or 6 ml (per 100 mm plate) of PBS. Next, PBS was aspirated and replaced with 1 ml (per 60 mm plate) or 2 ml (per 100 mm plate) of trypsin-EDTA solution. Cells were dissociated for 5 minutes at 37°C. After the incubation, 1 ml (per 60 mm plate) or 2 ml (per 100 mm plate) of maintenance medium was added and cells gently resuspended and the cell suspension transferred into 15 ml Falcon tube. Cells were pelleted by centrifugation at 1000 rpm (180 x g) for 5 minutes at room temperature. Next, the supernatant was aspirated off and cell pellet resuspended in 1 ml (per 60 mm plate) or 2 ml (per 100 mm plate) of maintenance medium. From this cell suspension, 20 μl was mixed with equal volume of trypan blue dye, which is excluded from live cells, but labels dead cells in blue. Concentration of cells was determined with a haemocytometer and 1.5 x 10^5 cells were added per 60 mm plate, for the larger 100 mm plate 4.2 x 10^5 cells were plated. In case of cultures passaged on a Friday and grown over the weekend, the starting inoculum was halved and therefore 7.5 x 10^4 or 2.1 x 10^5 cells were plated for each of the plate sizes. Required volume of cell suspension was added either into 4 ml (per 60 mm dish) or 9 ml (per 100 mm dish) of maintenance medium containing 2

µl of LIF working solution per ml of medium. After mixing, medium with cells was added onto gelatin-coated plates and cells grown in an incubator at 37°C in 5% CO_2.

II.V.I.II. Freezing mouse ES cells

Mouse ES cells were seeded to be subconfluent (less than 30% confluency) on the day of freezing. PBS, 0.25% trypsin-EDTA solution and maintenance medium were pre-heated for 10 minutes in a water bath set at 37°C. Cell culture medium was aspirated before cells were washed with 6 ml of pre-heated PBS (Life Technologies Ltd, UK). PBS was then aspirated off and cells enzymatically dissociated using 2 ml of 0.25% trypsin-EDTA solution (Life Technologies Ltd., UK) at 37°C for 5 minutes. 2 ml of maintenance medium was then added and cells resuspended into a homogenous solution. Cell suspension was transferred into a 15 ml Falcon tube and any remaining cells washed out by adding another 2 ml of maintenance medium. Cells were pelleted by centrifugation at 180 x g (1000 rpm) for 3 minutes at room temperature and the supernatant removed. Subsequently, cells were resuspended in 750 µl of pre-chilled freezing medium containing 10% (v/v) dimethyl sulfoxide (Sigma-Aldrich Ltd, UK) as a cryoprotectant. Cell suspension was distributed into three cryovials (250 µl each) and frozen in a pre-cooled cell freezing container, which was immediately transferred into -80°C after adding cryovials with cells.

II.V.I.III. Thawing frozen stocks of mouse ES cells

Approximately 30 minutes prior to thawing cryovials containing frozen ES cells, 60 mm tissue culture-treated dishes were coated using 0.1% gelatin solution at 37°C and 15 minutes prior maintenance medium was pre-warmed in a water bath at 37°C. Cryovial containing the cells was briefly placed in the water bath and removed with some ice crystals still visible. Cells were then collected into 20 ml of pre-warmed maintenance medium, cells remaining in the cryovials washed out with a small volume of medium and the whole cell suspension centrifuged at 180 x g (1000 rpm) for 3 minutes at room temperature. Supernatant was subsequently removed and cells resuspended in 4 ml of maintenance medium containing LIF working solution at 2 µl/ml. This cell suspension was well mixed and added to the pre-coated plates. This culture was incubated at 37°C in 5% CO_2 overnight. Following day medium was replaced for fresh maintenance medium with LIF. Cultures were passaged every 48-72 hrs and cultured for at least a week after thawing before proceeding with differentiation.

II.V.II. 3D suspension retinal differentiation

Three mouse embryonic stem cell lines were differentiated in this study: CCE E16 line or Crx:GFP and Chrnb4:GFP transgenic lines. Typical differentiation experiment

followed a timeline outlined below (composition of the media used are listed in the table following).

II.V.II.I Differentiation day 0

Prior to differentiation, differentiation medium, 0.25% Trypsin-EDTA and PBS (without Mg^{2+} and Ca^{2+}) were pre-warmed in a water bath at 37°C for at least 15 minutes. Maintenance cultures were then dissociated as for passaging: cell culture medium aspirated and cells washed with 3 ml or 6 ml (per 60 mm and 100 mm dish, respectively) of pre-warmed PBS (Gibco, UK; pH 7.4); PBS aspirated and 1 or 2 ml of 0.25% trypsin-EDTA (Life Technologies Ltd, UK) added (per 60 mm and 100 mm dish, respectively). Cells were incubated with trypsin for 5 minutes at 37°C in a tissue culture incubator. Equal volume (1 or 2 ml) of differentiation medium containing knockout serum inactivating trypsin was then added, cells pipetted into suspension which was transferred into a 14 ml falcon tube (BD Biosciences Ltd, UK) centrifuged at 180 x g for 5 minutes at room temperature. Supernatant was removed and cell pellet brought into suspension with either 1 or 2 ml of differentiation medium. Small volume of suspension (20 µl) was used for assessing cell number. 20 µl of cell suspension was mixed with trypan blue solution (Life Technologies Ltd, UK), pipetted into the chamber of a Neubauer haemocytometer (VWR Ltd, UK) and live cells (excluding the blue dye) were counted in two of the large grid boxes. Cells were subsequently plated into Nunclon Sphera ultra low-binding 96-well plates (Thermo-Fisher Scientific Ltd, UK). Total of 3.0 x 10^5 cells was resuspended in 10 ml of differentiation medium, mixed well through pipetting and 100 µl of suspension added per well of the 96-well plate, so that an average of 3000 cells was plated into each well. Cells were placed into a tissue culture incubator at 37°C and 5% CO_2 overnight and during this incubation spherical embryoid body formed in each well.

II.V.II.II. Differentiation day 1

Around 24 hours after plating, differentiation medium was pre-warmed at room temperature for about 30 minutes, aggregates were examined under a light microscope to assess embryoid body formation followed by addition of matrigel solution to trigger continuous retinal neuroepithelia formation. Matrigel solution was prepared by rapidly dissolving 1 ml of growth factor reduced (GFR) Matrigel working solution (1:35 dilution) in 4 ml of differentiation medium in a 14 ml falcon tube. Next, 50 µl of this freshly prepared Matrigel solution was added per well of the 96-well plate to give a final concentration of 2% Matrigel. Following Matrigel addition aggregates were cultured for another 8 days at 37°C in 5% CO_2 in a tissue culture incubator.

II.V.II.III. Differentiation day 9

Nine days after plating aggregates were assessed for optic vesicle and optic cup formation under a light microscope. Retinal maturation medium was pre-warmed in a water bath at 37°C for around 30 minutes and embryoid bodies transferred into a low-binding 24-well tissue culture plate (Thermo-Fisher Scientific Ltd, UK) using wide bore pipette tips (VWR Ltd, UK), 12 aggregates per single well of a 24-well plate. Differentiation medium carried over with the embryoid bodies was gently aspirated using a 1 ml pipette and replaced with 1 ml of pre-warmed retinal maturation medium (RMM). Cells were subsequently cultured for next 3 days at 37°C in 5% CO_2 in a tissue culture incubator.

II.V.II.IV. Differentiation day 12

At day 12 of differentiation, RMM again was pre-warmed at 37°C in a water bath, embryoid bodies examined under a light microscope, medium gently removed from above the floating aggregates and 1 ml of fresh RMM medium added per well of the 24-well plate.

II.V.II.V. Differentiation day 14

As previously, also at day 14 embryoid bodies were examined under a light microscope, at this stage nearly all aggregates showed differentiation of pigmented RPE cells. RMM medium was pre-warmed in a water bath at 37°C, on this day 5 µl of retinoic acid working solution was added per ml of RMM (500 nM final concentration) and 3 µl per ml of taurine working solution (150 nM final concentration). Medium was replaced with RMM containing retinoic acid and taurine.

II.V.II.VI. Differentiation days 16-30

From day 16 onwards, aggregates were cultured in RMM with added 3 µl of taurine working solution per ml (150 nM final concentration). Medium was replaced every 48-72 hours. Crx:GFP cells were processed for transplantation at day 16, whilst E16 CCE cells following cone precursor labelling at day 26-30.

Table 6. Retinal differentiation culture media composition.

Maintenance medium	Retinal differentiation medium	Retinal maturation medium
510 ml GMEM 5.1 ml Non-essential amino acids 5.1 ml Pyruvate (1 mM) 0.51 ml 2-Mercaptoethanol	130 ml MEM-E HEPES 65 ml HBSS 1 g Glucose 2 ml Heat-inactivated FBS 2 ml N2 supplement	500 ml DMEM/F-12 GlutaMAX 5 ml N2 supplement 2.5 ml Penicillin/Streptomycin

58 ml KSR (10%) 5.8 ml Heat-inactivated FBS (1%)	1 ml Penicillin/Streptomycin 0.2 ml L-Glutamine	

II.V.III. Treatment of cultures with Notch inhibitors DAPT and RO4929097

Embryoid bodies at either day 16 or 21 of culture had their media replaced with pre-warmed RMM supplemented with 150 nM taurine and containing DMSO as a vehicle control or 10 µM final concentration of DAPT (Sigma-Aldrich Ltd, UK) or RO4929097 (BioVision Inc., USA; 1 µl of 10 mM working solution and 10 µl of 1 mM working solution, respectively). Cells were next incubated with inhibitors for 48 hours before processing for analysis by flow cytometry or collection for quantitative PCR.

II.V.IV. BrdU proliferation analysis

To assess the abundance of cells in the synthesis phase of the cell cycle, 3D differentiated embryoid bodies were pulsed with 5-bromo-2'-deoxyuridine (BrdU; Sigma-Aldrich Ltd, UK). Replicate wells each containing 12 aggregates had their media replaced with media containing 10 µM BrdU (1 µl of 10mM working solution per 1 ml of culture medium). Cells were incubated with BrdU in a cell culture incubator for 1 hour before washing with PBS and collection. Collected aggregates were then fixed with a 4% paraformaldehyde (PFA) solution for 1 hour; PFA was removed and samples washed with PBS and then placed in a 20% sucrose (Sigma-Aldrich Ltd, UK). Samples were subsequently snap-frozen and processed for histology.

II.V.V. T4 stimulation

L-Thyroxine (≥98% HPLC; Sigma-Aldrich Ltd, UK) was dissolved in ethanol at 65 mmol for stock solution. Working solution was prepared in ethanol and then appropriately dissolved to final concentration in culture medium.

II.VI. Methods of cell labelling, isolation and transplantation

II.VI.I. Viral vector transduction

II.VI.I.I. Adeno-associated viral vector infection

Suspension cultures between day 20 and 22 were used for viral labelling. RMM medium containing 150 nM taurine was pre-warmed in water bath. Purified and concentrated rAAV2/9 viral vector preparations were used at titers between $5x10^{12}$-$1x10^{13}$ viral genomes per ml (assessed by qPCR). 250-350 µl of such preparation was used to infect a 24-well plate with 12 aggregates in each well. Estimated multiplicity of infection was in the range of several thousand viral particles per cell. To perform the infection, vector preparation was dissolved in 650-750 µl of RMM medium with taurine to obtain 1 ml solution. This was sterile-filtered using a 0.22 µm membrane filter (Merck Milipore Ltd, UK). This solution was further diluted to a volume of 8.5 ml with RMM with taurine and 250 µl added to each well in the plate, which had the old medium removed. One such 24-well plate was used for one transplantation experiment. In smaller scale experiments the quantities used were scaled down as appropriate. Cells were incubated overnight with the plate tilted, so that the aggregates could remain suspended in the small volume of media. Following day, 250 µl of fresh RMM medium with taurine was added in the morning and another 500 µl in the evening. This protocol allowed labelling of a large proportion of cells in culture, around 25-40% of all retinal cell types as determined using a vector containing an RFP fluorescent reporter under the control of a ubiquitously expressed CBA promoter on cryosections of infected aggregates.

II.VI.I.II. Lentiviral vector infection

Embryoid bodies at day 9 in culture were used for lentiviral vector infection. Lentiviral vectors were concentrated by ultracentrifugation and dissolved in DMEM culture medium with 10% FBS (Life Technologies Ltd, UK). Typical preparation of lentiviral vectors gave an infectious titer of approximately 10^8 transducing particles per ml. Embryoid body cell aggregates were transferred from 96-well to 24-well plate, 12 per well of 24-well plate, most medium removed and a small volume of 200-250 µl of concentrated vector solution in culture medium added to each well. The plate was incubated tilted in a tissue culture incubator at 37°C and 5% CO2 for 6 hours. Next, 750 µl of RMM medium supplemented with antibiotic-antimycotic solution at 50x dilution (Thermo-Fisher Scientific Ltd, UK) to prevent contamination from non-sterile

produced vector. Cells were cultured in antibiotic-antimycotic supplemented medium until collection.

II.VI.II. Cell isolation for fluorescence-activated cell sorting (FACS)

Embryoid bodies infected with viral vectors driving a fluorescent reporter (either GFP or RFP) were examined under a fluorescent microscope for reporter expression prior to dissociation. For dissociation papain-based Miltenyi Biotec Neural Tissue Dissociation Kit (Miltenyi Biotec GmbH. Germany) was used according to manufacturer's recommendations. Briefly, neural tissues can be dissociated into single cell suspensions by enzymatic degradation of cell adhesion proteins that serve to maintain the structural integrity of the tissue and papain was found to be the enzyme of choice for dissociation of retinal tissue. First, solution 2 from the kit was pre-warmed for 15 minutes in a water bath set at 37°C, 960 µl was used per 70-100 aggregates. Embryoid bodies were collected with wide-bore pipette tips into 14 ml Falcon tubes (aggregates from 6-8 wells into a single tube). Embryoid bodies were left for several minutes to sink down to the conical bottom of the tube. Next RMM medium was removed from above the aggregates and they were washed with 10 ml of PBS (without Ca^{2+} and Mg^{2+} ions; Thermo-Fisher Scientific Ltd, UK). PBS was then carefully aspirated and aggregates suspended in pre-heated solution 2. To each tube 25 µl of solution 1, 10 µl of solution 3 and 5 µl of solution of 4 was added and mixed with the embryoid bodies in suspension. The falcon tubes were then incubated at 37°C in a water bath for 15-25 minutes, mixed every 3-5 minutes. Following the incubation, embryoid bodies were mechanically dissociated by gentle trituration with a P1000 pipette. Partially dissociated samples were then incubated at 37°C for another 5 minutes and again gently triturated. Tubes were then centrifuged at 1000 rpm for 7 minutes. Supernatant was aspirated and cells resuspended in 1 ml of resuspension solution composed of 66% Eagle's Minimum Essential Medium (MEM-E HEPES), 33% Hank's Balanced Salt Solution (HBSS), 1% heat-inactivated FBS (all Thermo-Fisher Scientific Ltd, UK) and supplemented with 10 µl/ml of DNase I (Sigma-Aldrich Ltd, UK). Once homogenous, the solutions were pooled and passed through a 40µm cell strainer lid into a FACS tube (BD Biosciences Ltd, UK). The tube was placed on ice and transferred to the flow cytometry facility.

II.VI.III. Fluorescence-activated cell sorting (FACS)

Cell sorting was performed either at UCL Institute of Ophthalmology or the Institute of Child Health using BD Influx Cell Sorter (Beckman Dickinson Inc., USA) or MoFlo XDP (Beckman Coulter Inc., USA) cell sorters, respectively. Both sorters were fitted with a 200 mW 488 nm blue laser (adjusted to 150 mW for sorting) that was used to excite

GFP or RFP with the GFP signal detected in 530/40 nm channel, whilst RFP signal in 613/20 nm channel. Sorting of photoreceptor cells was performed at 50 psi and a 70 nozzle was used. Flow-sorted mESC-derived GFP+ cells were on average >95% pure GFP-positive, and >80% viable.

II.VI.IV. Cell isolation for flow cytometry analysis

Cells for flow cytometric analysis were isolated according to the same protocol as for FACS. To determine cell viability, Annexin V-eFluor 450 (eBioscience, 88-8006) was added to samples at a 1:20 dilution in 1x Binding Buffer and incubated for 15 minutes at room temperature. Next, the cells were washed once in 1X Binding Buffer and resuspended in PBS. DRAQ7 (Biostatus, DR71000) dead cell stain was then added to the samples at a final concentration of 0.3µM for 5 minutes at room temperature, followed by sample acquisition. All of the samples were analysed using a BD LSRFortessa X-20 flow cytometer (Beckman Dickinson Inc., USA), fitted with with 5 lasers (i.e. 355nm, 405nm, 488nnm, 561nm & 640nm lasers). Results were subsequently analysed using FlowJo software.

II.VI.V. Preparation of sorted cells for transplantation

Cells sorted into 14 ml Falcon tubes were centrifuged for 10 minutes at 1000 rpm. During centrifugation resuspension solution was prepared by mixing 900 µl of HBSS with 50 µl of DNase I working solution and placed on ice. Supernatant from above the cell pellet was carefully aspirated and cells resuspended in around 75 µl of resuspension solution, final volume was noted at this point. 2 µl of cells were dissolved in 8 µl of resuspension solution (1 in 5 dilution). This was diluted 1:1 with trypan blue solution giving 20 µl, which was used to add to the counting chamber of a Neubauer haemocytometer (VWR Ltd, UK). Live cells in five squares were counted and the total number of cells calculated based on a formula:

Total number of cells = [count from 5 squares * 2 * 10^4 * volume resuspended in]/1000 µl

Final volume to resuspend cells for injections was established by dividing the obtained number of cells by 10^5, to obtain a 10^5 cells/µl final soluton. Before cells were resupended in the final volume for injections they were again centrifuged for 10 minutes at 1000 rpm, but this time in a clear 0.5 ml PCR tube (Thermo-Fisher Scientific Ltd, UK), supernatant was carefully removed and cell pellet resuspended in the calculated final volume for injections. 1 µl of cell suspension (10^5 cells) was injected into the superior and another 1 µl to the inferior retina, giving a total of 2x10^5 cells injected into a single eye.

II.VI.VI. Animal models

For the majority of experiments wild-type C57BL/6J mice were used. In addition, an $Nrl^{-/-}$ animal model of a rod-less retina was used (Mears *et al*., 2001). Care of all animals used in this study was according to standards described in the Animal (Scientific Procedures) Act 1986. All the procedures were performed in accordance with the Association for Research in Vision and Ophthalmology (ARVO) Statement on the Use of Animals in Ophthalmic and Vision Research. Transplantation of photoreceptor precursors was performed at 8-16 weeks of age. $Nrl^{-/-}$ animals were transplanted between 8-12 weeks of age, at this stage the retina in this model contains multiple rosettes, but does not show thinning of the outer nuclear layer due to loss of photoreceptors. Animals used were housed in conditions of standard 12 hour light-darkness cycle with food and water *ad libitum*.

II.VI.VII. Anaesthesia

Prior to performing intraocular injections animals were anaesthetised by intraperitoneal injections of an anaesthetic solution composed of Dormitor (1 mg/ ml, Pfizer Pharmaceuticals Ltd, UK) and ketamine (100 mg/ml, Fort Dodge Animals Health Ltd, UK) mixed with sterile water for injections (Thermo-Fisher Scientific Ltd, UK) in a ratio of 5:3:42. Young adult animals that were used for subretinal injections weighing approximately 200g received 0.2 ml of anaesthetic solution. Once anaesthetised, a small drop of Viscotears (Alcon Ltd, UK) was used topically on the cornea to prevent it from drying during the procedure. After the injections, in order to reverse the effects of the anaesthetic, 0.2 ml of Antisedan (0.1 mg/ml, Pfizer Pharmaceuticals Ltd, UK) was administered through intraperitoneal injection and the mice were placed on a heat mat until they regained normal motility.

II.VI.VIII. Subretinal injections

Before surgery, pupils of the animals were dilated by topical administration of 1% Tropicamide solution (Chauvin Pharmaceuticals Ltd, UK). Surgery was performed under direct retinoscopy utilising an operating microscope (Leica AG, Germany). In preparation for injections, the eye was protruded forward by application of small pressure on both sides of the eye and kept in place by holding a section of conjunctiva and extraocular muscle using a pair of forceps. By placing a coverslip on the cornea covered in Viscotears solution (Alcon Ltd, UK) acting as coupling medium, a contact lens system was created enabling visualisation of the fundus. Injections were performed with a 1.5 cm, 34-gauge hypodermic needle mounted on a 5 µl Hamilton syringe (Thermo-Fisher Scientific Ltd, UK). Tip of the syringe was placed underneath the coverslip and then guided to the sclera and then inserted tangentially through it

creating a wound tunnel that self-seals. Once the needle was inserted its tip was brought into focus between the retina and the RPE and 1 µl of cell suspension containing 10^5 cells selected for GFP expression was injected. This procedure was performed for the superior and inferior hemispheres of the eye.

II.VI.IX. Eye cup dissection and fixation

In most cases, at three weeks post-transplantation, animals that received cell injections were culled by spinal dislocation and the eye extracted. Cornea, iris and lens were removed and the dissected eye cup immediately immersed in fixative solution. 1% or 4% PFA was used depending on intended staining protocol. Eye cups were fixed for 1 hour at room temperature, washed with PBS and transferred to 20% sucrose (Sigma-Aldrich Ltd, UK) solution in PBS, in which they were incubated overnight at 4°C before embedding and snap-freezing.

II.VII. Methods of histology

II.VII.I. Cryosections

Following fixation, embryoid bodies or dissected eye cups were embedded in O.C.T. matrix (Pyramid Innovation Ltd, UK) and snap-frozen by submerging in liquid nitrogen. Samples were transferred from liquid nitrogen for storage at -20°C. Specimens were cut into 18 µm-thick cryosections on a Bright cryostat (Bright Instrument Co. Ltd., UK) onto Superfrost Plus glass histology slides (Thermo-Fisher Scientific Ltd, UK) and stored at -20°C.

II.VII.II. Immunohistochemistry

Cryosections to be used for immunostaining were air-dried for 15 minutes after removal from -20°C. Sections were washed with PBS for 5 minutes to remove O.C.T. Next, they were blocked for 2 hours in a PBS-T solution composed of 1% Bovine serum albumin (BSA; Sigma-Aldrich Ltd, UK), 0.1% Triton X-100 (Sigma-Aldrich Ltd, UK) and 5% serum (either goat or donkey, depending on the species in which the primary antibody was raised in). After blocking, primary antibody was added at an appropriate dilution in PBS-T solution and incubated on the slides overnight in a humid chamber at 4°C. Following day, slides were briefly washed with PBS five times, and then Alexa Fluor secondary antibodies (Thermo-Fisher Scientific Ltd, UK) were added in PBS-T solution for 2 hours at room temperature. Secondary antibodies were normally used at 1:400 dilution. Slides were next washed five times with PBS and nuclei counterstained

with 4',6-diamidino-2-phenylindole (DAPI) for 15 minutes before mounting in DAKO fluorescent mounting medium (Thermo-Fisher Scientific Ltd, UK).

II.VII.III. Immuno-detection of BrdU incorporation

Cryosections were rehydrated with PBS, followed by incubation with 2M HCl solution for 30 min. at 37°C followed by incubation in 1M solution of Na Borate for 10 min. at room temperature. Sections were then washed three times with PBS. Next, sections were blocked with a solution of 5% goat serum, 1% BSA, 0.05% Triton X-100 in PBS for two hours at room temperature. BrdU antibody was then added at 1:100 dilution in 1% BSA, 0.05% Triton X-100 in PBS overnight at 4°C. Next day, sections were washed 3 times with PBS prior to incubation with goat anti-rat AlexaFluor® 546 secondary antibodies diluted 1:300 in 1% BSA, 0.05% Triton X-100 in PBS. Sections were next washed 3 times with PBS before DAPI (1:1000 dilution in PBS) was added for 15 min. at room temperature and then slides were mounted.

II.VII.IV. Detection of EdU incorporation

The Click-iT® EdU Alexa Fluor® 594 Imaging Kit (ThermoFisher Scientific Ltd., UK) was used for detection of EdU (5-ethynyl-2'-deoxyuridine) by fluorescent microscopy. EdU is a nucleoside analog of thymidine that gets incorporated into newly synthesised DNA during the S phase of the cell cycle in proliferating cells. In contrast to BrdU histological detection, Click-iT® EdU requires only mild fixation and detergent permeabilization for the small molecule-based Click-iT® EdU detection reagent to gain access to the DNA, facilitating antibody co-staining and examination of cell morphology. The assay was performed on 4%-fixed cryosections according to manufacturer's guidelines.

II.VII.V. Confocal imaging

Stained cryosections were visualised on a Leica DM5500Q confocal miscroscope (Leica AG, Germany). Cells staining for selected markers were identified using the epifluorescence illumination mode on the microscope. Once the desired field of view was identified, a series of XY optical sections between 0.5-1 µm thick through the depth of the object was acquired. Using Leica AF Lite Software (Leica AG, Germany) from a stack of those individual XY scans a projection image was created. Images were exported in TIFF format and analysed using ImageJ software (Schneider et al., 2012).

II.VII.VI. Statistical analysis

Means of repeated measures are presented ± standard error of the mean (SEM) or ± standard deviation (SD), as indicated. *N* denotes the number of independent experiments, *n* the number of samples analysed (e.g. images of sections, individual RNA samples or injected eyes). GraphPad Prism 5 software (GraphPad Software Inc.,

USA) was used to process the results, generate graphs and perform statistical analysis. Results of statistical analysis are presented with * indicating $p<0.05$, **, $p<0.01$ and ***, $p<0.001$.

II.VIII. Contributions

All of the results presented in this thesis were produced by the author, apart from quantification of the Onecut1-, Olig2- and Otx2-positive cells presented in Figure 1.1 g and quantification of RFP-expressing cells following viral vectors transduction presented in Figure 3.4 d performed by Mindaugas Jonikas and staining for S opsin, Arrestin3 and Rhodopsin in retinal organoids at day 37 in Figure 1.5 f,g performed by Dr Emma West. Dr Anastasios Georgiadis helped with the design of the *Nrl* and *Nr2e3* knockdown constructs used in Chapter 3. Selina Azam and Ryea Maswood performed FPLC purification step for rAAV viral vector production. Arifa Naeem and Samuel Blackford helped with mESC maintenance cultures. Robert Sampson and Ayad Eddaoudi operated the cell sorters and contributed with the flow cytometry analysis. Dr Emma West and Dr Anai Gonzalez-Cordero helped with experimental design.

III. Results chapters

Chapter 1. Characterization of cone photoreceptor differentiation in retinae derived from mouse embryonic stem cells.

1.1. Background

Photoreceptors arise from a pool of multipotent retinal progenitors. Retinal progenitors are a population heterogeneous at the gene expression level (Trimarchi et al., 2008 and reviewed in Cepko, 2014) and undergo a temporal programme of competence whereby they produce subsets of retinal neurons within specific time windows during development (reviewed in Cepko, 2014; Swaroop, Kim and Forrest, 2010). In mice, photoreceptors are generated over a prolonged period starting from around embryonic day 11 (E11) when the first cone precursors become post-mitotic until postnatal day 10 (P10) when the last rod precursors are born (Carter-Dawson and LaVail, 1979). Cone genesis occurs earlier in retinal development and is complete by birth, whilst rods are made over a longer time frame between E12 and P10, with a peak at around birth (Carter-Dawson and LaVail, 1979; Rapaport et al., 2004). Signalling through the Notch receptor regulates initial stages in photoreceptor specification with high levels of Notch signalling maintaining cycling progenitors, whilst low levels permitting photoreceptor neurogenesis (Yaron et al., 2006; Jadhav et al., 2006; Mizeracka et al., 2013). While a detailed description of the molecular events in the terminally dividing retinal progenitors generating photoreceptor precursors still awaits, some of the molecular markers of progenitors biased towards photoreceptor production have been identified (reviewed in Cepko, 2014).

Single cell gene expression analysis revealed expression of the basic helix-loop-helix transcription factor Olig2 in a subset of retinal progenitor cells (Hafler et al., 2012). Fate mapping using Cre recombinase for marking showed that the majority of cones and rods have a history of Olig2 expression (Hafler et al., 2012). Analysis of clones arising from Olig2-expressing retinal progenitors yielded striking results. When marking of clones using retrovirus was initiated early in retinal development, at E13.5-14.5, the clones obtained were composed of only one or two cells, meaning that Olig2 is expressed in terminally dividing progenitors, and consisted nearly solely of cones and horizontal cells. This is a very significant bias since cones and horizontal cells are the rarest cell types in the retina. Ganglion cells, which are also made at this stage were not present amongst Olig2 progeny. Labelling of clones generated at late

developmental stages at P0-P3 resulted again in small clone size and a bias in the type of progeny, at this stage almost entirely to rods with a small proportion of amacrine cells (Hafler et al., 2012). Therefore, these observations show that Olig2 is a marker of retinal progenitors undergoing terminal divisions that are heavily biased towards generating photoreceptors, early in development cones whereas at late stages rods.

Thyroid hormone receptor beta 2 (Trβ2) is an early marker of cone precursors. A live imaging study in zebrafish expressing a fluorescent reporter based on zebrafish *thrb*, which is a marker of long-wavelength opsin-expressing cones (L cones) revealed reporter expression in terminally dividing retinal progenitors that made predominantly L cones as their progeny with a few horizontal cells as siblings (Suzuki et al., 2013). *THRB* reporter in the chick has also been studied (Emerson et al., 2013). A small conserved regulatory region was found expressed in a subset of retinal progenitor cells, cone precursors and developing horizontal cells. Retroviral lineage study of cells expressing this reporter showed that progenitors expressing this genetic element divide to produce horizontal cells and photoreceptors. Further analysis of this conserved sequence in the mouse identified binding sites for transcription factors Otx2 and Onecut1. Otx2 is a known factor involved in photoreceptor differentiation expressed in progenitors and early post-mitotic photoreceptor precursors (Nishida et al., 2003). A novel role was identified for Onecut1 in photoreceptor genesis in addition to the requirement for this factor in horizontal cell differentiation (Wu et al., 2013; Klimova et al., 2015) and explained its expression in early post-mitotic photoreceptors isolated from embryonic retina (Muranishi et al., 2010). Expression of Onecut1 is proposed to define the context in which terminally dividing retinal progenitors give rise to cone as opposed to rod precursors, since Onecut1 expression is restricted to the embryonic retina and its misexpression at later stages led to a significant increase in the proportion of progeny expressing the cone marker RXRγ (Emerson et al., 2013). Altogether, combined with the data on Olig2 expressing progenitors, these findings suggest existence of terminally dividing progenitors, marked by Olig2, in which commitment to cone fate is triggered by collaborative action of Otx2 and Onecut1 through binding to regulatory sequences of an early cone gene *Thrb*.

Expression of Trβ2 in early post-mitotic cone precursors commences at around E10.5, at which stage sparse faintly positive cells begin to appear in the neuroblastic layer (Ng et al., 2009). With the progress of retinal neurogenesis these cells become more abundant and their numbers peak at around E17-E18. Expression in single cells dips neonatally, but increases again around P2 and strong expression remains until around P10, after which expression decreases and becomes very weak by the second

postnatal week. Trβ2 acts together with another early cone marker RXRγ to impose the dorsal to ventral gradient of M and S opsins characteristic of the mouse retina (Ng et al., 2001; Roberts et al., 2005). Similarly to Trβ2, RXRγ is also expressed from early stages in cone differentiation, with the first cells positive for this marker being detected from E14.5, and like Trβ2 its levels temporarily decrease around birth. From P5 cones re-express RXRγ and remain clearly positive for this marker in the adult eye. The transient downregulation of these two markers appears to allow expression of S opsin in the ventral retina (Roberts et al., 2005). This specific temporal expression pattern highlights that the differentiation of post-mitotic cone precursors is a dynamically regulated process.

Towards the end of embryonic development cone precursors begin to mature and at around E18 S opsin visual pigment begins to be expressed. Expression of M opsin lags behind and is only induced around P6 through a rise in levels of thyroid hormone that by binding to Trβ2 receptor triggers M opsin expression in a dorsal-high to ventral-low gradient (Ng et al., 2001; Ng et al., 2009; Lu et al., 2008). However, in the mouse most if not all cones are believed to express some level of M opsin, whilst S opsin is repressed in some cones (Applebury et al., 2000) through the cooperative action of Trβ2 and RXRγ (Ng et al., 2001; Roberts et al., 2005). From as early as P3 developing cones start to form synaptic connections with horizontal cells (Rich et al., 1997) shortly before their nuclei lose the apical location and become dispersed throughout the developing outer nuclear layer between P4 and P12. At P12 cone nuclei finish an upward movement and attain their final location at the apical edge of the outer nuclear layer (Rich et al., 1997). In addition to the M opsin visual pigment, in the second postnatal week the expression of phototransduction proteins commences with cone arrestin being detectable from P9 (Zhu et al., 2002), subsequently outer segments extend and cones reach full functional maturation before eye opening at P14.

Advances in stem cell technology led to establishment of protocols for differentiation of retinal cell types from mouse and human embryonic and induced pluripotent stem cells (Eiraku et al., 2011; Ikeda et al., 2005; Kuwahara et al., 2015; Nakano et al., 2012; Osakada et al., 2008; Reichman et al., 2014; Zhong et al., 2014). In a groundbreaking study, Eiraku and colleagues reported self-formation of optic vesicles and differentiation of retinal cell types *in vitro* closely resembling *in vivo* development (Eiraku et al., 2011). Later studies using similar methods characterized rod photoreceptor differentiation in further detail (Gonzalez-Cordero et al., 2013; Decembrini et al., 2014). Cone differentiation, however, received much less attention and remains to be closely examined.

1.2. Aims

A seminal study from the Y. Sasai laboratory (Eiraku et al., 2011) has shown the feasibility of recapitulating optic cup morphogenesis and retinal cell types genesis *in vitro* from mouse ES cells. Previous work from this laboratory has confirmed and optimized this culture protocol for the generation of rod photoreceptor precursors for transplantation (Gonzalez-Cordero et al, 2013). However, both of these studies concluded that cone precursor differentiation is poor in this setting based on the scarcity of cells staining for blue cone opsin at postnatal equivalent stages of development. The aims of this chapter were to further characterise the development of cone photoreceptors in culture and in particular to:

(1) examine the expression of recently identified molecular markers of progenitors biased towards cone and horizontal cell precursors generation,

(2) establish if altered expression of Onecut1, the main determinant of this bias, affects cell fate *in vitro*,

(3) analyse mESC-derived retinal expression of Trβ2, a transcriptional target of Onecut1 and an early cone marker,

(4) perform a more detailed characterisation of cone precursor gene and protein expression in 3D retinal differentiation cultures

(5) quantify the proportion of retinal cells that develop into cone precursors.

1.3. Transcriptional regulators determining the competence of retinal progenitors to generate cone and horizontal cells are expressed *in vitro* in a dynamic fashion as *in vivo*.

To differentiate mouse embryonic stem cells (mESC) into retinal lineages a protocol previously developed in the laboratory (Gonzalez-Cordero et al., 2013) adapted from a study by Eiraku and colleagues (Eiraku et al., 2011) was utilised (schematically represented in Diagram 1.1). Briefly, $3x10^3$ dissociated undifferentiated mESC (maintained as described in the Methods section) were plated per well of an ultra-low binding round bottom 96-well plate to form an embryoid body (Figure 1.1 a). The dissociated mESC spontaneously reaggregated forming a round embryoid body at the

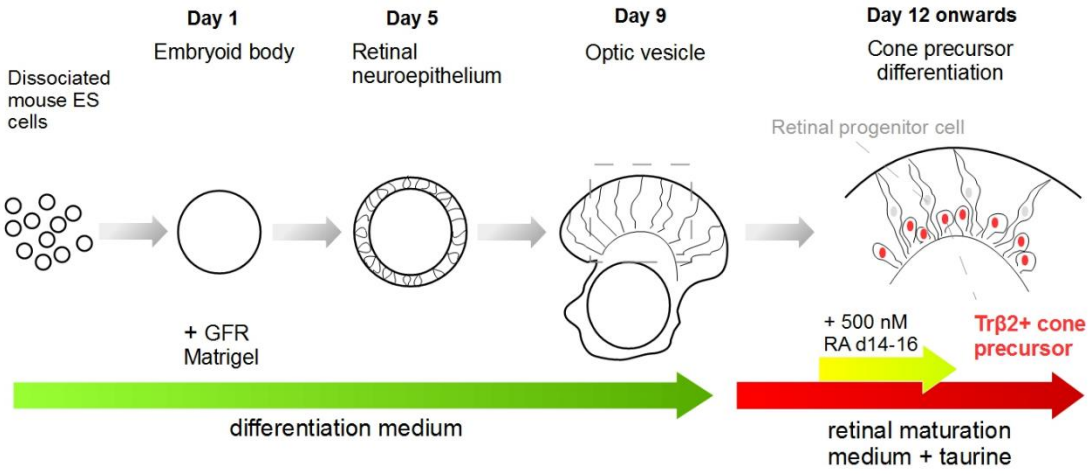

Diagram 1.1. Retinal differentiation of mESCs for study of cone precursor genesis *in vitro*.

Colonies of mESCs were dissociated and added in suspension to 96-well ultra low-binding round bottom plates (3000 cells per well) to form embryoid bodies. On day one a solution of growth factor-reduced (GFR) Matrigel was added to induce formation of continuous rigid neuroepithelia. By day 5 thick, pseudostratified retinal neuroepithelium became clearly visible. In the next 4-5 days retinal neuroepithelia further developed to form optic vesicles evaginating from the aggregate. At day 9 aggregates were transferred into a 24-well plate with retinal differentiation medium. Retinal maturation medium was supplemented with retinoic acid on days 14-16 and taurine added from day 14 onwards. From day 12 differentiation post-mitotic cone precursors was observed.

bottom of the well (Figure 1.1 a). The following day a solution of growth factor reduced Matrigel basement membrane matrix was added to the wells to initiate formation of continuous neuroepithelia on the surface of the aggregates; these structures became clearly visible by light microscopy by day 5 in culture (Figure 1.1 b). By day 9 after plating, thickened retinal neuroepithelia evaginated forming optic vesicle and optic cup-like structures (Figure 1.1 c). At day 9, 12 embryoid bodies (EBs) were transferred per well into a low-binding 24-well plate. Remainders of differentiation medium were aspirated and EBs placed in retinal maturation medium. Optic vesicles considerably grew in size over the next three days and from day 12 (Figure 1.1 d) samples were collected for gene expression analysis and immunostaining.

Studies in fish, chicken and mouse developing retinas presented evidence that cone photoreceptors share a common progenitor with horizontal cells (Emerson et al., 2013; Hafler et al., 2012; Suzuki et al., 2013) that is marked by expression of the transcription factor Olig2 (Hafler et al., 2012). Moreover, analysis of conserved regulatory elements in the *Thrb2* locus, which encodes thyroid hormone receptor beta 2, an early cone marker, revealed regulation by Onecut1 and Otx2 transcription factors, with the window of Onecut1 defining the competence for cone precursor production. To interrogate the competence of mESC-derived retinal progenitors in our 3D suspension retinal differentiation protocol to generate cone precursors, expression of Onecut1, Olig2 and Otx2 was determined using qPCR and immunohistochemistry (Figure 1.1 e-h).

Firstly, qPCR assays were used to determine the changes in expression levels of Onecut1 and Olig2 from day 12 in culture, around the onset of neurogenesis in our *in vitro* retinal differentiation system, to day 24, corresponding to second half of the first post-natal week, a time when photoreceptor generation should be mostly complete. Since Otx2 is highly expressed in retinal pigment epithelium in addition to the neuroepithelium, it was omitted from mRNA analysis. Apart from retina, Onecut1 is predominantly expressed in cerebellum, which is not formed in this culture paradigm. Olig2 is also expressed in specific, restricted domains of the brain such as ventricular zone and in the spinal cord, and whilst posterior neuronal identities are not prominent in these cultures, some contribution of expression in non-retinal neurons cannot be excluded. This analysis shows that Onecut1 expression is higher at early stages in culture, day 12 and day 16, and declines at later stages, day 20 and day 24 (Figure 1.1 e). Regarding Olig2, levels of this transcriptional regulator peak at around day 16 in culture and, similarly to Onecut1, drop at later stages, day 20 and day 24 ((Figure 1.1 e).

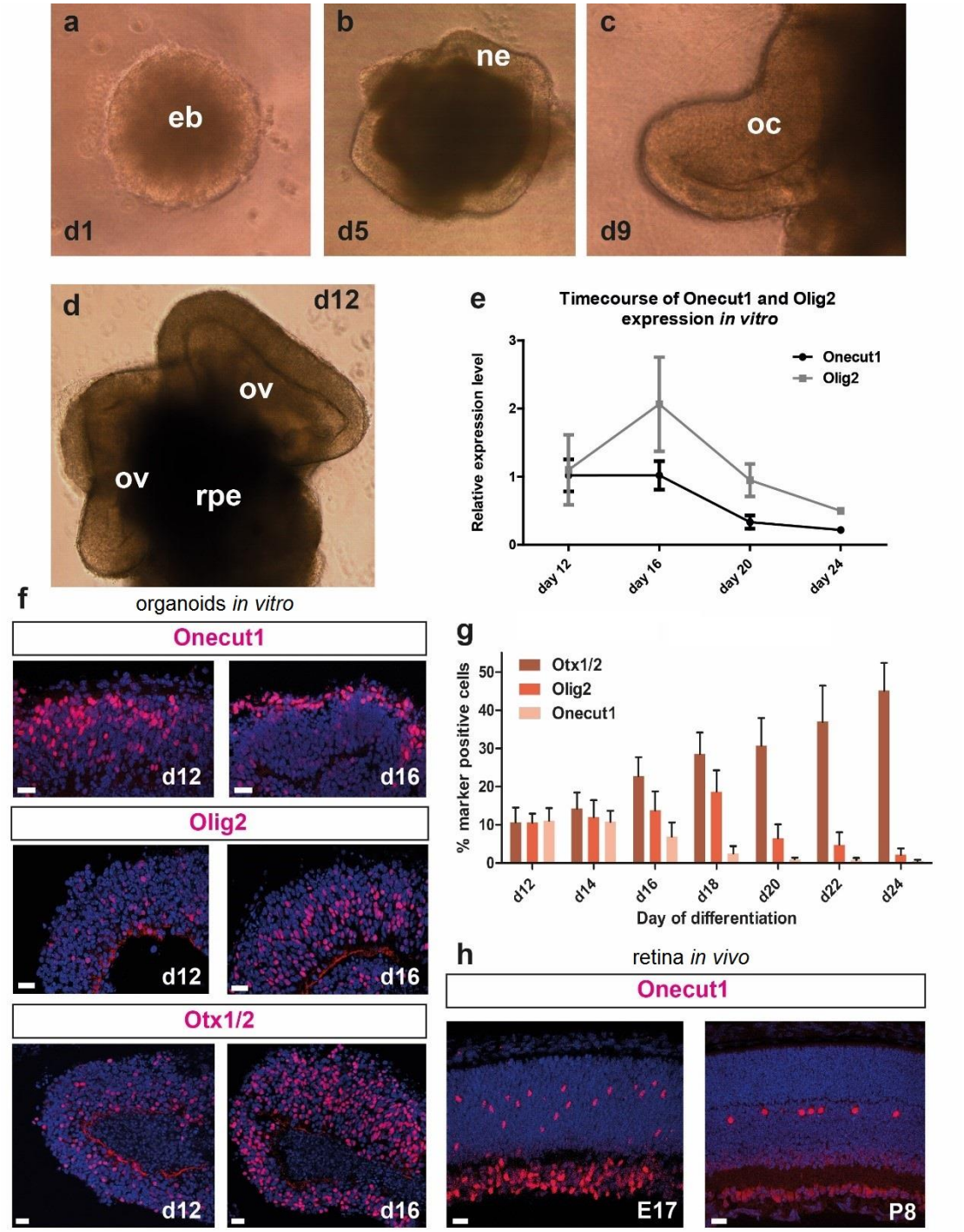

Figure 1.1. Markers of retinal progenitors biased towards cone production exhibit dynamic patterns of expression resembling *in vivo* development.

(**a-d**) Bright field images of ES aggregates at different stages of retinal differentiation. (**a**) Embryoid body (eb) at d1 of culture. (**b**) Formation of retinal neuroepithelia (ne) on day 5. (**c**) Bi-layered optic cup (oc) at d9. (**d**) Embryoid body showing evaginated optic vesicles at day 12 of culture. (**e**) qPCR timecourse of Onecut1 and Olig2 in 3D retinal differentiation cultures between day 12 and day 24. Note decreasing expression past

day 16. (**f**) Immunohistochemistry showing expression of Onecut1, Olig2 and Otx2 in retinal neuroepithelia at day 12 and day 16 in culture. From day 16 Onecut1 expression becomes more pronounced in prospective interneuron layer. (**g**) Quantification of Onecut1, Olig2 or Otx2 immunostained nuclei on sections. At least 15 images of different organoids from 3 differentiation cultures were used, data expressed as mean ±SEM. (**h**) Onecut1 immunostaining on sections from E17 (left panel) and P8 (right panel) mouse retina. Scale bar in all images 10 µm.

Next, the expression of Onecut1, Olig2 and Otx2 at the protein level was assessed. Samples of differentiation cultures at day 12, 14, 16, 18, 20, 22 and 24 were collected for cryosectioning and immunohistochemistry. In all cases antibodies used in the study gave expected nuclear localization, as verified by antibody staining using wild-type retina control specimens, allowing quantification of the proportion of cells in optic vesicles expressing each marker. Nuclei labelled with each of the antibodies were counted only in well-formed neural retina regions since these proteins are also expressed in other brain regions and immunoreactivity in possibly non-retinal cells was observed. In the neural retina, positive cells were localized throughout the neuroblastic layer, consistent with expression in progenitors and early precursor cells (Figure 1.1 f). Quantitative assessment of staining revealed immunoreactivity patterns consistent with the mRNA levels analysis. Specifically, the highest percentage of Onecut1 immunoreactive nuclei was observed between day 12 and 16, dropping dramatically beyond day 18 (Figure 1.1 f, g). Expression from day 16 appeared to shift towards the basal side of the developing neuroblastic layer, on which side interneurons are later found. With respect to Olig2, immuno-positive cells were most abundant at day 18 of differentiation, in alignment with Olig2 being expressed also in progenitors giving rise to rods, birth of which peaks around this time (Eiraku et al., 2011). Past day 18 the proportion of Olig2-positive cells dropped significantly (Figure 1.1 f, g). Finally, the proportion of cells immunolabeled for Otx2 was found to increase over time in the differentiation cultures (Figure 1.1 f, g). This is expected, given that Otx2 labels differentiating photoreceptor precursors, which increase in numbers at the timepoints examined.

Collectively, these results show dynamic expression patterns of Onecut1, Olig2 and Otx2 during the retinal neuroepithelium development. Thus, were consistent with those observed *in vivo*, where Onecut1 is expressed in retinal progenitors in the embryonic retina becoming restricted to horizontal interneurons at postnatal stages (Fig. 1.1 h), Olig2 expression levels peak neonatally, whilst Otx2 expression is found in progenitors and post-mitotic photoreceptor precursors from early stages of development onwards.

1.4. Misexpression of Onecut1 increases horizontal cell genesis mESC-derived retinae

1.4.1 Developing Onecut1 overexpression strategy.

Since studies *in vivo* indicate that Onecut1 is a critical determinant of the commitment to cone and horizontal cell lineages we sought to determine whether it also plays a role in specification of these cell types in our differentiation system. To this end an

overexpression strategy was developed using lentiviral vectors, which can stably transduce dividing cells such as retinal progenitors. Moreover, retroviral and lentiviral vectors have been extensively used in cell lineage studies in the retina and other systems. First, infection with concentrated lentiviral vectors was optimized. We observed that significant transduction with GFP reporter encoding vector under the control of CMV promoter could only be achieved by adding the vector preparation at very early stages of differentiation at the optic vesicle stage, at day 9 of culture (Figure 1.2 a and b). Infection with lentiviral vectors at the same multiplicity of infection (MOI=6) at later timepoints (day 15 and day 20) did not lead to any significant transduction in the neuroblastic layer. At day 9, cycling progenitors constitute the majority of cells in the optic vesicle *in vitro* and few if any post-mitotic cells are present at this stage in culture (Eiraku et al., 2011; Gonzalez-Cordero et al., 2013; Decembrini et al., 2014). Therefore, the use of lentiviral vectors in this 3D retinal differentiation system allows targeting of early retinal progenitors, when applied at relevant stages of development.

To overexpress mouse Onecut1 a lentivirus expression vector was purchased from GeneCopoeia™ that contains Onecut1 mRNA driven by CMV promoter and followed by an internal ribosome entry site (IRES) allowing the expression of an enhanced GFP reporter from a single transcript (Figure 1.2 a). Lentivector was made using this construct as described in the Methods section. Purified and concentrated vector was initially used to infect 661W cells, an immortalized cell line derived from a cone photoreceptor (Tan et al., 2004) and expressing some cone-specific genes, to assess the overexpression capacity in a neuronal- and photoreceptor-like cell type. GFP reporter expression was similar to that observed with control CMV.GFP lentivirus (Figure 1.2 c, c' and b, b', respectively). RNA was isolated from the cells and quantitative PCR was performed, which confirmed a robust increase in Onecut1 mRNA levels with the overexpression construct, compared to a control CMV.GFP vector (Figure 1.2 d). Together, this data set serves to validate the outlined strategy for Onecut1 misexpression.

1.4.2 Forced expression of Onecut1 leads to increased production of horizontal cell precursors and small cell clones.

To examine the effects of Onecut1 misexpression in mESC-derived retinal progenitors, concentrated CMV.Onecut1.IRES.GFP lentivector or a control CMV.GFP vector were added to 3D retinal differentiation cultures at day 9 of differentiation (Figure 1.3 a) at an MOI=6. Infected aggregates were cultured for another 12 days until day 21, a stage in culture comparable to neonatal retina (~P1). At this stage nearly all horizontal cells and cones should be born and express early markers of differentiation.

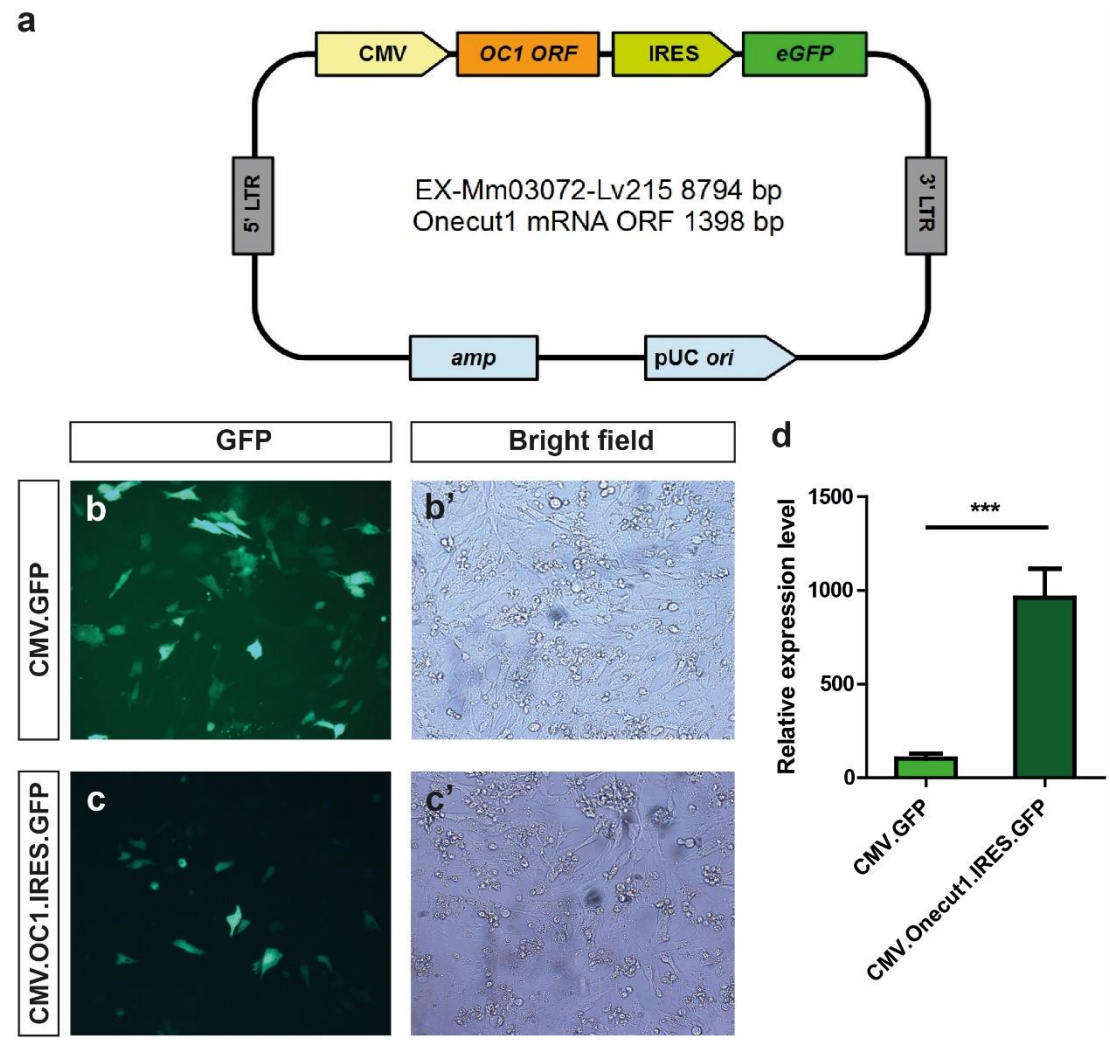

Figure 1.2. Strategy for Onecut1 overexpression.

(**a**) Schematic depicting the design of lentiviral vector construct used for Onecut1 overexpression. CMV – cytomegalovirus promoter; OC1 ORF – mouse Onecut1 mRNA open reading frame; IRES – internal ribosome entry site; eGFP – enhanced green fluorescent protein coding sequence; LTR – long terminal repeat; *amp* – ampicillin resistance gene; pUC *ori* – pUC plasmid origin of replication (**b**, **b'**, **c**, **c'**) Green fluorescence (**b**, **c**) and corresponding bright field images of 661W cells transfected with either control CMV.GFP lentivector plasmid (**b**, **b'**) or Onecut1 overexpression construct (**c**, **c'**). (**d**) qPCR quantification of Onecut1 mRNAs levels in cells transfected with CMV.GFP control plasmid or the Onecut1 overexpression construct. *** $p<0.001$; Student's *t* test.

Immunohistochemistry for cone and horizontal cell-specific proteins was performed on the transduced aggregates. Technical difficulties in combining cone precursor staining with GFP reporter detection precluded assessment of the effect of Onecut1 misexpression on the numbers of cones generated from transduced progenitors. Namely Trβ2 staining required very low fixation with use of detergent and therefore was not compatible with preserving the GFP reporter signal. Apart from one lot of RXRγ antibody, which produced specific signal in both cone and ganglion cell precursors (presented in the following section), all subsequent batches of the antibody detected ganglion cell expression but failed to produce a reliable signal in the cone cells, an observation confirmed on mouse retina sections by the author and several other researchers in our and other groups. This is not an uncommon situation with polyclonal antibodies, which are heterogenous preparations and their specificity and composition is dependent on the immunisation. Continued expression of Onecut1 does not allow for expression of mature cone markers (Emerson et al., 2013), therefore use of antibodies to more mature cone-specific proteins such as S opsin or Arrestin3 was not possible. Due to tropism of lentiviral vectors toward RPE cells, the predominant population within the cultures transduced with the vectors was developing RPE, precluding reliable analysis of gene expression in GFP+ cells using FACS. However, staining for the horizontal cell marker calbindin was robust and reliable, labelling cells predominantly on the basal side of the neuroblastic layer extending processes parallel to the plane of the neuroepithelium (Figure 1.3 b'',c''), enabling quantification of the proportion of calbindin-positive horizontal cell precursors amongst the GFP reporter-expressing cells (Figure 1.3 b,c and d). This analysis revealed a pronounced increase in the percentage of GFP reporter-expressing cells that co-expressed calbindin (Figure 1.3 d). In addition, the number of cells expressing the GFP reporter was significantly lower following CMV.Onecut1.IRES.GFP transduction, compared with CMV.GFP vector (Figure 1.3 e), despite using the same quantity of both vectors (MOI=9). Since the GFP reporter expression in 661W cells transduced with CMV.Onecut1.IRES.GFP was robust and comparable to that obtained with CMV.GFP vector (Figure 1.2 c,d), this is unlikely a result of the reporter being driven by the weaker IRES sequence. This observation is suggestive of either Onecut1 expression resulting in smaller clone size or, alternatively, the misexpression causing death of the transduced cells.

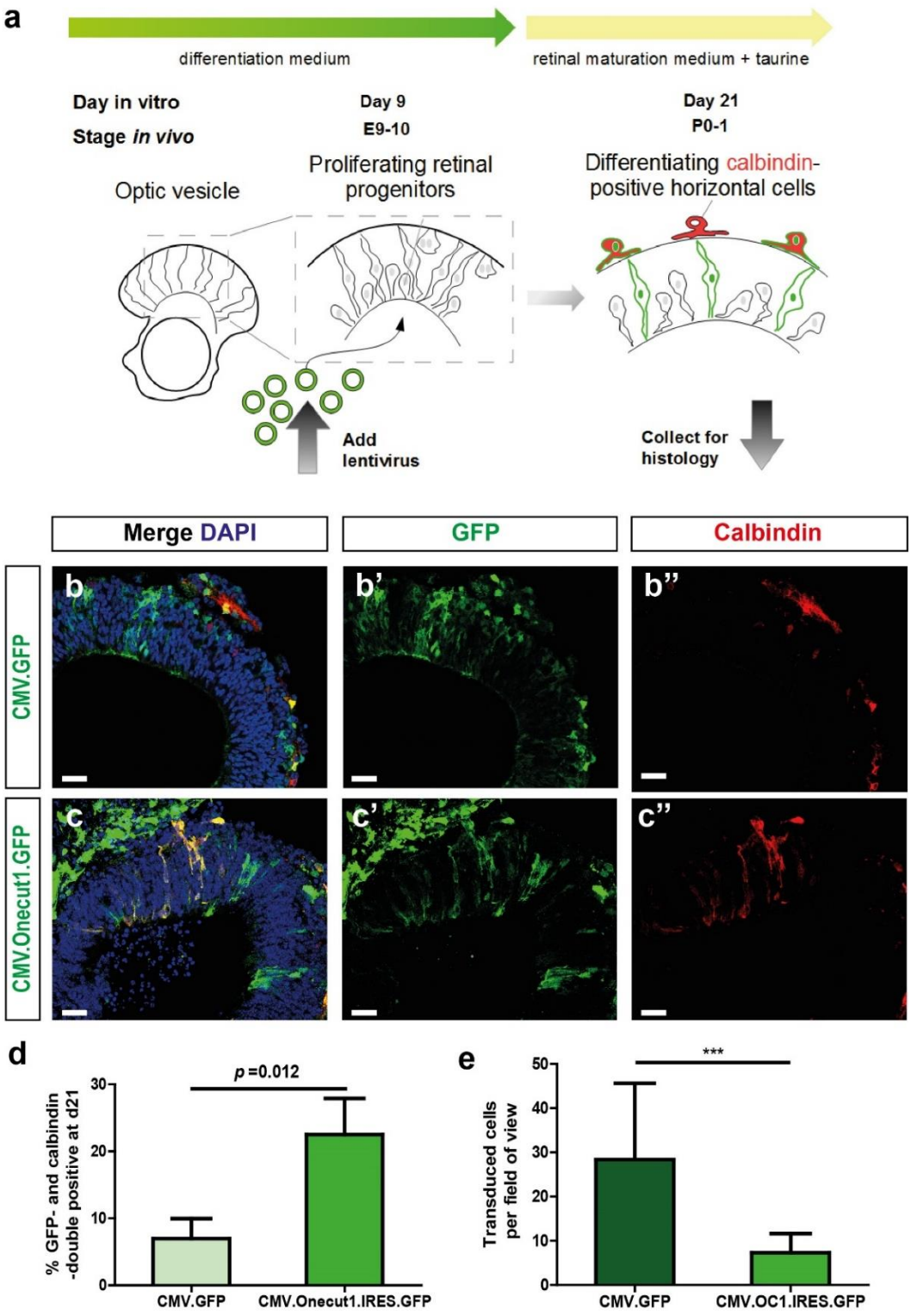

Figure 1.3. Forced expression of Onecut1 at early stages of development leads to increase in horizontal cell production and small clones.

(**a**) Schematic showing the approach used to transduce retinal progenitors in 3D retinal differentiation cultures with lentiviral vectors. Concentrated vector was added at day 9 of differentiation, before the onset of post-mitotic neuron production. Samples were

collected for immunostaining at day 21, stage similar to neonatal retina. (**b**, **b'**, **b''**, **c**, **c'**, **c''**) Immunohistochemistry for vector GFP (**b'**, **c'**) and horizontal cell marker calbindin (**b''**, **c''**); overlay with DAPI counterstain shown in (**b**, **c**). Mouse ES-derived retinal tissues were transduced with control CMV.GFP lentiviral vector (**b**-**b''**) or Onecut1 overexpression vector (**c**-**c''**). Note more co-localization of GFP signal with calbindin staining in Onecut1 overexpression sample. (**d**) Percentage of transduced cells (GFP-positive) immunoreactive for calbindin. Over 40 sections from 3 independent experiments were used for each vector, data shown as mean ±SEM; *p=0.012*, Student's *t* test. (**e**) Quantification of number of cells per field of view after transduction with vectors at approximately same MOI. Over 40 sections from 3 independent experiments were used, data shown as mean ±SD; *** *p<0.001*, Student's *t* test.

1.5. Early cone precursors expressing RXRγ and Trβ2 are efficiently generated in mESC-derived retinae

Given that expression analysis of Onecut1, Olig2 and Otx2, markers of progenitors biased towards generation of cone and horizontal cell precursors, revealed expression patterns similar to those observed *in vivo* (please see section 1.3) and misexpression of Onecut1 in retinal progenitors increased the proportion of horizontal cells, which are cone precursors siblings sharing a terminally dividing progenitor, we decided to directly examine early cone precursor genesis *in vitro*. During development, shortly after terminal mitosis, cone precursors start expressing thyroid hormone receptor β2 (Trβ2) followed by retinoid X receptor γ (RXRγ). Trβ2-positive cells can be detected by immunostaining as early as E10.5-12.5 (Ng et al., 2009), whilst the first RXRγ labelling can be observed at E14.5 (Roberts et al. 2005). We therefore investigated the expression of those two early cone markers in our 3D retinal differentiation system.

Initially, expression patterns of mRNA transcripts of these receptors (*Rxrg* and *Thrb2* genes) were examined from day 12 to 24 of the differentiation protocol, corresponding to the beginning of retinal neurogenesis and onset of photoreceptor maturation, respectively. We found that the level of transcripts for both receptors peaked around day 20 *in vitro* (approximately P0-1 *in vivo*; Figure 1.4 a).

Immunohistochemistry was performed then for RXRγ, which labels cones and ganglion cells, at the peak of its mRNA expression at day 20 of differentiation, immunoreactive nuclei aligned at both basal and apical sides of the mESC-derived neuroblastic layer (Figure 1.4 b, #-basal, *-apical). Cells located at the basal side can be identified as differentiating ganglion cells with large round nuclei (Figure 1.4 b, denoted by #), whilst cells localized to the apical edge show more elongated nuclei reminiscent of developing cone photoreceptor precursors (Figure 1.4 b, denoted by *).

In vivo, in Olig2-positive retinal progenitors, Otx2 and Onecut1 induce commitment to the cone precursor lineage through collaboratively binding to regulatory sequences in the *Thrb2* locus (Emerson et al., 2013). Given that Otx2 and Onecut1 are expressed in our retinal differentiation cultures (Figure 1.1), we also examined Trβ2 expression using immunostaining from early stages (day 12) to a stage equivalent to P4-6 postnatal retina (day 26). This analysis showed the appearance of the first Trβ2-positive cells at day 12 of differentiation (Figure 1.4 c), stained nuclei became more abundant with the progression of differentiation (Figure 1.4 d), with the positively stained nuclei still present at day 26 of culture, the last timepoint examined (Figure 1.4 e).

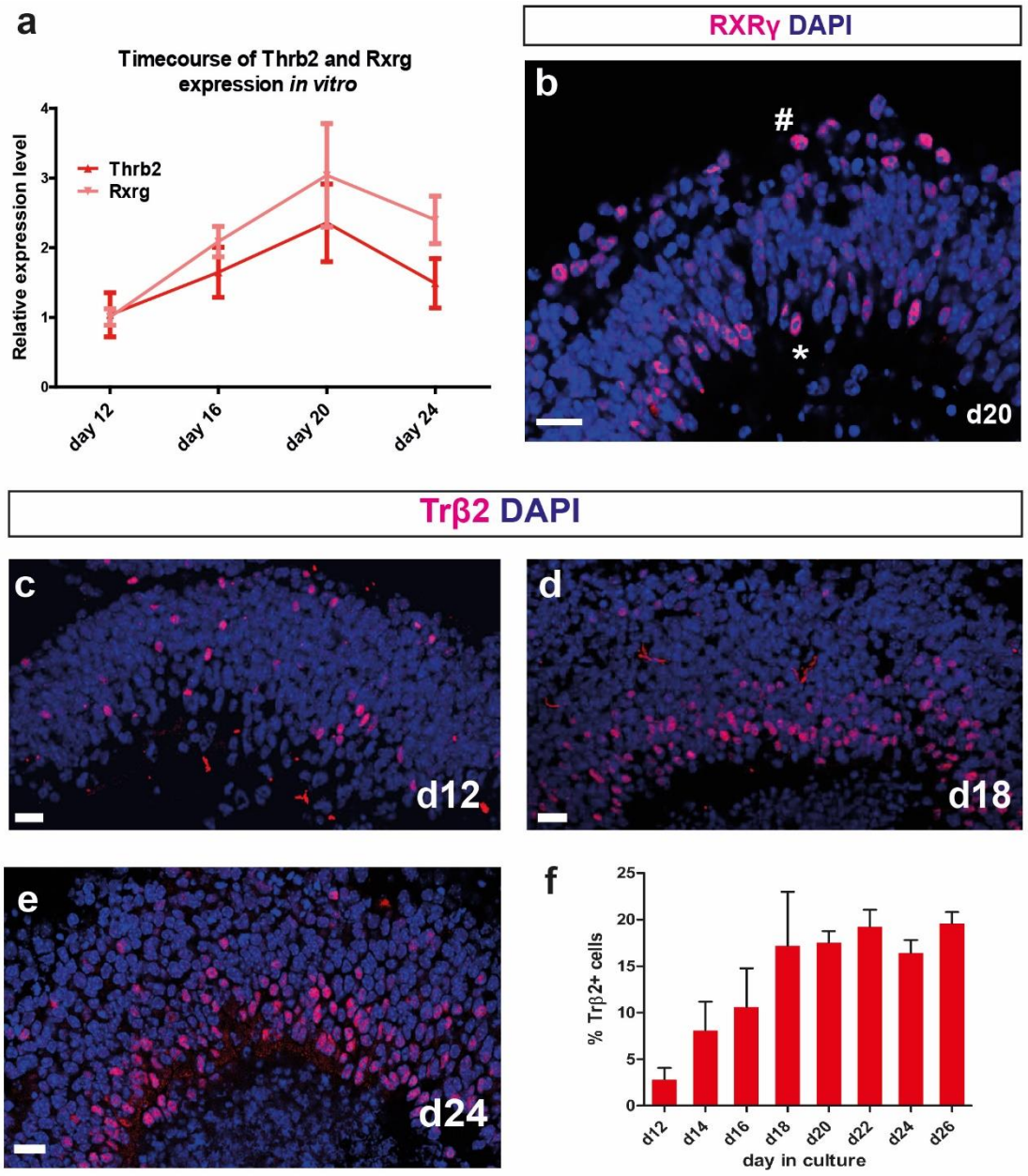

Figure 1.4. Early cone precursors expressing Trβ2 and RXRγ increase in abundance as differentiation *in vitro* progresses.

(**a**) qPCR timecourse of *Thrb2* and *Rxrg* expression in mES 3D retinal differentiation cultures between day 12 and day 24. (**b**) Immunostaining for RXRγ at day 20 of differentiation. Note RXRγ-positive nuclei of cone precursors at the apical edge of the neuroblastic layer (*) and the nuclei of ganglion cells at the basal side (#). (**c**, **d**, **e**) Immunostaining showing expression of the early cone precursor marker Trβ2 at day 12 (c), day 18 (d) and day 24 (e) of differentiation. As with RXRγ, Trβ2-positive cone precursors are more abundant at the apical edge of the ES-derived developing retina (d and e). (**f**) Percentage of retinal neuroepithelia cell nuclei immunoreactive for Trβ2 between day 12 and day 26 in culture. Notice that the percentage of cone precursors starts to plateau from day 20. At least 15 images of individual organoids used for quantification at each timepoint. Data expressed as mean ±SD.

The proportions of Trβ2-positive nuclei present in the mESC-derived retinal neuroepithelia were then quantified on sections from different stages of culture. This demonstrated a steady increase in the number of Trβ2-positive nuclei from day 12, at which they are first detectable (mean of 2.8% ±1.3%, *n*=12 sections of different organoids), to around day 18 (mean of 17.2% ± 5.8%, *n*=20 sections), from when the proportion of Trβ2 immunoreactive cells plateaued at between 15-20% of all cells in the retinal neuroepithelium (Figure 1.4 e). The abundance of cone precursors *in vitro* at equivalents of postnatal stages (day 24-26) appears higher than *in vivo* (Ng et al., 2009), however this can be skewed by poor development of interneuron and ganglion cell layers using this protocol (Gonzalez-Cordero et al., 2013).

Collectively, these observations show that early cone precursors are robustly generated in these retinal differentiation cultures.

1.6. Cone photoreceptor precursors survive and mature to postnatal stages of development in retinae derived from mESCs

In mouse photoreceptor development cone genesis commences at embryonic day 11 (E11) and is largely complete by birth. At late embryonic stages S opsin begins to be expressed, whilst expression of M opsin lags behind and only starts around P6 (Swaroop, Kim and Forrest, 2010). At the beginning of second postnatal week (~P9) cone arrestin, a protein involved in the phototransduction cascade, begins to be expressed (Zhu et al., 2002). Having confirmed expression of early cone differentiation markers *in vitro*, we then examined whether these following steps of cone maturation are also recapitulated in our 3D retinal differentiation system.

RT-PCR was first used to examine the presence of transcripts of a set of cone differentiation markers at later stages of differentiation from day 22 to day 33 (corresponding from around P1-2 to late second postnatal week *in vivo*; Figure 1.5 a). Primer sets for RXRγ, S opsin, M opsin, cyclic nucleotide gated channel alpha 3 (CNGA3), cone arrestin, cone cGMP-specific phosphodiesterase 6C (PDE6C) were used for this analysis with beta actin used as loading control. This analysis showed that from day 22 to day 33 expression of all these cone-specific genes could be detected at the mRNA level (Figure 1.5 a), consistent with the onset of cone maturation *in vivo* in late second postnatal week.

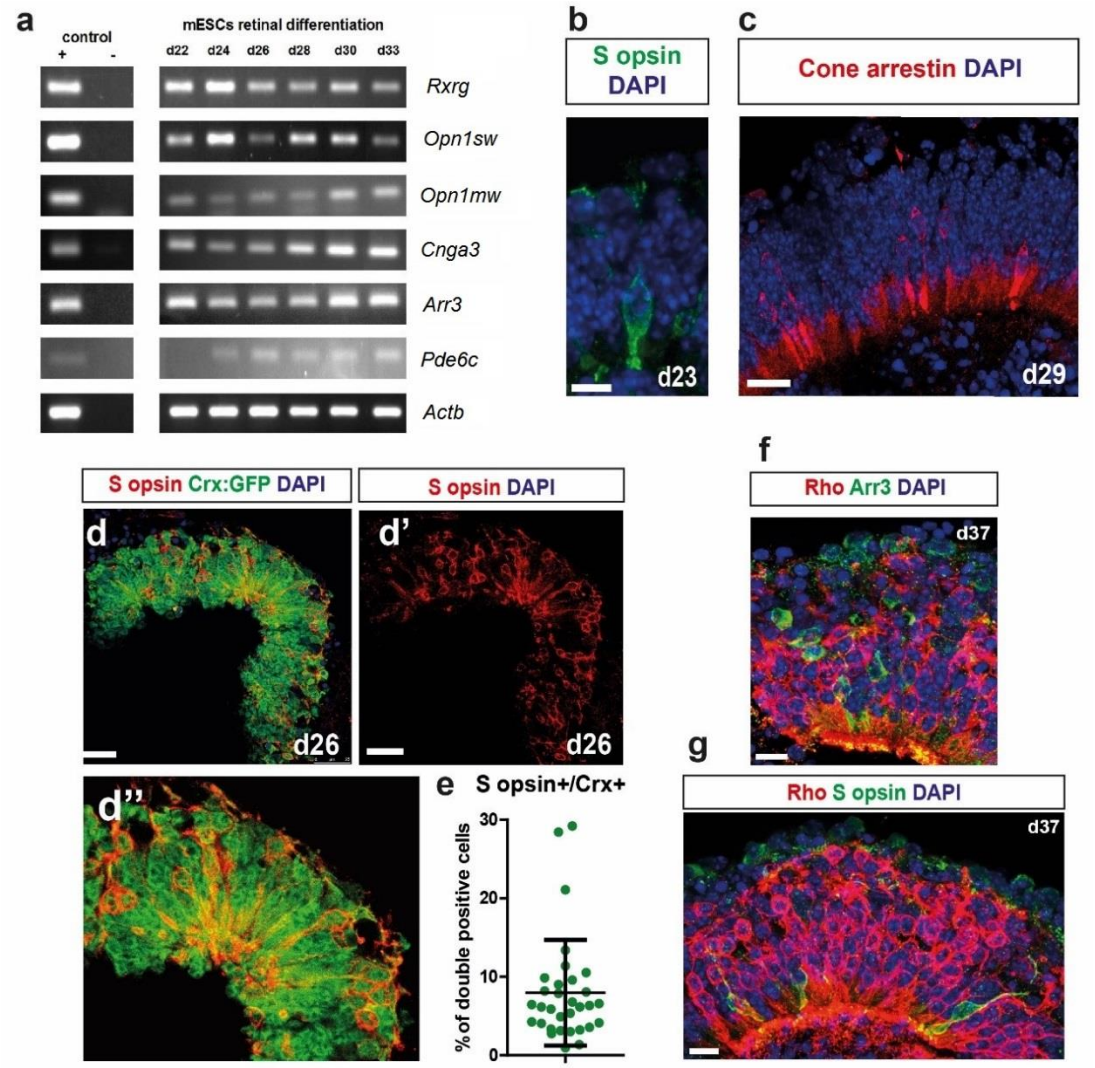

Figure 1.5. Markers of cone maturation are expressed in mESC-derived retinae *in vitro*.

(**a**) RT-PCR analysis of cone gene expression in 3D retinal differentiation cultures. Transcripts of markers of cone maturation such as cone opsins (*Opn1sw* and *Opn1mw*) and other phototransduction cascade components (*Cnga3, Arr3, Pde6c*) are all expressed at later stages (beyond day 24) *in vitro*. (**b**) Immunostaining for S cone opsin at d23 of differentiation. (**c**) Immunostaining showing cone precursors expressing cone arrestin protein at day 29 in culture. Observe stronger staining in the inner segment region of positive cells. (**d-d''**) S opsin protein (d') is co-expressed (d and d'') with reporter GFP (d and d'') in the Crx::GFP mES line differentiated into retina at day 26 in culture. (d'') Higher power image showing cell morphology. Single 1µm confocal planes shown. Scale bars 20 µm. (**e**) Quantification of Crx+ cells expressing S opsin. Data from *n*=32 sections from 3 differentiation cultures. (**f,g**) Immunostaining for Rhodopsin (in red) and cone-specific proteins Arrestin3 (f) and S opsin (g) at day 37 of culture.

Next, expression of S opsin and cone arrestin proteins was analysed using immunohistochemistry. At day 23 clear labelling for S opsin could be detected (Figure 1.5 b), whilst cone arrestin-positive cells appeared later at day 29 of differentiation (Figure 1.5 c), equivalent to P6-9 *in vivo* retinal development. To confirm that cells expressing S opsin were indeed photoreceptor precursors we performed S opsin staining on Crx::GFP ES line (Decembrini et al., 2014) differentiated according to the same protocol, this showed at day 26 clear co-labelling of cells in the photoreceptor precursor layer (Figure 1.5 d-d''). On no occasion was S opsin staining found in GFP-negative cells. The proportion of GFP-positive cells expressing S opsin was determined using confocal microscopy. A mean of 7.97% ±1.91% (*n*=32 sections, aggregates from 3 independent differentiation cultures) of Crx::GFP photoreceptors stained for S opsin (Figure 1.5 e), significantly higher than *in vivo*, where approximately 3% of photoreceptors are cones and only a subset of these express S opsin (Applebury et al., 2000). Full functional maturation of photoreceptors in these cultures does not occur with lack of outer segment biogenesis and light sensitivity (Decembrini et al., 2014; Eiraku et al., 2011; Gonzalez-Cordero et al., 2013). Beyond day 34 differentiation cultures lost clear laminar organisation and retinal rosettes formed (Figure 1.5 f; at d37). However, even at these late stages some S opsin- and Arrestin3-positive cones persisted (Figure 1.5 f,g; at day 37), suggesting that at least some cone photoreceptors survived in long-term culture.

Altogether, this data set shows that not only are markers of specialised cone and horizontal cells-generating retinal progenitors and early cone precursors markers such as RXRγ and Trβ2 present in mESC-derived retinal neuroepithelia, but also cone precursors develop to express marker of the onset of maturation such as S opsin and cone arrestin.

1.7. Conclusions and discussion

Cone photoreceptors are one of the rarest cell types in the mouse retina constituting only around 2% of all retinal neurons (and 3% of photoreceptor cells; Swaroop, Kim and Forrest, 2010). However, human vision is highly dependent on cone cells since they mediate colour vision and permit high visual acuity both required for many of our daytime activities, for example reading and driving. Moreover, many highly prevalent conditions such as age-related macular degeneration lead to the loss of these cells and therefore from a perspective of developing cell therapies in the retina this is one

the most relevant cell populations (Jayakody et al., 2015). The scarcity of cone cells hampered research into their cell biology and development. Only recent technological advances and deepened understanding of retinal development has revealed a more detailed picture of the mechanisms involved in their generation *in vivo* as well as molecular details of cone-mediated vision (Mustafi, Engel and Palczewski, 2009). As developmental biology studies provided more and more insights in this area, the advent of stem cell biology led to the development of protocols allowing differentiating physiologically-relevant retinal tissue in a culture dish (Eiraku et al., 2011; Ikeda et al., 2005; Nakano et al., 2012; Osakada et al., 2008; Zhong et al., 2014). The most remarkable of these studies came from the Sasai group at RIKEN, who first reported the generation of self-organising optic cups *in vitro* (Eiraku et al., 2011). A study from our group showed adaptation of this protocol for the isolation of rod precursors for transplantation (Gonzalez-Cordero et al., 2013). Both of these studies reported very low numbers of differentiating cone photoreceptors (less than 0.1%), albeit the set of examined markers was very limited, consisting of RXRγ, S opsin and neuron-specific enolase (NSE). A more recent study from the Arsenijevic group using a Crx:GFP ES mouse reporter line reported that a considerable percentage of the GFP-expressing photoreceptors co-labelled with RXRγ (between 38% at day 16 and 12% at day 23 of differentiation). Here, through the use of immunohistochemistry for Trβ2, a highly specific and early marker of developing cone precursors we determined that the generation of this cell type in mESC-derived retinae is efficient (Figure 1.4) with up to 15-20% of cells in optic vesicles expressing Trβ2 (Figure 1.4 f). There can be several reasons for the discrepancies between the observed abundance of cone precursors between the studies: (1) the three differentiation protocols differ slightly in culture conditions used, for instance in the original protocol (Eiraku et al., 2011) optic vesicles were manually dissected and subsequently cultured in isolation, whilst in both more recent protocols the aggregates were kept as a whole throughout the culture period; (2) immunostaining protocols may differ from study to study as well as the specificity of polyclonal antibodies used for each staining and indeed in this study we found that from several batches of RXRγ antibody only one gave clear, specific and robust signal in cryopreserved samples of the differentiated mESC aggregates; (3) the stage of differentiation examined in culture, for example we found that S opsin staining until around day 26 in culture is relatively weak and using the antibody at low concentrations might not reveal all the precursors expressing the marker present at those stages.

To characterize in much greater detail the competence of mESC-derived retinal neuroepithelia to give rise to cone precursors, we took advantage of recent

developments in our understanding of cone genesis *in vivo* that came primarily from retinal lineage studies in the Cepko group at Harvard. These studies identified a specialised progenitor heavily biased towards generating cone and horizontal precursors (Hafler et al., 2012; Emerson et al., 2013). At the molecular level this progenitor is characterized by expression of the basic helix-loop-helix transcription factor Olig2 and the competence to trigger cone differentiation derives from cooperative action of the transcription factors Otx2 and Onecut1 binding the regulatory elements in the *Thrb* locus to stimulate Trβ2 expression (Emerson et al., 2013). In this study we characterized the expression of these transcriptional regulators in mESC-derived optic tissue. This analysis showed that expression of Onecut1 in the neuroblastic layer, as during *in vivo* development, is restricted mainly to the early stages of differentiation (few Onecut1-positive cells are found from day 20 onwards). Olig2 expression peaks around day 18 in culture, a timepoint that has been identified as the peak of rod birth *in vitro* (Eiraku et al., 2011), consistent with Olig2 marking also progenitors that give rise to clones composed of rods and amacrine cells at neonatal stages (Hafler et al., 2012). As expected the numbers of cells expressing Otx2, expressed by a subset of progenitors and developing photoreceptor precursors was found to increase with the progress of differentiation (Figure 1.1).

Forced expression of Onecut1 in mESC-derived retinal progenitor cells at early stages of differentiation using a lentiviral construct led to an increased proportion of calbindin-positive horizontal cell precursors in the population transduced with Onecut1 overexpression construct versus control vector (Figure 1.3 d). Due to technical difficulties it was not possible to reliably determine the effect on cone precursor abundance at this stage. What is clear however, is that Onecut1 misexpression affects fate choice in mESC-derived retinae introducing bias towards generation of horizontal cells, the proposed siblings of cone precursors (Hafler et al., 2012; Emerson et al., 2013). It was also noted that in experiments using vectors at the same MOI (MOI=9), 12 days following infection clusters of reporter expressing cells were much smaller in case of Onecut1 overexpression (Figure 1.3 e). No major difference in transduced cell numbers could be observed following overexpression of Onecut1 in 661W cell line, suggesting that the effect might be specific to retinal progenitors. Noteworthy, Olig2 is expressed in terminally dividing cells and as a result clones from Olig2-expressing progenitors are of small size (Hafler et al., 2012). Small clusters in Onecut1 overexpression might be a consequence of this factor triggering cell cycle exit or, alternatively, compromising cell survival.

Further analysis showed that the transcriptional target of Otx2 and Onecut1 the cone marker Trβ2 is induced in differentiating mESC-derived retinae (Figure 1.4). In the developing retina the first Trβ2-positive cone precursors can be detected by immunostaining from E10.5-12.5 with their number increasing to around birth. In culture we found the first Trβ2 immunolabelled cells at day 12 (Figure 1.4 c), which allows us to correlate developmental timing with respect to cone genesis, placing day 12 as corresponding to E11-12. Similar to the situation *in vivo*, numbers of cone precursors, found mainly aligned on the apical side of the neuroepithelium, increased *in vitro* to around day 18 (Figure 1.4 d), from when the percentage of retinal cells they constituted started to plateau at around 15-20% (Figure 1.4 f). Staining for another early cone marker protein RXRγ also showed apically located cone precursor nuclei at day 20 of differentiation (Figure 1.4 b). This apical location became more dispersed at later stages (day 24-26, Figure 1.4 e) reminiscent of the displacement of Trβ2-stained nuclei associated with movement of cone nuclei within the first postnatal week in development (Ng et al., 2009). Detection of markers signalling the onset of cone maturation was also possible with staining for S opsin found from day 23 (Figure 1.5 b) onwards and cone arrestin being detectable from day 29 of differentiation (Figure 1.5 c). Cone arrestin protein is first detected in the mouse retina from P9 (Zhu et al., 2002), therefore day 29 in culture appears to correspond to around P9 *in vivo*, consistent with previous work from the laboratory placing day 26 at around P4-6 (Gonzalez-Cordero et al., 2013). Collectively, the observations regarding transcriptional regulators expressed in biased progenitors and developing cone precursors suggest that cone genesis in our mESC 3D retinal differentiation culture system largely resembles that in the developing mouse.

However, several differences between cone genesis *in vitro* and *in vivo* were noticed. Firstly, despite cultures reaching a stage equivalent to P6, when M opsin expression commences, we could not detect M opsin protein at day 26, 29 and 35 *in vitro*. Extrinsic factors such as bone morphogenetic protein (BMP), retinoic acid and thyroid hormone are implicated in regulating expression and establishing the dorsal-ventral gradients of S and M opsins in the mouse retina (Alfano et al., 2011; Lu et al., 2009; Satoh et al., 2009 also discussed in Chapter 3). We can speculate that the lack of detectable M opsin protein in culture might stem from missing extrinsic signal(s) required for triggering its expression. Moreover, despite the high propensity for self-organisation in mouse 3D retinal differentiation cultures used in this study, no outer segment growth occurs spontaneously in this system (Eiraku et al., 2011; Gonzalez-Cordero et al., 2013; Decembrini et al., 2014), with some degree of segment formation triggered by

forced expression of a sensory organ-enriched microRNA cluster (Busskamp et al., 2014). This stands in contrast to recent work showing outer segment formation and light responsiveness in cultures of human induced pluripotent stem cells differentiated into retina (Zhong et al., 2014). The lack of this feature of terminal differentiation and maturation of photoreceptors, did not allow us to test if cone precursors generated *in vitro* would reach full functional maturation. Finally, the number of cone precursors present in cultures is much larger than expected, even at day 26 *in vitro*, a stage similar to the second half of the first postnatal week, cone precursors labelled with Trβ2 antibody constitute nearly 20% of cells within the retinal neuroepithelium. At similar stage *in vivo* cones are much less abundant since most rods and bipolar cells are generated by that time. One reason for high percentage of cones could be that cells of inner nuclear layer facing the exterior of the optic vesicle gradually detach and are lost to the culture medium. A second possibility is that rod genesis in culture is incomplete and therefore the proportion becomes skewed in favour of cone cells. An interesting alternative is also that cone numbers are regulated by negative feedback mechanism similar to that described for ganglion cells (RGCs) in the retina. In the developing retina, the number of retinal ganglion cells was found to be regulated by growth and differentiation factor 11 (GDF11), a soluble factor of the transforming growth factor β superfamily. Secreted GDF11 negatively regulates the expression of the neurogenic factor Math5, which confers the competence of retinal progenitors for RGC production, without affecting their proliferation. In the absence of GDF11 the time window of RGC production is extended and an excess of RGCs is made at the expense of rods and amacrine cells (Kim et al., 2005). This shows that an early born cell type can signal to the progenitor cell pool to affect its competence for generation of specific cell types. One could speculate that the high number of cone precursors seen in the differentiation cultures might arise as a result of a soluble factor mediating negative feedback to the progenitor cells diffusing out of the mESC-derived optic vesicles to the large volume of culture medium in which the aggregates are suspended and not attaining a high enough concentration to limit cone precursor genesis.

Collectively data presented here indicate that cone genesis and subsequent development occurs in mESC-derived retinae *in vitro* and that this process follows a timecourse resembling the *in vivo* differentiation of this cell type. Moreover, analysis of the number of cone precursors formed in culture shows that their generation is highly efficient, possibly exceeding that *in vivo*. This raised the question whether the developmental pathways modulating cone development *in vivo* also operate in differentiation cultures *in vitro*.

Chapter 2. Notch signalling limits the competence for photoreceptor generation in mESC-derived retinae

2.1. Introduction

During the course of neurogenesis a balance is attained between proliferation and differentiation so that sufficient numbers of progenitors are maintained to generate the whole cellular composition of the central nervous system. During retinal development, progenitor cells pass through competence states in which only subsets of cell types are generated. This process underlies the evolutionary conserved birth order of the six retinal neurons and one glial cell type present within the adult retina (reviewed in Cepko, 2014; Swaroop et al., 2010). The Notch pathway acts to maintain the balance of proliferation and differentiation during both invertebrate as well as vertebrate neurogenesis (Lewis, 1996) with an important role in retinal development (reviewed in Bassett and Wallace, 2012; Swaroop et al., 2010; Xiang, 2013; Zagozewski et al., 2014). Three Notch receptor family members are expressed in the developing eye (Lindsell et al., 1996). Notch2 is required for proper development of the ciliary epithelium (Zhou et al., 2013), whereas Notch1 and Notch3 were found to control neural retina formation. Activity of Notch3 is required early to limit retinal ganglion cell production and maintain a pool of proliferating progenitors (Riesenberg et al., 2009). Notch1 is also necessary early in retinal development to restrict cone photoreceptor precursor genesis and preserve a pool of dividing progenitors for later stages of retinogenesis (Jadhav, 2006; Yaron, 2006). Genetic ablation of *Notch1* in an early phase of retinal development leads to the overproduction of cone precursors, loss of proliferating progenitors and is associated with reduction in organ size and retinal architecture resulting in a loss of lamination (Jadhav, 2006; Yaron, 2006). Inactivation of Notch1 at a later stage of development (P0-P3), resulted in nearly exclusive generation of rod precursors at the expense of bipolar and Müller cells (Jadhav, 2006). This suggests a specific role of Notch1 in restricting photoreceptor production in the mammalian retina (Diagram 2.1).

Notch pathway is a cell-cell contact-dependent signalling mechanism, whereby binding of ligands expressed on the surface of neighbouring cells initiates intracellular signal transduction (Lewis, 1996). Notch signalling can be divided into canonical and non-canonical (Lewis, 1996). In the canonical pathway, binding of a ligand to the membrane spanning Notch receptor allows interaction with the γ-secretase/presenilin complex. Proteolytic activity of γ-secretase leads to cleavage and release of the Notch internal cytoplasmic domain (NICD). NICD translocates to the nucleus where it participates in

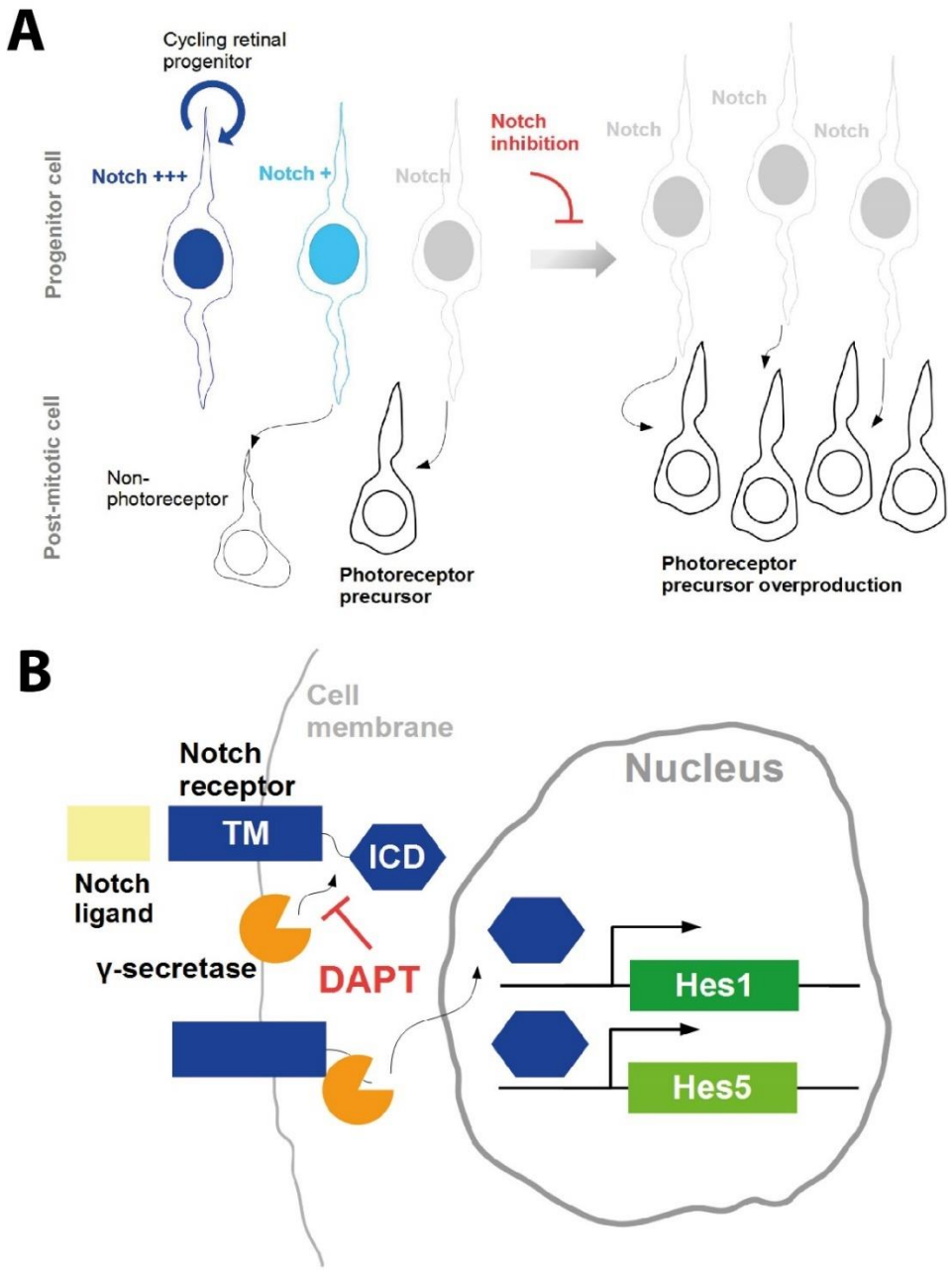

Diagram 2.1. Notch signalling in retinal neurogenesis

(**A**) Notch activity is required for maintenance of a pool of cycling retinal progenitors. At least a low level of Notch activity in terminally dividing progenitors is required for acquisition of non-photoreceptor cell fates (left panel). Inhibition of Notch activity leads to overproduction of photoreceptor cells (right panel). (**B**) Notch is a transmembrane receptor with a membrane spanning domain (TM) and intracellular domain (ICD). Activation of Notch signalling by extracellular ligands requires proteolytic cleavage by γ-secretase enzyme to release the ICD, which then translocates to the nucleus to activate expression of Notch target genes including *Hes1* and *Hes5*. Signalling downstream of Notch receptor can be blocked by pharmacological inhibitors of γ-secretase such as DAPT.

the activation of Notch target genes such as the bHLH transcription factors Hes1 and Hes5 (Lewis, 1996; schematically represented in Diagram 2.1). High affinity small molecule inhibitors targeting γ-secretase have been developed and their effects shown to phenocopy Notch pathway loss of function mutations (De Kloe and De Strooper, 2014; Nelson et al., 2007). Application of one of these inhibitors, DAPT, to developing chick and mouse retinae closely mimicked Notch receptor loss of function phenotypes. In particular, when DAPT was applied at an early stage of retinogenesis overproduction of retinal ganglion cells and cone photoreceptor precursors, loss of progenitor proliferation and laminar organisation, as well as growth arrest were observed (Nelson et al., 2007).

Development of stepwise differentiation protocols to obtain telencephalic tissue, followed by induction of retinal neuroepithelia, retinal progenitor cells and finally photoreceptor precursors (Ikeda et al., 2005; Osakada et al., 2008) also saw an increase in Crx-positive photoreceptor precursor yield following the application of γ-secretase inhibitor DAPT (Osakada et al., 2008). This treatment facilitated both photoreceptor precursor as well as retinal ganglion cell genesis in these cultures, consistent with observations regarding the *in vivo* role of Notch (Osakada et al., 2008). Subsequently, a study by Sasai and colleagues showed retinal morphogenesis with formation of retinal neuroepithelia further developing into optic vesicles and optic cups by subjecting mESCs to appropriate culture conditions (Eiraku et al., 2011). The effect of DAPT on retinal progenitor cultures was also examined in that study, showing increased numbers of Crx-positive cells and disruption of laminar tissue organisation. However, the identity of the photoreceptor cells generated and the maturation of these cells following DAPT treatment, were not examined (Eiraku et al., 2011).

Here, using a mouse ES cell 3D retinal differentiation system, we interrogated the role of the Notch pathway in the genesis of both photoreceptor subtypes *in vitro*, with a particular focus on the differentiation of cone precursors.

2.2. Aims

Notch signalling has a well-established role in limiting progenitor competence for photoreceptor genesis *in vivo* allowing generation of other retinal neuronal cell types, as well as Müller glia (Jadhav, 2006; Mizeracka et al., 2013; Nelson et al., 2007; Yaron, 2006). It has been also used in the retinal differentiation of pluripotent stem cells to increase the yield of photoreceptors (Osakada et al., 2008). The goal of the work presented in this chapter was to investigate its role related to cone genesis in the 3D retinal differentiation of mESCs. To this end the following aims were set out:

1) confirm whether pharmacological inhibition of Notch results in upregulation of photoreceptor markers in the culture system used;
2) quantify the effect of Notch inhibition on photoreceptor differentiation and examine isolated photoreceptors following treatment;
3) test the hypothesis that inhibition of Notch signalling at the time of cone genesis will lead to overproduction of this cell type and skew the ratio of photoreceptor subtypes towards a higher proportion of cones.

2.3. Notch inhibition results in loss of retinal progenitors

Notch is a transmembrane receptor activated by interaction with ligands expressed on the surface of surrounding cells. Activation of downstream molecular effectors occurs when the intracellular domain of Notch is proteolytically cleaved by the protease γ-secretase (Nelson et al., 2007). Several high affinity small molecule inhibitors of γ-secretase have been developed and embraced in basic developmental biology research. Amongst those, two molecules γ-secretase inhibitor IX (DAPT) and RO4929097 became routinely used due to their favourable biochemical and toxicological properties (De Kloe and De Strooper, 2014). To interrogate the role of Notch activity on photoreceptor development in the 3D retinal differentiation system, Notch inhibitor DAPT was used at 10 µm, as previously described (Eiraku et al., 2011; Osakada et al., 2008). Day 16 of differentiation was chosen for treatment as a time when the proportion of Trβ2-positive cone precursors is increasing (please refer to Figure 1.4), but before the peak of rod birth at day 18-20, as observed in similar cultures (Eiraku et al., 2011). Aggregates of E16 CCE line cells were kept in the medium containing DAPT for 48 hours, much longer than the minimal 6 hour treatment required for permanent effects on retinal neurogenesis (Nelson et al., 2007), to ensure maximal effects.

Given the importance of Notch signalling for the maintenance of cycling retinal progenitors, we first examined the impact of Notch inhibition on the expression of proteins associated with dividing progenitors. Immunostaining for Ki67, a protein expressed in mitotic cells, showed loss of large, strongly Ki67-positive progenitors undergoing mitosis (Figure 2.1 A; N=3 differentiation cultures, n=12 organoids each). Furthermore, antibody staining for Sox9, a transcription factor expressed in retinal progenitors and later in Müller glia, also displayed a reduction in immunoreactivity in the inhibitor-treated organoids (Figure 2.1 B; N=3 differentiation cultures, n=12 organoids each). Finally, we performed staining for Olig2, which is expressed in retinal progenitors biased towards production of specific lineages, a combination of cones with horizontal cells early in development and rods with amacrine cells at later stages

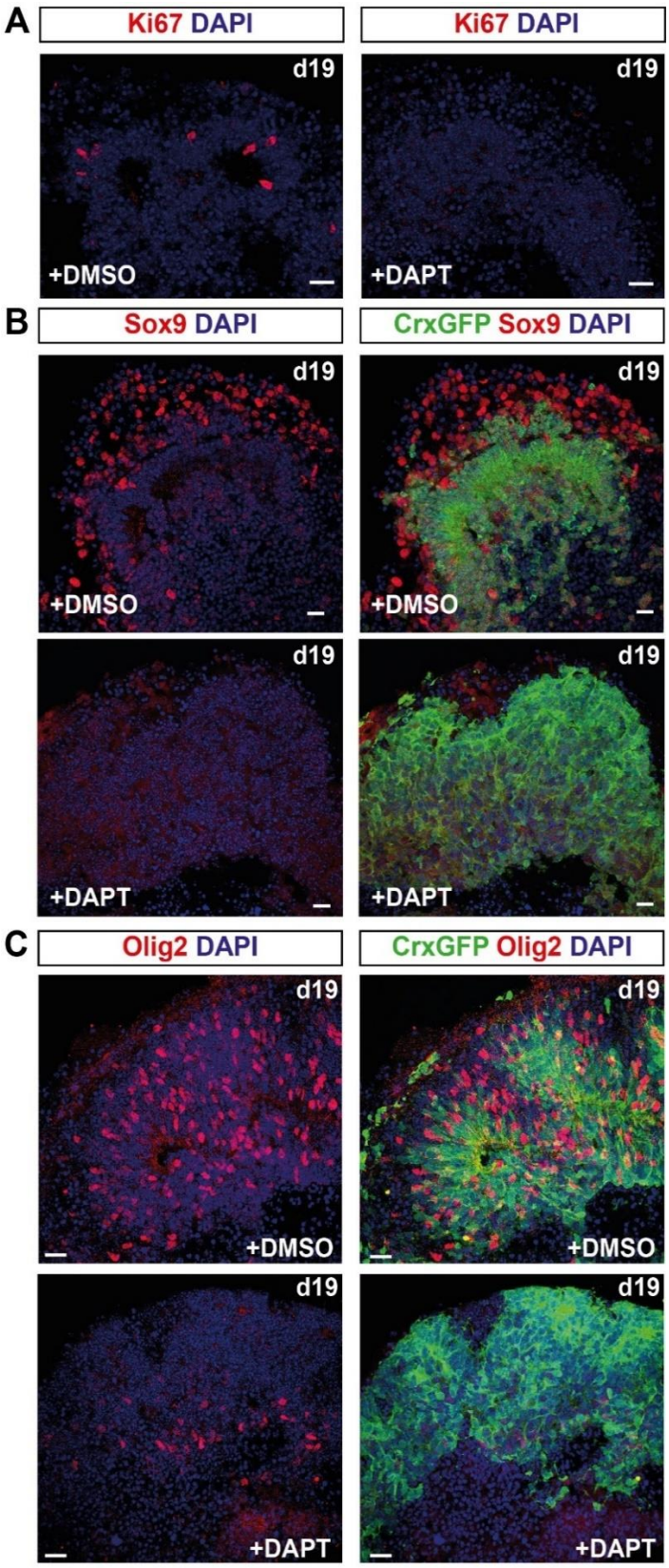

Figure 2.1. Inhibition of Notch signalling triggers cell cycle exit of retinal progenitors in organoids derived from mESC

Representative immunostaining of retinal organoids for the mitotic marker Ki67 (A) and retinal progenitor markers Sox9 (B) and Olig2 (C) at day 19 of retinal differentiation following treatment with vehicle control (DMSO) or DAPT at 10 µM on days 16-18 of differentiation. Please observe reduced expression of progenitor markers resulting from Notch signalling inhibition. Experiment performed in N=3 differentiation cultures with n=12 organoids each. Scale bar 10 µm in all images.

(Hafler et al., 2012). Similarly, a pronounced reduction in the expression of Olig2, normally present in numerous cells dispersed within the neuroblastic layer, was observed following treatment of aggregates with DAPT (Figure 2.1 C, N=3 differentiation cultures, n=12 organoids each). Altogether, these analyses demonstrate that maintenance of proliferating retinal progenitors requires Notch activity at the time of cone precursor genesis.

2.4. Photoreceptor neurogenesis is induced following Notch inhibition

We next sought to determine the impact of Notch signalling inhibition on formation of cones and rods. Histological analyses presented in Figure 2.1 included aggregates differentiated using the transgenic Crx:GFP mESC line (Decembrini et al., 2014). This line was derived from mice that carry a bacterial artificial chromosome engineered to allow GFP expression from the *Crx* locus (Samson et al., 2009). Subjected to the differentiation protocol described in detail in Chapter 1, this mESC line formed embryoid bodies that showed retinal neuroepithelia formation and photoreceptor differentiation (Figure 2.1 B,C and 2.2 c; for more details please refer to Figure 5.1 in Chapter 5). Concomitant with the reduction of retinal progenitor-specific proteins, expanded patches of GFP-positive cells formed (Figure 2.1 B,C), suggesting that the loss of proliferating progenitors is associated with the formation of photoreceptor precursor cells. To directly examine this, mESC-derived retinae treated with DAPT were antibody stained for the pan-photoreceptor marker Crx, revealing an increase in endogenous Crx expression (Figure 2.2 a). Furthermore, the rod-specific protein Rhodopsin appeared more abundant (Figure 2.2 b). These changes were associated with tissue disorganisation with the disruption of photoreceptor layer architecture in the cultures (Figure 2.2 a and b). QPCR was employed to determine the effects of DAPT treatment on the gene expression profile of retinal differentiation cultures. This analysis showed that of the direct transcriptional targets of Notch signalling, the progenitor bHLH genes *Hes1* and *Hes5*, *Hes5* mRNA transcription was nearly abolished (Figure 2.2 c), in accordance with reports *in vivo* (Riesenberg et al., 2009). With respect to photoreceptor genes, a significant increase in *Crx* as well as *Opn1sw*, *Nrl* and *Rho* expression was observed (Figure 2.2 c), suggesting that both cone and rod photoreceptor neurogenesis was increased by pharmacological inhibition of Notch signalling.

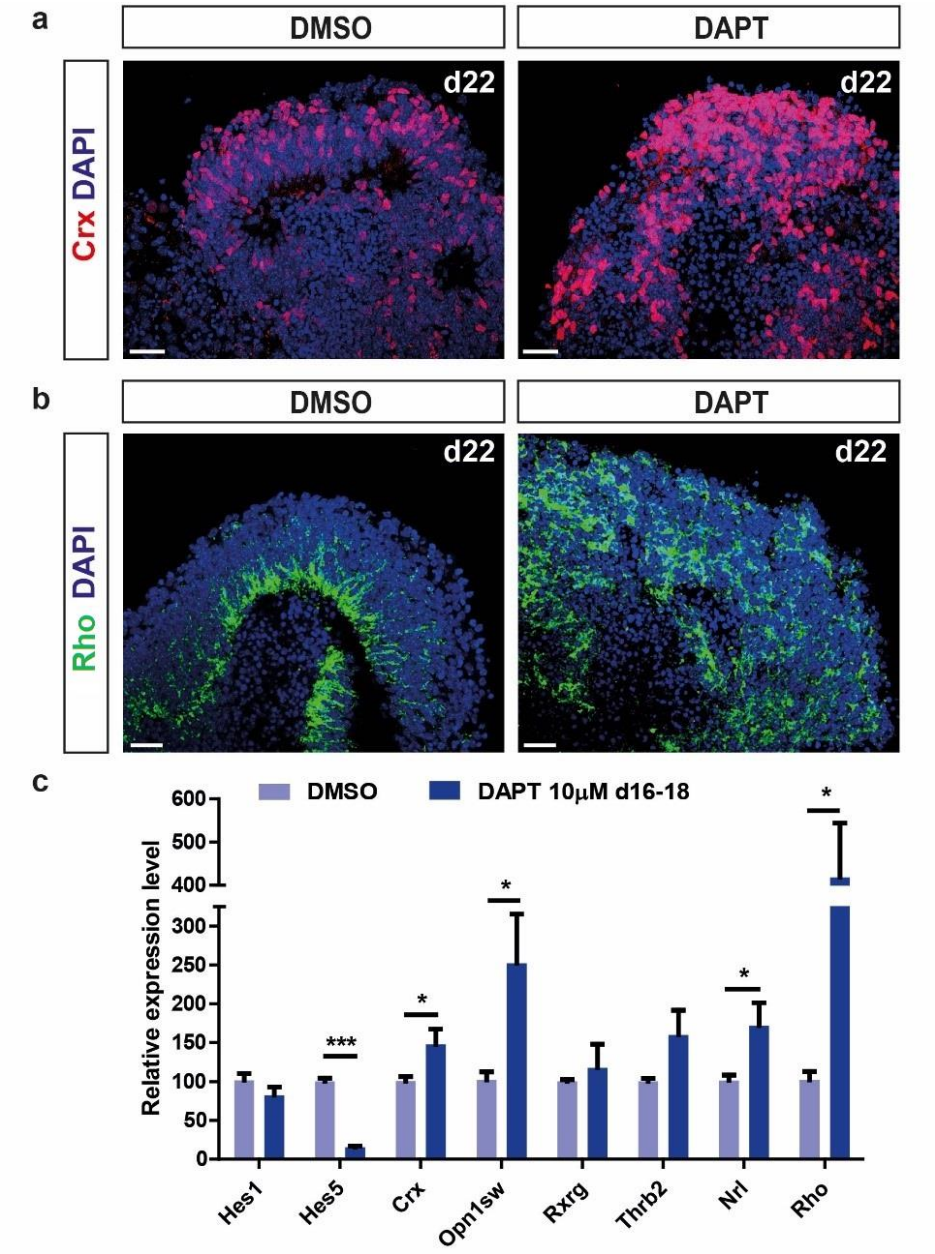

Figure 2.2. Notch inhibition at the time of photoreceptor genesis induces photoreceptor markers in mESC-derived retinae

(a) Immunohistochemistry showing increased staining for the photoreceptor precursor marker Crx (in red) following treatment with 10 μm DAPT at 16 of differentiation. **(b)** Immunostaining for the rod marker Rhodopsin in cultures treated with 10 μm DAPT at day 16 of differentiation. Note the loss of tissue organisation in the treated sample. Scale bar 20 μm in all images. **(c)** QPCR analysis at day 22 of differentiation of control cultures (DMSO) or treated with DAPT for 48 hours on day 16. N=3 differentiation cultures, n=6 RNA samples each from 12 organoids. *$p<0.05$; ***$p<0.001$, Student's *t*-test.

2.5. Proportion of Crx:GFP-positive photoreceptor precursors increases following Notch signalling inhibition

Having confirmed increased photoreceptor gene expression following the downstream blockade of Notch signalling in the retinal differentiation system, we next wanted to quantify the effect of photoreceptor fate induction. To this end, a Crx:GFP mouse embryonic stem cell line was used (Decembrini et al., 2014). Expression of GFP in all photoreceptor precursors allowed for the use of flow cytometry to quantify the proportion of cells in differentiation cultures that became photoreceptors. A papain-based neurosphere dissociation kit (Miltenyi Biotech, Germany) was used to reliably obtain single cell suspensions of differentiated mESC aggregates with good viability. Analogous to the experiments with the E16 CEE msESC line described in the previous section, Crx:GFP differentiated embryoid bodies at day 16 of culture were either treated with 10 µm DAPT, 10 µm RO4929097 or with control DMSO for 48hrs. 4 days following treatment, at day 22 the cells were dissociated and the percentage of cells expressing the GFP reporter was determined by flow cytometry. In the control DMSO condition an average 49.3% ± 5.8% of single live cells was GFP-positive, this percentage was substantially increased with treatment with both DAPT and RO4929097, to 67.2% ± 11.3% and 69.3% ± 6.3%, respectively (N=4 differentiation cultures, 36 organoids each; Figure 2.2 a and b). Treated aggregates were also collected for histological examination. This analysis confirmed upregulation of GFP reporter expression (Figure 2.2 c) and disorganisation of tissue morphology (Figure 2.2 c). Altogether these data show that Notch signalling limits cone and rod photoreceptor production in culture and modulation of this pathway offers potential to increase the yield of photoreceptors for transplantation.

2.6. An increased proportion of photoreceptors develop as cones following Notch inhibition at the time of cone genesis

During retinogenesis *in vivo* the peak of cone genesis precedes that of rod birth (reviewed in Swaroop et al., 2010). Inactivation of Notch was found to lead to overproduction of the photoreceptor type appropriate to the developmental stage at which it had been applied (Jadhav, 2006; Nelson et al., 2007; Yaron, 2006). Therefore, we hypothesised that blocking the downstream signalling of the Notch receptor at the time of cone genesis in mESC retinal differentiation culture will result in increased abundance of this cell type. To test this hypothesis treatment with 10 µm DAPT or RO4929097, or DMSO as vehicle control was performed at day 16 in culture or at day 21, a later stage at which some rod photoreceptors, bipolar cells and Müller glia are expected to be generated (Eiraku et al., 2011; Gonzalez-Cordero et al., 2013), but

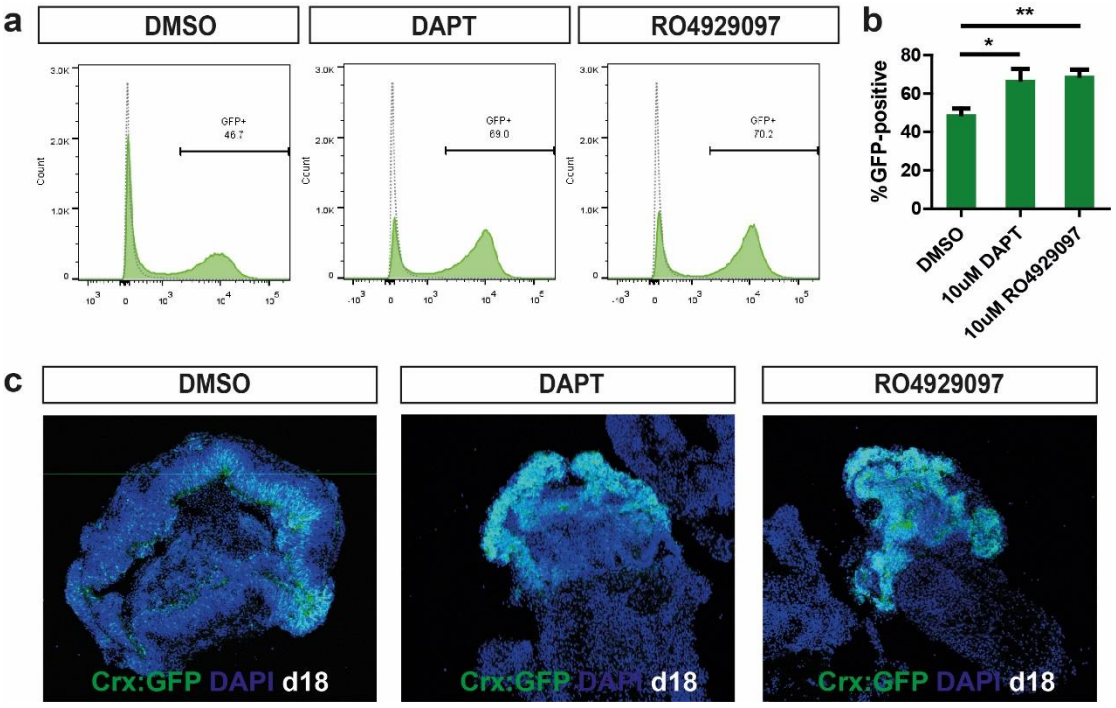

Figure 2.3. Proportion of Crx:GFP-positive photoreceptor precursors is increased by inhibition of Notch signalling

(a) Representative flow cytometry histograms of Crx:GFP line aggregates dissociated at day 19 of differentiation showing a shift towards higher percentage of GFP-positive photoreceptor precursors numbers following treatment with 10 µm DAPT or RO4929097 at day 16 (middle and right) versus DMSO control (left). **(b)** Quantification of the percentage of GFP-positive cells in samples described in (a); data represent results from 4 independent cultures. * *p<0.05*, ***p<0.01*, one-way ANOVA with Tukey's *post hoc* test. **(c)** Histological analysis using confocal microscopy of cryosections from DMSO control (on the left) and samples treated with DAPT or RO4929097 (middle and right) on day 16 of differentiation and collected at day 18. Please note the more pronounced GFP-expression, disorganisation and thinning of neural retina in treated samples.

cone genesis should be largely completed. Differentiating Crx:GFP ES line aggregates were then cultured as usual until day 26 when GFP-positive photoreceptors were collected by FACS (Figure 2.3 a). RNA was subsequently isolated from GFP-positive cells collected from each condition and qPCR analysis of photoreceptor gene expression was performed (Figure 2.3 b). Samples treated with either DAPT or RO4929097 at day 16 showed upregulation of cone markers *Thrb2* and *Rxrg*, which was not observed with inhibitor treatment at day 21 (Figure 2.3 b). Transcripts of S opsin (*Opn1sw*) were upregulated with inhibition performed at both time points (Figure 2.4 b), which could suggest some degree of regulation of this visual pigment expression by Notch signalling in post-mitotic precursors in addition to introducing bias in the type of progeny generated by progenitors. Differentiated embryoid bodies treated at day 16 with 10 µm DAPT were also collected for histological analysis at day 26. Immunostaining for S opsin was used to determine the percentage of Crx:GFP-positive photoreceptor precursors co-expressing S opsin (Figure 2.4 c and d). This analysis showed that aggregates treated with DAPT showed a significantly higher percentage of S opsin-expressing photoreceptor precursors compared to DMSO controls (Figure 2.4 c and d). Collectively, these results show that inhibition of Notch signalling at a stage when cone precursors are generated in mESC retinal differentiation yields a higher proportion of this photoreceptor subtype when examined at a more mature stage.

2.7. Photoreceptors show onset of maturation in mESC-derived retinae following Notch signalling inhibition

Notch inhibition, as in other systems examined (Jadhav, 2006; Nelson et al., 2007), led to disruption in tissue architecture and overproduction of developmentally appropriate cell subtypes. Since aspects of the developmental niche affect photoreceptor differentiation in retinal organoids (West et al., 2012), we wished to determine whether the photoreceptors generated in aggregates treated with DAPT develop to express phototransduction-related proteins at a stage equivalent to the onset of photoreceptor functional maturation *in vivo*. To address this we performed immunostaining for the visual pigments Rhodopsin (Fig 2.5 A) and S opsin (shown in Fig 2.4 c). The proteins were found expressed at day 28 and day 26 (equivalent to P4-8 *in vivo*), respectively, in the Crx:GFP-positive regions. At day 28 the DAPT-treated organoids also shown expression of the phototransduction-related protein Recoverin (Fig. 2.5 B) in the patches of GFP-positive photoreceptors. Moreover, neural retinae in the inhibitor-treated samples stained positive for the cone-specific marker Arrestin3 at day 28 of culture (Fig 2.5 C). These analyses show that, despite the loss of laminar

tissue organisation and partial disruption of the temporal neurogenesis programme triggered by pharmacological Notch signalling inhibition, photoreceptor precursors in this condition show expression of proteins associated with photoreceptor functional maturation.

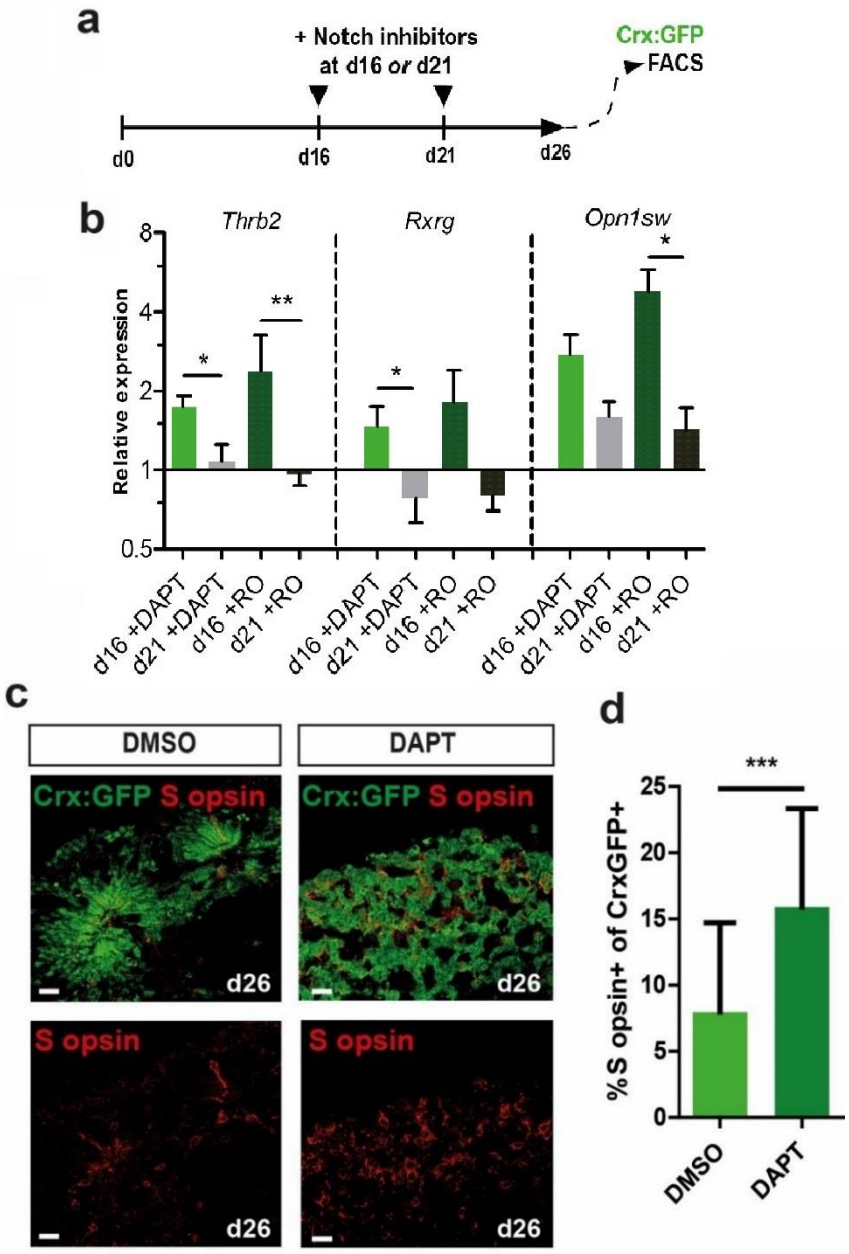

Figure 2.4. Increased proportion of photoreceptor precursors develops as cones following Notch inhibition at early stages of differentiation.

(a) Schematic depicting the protocol used for inhibition of Notch at early (day 16) versus late (day 21) stages of *in vitro* retinogenesis. GFP-positive cells were subsequently harvested by FACS for RNA isolation. **(b)** Gene expression analysis of samples obtained as depicted in (a). Note the clear increase in levels of cone-specific genes when Notch inhibition was performed at day 16, but not at day 21. Data represent flow-sorts of 8 independent differentiation cultures. Error bars ±SD. *$p<0.05$, **$p<0.01$, Student's *t*-test **(c)** Confocal microscopy images showing increase in Crx:GFP-positive cells co-labelling for S opsin on day 26 of differentiation (in red) following DAPT treatment at day 16. Scale bar 10 µm. **(d)** Quantification of Crx:GFP and S opsin co-labelling in control DMSO and cultures treated with 10 µm DAPT on day 16 of differentiation. Errors bars ±SD; ***$p<0.001$ Student's *t*-test.

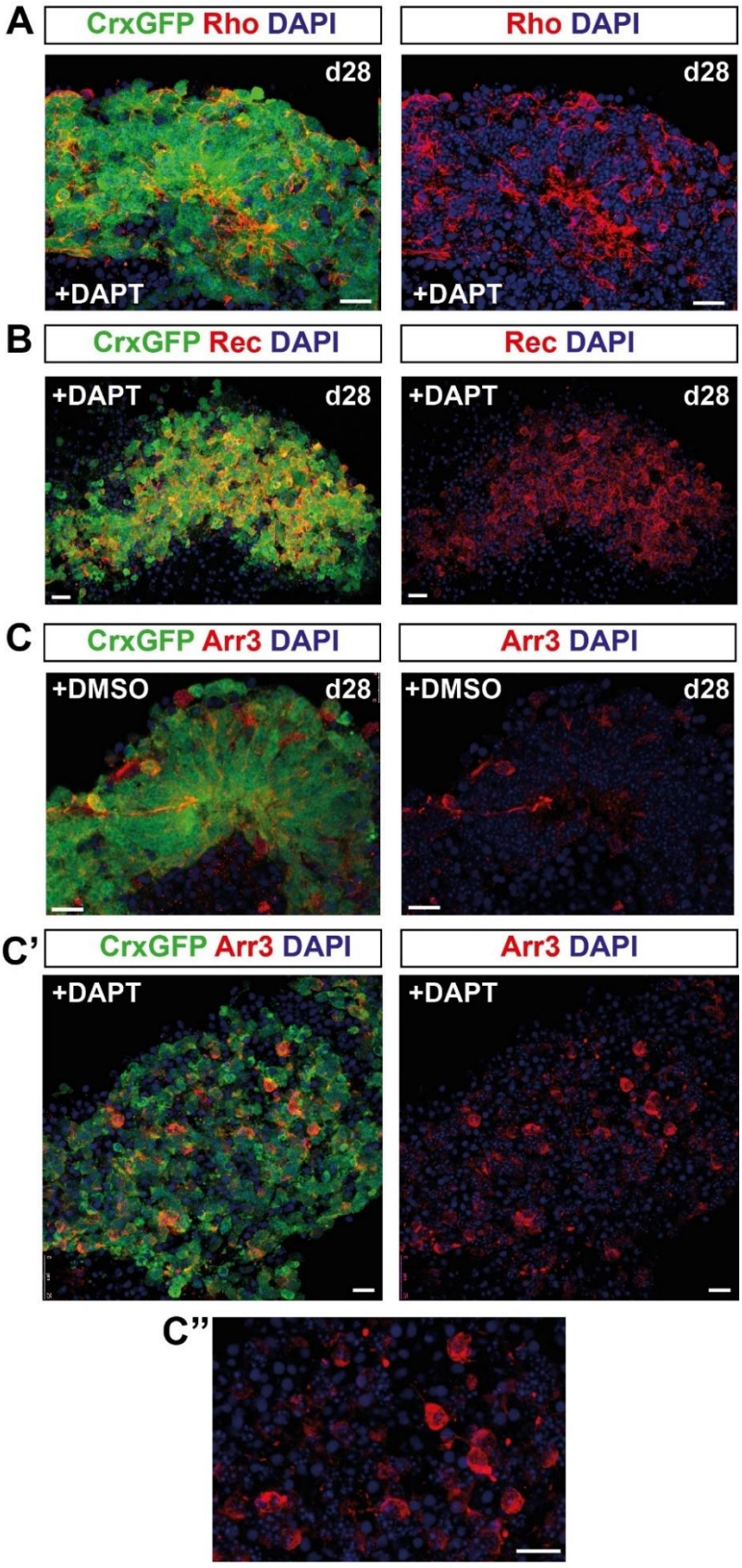

Figure 2.5. Photoreceptor maturation following Notch inhibition in mESC-derived retinae.

(A) Expression of the rod marker Rhodopsin in CrxGFP line aggregates treated with 10 µM DAPT at d16 of culture. **(B)** Immunostaining for the pan-photoreceptor marker Recoverin in differentiation cultures treated as in (A). **(C-C'')** Immunohistochemistry showing expression of Arrestin3 on day 28 in control cultures (DMSO, panel C) or cultures treated with 10 µM DAPT at d16 (C''). (C'') Higher power view showing morphology of the cells in (C'). Note the loss of organisation in the DAPT-treated organoids. Scale bar in all images 10 µm.

2.8. Conclusions and discussion

Notch signalling plays a critical role in regulation of neurogenesis by allowing maintenance of a cycling pool of progenitor cells and limiting precocious neurogenesis (Bassett and Wallace, 2012; Lewis, 1996). Pharmacological Notch inhibition using DAPT was performed in retinal organoids resulting in an increase in progenitor cell cycle exit, tissue disorganisation and, importantly, increase in Crx-positive cells (Eiraku et al., 2011). However, neither the photoreceptor subtypes made following Notch inhibition nor the temporal aspects of Notch action were examined.

In this chapter, the role of Notch signalling was investigated for the differentiation of cone and rod photoreceptor precursors using our retinal differentiation protocol. Treatment of mESC-derived retinae with the pharmacological inhibitor of Notch signalling DAPT at day 16 of differentiation revealed induction of both cone and rod genes as well as a pronounced decrease in progenitor marker *Hes5*. Analysis of the early cone cell specific marker Trβ2 in our culture system, showed that Trβ2-positive cone precursors are first detectable from day 12 with numbers increasing until around day 20, beyond which point they stabilise (please refer to Figure 1.4). As Trβ2 is expressed soon after exit from terminal mitosis (Ng et al., 2009), day 16 is likely to be close to the peak of cone genesis in this system. Rod precursors are born over a longer temporal window *in vivo* starting at around E12 and finishing before P10 (Swaroop et al., 2010). In the 3D suspension mESC retinal differentiation system used here rod genesis is most pronounced between days 18 to 20 (A. Gonzalez-Cordero, unpublished results) and therefore Notch inhibition at day 16 falls at an earlier phase of rod genesis preceding the birth peak of this photoreceptor subtype.

Similar to previous observations *in vivo* (Jadhav, 2006; Nelson et al., 2007; Yaron, 2006) and *in vitro* (Eiraku et al., 2011) we observed disrupted tissue morphology with prominent loss of lamination following Notch inhibition *in vitro*. retinal tissue in treated samples appeared smaller in size by light microscopy and the total yield of flow-sorted cells was usually lower from treated samples, consistent with growth arrest reported in the pharmacologically treated chick and mouse retinae (Nelson et al., 2007). Nevertheless, this dysmorphic tissue still permitted photoreceptor differentiation with the appearance of mature phototransduction-related proteins such as S opsin, Rhodopsin, Recoverin and Arrestin3 as reported *in vivo* (Riesenberg et al., 2009; Yaron, 2006), but not previously examined *in vitro*. Importantly, this demonstrates that the use of Notch inhibition yields photoreceptors capable of at least the initial steps of functional maturation, potentially providing a means to increase the yield of photoreceptor precursors undergoing normal further differentiation.

Further quantitative assessment of the effects of pharmacological inhibition of Notch activity was possible with the use of a Crx:GFP reporter ESC line (Decembrini et al., 2014). Embryoid bodies formed from this mESC line differentiated into retinal tissue showed robust induction of the GFP reporter following treatment with two pharmacological γ-secretase inhibitors DAPT and RO4929097 at day 16 in culture. In this cell line, at day 16, cone precursors constitute 38% of Crx:GFP-positive cells, with the percentage progressively dropping beyond this stage suggestive of the appearance of the rod precursor birth peak (Decembrini et al., 2014). In this study, Crx:GFP line aggregates treated with the Notch inhibitor DAPT at day 16 showed an increased proportion of S opsin-positive cells amongst GFP-expressing photoreceptor precursors, by immunostaining, when cultured until day 26. To test whether this increase was stage dependent, we treated cultures either at day 16 or later at day 21, when the late-born cell types such as rod, bipolar and Müller cells would be generated. Photoreceptors isolated from these cultures showed that cone markers were much more prominently upregulated in cultures treated with DAPT or RO4929097 at d16 than at day 21, showing that the confinement of cone genesis to earlier stages of retinogenesis is most likely recapitulated in this mESC retinal differentiation system. This finding is consistent with the role of Notch in regulation of neurogenesis timing and limiting production of ganglion cells and cones at early stages of retina formation (Jadhav, 2006; Nelson et al., 2007; Riesenberg et al., 2009). Altogether, these results demonstrate that signalling through Notch receptors negatively regulates both cone as well as rod neurogenesis and timely inhibition of Notch signalling demonstrates the presence of progenitor cells with a bias towards cone genesis in the early stages of retinogenesis *in vitro*.

Since processing of all Notch receptor isoforms was inhibited in this study, differential effects of the individual Notch receptors could not be investigated. Therefore, there remain outstanding questions regarding the role of Notch pathway in this differentiation system. Are both Notch1 and Notch3 receptors expressed in this system? If so, would inhibition of Notch signalling at earlier stages than tested here trigger increased production of retinal ganglion cells as observed with genetic disruption of *Notch3 in vivo* (Riesenberg et al., 2009)? This question is of interest from translational research point of view since retinal ganglion cells are affected in glaucoma and cell therapy is considered a potential future treatment for this condition (reviewed in Sun et al., 2015; Wang and Xie, 2014). Another remaining question concerns the downstream molecular effectors of Notch signalling in limiting cone precursor differentiation. We found here a significant decrease in the mRNA transcripts for the downstream Notch

signalling target the bHLH transcription factor Hes5, however the more direct effectors of commitment to cone lineage remain uncharacterized. Some indication as to the downstream effectors of Notch1 signalling in late retinogenesis were described in a recent study by the Cepko group (Mizeracka et al., 2013). Gene expression comparison of wild-type and *Notch1*-knockout precursors revealed differentially expressed candidate regulators. Amongst them inhibitor of DNA binding factors Id1 and Id3 were strongly downregulated in *Notch1*-knockout cells and were subsequently found to drive Müller cell differentiation. In contrast, Notch-regulated ankyrin repeat protein (Nrarp) was found to be significantly upregulated following Notch1 deletion. Overexpression of this inhibitor of Notch signalling led to overproduction of rod cells at the expense of Müller glia. Similar analysis could reveal Notch effectors at the time of cone genesis and potentially provide valuable insights into how the decision between cone and other early fates is made.

In the aforementioned study (Mizeracka et al., 2013) *Notch1* deletion was specifically analysed in early post-mitotic cells, indicating a function for Notch signalling also following progenitor terminal division. Interestingly, we found that, when we performed pharmacological Notch inhibition at equivalents of early post-natal stages at day 21 in culture (Fig. 2.4 b), S opsin expression was increased without a concomitant induction of *Thrb2* or *Rxrg* expression. Since the effect size for *Thrb2* upregulation was similar with inhibition at the earlier day 16 timepoint, it is possible to speculate that this induction could reflect an increase in S opsin expression in differentiating early post-mitotic cone precursors rather than an increase in progenitors committing to cone fate. This observation could suggest a role of Notch signalling in regulation of differentiation in newly born cones.

In conclusion, results presented in this chapter demonstrate the role of Notch signalling in limiting photoreceptor genesis in mESC retinal differentiation *in vitro*. Pharmacological inhibition of Notch signalling by use of γ-secretase inhibitors DAPT or RO4929097 at the time of cone genesis lead to upregulation of cone precursor-specific proteins and an increased proportion of S opsin-positive cells amongst differentiating mESC-derived Crx:GFP-expressing photoreceptor precursors. Following inhibition, both cone and rod-expressed genes and proteins increased, as well as the percentage of GFP-positive photoreceptors differentiated from a Crx:GFP reporter line. This was associated with loss of lamination and tissue laminar morphology, however, disorganisation resulting from precocious photoreceptor neurogenesis did not prevent the expression of more mature phototransduction-related proteins such as the visual pigments Rhodopsin and S opsin, as well as

phototransduction cascade components Recoverin and Arrestin3. Finally, inhibitor treatment at early (day 16) but not late (day 21) stages of retinogenesis *in vitro* led to increased expression of cone genes, indicating that cone genesis is limited to an earlier stage of retinal neurogenesis, mimicking *in vivo* cone development.

Chapter 3. Levels of the rod specific transcription factors Nrl and Nr2e3 affect photoreceptor precursor differentiation in retinae derived from mouse embryonic stem cells.

3.1. Background

Photoreceptors, especially rods, are generated during an extended period in retinal histogenesis, long before the onset of functional maturation. The time from progenitor final mitosis to the acquisition of mature features and the onset of function is weeks to months, depending on the species (Swaroop et al., 2010). This prolonged lag period between final division of a progenitor and terminal differentiation raised interest in the potential fate plasticity during this phase.

Investigations into the evolution of the vertebrate visual system have revealed that cone-like photoreceptors were the first to emerge prior to the whole genome duplication around 550 million years ago in the Cambrian era that gave rise to vertebrates (Lamb, 2013). In accordance, studies examining the molecular evolution of opsins have shown short wavelength (blue) opsin to be the ancestral photoreceptor visual pigment (Lamb, 2013; Larhammar et al., 2009). It still remains unclear when exactly in the course of evolution rods appeared. However, recent reports characterized lamprey photoreceptors, that have cone-like morphology, but sensitivity to dim-light with single photon detection capability, a typical feature of rods (Asteriti et al., 2015; Morshedian and Fain, 2015). These studies indicate that the separation of the two photoreceptor types occurred before 400 million years ago, since then jawless lampreys diverged from jawed vertebrates (Asteriti et al., 2015; Lamb, 2013; Morshedian and Fain, 2015). Hence, evidence supports the hypothesis that rods emerged from ancestral cone cells in photoreceptor evolution.

The molecular pathways leading to the determination of rod versus cone phenotype have been an area of intense investigation (reviewed in Swaroop et al., 2010, summarised in Diagram 3.1.). Recently early steps in commitment to the cone lineage have been described with the Onecut family transcription factors acting collaboratively with Otx2 to induce expression of the early cone marker Trβ2 in progenitors biased towards cone genesis (Emerson et al., 2013). Moreover, introduction of the dominant-negative form of chicken Onecut1 homologue was shown to induce the rod-determining transcription factor L-Maf (Emerson et al., 2013) suggesting early binary determination of subsequent photoreceptor precursor fate in avian species. In accordance, misexpression of Onecut1 in neonatal mouse retinal progenitors leads to

increased generation of RXRγ-positive cone precursors and concomitant reduction in Nr2e3-expressing rod precursors (Emerson et al., 2013).

In contrast to the cone-dominant retinae of fish or birds, mammalian retinae are composed predominantly of rods. This was likely a critical adaptation for mammalian ancestors forced into nocturnal lifestyle during their early evolution. Only recently the molecular mechanism for this shift in retina composition in mammals has been proposed (Kim et al., 2016). In mammals a key determinant of the rod photoreceptor fate is the highly conserved neural retina leucine zipper (Nrl) transcription factor (Swaroop et al., 1992). With loss of Nrl in mice, all rod-specific gene expression is abolished and nearly all photoreceptors acquire an S cone-like phenotype (Mears et al., 2001). Conversely, forced expression of Nrl in all developing photoreceptor precursors using the *Crx* promoter leads to the loss of mature cone phenotype (Oh et al., 2007). In mice, but not zebrafish, most rods show an expression history of S opsin, determined by the use of permanent genetic tagging driven by S opsin promoter (Kim et al., 2016). Moreover, cone genes are transiently expressed in immature rods in mice (Kim et al., 2016). Taken together these observations strongly suggest that increased proportion of rods in mammals arises from recruitment of S cone precursors via Nrl activity.

This hypothesis is consistent with additional observations related to photoreceptor precursor plasticity. Histological analysis of developing retinae showed co-expression of cone (Trβ2, S opsin) and rod (Nrl) markers in a proportion of developing photoreceptor precursors (Kim et al., 2016; Ng et al., 2011). In addition, misexpression of Nrl from the S opsin promoter in an Nrl knockout background repressed cone markers, but did *not* result in generation of functional rods (since the promoter is only transiently active in immature rods; Oh et al., 2007). Similarly, inducible deletion of Nrl could only lead to full conversion into S opsin-expressing cone-like cells prior to P8, due to development of epigenetic modifications acting as a barrier to fate switch at later stages of development (Montana et al., 2013). Altogether, there is strong evidence supporting cell fate plasticity in immature photoreceptors.

Nrl plays a central role in the gene-regulatory network for rod differentiation (Diagram 3.1.). The retinoid orphan receptor RORβ, which is expressed in progenitors, photoreceptors and other cell types, initiates Nrl expression in early photoreceptor precursors destined to develop as rods. In these cells Nrl in a positive feedback loop induces expression of photoreceptor-specific isoform RORβ2, consolidating commitment to the rod fate (Fu et al., 2014). Using an Nrl:GFP reporter mouse line it

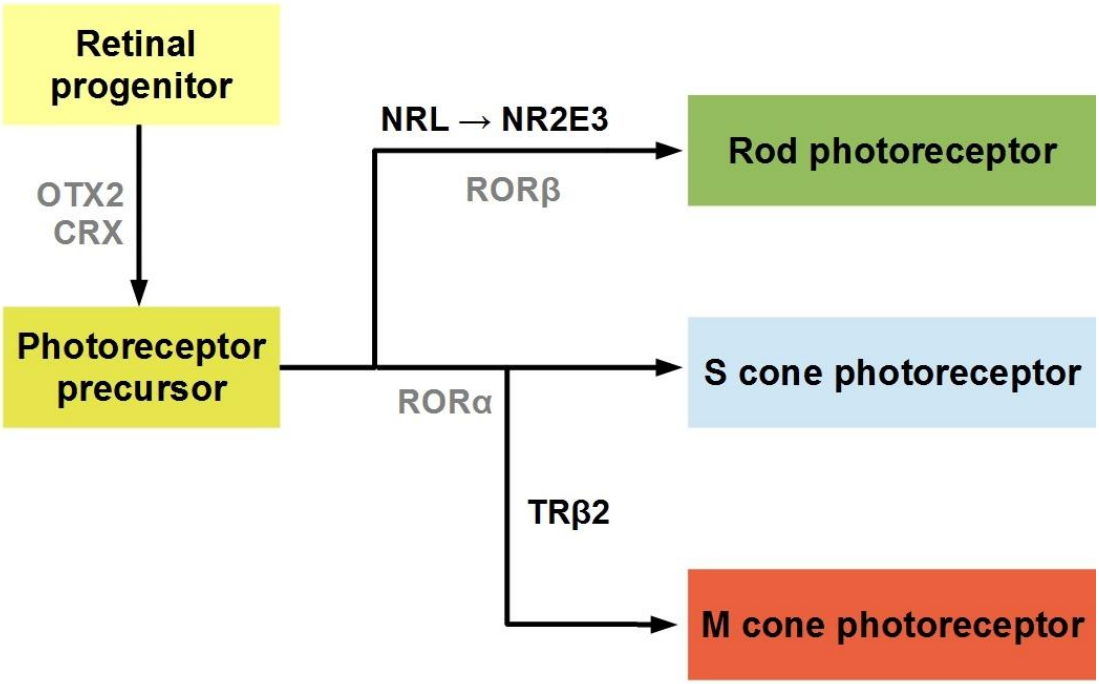

Diagram 3.1. Simplified model of photoreceptor specification through sequential activity of transcriptional regulators

In retinal progenitors poorly characterized events lead to upregulation of Otx2, which is necessary, but not sufficient for photoreceptor fate specification. Early in postmitotic photoreceptor precursors an Otx-like transcription factor Crx becomes expressed, which is required for induction of a large subset of photoreceptor-specific genes, including those encoding phototransduction cascade components and outer segment proteins. Orphan nuclear receptors RORα and RORβ also play an important role in the regulation of gene expression in developing cone and rod precursors. RORβ expression is critical for the induction of the rod determining transcription factor Nrl. In turn, Nrl induces expression of Nr2e3, which is necessary for suppression of cone-specific gene expression in rod cells. In cone precursors, thyroid hormone receptor Trβ2 is required for induction of M opsin expression.

was determined that Nrl expression in rod precursors commences as early as E12.5-E14.5 (Akimoto et al., 2006). Many rod-specific genes require Nrl for their expression, most notably Rhodopsin and the rod-specific orphan nuclear receptor Nr2e3. Activity of Nrl in inducing Rhodopsin expression is mediated through Nrl Responsive Element (NRE), an AP1-like binding sequence present in the promoter of the Rhodopsin gene. Crx acts in synergy with Nrl to induce transcription from the Rhodopsin locus, but not from the S opsin promoter region (Hennig et al., 2008).

Many of the effects of Nrl are mediated through its direct transcriptional target Nr2e3. Nr2e3 is a nuclear receptor with a zinc-finger DNA-binding domain at its N-terminus and a ligand-binding domain in the C-terminus, however, no physiological ligand has so far been identified for Nr2e3 (Milam et al., 2002). Nr2e3 expression is first detected around E18 in the mouse and is abolished in *Nrl*$^{-/-}$ retina demonstrating that Nrl is a key upstream inducer of Nr2e3 in the rod differentiation pathway. A spontaneous retrotransposon insertion in the Nr2e3 locus interfering with splicing and resulting in the loss of Nr2e3 protein expression (Chen et al., 2006) underlies retinal degeneration in the *rd7* mouse strain (Akhmedov et al., 2000). Nr2e3 deficiency results in the formation of hybrid photoreceptors, which express both rod and cone markers (Corbo and Cepko, 2005), indicating that the primary action of Nr2e3 is to suppress cone gene expression in rods. Since Nrl expression is not affected in the *rd7* mice this also highlights that Nrl is mainly an inducer of rod-specific genes, whilst negative regulation of cone genes in rods is mediated via Nr2e3 (Cheng et al., 2006; Corbo and Cepko, 2005). Additionally, loss of Nr2e3 in *rd7* mice results in formation of supernumerary S cones (around 2-3 fold increase; Corbo and Cepko, 2005) suggesting that Nr2e3 also plays some role in establishing the proper cone to rod ratio. Consistently, these mice show increased blue cone responses measured by electroretinogram (ERG; Cheng et al., 2006). The other hybrid photoreceptors do not express cone opsins, but do express certain cone-specific genes such as *Gnat2* and *Pde6c* in addition to rod genes (Corbo and Cepko, 2005). In summary, rod specification is dependent on the action of Nrl and its downstream effector Nr2e3. Loss of Nrl prevents formation of mature rods, whereas Nr2e3 is critical for suppressing cone-specific genes in rod cells (Diagram 3.1.).

3.2. Aims

In Chapter 2 we show evidence that inhibition of Notch signalling at early stages of retinal histogenesis *in vitro* leads to precocious neurogenesis increasing the ratio of cones to rods in resulting populations. In mouse post-mitotic photoreceptor precursors activity of Nrl and its downstream transcriptional target Nr2e3 directs recruitment of a large proportion of S cone precursors to the rod fate. Since genetic removal of Nrl in

donor mice has been employed to produce cone-like populations for transplantation (Santos-Ferreira et al., 2015; Smiley et al., 2016), we sought to test the utility of *Nrl* and *Nr2e3* gene silencing during equivalents of early post-natal development for cone enrichment *in vitro* by:

- developing and testing efficient *Nrl* and *Nr2e3* knockdown constructs,
- effective delivery of these constructs into developing mESC-derived retinae at an appropriate stage when early post-mitotic photoreceptors are present,
- evaluation of the effects of Nrl and Nr2e3 knockdown on gene expression in differentiating photoreceptor precursors.

We hypothesised that given the fate plasticity in immature photoreceptors reduction in *Nrl* and *Nr2e3* expression in immature photoreceptor precursors would prevent repression of S opsin and allow formation of cone-like cells.

Providing we achieve broad and efficient downregulation of *Nrl* and *Nr2e3*, our goal was to examine expression of cone specific genes such as *Thrb2* and *Rxrg* to compare resulting photoreceptors with cone-enriched populations formed by inhibition of Notch signalling. This would allow identification of most promising approaches for cone enrichment in mESC-derived donor population for transplantation studies.

3.3. Development of Nrl and Nr2e3 knockdown constructs

Previous studies from the group demonstrated that efficient downregulation of specific target gene expression in the retina can be achieved using short hairpin constructs based on endogenous microRNA structure and acting through the RNA interference pathway (Georgiadis et al., 2010). To directly evaluate the impact of *Nrl* and *Nr2e3* expression levels in developing photoreceptor precursors, we employed this gene expression silencing strategy. Artificial miRNAs targeting the coding sequences of mouse *Nrl* and *Nr2e3* genes were designed *in silico* using siDESIGN software (Dharmacon) and candidates with the highest targeting scores and lowest predicted off-target effects were cloned into expression plasmids (Figure 3.1 a). Efficiency of mRNA targeting was measured in HEK 293T cells transiently transfected with *shNrl* and *shNr2e3* expression vectors alongside Nrl and Nr2e3 overexpression constructs (Figure 3.1 a and b). RNA from transfected cells was harvested and analysed by qPCR. Expression of both *Nrl* and *Nr2e3* mRNAs was strongly downregulated in cells transfected with *shNrl* and *shNr3e3*, compared to a non-targeting control construct (Figure 3.1 b). This effect was particularly striking when the ratio of knockdown to overexpression plasmids was increased to 4:1 (Figure 3.1 b). These constructs were

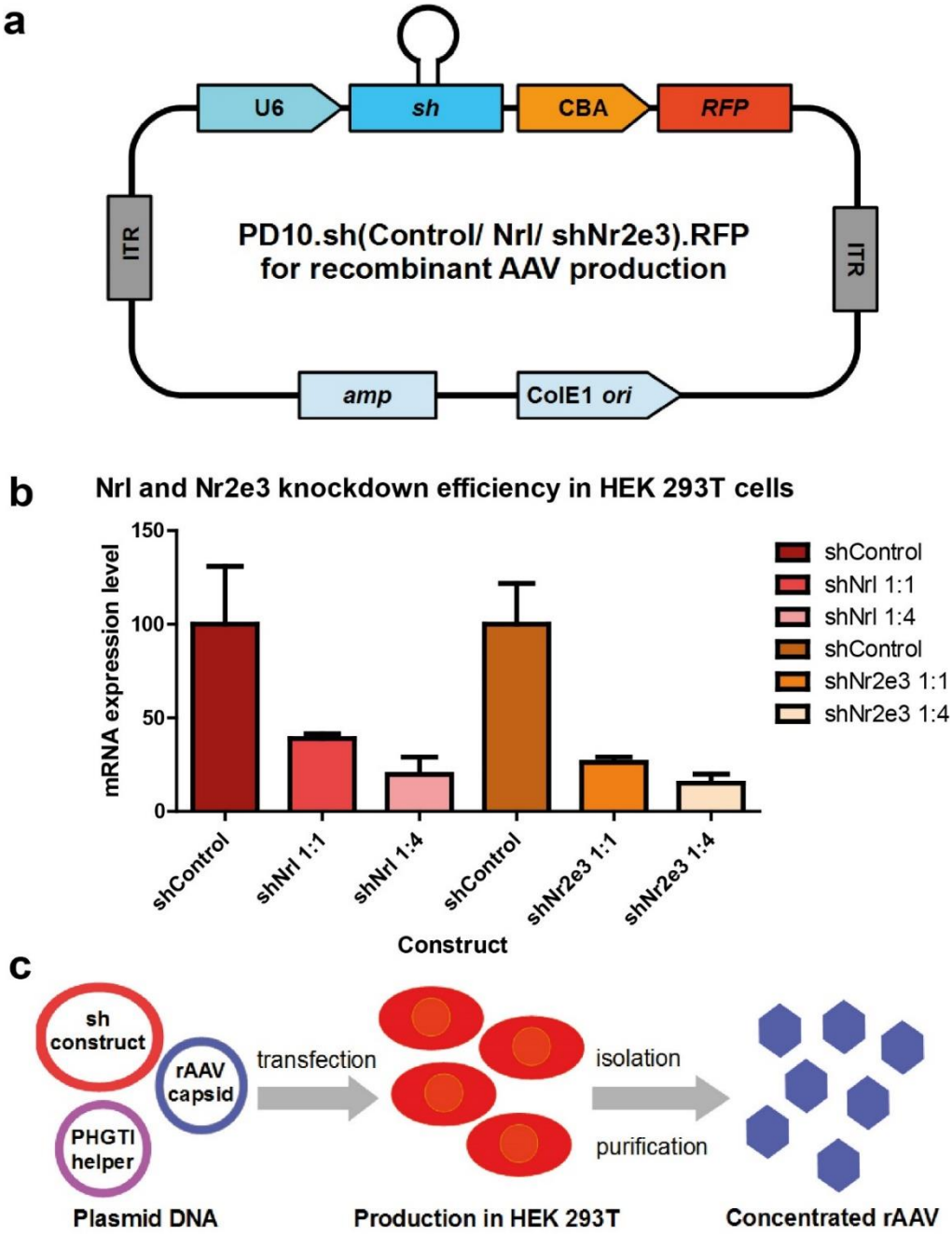

Figure 3.1. Development and production of *Nrl* and *Nr2e3* knockdown constructs in rAAV vectors

(a) Schematic map of knockdown construct plasmids. U6 – *U6* promoter sequence; sh – short hairpin; CBA – chicken beta actin promoter sequence; RFP – red fluorescent protein coding sequence; ITR – inverted terminal repeats; amp – ampicillin resistance gene coding sequence; ColE1 ori – ColE1 plasmid origin of replication sequence. **(b)** Quantitative PCR analysis of RNA isolated from HEK 293T cells transfected with Nrl or Nr2e3 overexpression vectors and control non-targeting short hairpin or shNrl or shNr2e3 constructs in 1:1 or 1:4 ratios. Average of triplicate samples from two independent transfections. **(c)** Graphical overview of the protocol for recombinant AAV vector production using a three plasmid system (on the left) in HEK 293T cells (middle).

used to produce recombinant adeno-associated viral vector (rAAVs) (Lai et al., 2002) using a three plasmid system (Figure 3.1 c). The RFP reporter present in the constructs allowed examination of transfection efficiency in HEK 293T cells used for vector production. Viral vector particles were isolated and purified using chromatography (Kaludov et al., 2002), followed by concentration (Figure 3.1 c). Vectors prepared in this way can be used to efficiently transduce photoreceptor cells both *in vivo* (Georgiadis et al., 2010) and *in vitro* (Gonzalez-Cordero et al., 2013; West et al., 2012).

3.4. Efficient transduction and downregulation of Nrl and Nr2e3 expression in the adult mouse retina

To test the effects of developed vectors in photoreceptor cells, purified and concentrated rAAV serotype 2/9 vector preparations were injected into the subretinal space of adult wild-type mice. Histological examination of injected eyes revealed widespread transduction assessed by reporter RFP expression, which was limited to the outer nuclear layer (Figure 3.2 a and b), where photoreceptors reside. Transduced photoreceptors were isolated by dissociation and FACS, followed by RNA isolation. Pronounced silencing of gene expression was observed for both *shNrl* as well as *shNr2e3*, compared to retinae transduced with a non-targeting control vector (Figure 3.2 c). Consistent with the requirement for Nrl in *Nr2e3* expression, levels of *Nr2e3* transcripts were diminished in retinae transduced with the *shNrl* vector (Figure 3.2 c). Notably, expression of the *Rhodopsin* gene, which is a direct transcriptional target of Nrl and Nr2e3, was also strongly suppressed following transduction with these vectors (Figure 3.2 d). Therefore, this set of experiments demonstrates that the Nrl and Nr2e3 knockdown vectors developed are effective in adult photoreceptor cells *in vivo*.

3.5. The expression level of Nrl and Nr2e3 impacts on S opsin transcription

In the rod differentiation pathway Nrl stimulates rod-specific gene expression, whilst Nr2e3 suppresses cone genes. Genetic ablation of each of these transcription factors leads to a widespread upregulation of S opsin visual pigment (Corbo and Cepko, 2005; Mears et al., 2001). Co-expression of Nrl and S opsin was detected in a subset of photoreceptor precursors (Kim et al., 2016; Ng et al., 2011). In order to determine how the transcription levels of Nrl and Nr2e3 affect opsin expression in developing photoreceptor precursors, we used the *shNrl* and *shNr2e3* vectors in the synthetic mESC-derived retina tissue culture system. First, to determine the appropriate time window for transduction, in which photoreceptors are primarily at the post-mitotic precursor stage, a BrdU pulse-chase experiment was performed. BrdU nucleotide analogue is incorporated into the newly synthesised DNA in the S phase of the cell cycle. The label is largely retained if exposure occurs during progenitor terminal

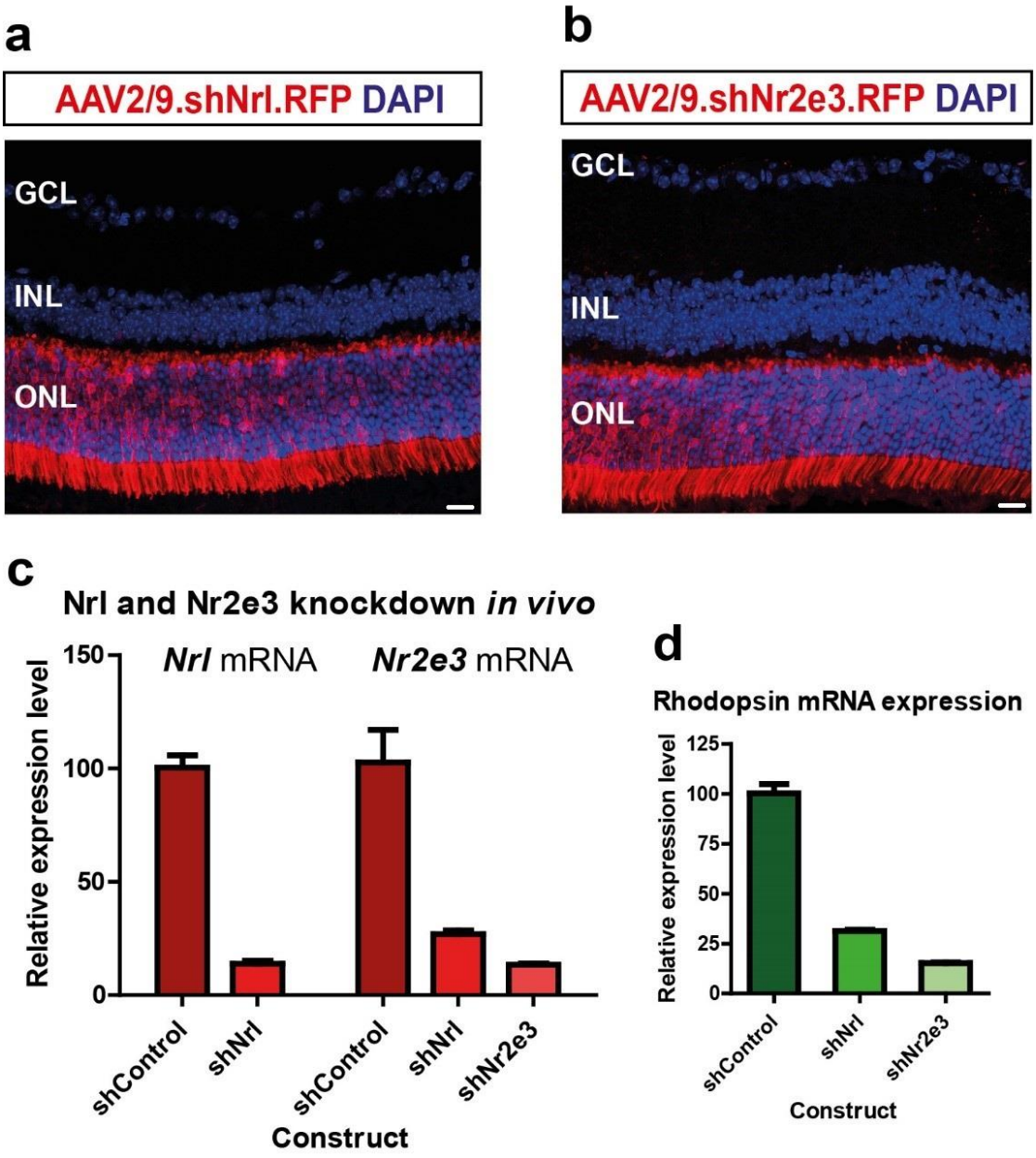

Figure 3.2. Efficient *Nrl* and *Nr2e3* knockdown *in vivo* using rAAV vectors

(a,b) Expression of RFP reporter in adult mouse retina transduced with AAV2/9.shNrl.RFP **(a)** or AAV2/9.shNr2e3.RFP **(b)** vectors delivered via subretinal injection. Note that reporter expression is limited to the outer nuclear layer. Scale bars 20 µm. **(c)** Quantitative PCR analysis of RFP-expressing cells isolated from transduced retinae and purified through FACS. Data from triplicate samples from three retinae. **(d)** QPCR Rhodopsin mRNA analysis in samples described in (c). Error bars ±SEM in both (c) and (d).

mitosis. This property was used to follow cell birth in our 3D mESC retinal differentiation cultures. Stem cell derived retinae were pulsed overnight with 10 µM BrdU at day 14, 16, 18 and 20 of culture and samples were collected for histological analysis at day 21. Immunohistochemical detection of BrdU showed that label incorporation was most prominent when the pulse was performed at day 16 and 18 (Figure 3.3 b and c), whereas much less labelling was observed with pulses at day 14 or day 20 (Figure 3.3 a and d). This is consistent with previous reports indicating that rod photoreceptor generation peaks around day 16-18 in culture (Eiraku et al., 2011). We therefore selected day 22 for vector transduction since few photoreceptor cells should be born before the expression from the constructs reaches high levels three days later (approximately on day 25 of differentiation). Since both Nrl and Nr2e3 are required for different aspects of rod fate commitment and Nrl is an upstream inducer of Nr2e3 (reviewed in Swaroop et al., 2010, also note the reduced expression of Nr2e3 following Nrl kockdown *in vivo* in Fig. 3.2 c), we only examined the molecular effects of simultaneous knockdown of both of these factors in mESC-derived retinae. With this experimental paradigm (Figure 3.4 a) expression of *shNrl* and *shNr2e3* occurs primarily at the post-mitotic photoreceptor precursor stage. Each vector was used at 3.5 x10^9 viral genome copies per retinal organoid, giving 7 x10^9 viral genome copies per aggregate when both knockdown constructs were used. In organoids infected with the vectors, strong RFP reporter expression was observed by day 29 (Figure 3.4 b-e'). At which stage tissues were harvested for histology and RNA analysis. Sectioned aggregates showed RFP-positive cells in the photoreceptor layer of mESC-derived retinae with strong signal in the inner segments (Fig 3.5 a-c). The percentage of transduced cells in the neural retinae derived from mESC were counted on sections counter-stained with nuclear Lamin B antibody for ease of identification of single transduced nuclei. In the case of each construct alone there were around 20% of neural retinal cells transduced, whereas combination of the two vectors at equivalent titres as each one on its own (approximately double the number of total viral particles) lead to around 35% of neural retinal cells expressing RFP (Fig 3.5 d). With this high transduction efficiency effects on gene expression in samples from whole cultures were observed. In RNA samples analysed by qPCR there was a clear reduction in mRNA transcripts of *Nrl* and *Nr2e3* associated with a significant increase in abundance of S opsin transcripts (n=6 samples from N=3 differentiation cultures; p<0.05 for all three genes, Student's t-test; Fig 3.5 e). No reduction in *Rho* expression was detected in these samples. Together these analyses show that Nrl and Nr2e3 knockdown constructs delivered and expressed in mESC-derived retinae at a stage when

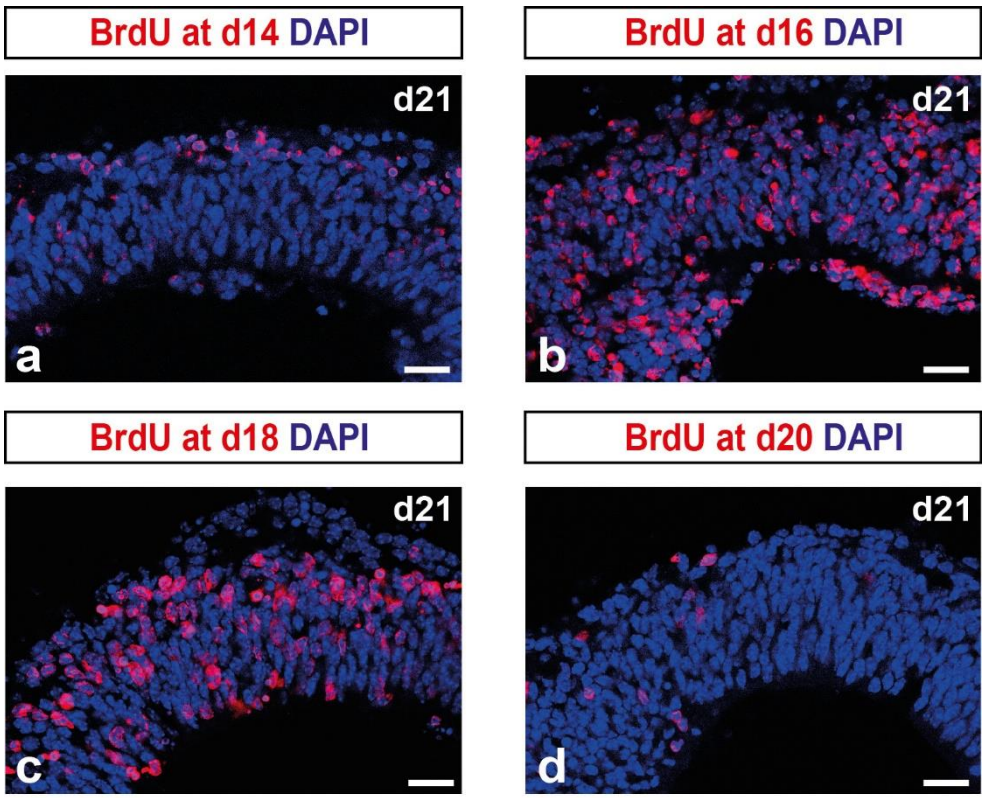

Figure 3.3. Analysis of proliferation in mESC-derived retinae using BrdU pulse labelling

Representative neural retinal regions in samples of aggregates treated for 8 hours with 10 µM BrdU at day 14 **(a)**, 16 **(b)**, 18 **(c)** and 20 **(d)**, before harvesting at day 21 of differentiation (n=2 differentiation cultures; 12 organoids per each timepoint). BrdU staining shown in red. Please note, the most prominent BrdU retention was present in samples treated at day 16 and 18, around the peak of rod photoreceptor genesis in culture. Scale bars 20 µm.

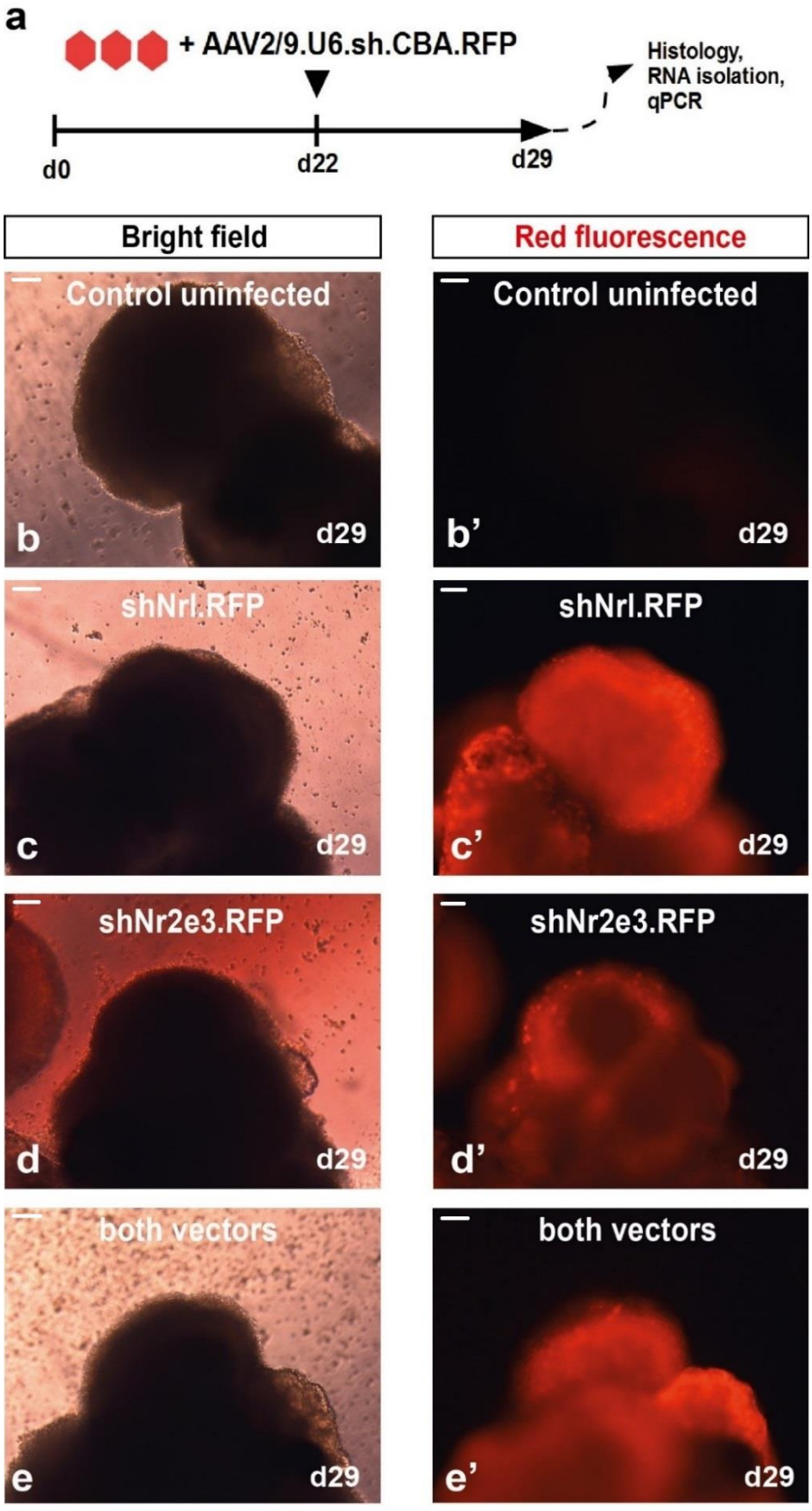

Figure 3.4. Transduction of mESC retinal differentiation cultures with rAAV2/9 *Nrl* and *Nr2e3* knockdown vectors

(a) Graphical depiction of the transduction protocol. Aggregates of mESCs differentiated into retina were infected at day 22 in culture and analysed 7 days later. **(b,c,d,e)** Bright field images of aggregates infected with control non-targeting vector **(b)**, shNrl **(c)**, shNr2e3 **(d)** or co-infected with both shNrl and shNr2e3 vectors **(e)**. Corresponding red fluorescence image showing RFP reporter expression in cultures transduced with control non-targeting construct **(b')**, shNrl **(c')**, shNr2e3 **(d')** or both shNrl and shNr2e3 vectors **(e')**. Scale bars 100 µm.

photoreceptors are post-mitotic precursors lead to reduction in *Nrl* and *Nr2e3* mRNA levels that correlates with upregulation of S opsin expression.

3.6. Identification of the most efficient AAV serotypes for photoreceptor transduction in mESC-derived retinae

Different AAV serotype-based vectors delivered to the developing retina have shown varied efficiencies for photoreceptor transduction (Watanabe et al., 2013). The tropism and efficiency of rAAV vectors in synthetic mESC-derived retinae are currently poorly characterized. Since the use of high-titer rAAV2/9 vector transduced only around a third of cells in the mESC-derived neural retina (Fig. 3.5) and as a part of ongoing research in the group, a panel of rAAV vectors based on different serotypes was examined for transduction efficiency in mESC-derived retinae *in vitro*, to identify the most potent serotypes in this context. We screened a panel of vector serotypes based on the wild-type AAV2 capsid including AAV2/2, AAV2/5, AAV2/8, AAV2/8Y(733), AAV2/9 and an artificially developed serotype ShH10. Each of the different serotype vectors carried a GFP reporter driven by the CMV promoter as the transgene. An equal number of viral particles (3.5 $x10^9$ viral genome copies per retinal organoid) were added in triplicate to wells with differentiating retinal organoids at day 22 of culture (Figure 3.6 a). Samples were collected for histological analysis a week later on day 29 of differentiation (Figure 3.6 a). Examination of reporter expression in the transduced aggregates showed very prominent GFP fluorescence in neural retinal regions following infection with the ShH10 serotype vector (Figure 3.6 h). This was in contrast to the relatively modest transduction of retinal neuroepithelium with AAV2/9 (Figure 3.6 g), AAV2/2 (Figure 3.6 c), AAV2/8 (Figure 3.6 e), AAV2/8Y(733) (Figure 3.6 f) and the sparse transduction with the AAV2/5 serotype (Figure 3.6 d). Given that intravitreal injection of the ShH10 vector was reported to lead to primarily Müller cell transduction, we investigated the cell type identity of reporter-expressing cells in the retinal cultures infected with this vector serotype (Figure 3.6 i-j''). Immunostaining for the Müller cell marker CRALBP revealed transgene expression in a large proportion of Müller glia in the vector-infected cultures (j-j''). In addition to the large elongated Müller cells that span the whole thickness of the synthetic neural retina, a large number of smaller cells with neuronal morphology was also observed (Figure 3.6 i,j). Staining with the rod photoreceptor marker Rhodopsin showed a high degree of co-localization with this population (Figure 3.6 i-i''), suggesting efficient transduction of developing rod precursors using this vector serotype. In conclusion, these observations suggest that the ShH10 capsid could be used to enhance photoreceptor transduction in mESC-derived retinal organoids.

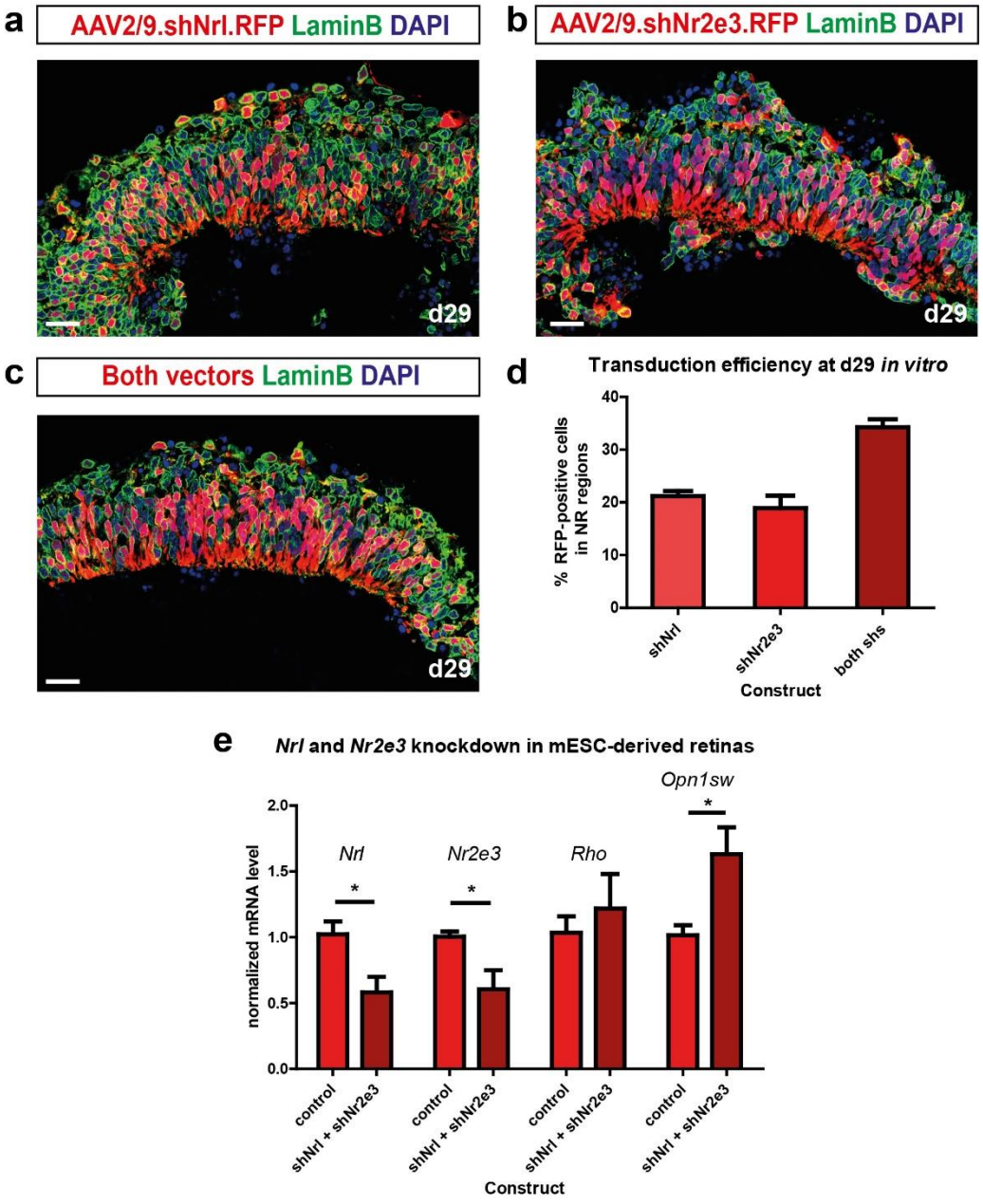

Figure 3.5. Reduction of *Nrl* and *Nr2e3* mRNA levels in mESC-derived retinal organoids induces S opsin transcription

(a-c) Immunohistochemistry showing expression of the RFP reporter in neural retinal regions of mESCs aggregates infected with shNrl **(a)**, shNr2e3 **(b)** or both vectors **(c)**. Sections were stained with LaminB antibody to visualize the nuclear envelope. Scale bar 10 µm. **(d)** Quantification of transduction efficiency in neural retinal regions of infected organoids. Percentage of RFP-positive cells in 10 fields of view from two infection experiments. **(e)** Quantitative PCR analysis of *Nrl*, *Nr2e3*, *Rho* and *Opn1sw* transcripts at day 29 of differentiation in control cultures or cultures transduced with both Nrl and Nr2e3 knockdown vectors. Note the significant reduction in Nrl and Nr2e3 expression and rise in Opn1sw transcripts. *N*=3 differentiation cultures, *n*=6 RNA samples; *$p<0.05$; Student's *t*-test

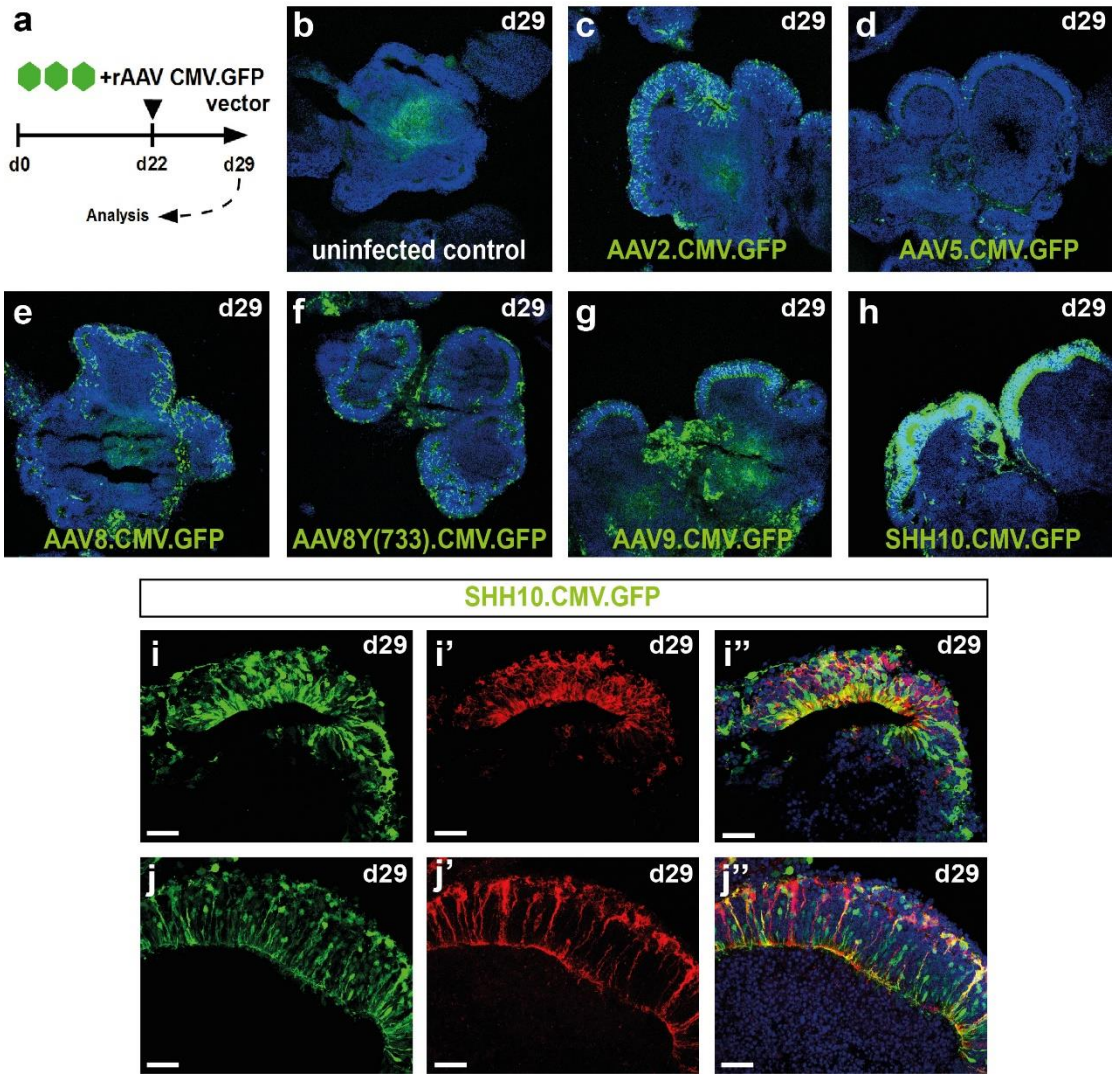

Figure 3.6. Tropism and transduction efficiency of selected rAAV serotypes in mESC-derived retinal organoids

(a) Schematic of infection protocol used. Titre-matched vectors were added at d22 of differentiation and samples were collected at d29. **(b)** Section of a control non-transduced aggregate. **(c-h)** Sections showing GFP reporter expression in aggregates infected with AAV2/2 **(c)**, AAV2/5 **(d)**, AAV2/8 **(e)**, AAV2/8Y(733) **(f)**, AAV2/9 **(g)** and ShH10 viral capsid serotypes. Each vector encoded a GFP reporter driven by the CMV promoter. **(i-j'')** Analysis of ShH10 vector capsid tropism in mESC-derived neural retina. Sections of ShH10.CMV.GFP transduced retinal organoids showing GFP reporter fluorescence **(i,j)** co-localised **(i'',j'')** with the rod marker Rhodopsin (i' in red) and the Müller cell marker CRALBP (j' in red), in neural retinal regions. Note that GFP expression is found both in Rhodopsin+ photoreceptors, as well as CRALBP+ Müller cells. Representative images of *N*=3 independent infections, 12 organoids each.

3.7. Decreased *Nrl* and *Nr2e3* expression in post-mitotic photoreceptor precursors does not induce transcription of cone genes *Thrb2* and *Rxrg*

The high extent of mESC-derived neural retinal transduction achieved using the ShH10 rAAV vector serotype enabled examination of the effects of Nrl and Nr2e3 downregulation directly in isolated post-mitotic photoreceptor precursors. This was achieved by using the Crx:GFP transgenic mESC line which underwent retinal differentiation and infection with the knockdown vectors (Figure 3.7). As with the E16 CCE retinal organoids, differentiation cultures were infected with purified vector at day 22 followed by dissociation into a single cell suspension and flow cytometry at day 29 (Figure 3.7 A-F). A clear GFP+ cell population was discernible in the scatter plots (Figure 3.7 B). As expected in the non-transduced cultures no RFP signal was found (Figure 3.7 A,B) and these samples were used to set the gating for the double-positive (GFP+/RFP+) transduced Crx:GFP photoreceptor precursor cells (Figure 3.7 A-D). The percentage of RFP+ cells was similar for both the control non-targeting vector (Figure 3.7 C and E) and the *Nrl* and *Nr2e3* knockdown constructs (Figure 3.7 D and F), with around 60% of viable cells transduced in culture (Figure 3.7 C and D). Of the GFP+ photoreceptor precursors, around 80% expressed the vector-delivered RFP reporter (Figure 3.7 E and F). RNA was isolated from the harvested cells and analysed by qPCR. Due to limited number of cells obtained the RNA yields were much lower and the quality of isolated RNA poorer than in experiments using whole cultures. For this reason we did not achieve reliable amplification of *Opn1sw* transcripts with the previously used assay in these samples. However, *Nrl*, *Ne2e3*, *Thrb2* and *Rxrg* showed good amplification curves, allowing assessment of their expression levels. This gene expression analysis did not show any trend towards upregulation of either *Thrb2* or *Rxrg* transcript levels (n=7 samples, N=6 differentiation cultures; p=0.109 and p=0.625, respectively, Wilcoxon matched pairs test, Figure 3.7 H), whereas transcripts of *Nrl* showed a significant nearly 70% reduction (n=7, N=6; p=0.016, Wilcoxon matched pairs test, Figure 3.7 H). Levels of *Nr2e3* transcripts were quite variable in this data set showing a strong but not statically significant trend towards decreased abundance in knockdown samples (n=7, N=6; p=0.078, Wilcoxon matched pairs test, Figure 3.7 H). Together, these results show that downregulation of Nrl and Nr2e3 does not lead to increased transcription of cone precursor-expressed genes *Thrb2* and *Rxrg*.

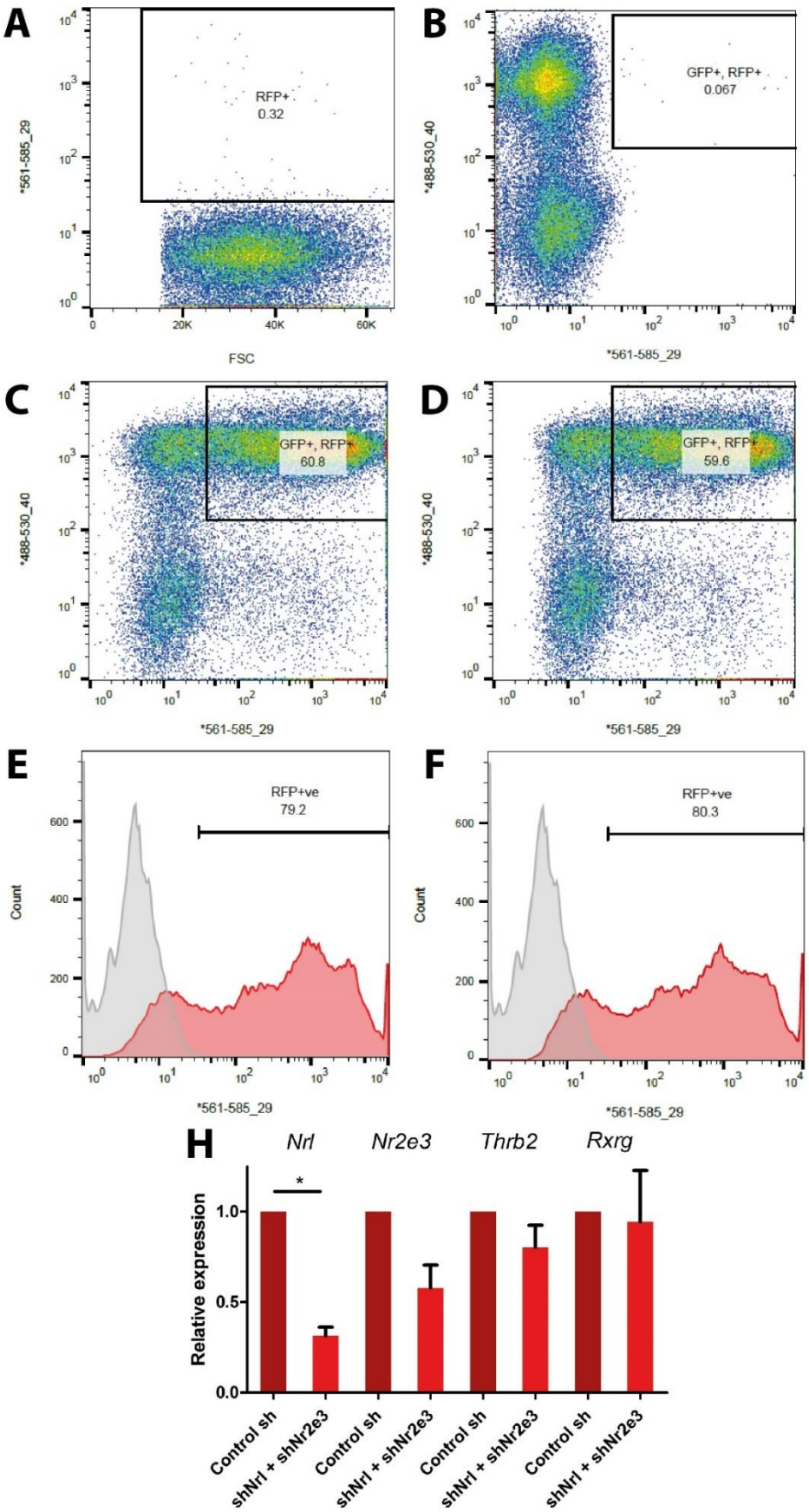
A
RFP+
0.32
*561-585_29
FSC
B
GFP+, RFP+
0.067
*488-530_40
*561-585_29
C
GFP+, RFP+
60.8
*488-530_40
*561-585_29
D
GFP+, RFP+
59.6
*488-530_40
*561-585_29
E
RFP+ve
79.2
Count
*561-585_29
F
RFP+ve
80.3
Count
*561-585_29
H
Nrl
Nr2e3
Thrb2
Rxrg
*
Relative expression
1.0
0.5
0.0
Control sh
shNrl + shNr2e3
Control sh
shNrl + shNr2e3
Control sh
shNrl + shNr2e3
Control sh
shNrl + shNr2e3

Figure 3.7. The reduction of *Nrl* and *Nr2e3* mRNA levels in post-mitotic photoreceptor precursors does not increase the expression of cone precursor markers *Thrb2* or *Rxrg*.

(A-F) Isolation and purification of post-mitotic photoreceptor precursors transduced with Nrl and Nr2e3 knockdown constructs by FACS. (A,B) Representative scatter plots showing gating strategy for collection of RFP+ **(A)** and GFP+ and RFP+ double positive cells **(B)** using non-transduced Crx:GFP dissociated control cultures. (C,D) Representative scatter plots showing collection of Crx:GFP photoreceptor precursors expressing non-targeting vector **(C)** or shNrl and shNr2e3 vectors **(D)**. Note the presence of a distinct GFP+RFP+ population in vector-transduced cultures (C,D), which is absent in control cultures (B). (E,F) Histograms showing RFP expression inCrx:GFP photoreceptor precursors transduced with non-targeting control **(E)** or infected with both shNrl and Nr2e3 vectors **(F)**. **(H)** QPCR gene expression analysis using RNA isolated from flow-sorted either control or knockdown construct transduced CrxGFP+ photoreceptor precursors; n=7 samples, N=6 differentiation cultures; *, $p<0.05$, Wilcoxon matched pairs test.

3.8. Conclusions and discussion

Discovery of the rod-determining transcription factor Nrl (Mears et al., 2001; Swaroop et al., 1992), its downstream target Nr2e3 (Cheng et al., 2006; Haider et al., 2000; Milam et al., 2002) and the requirement for thyroid hormone receptor Trβ2 in M opsin expression led to the postulation of a photoreceptor specification pathway in which two binary cell fate choices are directed by the action of two transcriptional regulators Nrl and Trβ2 (Ng et al., 2011; Swaroop et al., 2010). This model posits that the initial decision between the cone versus rod cell fate is determined by expression levels and/or activity of Nrl in post-mitotic photoreceptor precursors. In the next step, in cone precursors Trβ2 mediates determination of S versus M cone fate (Ng et al., 2011; Swaroop et al., 2010). In the mouse the latter fate choice is not exactly binary, since the majority of mouse cone photoreceptors co-express the two cone opsin photopigments (Applebury et al., 2000; Lukáts et al., 2005).

More recent work in several model systems suggested that cone photoreceptors and horizontal cells likely share a dedicated progenitor cell (Emerson et al., 2013; Hafler et al., 2012; Suzuki et al., 2013). Within this progenitor, expression of Otx2 and Onecut1 appear to determine the competence for cone genesis (Emerson et al., 2013). Interestingly, introduction of a dominant negative form of Onecut1 in the chick retina leads to upregulation of L-Maf, the chicken homologue of Nrl (Emerson et al., 2013). This observation suggests that Onecut1 likely induces a yet unidentified repressor of Nrl expression. Whether a similar gene regulatory network operates during mouse retinal development remains to be explored. In the nocturnal mouse, abundance of rods appears to arise from recruitment of S cone precursors by Nrl to the rod photoreceptor lineage (Kim et al., 2016). Whilst the mechanistic aspects of this switch in photoreceptor composition from ancestral cone-dominant retina remain to be fully understood, it is clear that a considerable proportion of prospective rods derive from precursors that would otherwise develop into S cones if not for Nrl activity.

In this study we experimentally tested the dependence of photoreceptor differentiation on expression levels of *Nrl* and *Nr2e3*. The dominant model for photoreceptor development suggests that the amount and activity of Nrl are critical to bias the post-mitotic photoreceptor precursor towards the rod fate, whereas reduction in Nrl would tip the balance towards S cone precursor differentiation (Swaroop et al., 2010). To address this question we developed knockdown constructs targeting *Nrl* and *Nr2e3* gene transcripts (Figure 3.1). The constructs mediated efficient reduction in levels of both *Nrl* and *Nr2e3* mRNAs in photoreceptor cells *in vitro* (Figures 3.5 and 3.7) and *in vivo* (Figure 3.2). Expression of these knockdown constructs in post-mitotic

photoreceptor precursors in the mESC-derived retinae did not lead to upregulation of cone precursor markers *Thrb2* and *Rxrg* (Figure 3.7), whilst transcription of S opsin was increased in whole cultures (Figures 3.5 and 3.7). These findings are somewhat surprising given that both Trβ2 and RXRγ are distributed uniformly across the retina in mouse cones (Ng et al., 2001; Roberts et al., 2005) and *Rxrg* transcripts show upregulation in adult *Nrl*$^{-/-}$ retina (Brooks et al., 2011). However, these data are in accordance with the recent observation that neither *Thrb2* nor *Rxrg* are increased in the *Nrl*$^{-/-}$ whole retinae in early post-natal development (Emerson et al., 2013). Since the presence of a significant contribution of non-photoreceptor cells in the whole retina at neonatal stages could mask more modest effects on the transcriptional profiles, it is of importance to confirm such analyses on purified photoreceptor populations, as in this study.

Lack of *Thrb2* or *Rxrg* induction following *Nrl* knockdown is in contrast to increases in expression of both genes following Notch signalling inhibition (please refer to Chapter 2, Figure 2.4). These insights suggest that, whilst *Nrl* gene silencing might be useful to obtain higher yields of S cone-like cells, there are molecular differences in their development compared to wild-type cones. Therefore, we conclude that a more appropriate approach to achieving a higher cone to rod ratio in mESC retinal differentiation cultures is timely pharmacological inhibition of Notch signalling, which results in formation of precursors expressing both Trβ2 and RXRγ and developing normally to equivalents of early postnatal development (Chapter 2, Figures 2.4 and 2.5). Surprisingly, despite developed transgenic mouse lines with retina specific *Notch1* deletion (Jadhav, 2006; Yaron, 2006), the *Nrl*$^{-/-}$ retina instead has been a tool of choice for transplantation studies so far (Santos-Ferreira et al., 2015; Smiley et al., 2016). It would be interesting to determine whether the difference in development correlates with transplantation outcomes. These experiments are of relevance for visual function following transplantation, since Trβ2 and RXRγ are required for M opsin induction and the majority of mouse and human cones express this visual pigment (Jeon et al., 1998).

Investigations into the evolutionary origins of photoreceptors provide some insight into how separation of photon detection into the cone and rod systems developed (Lamb, 2009, 2013; Larhammar et al., 2009). Recently two groups examined the morphology and physiology of lamprey photoreceptors. These jawless animals diverged early from the vertebrate phylogenetical tree (Lamb, 2013). Lamprey photoreceptors show cone-like morphology with short conical outer segments. However, two functional groups of photoreceptor cells already exist in these creatures (Asteriti et al., 2015; Morshedian

and Fain, 2015). One acts like a vertebrate cone cell, whereas the other is capable of single photon detection despite resembling a vertebrate cone cell with respect to morphological features (Asteriti et al., 2015; Morshedian and Fain, 2015). Recently, molecular and genetic analyses demonstrated recruitment of S cone precursors as an evolutionary mechanism for the switch from ancestral cone-dominant to extant rod-dominant retina in mammals (Kim et al., 2016). Interestingly, short conical outer segments similar to lamprey photoreceptors are observed in the *Nrl*$^{-/-}$ photoreceptors. Moreover, these cone-like cells only express S opsin, which is the ancestral visual pigment for vertebrate photoreceptors (Larhammar et al., 2009). Therefore, an alternative explanation for the resulting phenotype in the *Nrl*$^{-/-}$ animals could be reversion to a more primitive, ancestral photoreceptor form. This hypothesis is consistent with our observation that reduction in Nrl and Nr2e3 expression does not trigger the induction of cone precursor markers *Thrb2* or *Rxrg* expression, but does suggest the upregulation of S opsin transcription (Figures 3.5 and 3.7; Diagram 3.2). To further test this hypothesis, *Nrl* transcriptional silencing in single cells *in vivo* using the developed constructs could be employed to determine whether the immature morphology with very short segments is a cell autonomous feature of *Nrl*$^{-/-}$ photoreceptors or whether it is a result of the disrupted outer nuclear layer architecture.

Taking into consideration all the observations discussed above, it appears that the best interpretation of the results obtained with knockdown of Nrl and Nr2e3 in developing mESC-derived photoreceptor precursors is that preventing expression of Nrl and Nr2e3 maintains these cells in an immature developmental state. It is worth noting that both genes are rod-specific and therefore their downregulation only occurs in cells fated to become rods. Since S opsin is the ancestral visual pigment and abundance of rods in nocturnal animals evolved by recruitment of prospective S cones by expanded expression of *Nrl*, cells depleted of *Nrl* and *Nr2e3* gene expression likely revert into cells resembling primitive S cones, due to a block in rod fate acquisition. Hence, these precursors are stalled in their differentiation as an immature, primitive photoreceptor type rather than gaining a true cone cell fate.

Deeper understanding of the process of photoreceptor phenotype diversification is of relevance in the light of recent advances in the direct conversion of one mature somatic cell type into another (Buganim et al., 2012). Further methodological progress in this transdifferentiation approach could enable direct conversion of remaining rods into cones to enable some degree of daylight vision in conditions such as certain forms of age-related macular degeneration or Stargardt's macular dystrophy. One potential approach to execute this type of treatment would be the delivery of reprogramming

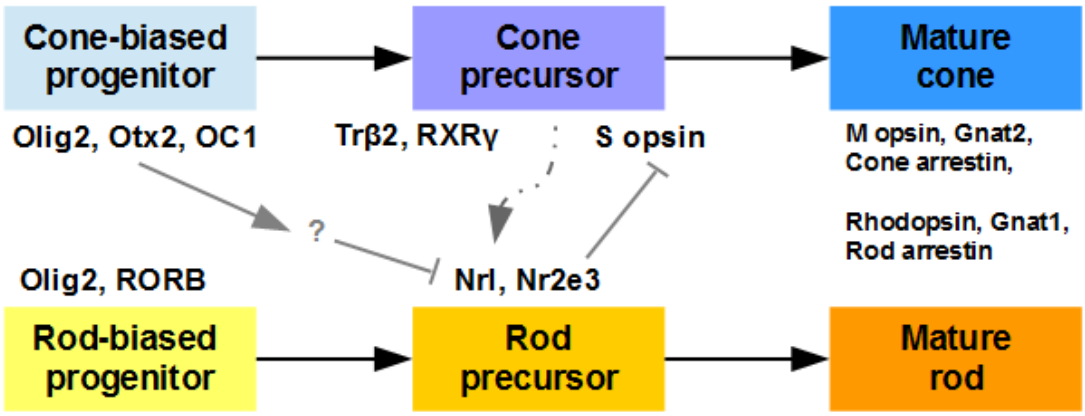

Diagram 3.2. Revised model of sequential acquisition of photoreceptor cell fate through action of specific transcription factors.

Recent advances in the understanding of photoreceptor fate determination suggest that diversification into cone and rod lineages occurs early, likely in terminally dividing progenitor cells through activity of transcription factors that create bias towards specific progeny fates, such as Otx2 and Onecut1 for cones (upper left panel). Through a yet unidentified mechanism, the rod pathway of differentiation is suppressed in cones (? in the graphic). Conversely, in rod precursors the cone transcriptional profile is repressed through induction of Nr2e3 (lower middle panel). In mammals, from the pool of S cone precursors the majority is recruited to the rod fate, through activity of Nrl (dashed arrow in middle section). During post-natal development precursor cells commence expression of proteins related to functional maturation (right panels) facilitating formation of mature features such as outer segments and synapses and cell fates are properly established.

factors using viral vectors. Here, we screened a panel of recombinant AAV serotypes to identify those most efficient at transducing photoreceptors in our *in vitro* retinal organoid culture system. Transgene delivery in this setting could be facilitated by the use of ShH10 vector, which was developed in a directed evolution approach to enhance infection of retinal cell types (Klimczak et al., 2009). *In vivo*, very efficient transduction and downregulation of the rod determining transcription factors Nrl and Nr2e3, as well as their transcriptional target Rhodopsin, was achieved using the rAAV2/9 capsid serotype (Figure 3.2). This downregulation combined with activation of a cone-specific transcriptional profile could present a paradigm for re-creation of cones from rods in conditions where the former are lost due to disease. A major hurdle for such an approach would be overcoming the epigenetic barrier for transdifferentiation (Montana et al., 2013). In principle this occurs in all reprogramming protocols for the generation of induced pluripotent stem cells from various adult somatic cell sources (Borooah et al., 2013) and, conceivably, the epigenetic barrier should be easier to overcome between more similar cell types (Buganim et al., 2012). Development of a transdifferentiation strategy utilising Nrl and Nr2e3 knockdown represents therefore an interesting avenue for future research.

In summary, development of knockdown constructs that effectively target Nrl and Nr2e3 expression both *in vitro* as *in vivo* allowed us to determine the effect of reduced levels of these rod fate determinants on ESC-derived photoreceptor precursor development. Our findings suggest that whilst Nrl and Nr2e3 are necessary to repress S opsin expression, the cone precursor transcription factors Trβ2 and RXRγ are regulated independently (Diagram 3.2). Given this difference in development compared to wild-type cones, we conclude that use of donor populations of either wild-type cone cells or cones generated using Notch inhibition approach are more appropriate for transplantation studies.

Chapter 4. The role of soluble factors retinoic acid and thyroid hormone in regulation of cone photoreceptor differentiation in retinae derived from mouse embryonic stem cells.

4.1. Background

Nuclear receptors are ligand-regulated transcription factors that play key roles in many aspects of development by linking hormonal signals with transcription of specific sets of genes (Huang et al., 2014). Nuclear receptors are highly enriched in the retina, suggesting an important role in the physiology of this organ (Forrest and Swaroop, 2012). In particular signalling via thyroid and retinoid receptors is implicated in various aspects of retinal development (Forrest and Swaroop, 2012; Swaroop et al., 2010).

Thyroid hormone signalling is primarily involved in cone maturation in mice. Thyroid hormone receptor β2 (Trβ2) is expressed from the terminal division in cone precursors, detectable as early as E10-12 (Ng et al., 2009). Trβ2 is required for M opsin induction in cones, since genetic ablation of this receptor leads to a loss of M opsin expression and all cones switching to S opsin expression (Ng et al., 2001). Hypothyroid mice show severely delayed M opsin appearance, indicating that thyroid hormone is required for M opsin expression induction via Trβ2 (Lu et al., 2009). However, precocious exposure to excess of thyroid hormone leads to developmental cone precursor death (Ng et al., 2010). Cones are protected from high levels of thyroid hormone during early stages of development through the activity of deiodinase 3, a hormone inactivating enzyme (Ng et al., 2010). Postnatal rise in thyroid hormone in circulation triggers the onset of M opsin expression (Lu et al., 2009; Ng et al., 2010) and there is indication that levels of thyroid hormone differ between dorsal and ventral parts of the retina with higher abundance in the dorsal region participating in establishment of dorso-ventral opsin gradient in mice (Roberts et al., 2006). Correspondingly, addition of thyroid hormone to *in vitro* cultures established from dissociated rat retinal cells stimulated expression of M opsin (Kelley et al., 1995).

Retinoic acid is a potent morphogen involved in a variety of developmental processes (Das et al., 2014; Huang et al., 2014; Janesick et al., 2015). With respect to eye development retinoic acid is generated in a dynamic pattern during eye morphogenesis. High activity of retinoic acid synthesising enzymes Raldh1, Raldh2 and Raldh3 in early eye development makes the optic cup extremely rich in retinoic acid (McCaffrery et al., 1993; Mic et al., 2000). Expression of these synthesising enzymes declines over time with correspondingly lower concentrations of retinoic acid found in neonatal and adult eye (McCaffrery et al., 1993). Exposure of fish eyes to

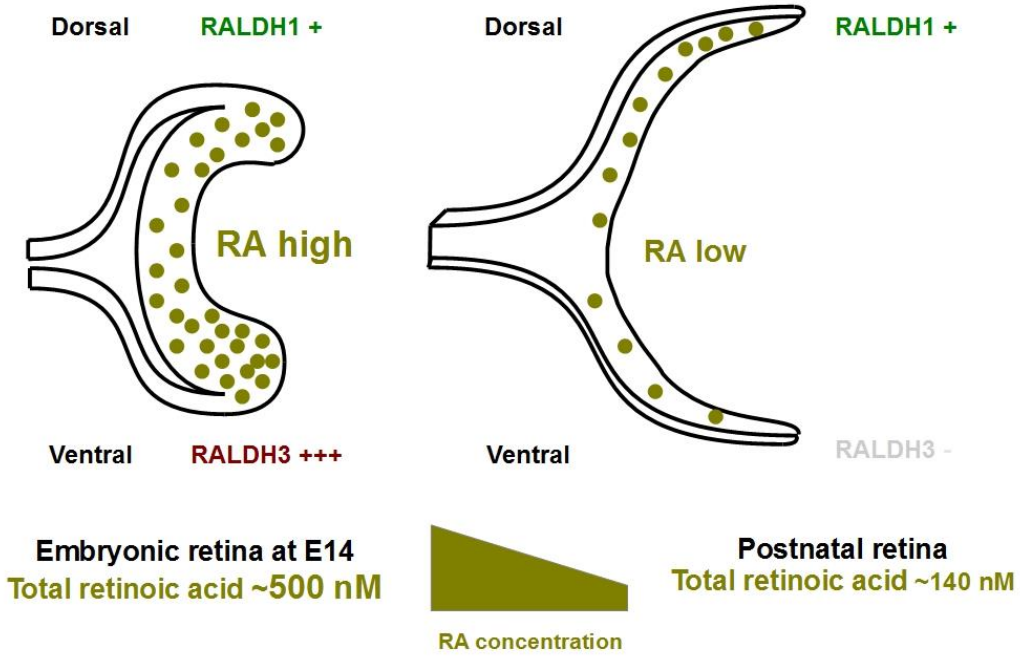

Diagram 4.1. Dynamic changes in retinoic acid synthesis during neural retinal development

Retinoic acid is synthesised in high quantities in early development at the optic vesicle and optic cup stages through the action of dorsally (Raldh1) and ventrally (Raldh3) localized enzymes. The ventral enzyme is more active producing higher levels of retinoic acid in the ventral part of the retina forming a dorsal-low to ventral-high gradient of this molecule in the embryonic retina (left panel). With the progress of retinal morphogenesis, expression levels of both enzymes decline leading to a decrease in retinoic acid abundance in the tissue. Expression and activity of the ventral enzyme Raldh3 becomes undetectable at late postnatal stages (right panel). As a result, at around P4-8 the gradient of retinoic acid shifts towards so a higher concentration is present in the dorsal part of the retina and this is maintained into adulthood.

excess of exogenous retinoic acid leads to hyperproliferation of progenitors and duplication of the retina (Hyatt and Dowling, 1997; Hyatt et al., 1992), suggesting that its high levels support cycling of retinal progenitors. From early stages a gradient of retinoic acid is established in the embryonic eye by expression of a lower activity dorsal synthesising enzyme Raldh1, retinoic acid catabolising enzyme Cyp26a1 in central retina and a high activity ventral enzyme Raldh3 (McCaffery et al., 1999). This gradient reverses within the second postnatal week in the mouse due to loss of the ventral enzyme expression (McCaffrery et al., 1993; summarized in Diagram 4.1). The formation of dorsal and ventral retinoic acid territories are regulated by the eye-specific homeobox gene Vax2, which regulates the establishment of the dorsal-ventral axis of the developing eye. Vax2 exerts its role through regulating expression of retinoic acid catabolising enzymes Cyp26a1 and Cyp26c1 and retinoic acid generating enzyme Raldh3. In Vax2 knockout mice expression of retinoic acid catabolising enzymes expands into ventral retina, whilst Raldh3 expression is diminished. This expansion of low retinoic acid zone leads to abnormalities in cone opsin patterning with loss of M opsin gradient resulting from expansion of its expression into ventral retina and downregulation of S opsin, which could be rescued by retinoic acid administration in utero (Alfano et al., 2011), suggesting that this phenotype is dependent on retinoic acid concentration. At later stages of photoreceptor differentiation addition of exogenous retinoic acid to zebrafish eyes results in precocious rod differentiation with more prominent rod outer segments and increased Rhodopsin expression. Concomitantly, cone maturation is impaired. Instead of well-formed cones, only immature miniature cones are observed (Hyatt et al., 1996). In accordance addition of retinoic acid stimulates rod differentiation in dissociated *in vitro* cultures of rat retinal cells and it also promotes rod differentiation in cultures of pluripotent stem cells (Eiraku et al., 2011; Gonzalez-Cordero et al., 2013; Osakada et al., 2008; Zhong et al., 2014). Collectively these observations show an important role for appropriate spatial and temporal regulation of retinoic acid levels for proper development of photoreceptors.

4.2. Aims

Signalling mediated by nuclear receptors of the steroid and thyroid families was found to play important roles in retinal development indicating that proper formation of this organ requires coordinated action of an intrinsic genetic programme, regulated by a set of transcription factors, with input from diffusible hormones and growth factors. Actions of two such soluble regulators, thyroid hormone and retinoic acid are best characterized in the retina. Thyroid hormone is implicated in opsin patterning, whereas

retinoic acid is necessary for early eye development and plays a role in photoreceptor maturation. The main objectives of the experiments presented in this chapter were to:

(1) determine whether M opsin expression could be initiated by timely addition of exogenous thyroid hormone to retinal differentiation cultures;
(2) characterize the expression of retinoic acid signalling pathway components *in vitro* to identify temporal changes relevant to photoreceptor differentiation;
(3) examine if photoreceptor genesis and maturation are dependent on the concentration of retinoic acid in cultures at specific stages of development.

We hypothesised that, given the important inductive roles of thyroid hormone and retinoic in cone and rod photoreceptor development, addressing the above outlined objectives with allow to better recreate environmental signals guiding cone cell specification through appropriate soluble factor supplementation regime in culture and therefore improve cone differentiation *in vitro*.

4.3. Thyroid hormone supplementation facilitates M opsin expression in mESC-derived retinae, but is associated with induction of cell death

Thyroid hormone mediates opsin patterning *in vivo* (Lu et al., 2009) and was found to increase cone differentiation in cultures of embryonic rat retinal cells established *in vitro* (Kelley et al., 1995). To determine the impact of thyroid hormone signalling on cone precursor development in mESC-derived retinae, differentiated aggregates were collected at the stages of cone precursor genesis and maturation (between day 13 and 29 of culture). Thyroid hormone is present in the circulation mostly in the form of thyroxine (T4). T4 is a prohormone with low biological activity, which is converted into the active triiodothyronine (T3) through enzymatic deiodination mediated by deiodinase 2 (Dio2). Both T4 and T3 can be inactivated by deiodination carried out by deiodinase 3 (Dio3; schematically represented in Figure 4.1 a). In developing cones the activity of T3 is mediated via thyroid hormone receptor β2 (Trβ2). Expression of the key components of thyroid hormone signalling, the enzymes *Dio2*, *Dio3* and *Thrb2* receptor, was assessed in RNA samples of day 13 to 29 aggregates by RT-PCR (Figure 4.1 b). This analysis showed that all three genes are expressed throughout the course of cone differentiation in mESC-derived retinae (Figure 4.1 b). The presence of *Dio2* transcripts is unexpected since this enzyme is not normally expressed in the developing retina *in vivo*. This expression could come from non-retinal forebrain neurons present in the differentiation cultures. Non-neural retina regions could also contribute to the detected expression of *Dio3*, since this enzyme is present in many foetal tissues (reviewed in Huang, 2005). Thrb2 expression is much more specific, being present only in the retina, cochlea of the inner ear and the pituitary

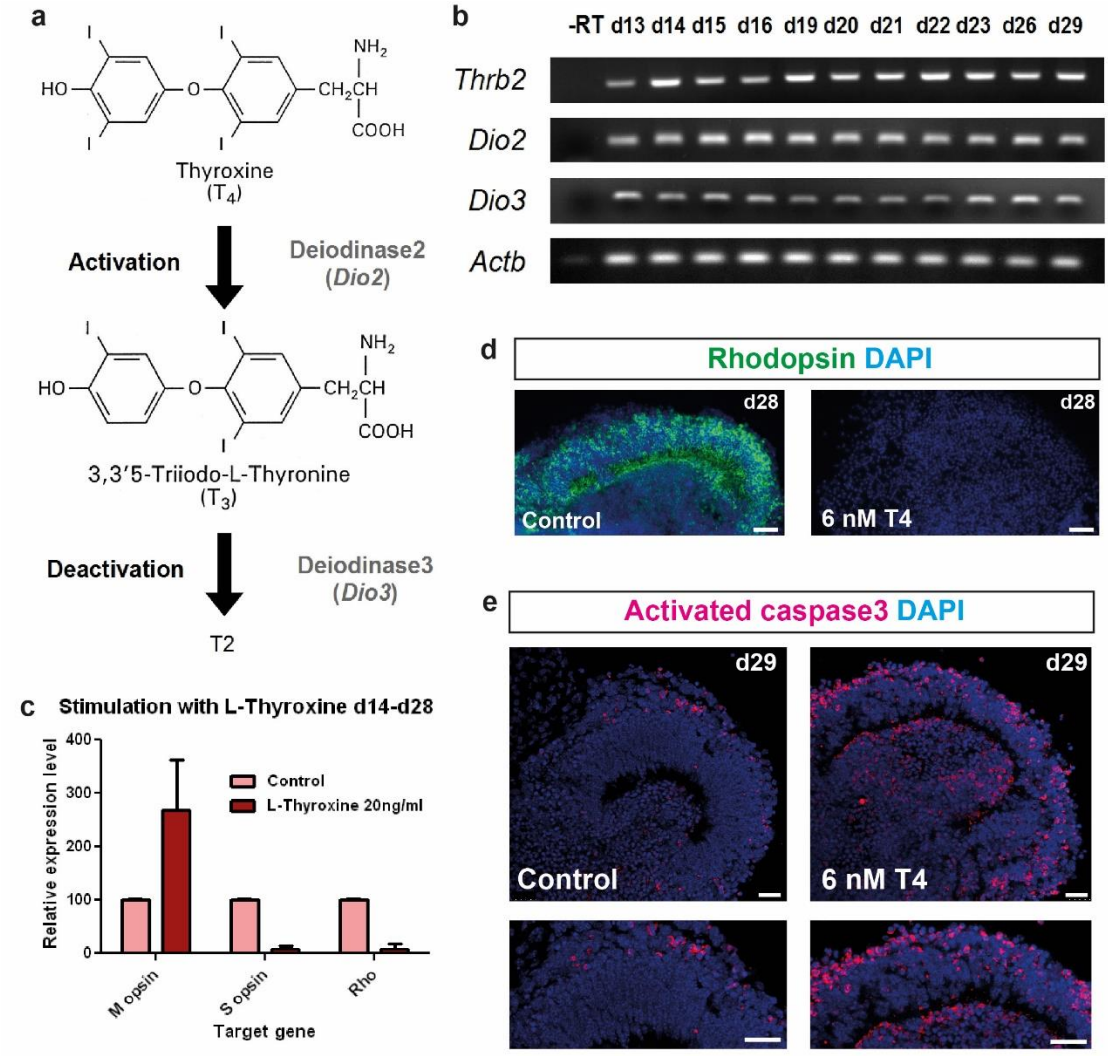

Figure 4.1. Thyroid hormone affects photoreceptor differentiation in mESC-derived retinae

(a) Schematic depiction of thyroid hormone metabolism. Thyroxine (T4) with low biological activity is converted into active T3 by deiodinase 2. Deiodinase 3 is a hormone de-activating enzyme removing iodine atoms from T3 and T4. **(b)** RT-PCR analysis of retinal differentiation samples between d13 and d29. –RT is a no template control. **(c)** QPCR analysis of transcripts of photoreceptor genes M opsin, S opsin and Rhodopsin in control and samples treated with T4 at 25 nM (20 ng/ml) between d14 and d28. Note the upregulation of M opsin in treated samples. *N*=3 differentiation cultures, *n*=3 RNA samples. **(d)** Immunostaining for Rhodopsin in control and 6 nM (5 ng/ml) T4-treated samples. Rhodopsin signal is lost in T4 treated samples. **(e)** Immunostaining for cleaved Caspase3 showing an increase in apoptotic cells in neural retina (neural retina fragments shown for comparison in the lower panel) following treatment with 6 nM T4. Nuclei counterstained with DAPI. Scale bar 20 µm in all images.

(Jones et al., 2007) and, indeed, immunostaining for Trβ2 was only found in the retinal neuroepithelia regions of the organoids (please refer to Figure 1.4 in Chapter 1).

Given the presence of both metabolizing enzymes as well as thyroid hormone receptor transcripts, next the effect of stimulation of cultures with T4 was determined. Initially, the cultures were supplemented with 20 ng/ml (~25.6 nM) of T4 from day 14 to day 28 of differentiation. Biochemical measurements showed a range of 5-15 nM of T4 in the developing mouse retina (Roberts et al., 2006). We chose a single, slightly higher than physiological concentration for the preliminary experiments, because culture medium in this differentiation system is only replaced every 48 hours and therefore hormone levels are likely to decline between re-feeding. This supplementation resulted in increased expression of M opsin, but a concomitant loss of both S opsin and Rhodopsin expression was determined by qPCR analysis (Figure 4.1 c). *In vivo* levels of thyroid hormone in circulation rise substantially shortly after birth (Lu et al., 2009) and excess of thyroid hormone at inappropriate developmental stages triggers cone precursor death (Ng et al., 2010). Having observed loss of S opsin and Rhodopsin photoreceptor markers with extended exposure to thyroid hormone (Figure 4.1 c), we subsequently examined restricting stimulation with T4 to the equivalent of early postnatal development. Cultures at day 26, a stage resembling P4-6 *in vivo* (Gonzalez-Cordero et al., 2013), were supplemented with 5 ng/ml (6 nM) of T4 for 48 hours before samples were collected for histological examination. The selected concentration of T4 was previously used to stimulate rat dissociated retinal cell cultures *in vitro* without any significant toxic effects (Kelley et al., 1995) and lies within the lower range of T4 concentrations measured in the early postnatal mouse retina (Roberts et al., 2006). Immunohistochemistry revealed a loss of Rhodopsin expression in T4-treated samples (Figure 4.1 d). We next determined whether this was associated with induction of cell death in the mESC-derived retinal tissue by immunostaining for cleaved Caspase3 (Figure 4.1 e). Sections of aggregates treated with T4 showed a strong increase in activated caspase3 immunoreactivity, predominantly in cells located in the retinal neuroepithelium (Figure 4.1 e, lower panel). Collectively, these data demonstrate that whilst thyroid hormone application induces M opsin transcription, it also triggers apoptosis in the mESC-derived neural retina.

4.4. Components of retinoic acid signalling pathway are expressed in a temporally dynamic pattern in mESC-derived retinae

Retinoic acid is a key morphogen required for the formation of the neural retina and subsequent photoreceptor differentiation (Hyatt and Dowling, 1997). Retinoic acid is generated in the neural retina from retinol (vitamin A) by the action of synthesising

enzymes Raldh1 and Raldh3 (McCaffrery et al., 1993), whereas Cyp26a1 enzyme mediates its degradation (McCaffery et al., 1999). To establish if regulators of retinoic acid metabolism are expressed in mESC-derived retinae in a manner resembling *in vivo* development, we used qPCR to examine the timecourse of *Raldh1*, *Raldh3* and *Cyp26a1* expression in this system (Figure 4.2 a). This analysis showed that expression levels of all three enzymes diminish in the course of differentiation and show substantial reduction in transcripts at a stage corresponding to neonatal retina (day 24, equivalent to P3-4). This pattern of expression is reminiscent of reductions in mRNAs and protein activity of the examined enzymes with the progress of in development *in vivo* (McCaffery et al., 1999; McCaffrery et al., 1993; Mic et al., 2000). Next, we used immunohistochemistry to determine whether the asymmetrical distributions of Raldh1 enzyme is preserved in retinae generated from mESCs. Indeed, Raldh1 protein was found localized to a single peripheral margin of the mESC-derived neural retina, indicating that spatial patterning of this enzyme expression is recapitulated *in vitro* (Figure 4.2 c).

Retinoic acid generated in the retina acts on its receptors belonging to the nuclear receptor superfamily. These molecules show temporally dynamic and spatially confined expression patterns in retinogenesis (Mori et al., 2001). To determine the temporal expression of retinoid receptors with known roles in photoreceptor development we used again qPCR as a quantitative readout of expression levels of *Rara* and *Rorb* transcripts in addition to timecourse of *Rxrg* expression presented in Chapter 1 (Figure 1.4 a). RARα transcripts showed relatively stable expression level at stages of photoreceptor differentiation in retinae derived from mESCs (Figure 4.2 b), consistent with its expression initially in progenitors/precursors embryonically followed by localization to a subset of interneurons at early postnatal stages reported *in vivo* (Mori et al., 2001). Additionally, immunostaining with RARα antibody showed diffuse labelling of cells in the mESC-derived neuroblastic layer at day 14 of differentiation (Figure 4.2 d), resembling the staining pattern in cryosections of the the developing hippocampus using the same antibody (Aoto et al., 2008). Levels of RORβ transcripts remained similarly abundant from day 12 to 20 of differentiation, consistent with its role in progenitors and early in photoreceptor precursors, and showed reduction in more mature tissue at day 24 (Figure 4.2 b). These analyses suggest that receptors for retinoic acid also display expression profiles similar to those in the developing mouse eye.

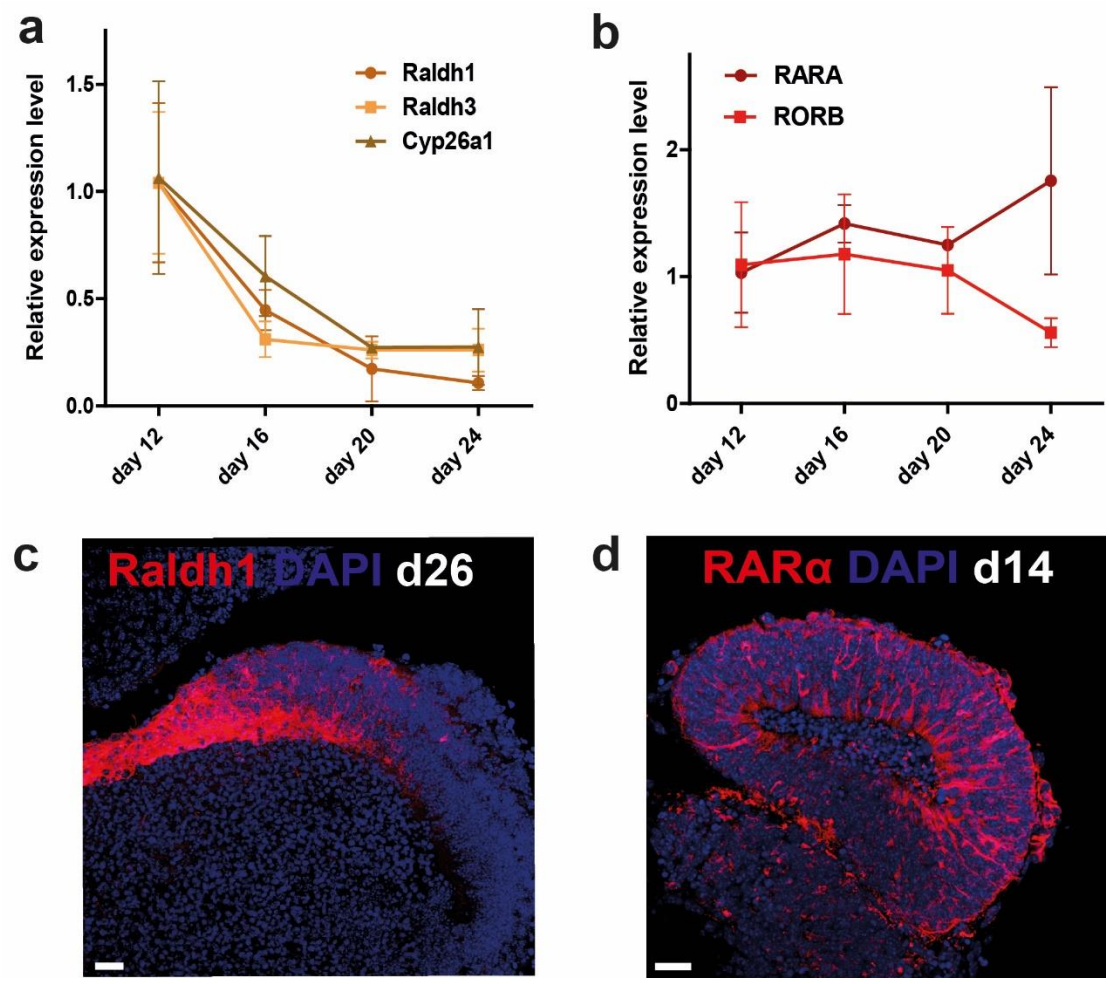

Figure 4.2. Retinoic acid metabolising enzymes and receptors are expressed in mES-derived retinae in a temporally dynamic pattern.

(a) QPCR expression timecourse of retinoic acid metabolising enzymes genes *Raldh1*, *Raldh3* and *Cyp26a1* in mESC retinal differentiation cultures between d12 and d24. Note the decline in expression with the progress of differentiation. **(b)** QPCR expression timecourse of retinoic acid receptor genes *Rara* and *Rorb*. In both (a) and (b) biological triplicates were used, each of which was run in a triplicate reaction. **(c)** Immunostaining for Raldh1 at d26 of differentiation showing a clear confinement to the peripheral part of the ESC-derived neural retina. **(d)** Antibody staining for RARα (in red) showing diffuse localization throughout the mESC-derived optic cup at d14 of culture. Scale bar in both images 20 µm.

4.5. Retinoic acid levels affect progenitor cell cycle in retinae derived from mESCs

Retinoic acid in the eye was found to promote hyperproliferation of ventral retina precursors and formation of a second retina in zebrafish embryos (Hyatt et al., 1992). In other systems however retinoic acid signalling is usually associated with induction of neural differentiation (reviewed in Janesick et al., 2015), suggesting that retinoic acid effects are context dependent. In order to determine the effects of retinoic acid on cycling retinal progenitors in this system, we supplemented culture medium with exogenous all-*trans* retinoic acid at 500 nM for 48 hours between day 14 and 16 of differentiation (Figure 4.3 a-c), an early stage corresponding to approximately E15 *in vivo*. A short 1 hour pulse of bromodeoxyuridine (BrdU) at 10 µM just before harvesting the samples was used to label progenitors in S phase of cell cycle. A similar approach in the retina allows labelling of up to 50% of cycling progenitors undergoing DNA synthesis, avoiding detection of newly generated post-mitotic cells, since the M phase of the cell cycle takes around 3 hours and therefore cannot be completed by progenitors labelled at the very end of S phase (Alexiades and Cepko, 1996; Hafler et al., 2012). Next, the relative abundance of S phase cells in the control and retinoic acid treated samples was assessed by quantifying the proportion of cells that incorporated the BrdU nuclear label in sections of mESC-derived optic vesicles (Figure 4.3 a-c). This analysis showed a modest but significant increase in BrdU-labelled nuclei (11.3% ± 0.85% in control samples, n=51 sections, versus 14.1% ± 0.72% in retinoic acid-treated samples, n=49 sections; p=0.0154, Student's t-test), indicating that retinoic acid levels have an impact on the cell cycle status of retinal progenitors differentiated from mESCs *in vitro*.

4.6. Effect of retinoic acid on gene expression in early photoreceptors

Studies examining the role of retinoic acid in photoreceptor genesis suggested it affects primarily the expression of photoreceptor maturation markers in post-mitotic cells (Alfano et al., 2011; Hyatt et al., 1996; Wallace and Jensen, 1999). However, some observations also raised the possibility of preferential generation of rod precursors following retinoic acid treatment (Kelley et al., 1994; Stevens et al., 2011). To determine the effect of retinoic supplementation on the appearance of post-mitotic photoreceptor precursors, differentiated cultures of either the E16 CCE or Crx:GFP ESC lines were treated as described in the previous section with all-*trans* retinoic acid at 500 nM between days 14 and 16 of differentiation. At this stage of culture cone and early-born rod precursors are generated. Tissue samples were collected following retinoic acid treatment and examined using fluorescence microscopy (Figure 4.4). Quantification of the percentage of fluorescent reporter-expressing cells in Crx:GFP

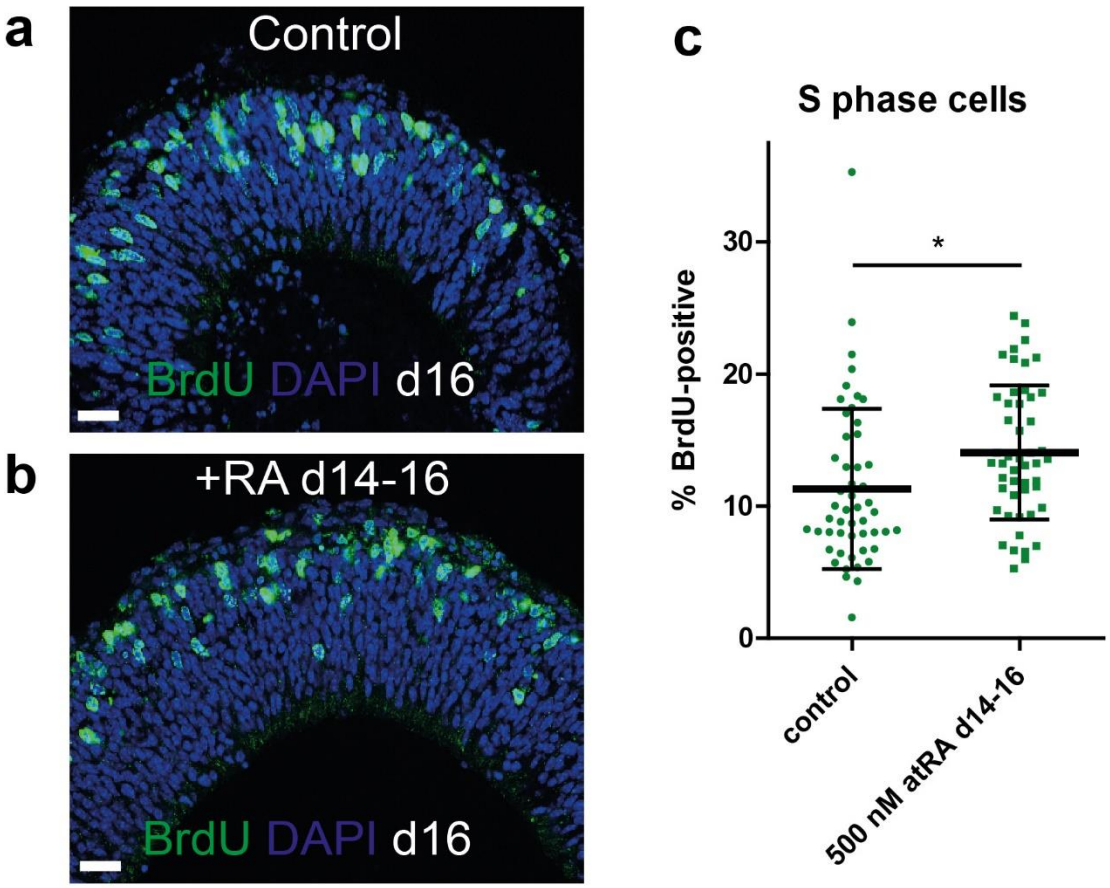

Figure 4.3. Effects of exogenous retinoic acid on cell proliferation at early stages of mESC retinal differentiation

(a,b) Confocal microscopy showing antibody staining for Bromodeoxyuridine (BrdU) incorporation following a short 1 hr pulse of 10 µM BrdU, which is expected to solely label cells in S phase of the cell cycle. Control shown in (a), sample treated with 500 nM all-*trans* retinoic acid shown in (b). Scale bar in both images 10 µm. **(c)** Quantification of the percentage of cell nuclei in the neural retina co-labelled for BrdU. Note the modest but significant increase in BrdU uptake in the retinoic acid-treated sample. *, $p<0.05$, Student's *t*-test. Control $n=51$ sections, retinoic acid-treated mESC-derived retinae $n=49$ sections, samples from aggregates derived from 3 independent differentiation cultures.

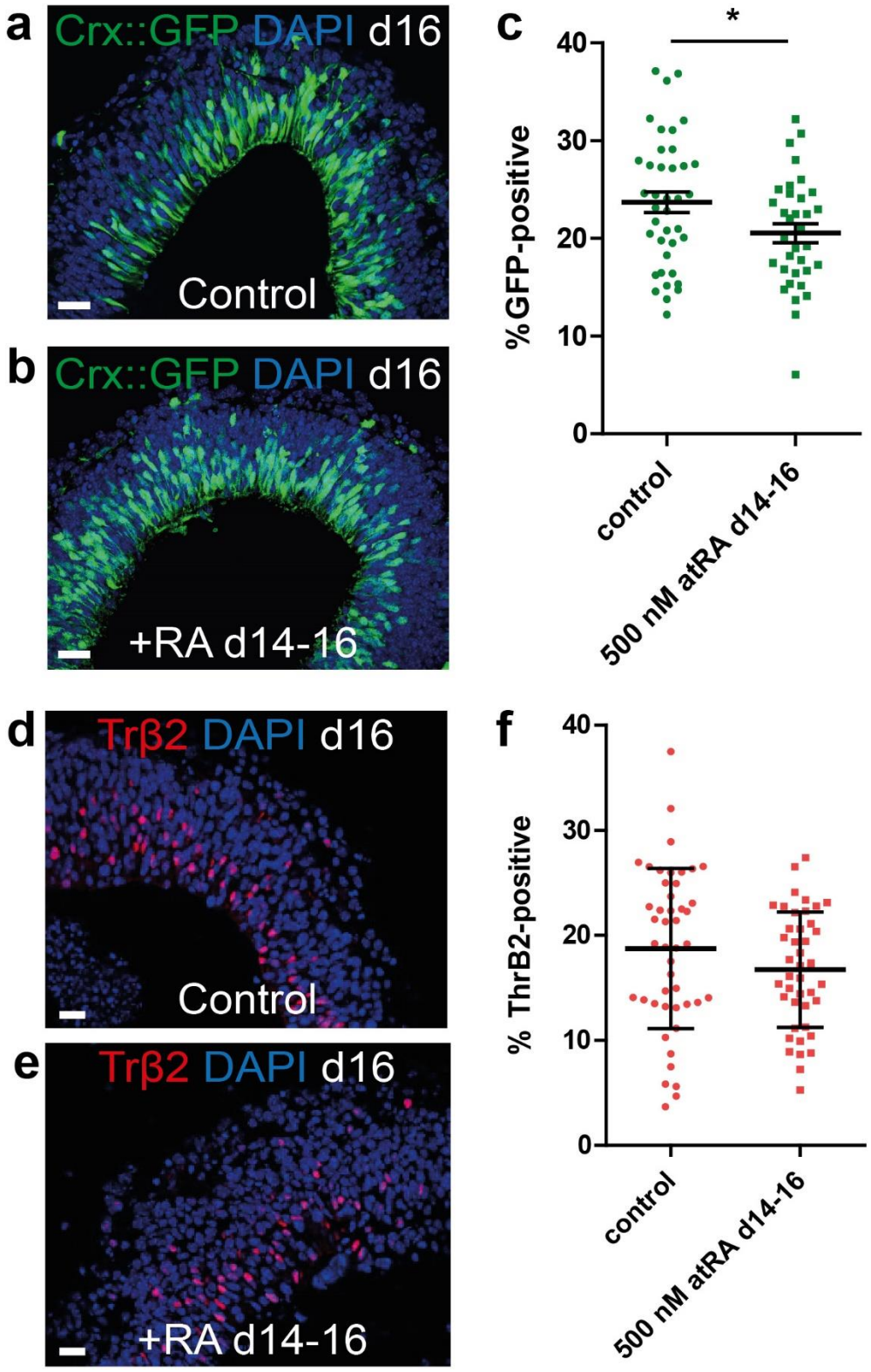

Figure 4.4. Expression of photoreceptor markers following retinoic acid treatment at d14-16

(a,b) Immunohistchemistry showing expression of Crx:GFP reporter in control (a) and treated with 500 nM retinoic acid between d14 and d16 (b) samples. Scale bar 10 µm. **(c)** Quantification of the percentage of GFP-expressing cells in the mESC-derived neural retinae at d16. Note small but statistically significant reduction in the number of GFP-positive cells in retinoic acid-treated samples. *, $p<0.05$, Student's *t*-test. For control $n=40$ sections were scored and $n=34$ sections from the retinoic acid-treated mESC-derived retinae, samples of aggregates derived from 3 independent differentiation cultures. **(d,e)** Antibody staining for Trβ2 in control samples (d) and from aggregates treated with 500 nM retinoic acid between d14 and d16 (e). **(f)** Quantification of the percentage of Trβ2-expressing cells in the mESC-derived neural retinae at d16. No statistically significant difference was found. In control $n=40$ sections were scored and in treated samples $n=34$ sections, samples of aggregates derived from 3 independent differentiation cultures were used for assessment.

mESC-derived neural retinae (Figure 4.4 a-c) revealed a modest, nevertheless, statistically significant decrease in numbers of GFP-positive cells (Figure 4.4 a-c; 23.69% ± 1.05% in control samples, *n*=40 sections, versus 20.53% ± 0.98% in retinoic acid-treated samples, *n*=34 sections; *p*=0.0325, Student's *t*-test). To examine if this reduction was caused specifically by decreased production of cone precursors, samples of E16 CCE line treated in the exact same manner were stained for the early cone marker Trβ2 (Figure 4.4 d,e). The percentage of cells in mESC-derived neural retinae that stained positive for Trβ2 was quantified showing no significant difference in the ratio of cone precursors (Figure 4.4 d-f; 18.74% ± 1.13% in control samples, *n*=46 sections, versus 16.73% ± 0.84% in retinoic acid-treated samples, *n*=43 sections; *p*=0.16, Student's *t*-test). Examining the changes in the proportion of precursors that express the pan-photoreceptor Crx or cone-specific Trβ2 markers, it appears that retinoic acid treatment causes a reduction in Crx-expressing cells by approximately 13.3% and a corresponding small reduction in Trβ2-expressing cells by 10.7%, indicating that there is no preferential reduction in cone precursor differentiation following retinoic acid treatment. This also suggests that it is highly unlikely that there could be a shift to rod precursor genesis. Unfortunately, direct examination of rod differentiation in this setting could not be performed due to lack of reliable immunohistochemical markers for rod precursors *in vitro* at this early stage. Nonetheless, results presented in Figures 4.2-4.4 are consistent with the hypothesis that high levels of retinoic acid participate in conferring early retinogenesis characteristics: higher proportion of cycling progenitors and lower levels of photoreceptor neurogenesis.

4.7. Retinoic acid regulates photoreceptor maturation in mESC-derived retinae

Application of exogenous retinoic acid to zebrafish eyes at the time of photoreceptor maturation leads to precocious rod differentiation and blocks cone maturation (Hyatt et al., 1996). Addition of retinoic acid to *in vitro* cultures of dissociated rat retinal cells and retinal differentiation culture of pluripotent stem cells facilitates rod marker gene expression (Kelley et al., 1994; Osakada et al., 2008; Wallace and Jensen, 1999). To examine the impact of retinoic acid levels on photoreceptor precursor development we examined photoreceptor gene expression in differentiation cultures treated with 500 nM all-*trans* retinoic acid either only at early stages or in which retinoic acid was continuously added until a stage equivalent to early postnatal development (schematically depicted in Figure 4.5 a).

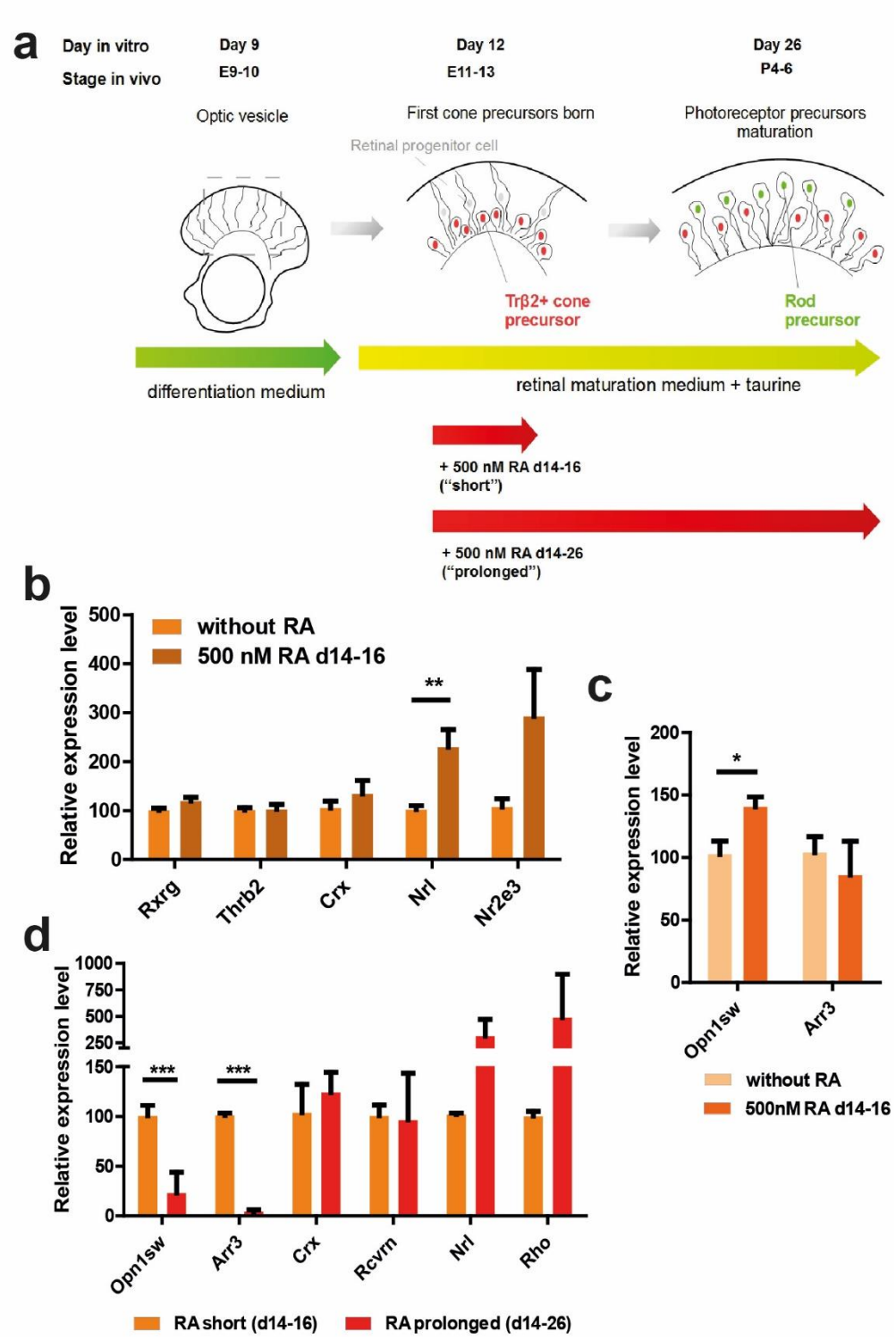

Figure 4.5. The effects of retinoic acid on mESC-derived photoreceptor differentiation are stage-dependent.

(a) Schematic depiction of exogenous retinoic acid addition regime. **(b)** QPCR analysis of the effect of exogenous retinoic acid stimulation at a differentiation stage equivalent to embryonic development, on genes specific for early cone and rod photoreceptor precursors. Note significant induction of Nrl expression. **(c)** QPCR analysis of control cultures and cultures treated with retinoic acid at d14-16, showing significant induction

of S opsin expression without effect on *Arr3* transcript levels. **(d)** QPCR analysis of cultures treated with retinoic acid only on d14-16 or from d14 until d26. Note significant suppression of S opsin (Opn1sw) and Arrestin3 (Arr3) expression resulting from prolonged levels of retinoic acid. In all experiments at least 3 samples from 3 independent differentiation cultures were run in triplicate. *, $p<0.05$; **, $p<0.01$; ***, $p<0.001$; Student's *t*-test. In (d) *Nrl*, $p=0.08$; *Rho*, $p=0.1$.

Results presented in previous sections suggested that immediately after treatment with retinoic acid between day 14 and 16 the numbers of photoreceptors generated were slightly lower, however proliferating progenitors in S phase of the cell cycle were more abundant (Figures 4.3 and 4.4). To examine the impact of this treatment on subsequent photoreceptor differentiation we performed gene expression analysis of differentiated embryoid bodies treated with retinoic acid followed by culture until day 21 of differentiation (a stage resembling the neonatal retina). Expression of cone photoreceptor transcripts *Rxrg* and *Thrb2* as well as the pan-photoreceptor marker *Crx* were similar in both treated and control conditions (Figure 4.5b?). In contrast, levels of rod precursor markers were elevated with a significant increase in *Nrl* expression and a strong trend for increased *Nr2e3* transcripts (Figure 4.5 b), suggesting a specific effect in stimulating rod specific genes.

Levels of retinoic acid during embryonic development were found to have an impact on induction of S opsin in ventral retina (Alfano et al., 2011). We therefore next determined the impact of the retinoic acid stimulation at early stages on S opsin expression. For this purpose, cultures treated with retinoic acid between days 14 and 16 were then further cultured until day 26. Gene expression analysis of these specimens revealed significant upregulation of S opsin, but not cone arrestin transcripts (Figure 4.5 c), suggesting that retinoic acid plays a role in S opsin induction *in vitro* as it occurs *in vivo*.

Exposure of developing zebrafish cones to excess retinoic acid prevents their maturation, whilst inducing precocious rod differentiation (Hyatt et al., 1996). In order to evaluate the effect of high concentrations of retinoic acid on photoreceptor maturation in this system, we exposed the cultures to 500 nM of retinoic acid either only between day 14 and 16 or kept this high level continuously until day 26, when specimens were collected for gene expression analysis (schematically depicted in Figure 4.5 a). QPCR performed on these samples showed potent suppression of S opsin and Arrestin3 transcription (4.4- and 23.8-fold reduction, respectively, N=4; Figure 4.5 d). Levels of pan-photoreceptor markers Crx and Recoverin were not affected by the treatment, whereas there was a strong trend for an increase in rod markers Nrl and Rhodopsin (Figure 4.5 d). Results of this analysis indicate that persistent high levels of retinoic acid in the culture environment blocks transcription of mature markers in cones developing in mESC-derived retinae.

To examine whether this effect on S opsin and Arrestin3 transcription corresponded to changes in protein levels we used CrxGFP line retinal organoids and also treated these

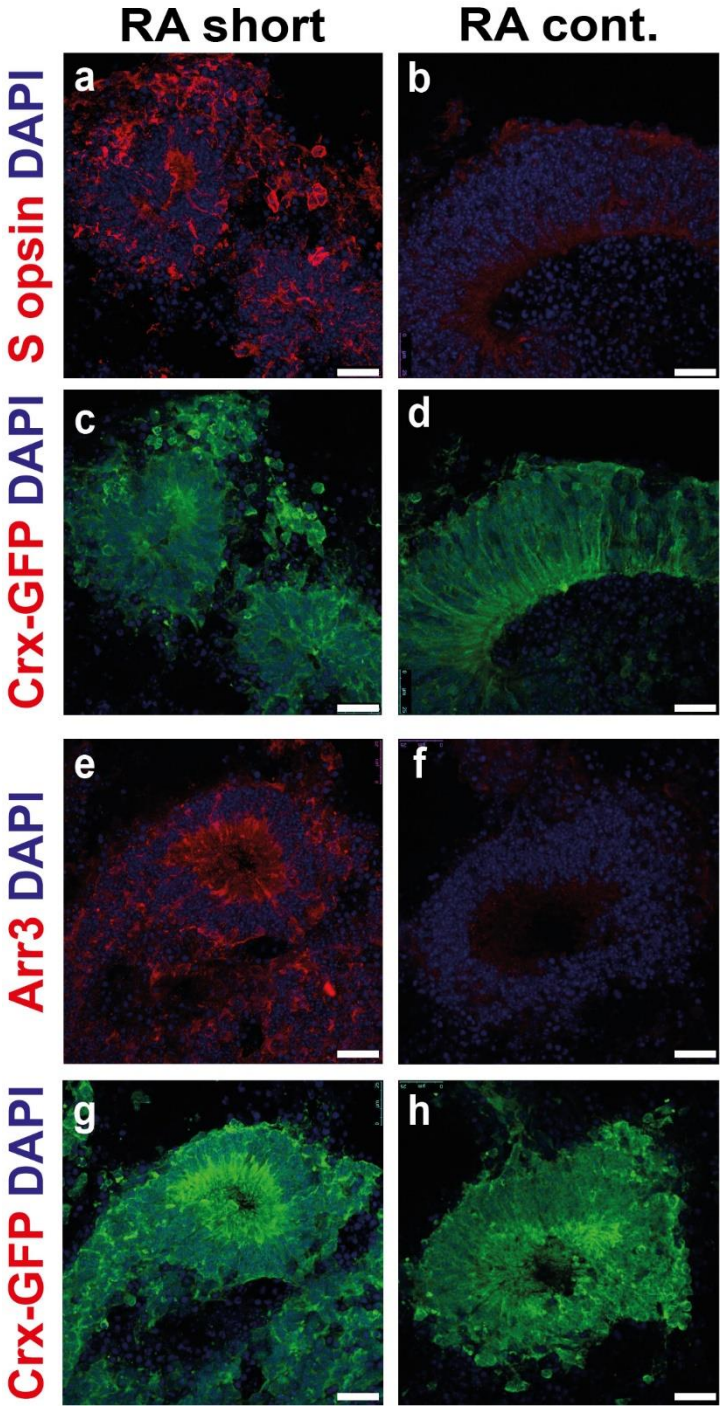

Figure 4.6. Prolonged exposure to retinoic acid suppresses expression of proteins related to cone maturation.

(a-h) Immunostaining for S opsin (a,b) and Arrestin3 (e,f) in CrxGFP line cultures treated with retinoic acid either at days 14-16 ('RA short'; a,c,e,g) or 14-26 ('RA cont.'; b,d,f,h). GFP reporter signal in each condition shown in (c,d,g,h). Note loss of immunoreactivity to S opsin and Arrestin3 in cultures continuously stimulated with retinoic acid ('RA cont.'; b,f versus a,e), despite equivalent CrxGFP reporter expression (c,d,g,h). Also observe more rosette-like morphology of neural retina in shorter stimulation condition ('RA short'; a,c). Scale bar 20 μm.

with 500 nM retinoic acid either at days 14-16 or 14-26, but instead collected for immunohistochemistry at day 26 (Figure 4.6 a-h). Immunostaining showed loss of both S opsin and Arrestin3 in neural retinae of organoids exposed continuously to high concentration of retinoic acid until day 26 ('RA cont.', Figure 4.6 b,f), compared to only days 14-16 ('RA short', Figure 4.6 a,e). No difference could be observed in expression of the CrxGFP reporter indicating that no general loss of photoreceptors occurred (Figure 4.6 c,d,g,h). However, the neural retinae in aggregates exposed to retinoic acid only at days 14-16 showed more frequent formation of photoreceptor rosettes (Figure 4.6 a,c), which are normally observed at late stages in culture, an observation consistent with high concentrations of retinoic acid conferring earlier retinal development characteristics.

4.8. Conclusions and discussion

Apart from the intrinsic genetic programmes operating cell-autonomously during retinal development, cell to cell signals are also required for formation and maturation of the neural retina. In Chapter 2 the important roles of direct cell to cell contact signals mediated by the Notch pathway have been discussed. Additionally, a number of studies identified the importance of soluble factors for the appropriate differentiation of retinal cell types. Signalling mediated by secreted growth and differentiation factor 11 (GDF11) is required for establishing the proper number of retinal ganglion cells in the developing retina (Kim et al., 2005). Soluble signals have also been implicated in photoreceptor differentiation. In early studies by Watanabe and Raff (Watanabe and Raff, 1990, 1992) the authors developed a re-aggregate retinal cell culture system to study retinal development *in vitro*. In this system co-culture of embryonic E15 retinal cells with postnatal P1-3 retinal cells resulted in an increase in rod generation by the embryonic cells. This effect was found to be mediated by soluble factor(s), since it was not blocked by separation of the cells from different stages by a milipore filter (Watanabe and Raff, 1992). Moreover, differentiation of neural progenitors derived from pluripotent stem cells into cells expressing markers of photoreceptors was achieved by co-culture with P1 retinae (Zhao et al., 2002), adding support to the observations from the heterochronic co-culture of dissociated retinal cells. Further studies sought to identify the soluble factors promoting photoreceptor differentiation *in vitro*. Retinoic acid and taurine were identified as most potent in induction of rod markers (Kelley et al., 1994; Osakada et al., 2008; Wallace and Jensen, 1999). With respect to cone photoreceptors, thyroid hormone T3 was identified to promote expression of markers of this cell type in rat retinal neurons cultured *in vitro* (Kelley et al., 1995). Here, we find that retinoic acid levels impact on the differentiation of both

cone as well as rod precursors in mESC-derived retinae, facilitating induction of both *Nrl* and *Opn1sw* (S opsin). However, prolonged exposure to retinoic acid, until stages equivalent to the early postnatal period suppressed markers of cone maturation. In addition, the application of thyroid hormone to cultures increased M opsin expression in cone photoreceptors, but simultaneously induced apoptotic cell death in this system.

Genetic studies have shed light on the molecular effectors of these diffusible molecules identifying their receptors expressed in the eye. Both retinoic acid as well as thyroid hormone exert their biological actions through nuclear receptors (Huang et al., 2014; Ng et al., 2001). Expression of several retinoid receptors has been reported for the developing neural retina including RARα, RXRα, RXRβ and RXRγ (Mori et al., 2001) and the retinoid orphan receptor RORβ (Jia et al., 2009). In this study, we examined expression of these molecules during the course of photoreceptor differentiation in mESC-derived retinae. A timecourse of QPCR analysis showed relatively stable expression of RARα, consistent with its broad expression pattern in the embryonic and early postnatal retina. In addition, immunohistochemistry showed diffused expression of this receptor across the mESC-derived optic vesicle at d12 of differentiation. RXRγ is specifically expressed in developing cones and ganglion cells (Roberts et al., 2005). RXRγ expression increased from day 12 until day 20 of differentiation followed by some decrease at day 24, which resembles temporary downregulation of RXRγ at the time of S opsin induction (Roberts et al., 2005). At the peak of its expression at day 20, immunohistochemistry confirmed RXRγ expression in two distinct populations, one at the apical and the other at basal side of the neural retina derived from mESCs, corresponding to developing cones and ganglion cells, respectively. The orphan retinoid receptor RORβ showed stable levels of expression until day 24, at which point some reduction in its transcripts were observed. This pattern is in accordance with *in vivo* studies, which show high expression patterns in progenitors and early photoreceptor precursors, as well as a later requirement for the development of outer segments (Fu et al., 2014; Jia et al., 2009). With respect to thyroid receptors, thyroid hormone receptor β2, expression, which is restricted to developing cone precursors, was observed at both the mRNA and protein level from day 12 of differentiation, with expression peaking around day 20 (similar to RXRγ; Figure 1.4; Chapter 1). Altogether, the expression of nuclear receptors for retinoids and thyroid hormone in mESC-derived retinae appear similar to that observed throughout the course of retinogenesis *in vivo*, suggesting that the effects of these ligands may also correspond in the culture system.

The activity of retinoid and thyroid ligands are dependent upon and extensively modified by metabolising enzymes. We examined the patterns of expression of these

molecules in mESC retinal differentiation cultures. In the circulation the majority of thyroid hormone is in the form of T4, which has low biological activity. Tissues that require thyroid hormone activity usually express deiodinase 2, an activating enzyme that converts T4 into the more potent T3. The retina expresses little if any deiodinase 2, however deiodinase 3, an enzyme that inactivates thyroid hormone is present in the developing retina. QPCR analysis of these two enzymes in mESC retinal differentiation cultures demonstrates expression of deiodinase 3 as seen in the developing retina, as well as deiodinase 2 (Figure 4.1 b). The unexpected expression of deiodinase 2 most likely derives from non-retinal forebrain neurons that can also differentiate within the cultures. Presence of this enzyme could explain the toxic effects of thyroid hormone observed even at relatively low concentrations in our culture system, since protection from thyroid hormone by deiodinase 3 is required for cone survival and proper M opsin induction *in vivo* (Ng et al., 2010). Conceivably, activating enzyme action could cause imbalance in the forms of thyroid hormone present, resulting in toxic effects. Suppressing thyroid hormone signalling was indeed found to protect cones and rods in retinal degeneration models (Ma et al., 2014). With respect to retinoic acid metabolism, synthesis of this molecule is very high at early embryonic stages, but enzymes involved in its metabolism decline or cease to be expressed around birth. Similarly, transcript levels of retinoic acid synthesising enzymes *Raldh1* and *Raldh3* as well as catabolizing enzyme *Cyp26a1* were high early in differentiation at day 12 and progressively decreased with time (Figure 4.2 a). Collectively, molecules involved in metabolism of thyroid hormone and retinoic acid are mostly expressed in patterns mimicking *in vivo* development with the exception of the presence of deiodinase 2 in differentiation cultures. Deiodinase2 is not normally expressed in retinal tissue and the detected expression could derive from non-retinal forebrain neurons present in the cultures given its broad expression pattern in forebrain tissues (Croteau et al., 1996).

Having observed a close resemblance in the temporal expression patterns of components of retinoic acid signalling between retinogenesis *in vivo* and mESC retinal differentiation cultures, we decided to determine how retinoic acid levels affect photoreceptor differentiation in this system. Addition of exogenous retinoic acid at early stages of retinal development stimulates excessive proliferation of progenitors leading to formation of a second retina in zebrafish (Hyatt et al., 1992). In our system, addition of exogenous retinoic acid at a high concentration of 500 nM between days 14 and 16 (corresponding to around E15) increased the proportion of cells in S phase of the cell cycle as determined by a BrdU pulse. This effect was modest however, suggesting that retinoic acid does not strongly influence proliferation of progenitors at this stage.

Quantification of the proportion of cells that showed expression of photoreceptor markers was performed immediately after this exposure to exogenous retinoic acid. The number of Crx:GFP reporter expressing cells decreased, while no significant change in the percentage of Trβ2-positive cone precursors was detected. These observations are most consistent with the hypothesis that retinoic acid confers some early characteristics to the retina such as a higher proportion of proliferating progenitors and lower photoreceptor neurogenesis. Two studies reported an effect of retinoic acid on cell fate choice in the retina. Retinoic acid was suggested to promote acquisition of rod fate in the study by Kelley and colleagues (Kelley et al., 1994) and Stevens and colleagues (Stevens et al., 2011). In contrast, subsequent studies reported effects on expression of cone-specific genes in differentiating post-mitotic cells (Alfano et al., 2011; Hyatt et al., 1996; Wallace and Jensen, 1999). In both reports suggesting fate choice alterations, the data presented appears to poorly support the conclusions drawn. Kelley and colleagues added BrdU 4-24 hours prior to dissociation of embryonic rat retinal cells and further culture *in vitro* with the addition of retinoic acid. Since the length of S phase, when incorporation of BrdU occurs, is approximately 6 hours at this stage in the rat (Alexiades and Cepko, 1996) most cells would exit the cell cycle and become post-mitotic before treatment with retinoic acid. Therefore, an increase in BrdU- and rhodopsin-positive cells is more likely to reflect precocious expression of genes involved in photoreceptor maturation in newly born cells rather than a cell fate switch. In the study by Stevens and colleagues (Stevens et al., 2011), the authors do not observe an effect of retinoic acid on the photoreceptor mosaic formed when stimulation with this factor is limited to a stage when solely proliferating progenitors are present. This again supports the notion that effects of retinoic acid are primarily on progenitor proliferation or levels of cell-specific gene expression, rather than the final proportions of particular cell types made.

We also probed the effects of retinoic acid in the differentiation system used in this study on photoreceptor-specific gene expression levels. Early treatment with retinoic acid significantly increased transcription of the rod-determining transcription factor Nrl. In accordance with the observations *in vivo* regarding the requirement of retinoic acid for S opsin induction (Alfano et al., 2011), we detected upregulation of S opsin following treatment at a stage corresponding to embryonic retina. However continuous addition of retinoic acid until the equivalent of early postnatal stages had an opposite effect, suppressing expression of S opsin and Arrestin3, markers of cone maturation, on both the transcript and protein levels. This is very similar to the effect of exogenous retinoic acid application on zebrafish photoreceptor maturation (Hyatt et al., 1996). In that

model system retinoic acid supplemented at later stages of photoreceptor development induced precocious expression of rod markers whilst blocking cone maturation (Hyatt et al., 1996). We also observed stimulation of rod markers with continuous addition of retinoic acid until late stages, therefore the differential effects of this molecule on cone versus rod photoreceptor differentiation appear to be evolutionarily conserved. One could speculate that retinoic acid signalling may act to synchronize photoreceptor development. Maturation of early born cones is blocked by high levels of retinoic acid in the embryonic retina, whereas it stimulates differentiation of later born rods, which only encounter diminishing levels of this molecule. Low levels of retinoic acid at neonatal stages are permissive for cone maturation correlating with an increase in circulating thyroid hormone shortly after birth that leads to induction of M opsin (Lu et al., 2009). Retinoic acid could thus maintain cones in an immature state until cone opsin patterning is complete in early postnatal period (represented schematically in Diagram 4.2).

A remaining question is which receptors mediate retinoic acid actions in this context? An intriguing possibility is that some of these effects are not mediated by conventional high affinity receptors, but by retinoid orphan receptors RORβ and COUP-TFs I/II. RORβ possesses a large ligand-binding pocket and structural studies have shown association of all-*trans* retinoic acid with this receptor. Binding of all-*trans* retinoic acid could repress RORβ transcriptional activity in a cell type-specific manner (Stehlin-Gaon et al., 2003). RORβ is expressed in retinal progenitors and implicated in their proliferation (Chow et al., 1998). Moreover, RORβ regulates many aspects of photoreceptor development including formation of outer segments and synapses (Jia et al., 2009). Importantly, two RORβ binding sites have been identified in the S opsin promoter (Srinivas et al., 2006) and RORβ deletion causes significant developmental delay in S opsin expression. A binding site for RORβ is also present in the *Nrl* promoter region and Nrl expression is abolished in RORβ knockout animals (Jia et al., 2009). It is possible that high concentrations of retinoic acid lead to its binding to RORβ. Since this binding represses RORβ-mediated transcription, as a result S opsin expression is suppressed at early stages of development. In progenitor cells this could limit Nrl expression, restricting rod generation to later stages of retinogenesis. At neonatal stages retinoic acid levels are much lower and there is a shift of retinoic acid production to the dorsal retina. This could facilitate S opsin patterning, by permitting S opsin expression in the ventral retina, whilst limiting it in the dorsal part through RORβ. With respect to rod development, at neonatal stages ligand-free RORβ could mediate Nrl induction and allow for the peak in rod genesis. Since RORβ also regulates mature

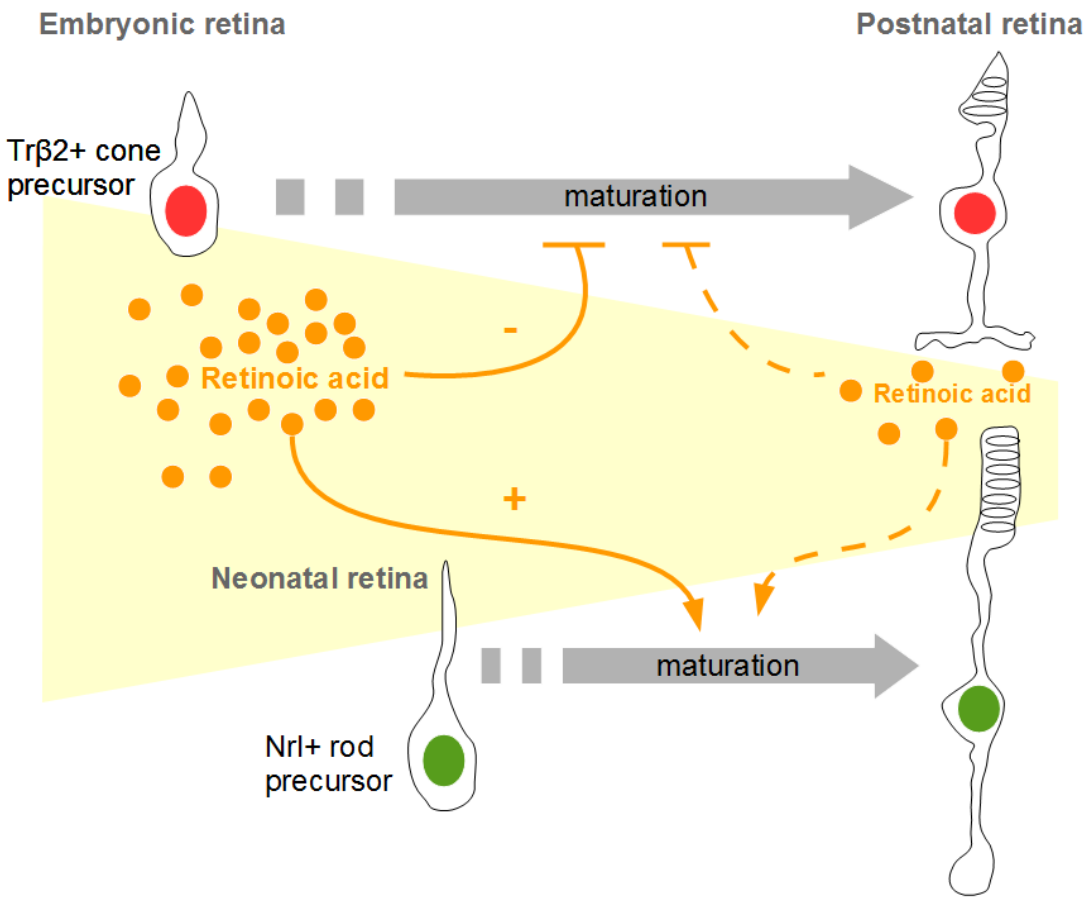

Diagram 4.2. Effects of retinoic acid levels on photoreceptor maturation

Retinoic acid concentrations in retinal tissue are high during embryonic stages but progressively decrease with development. Levels of retinoic acid at the peak of rod birth are only around one third of those at the peak of cone genesis. High abundance of retinoic acid is likely to prevent precocious maturation of cone cells (left side), whereas the neonatal decrease in its levels allow for the maturation of this cell type (on the right). With respect to rod cells, which are born later in retinogenesis when retinoic acid levels are lower, this molecule stimulates rod-specific gene expression in post-mitotic rod precursors. This could potentially provide a mechanism to synchronize the maturation of the two cell types, despite the time lag between their birth peaks.

features such as synapse formation and biogenesis of outer segments, inhibition of its transcriptional activity by high levels of all-trans retinoic acid could prevent precocious maturation and help to explain the lag between photoreceptor birth and acquisition of fully mature phenotype. Orphan receptors COUP-TFs I/II on the other hand are expressed in opposing gradients across the retina with COUP-TF II localised to the dorsal retina (Satoh et al., 2009). COUP-TF II was found to bind retinoic acid leading to activation of its transcriptional activity (Kruse et al., 2008). Since COUP-TF II is required for suppression of S opsin, it is conceivable that this activity is induced by binding of retinoic acid generated by the dorsal Raldh1 enzyme. Further future studies using developmental stage- and cell type-specific genetic deletion, agonist/antagonist treatment and use of luciferase transcriptional activity reporter assays based on specific binding sites are clearly necessary to reveal the detailed modes of action of these transcriptional regulators in photoreceptor development. In conclusion, orphan receptors could play an important role in linking the dynamic spatiotemporal pattern of retinoic acid generation in the retina with the regulation of gene transcription involved in many aspects of photoreceptor differentiation.

To summarize, ligands of nuclear receptors, retinoic acid and thyroid hormone, play important roles in the differentiation of mESC-derived photoreceptor precursors. Expression analysis of components of the retinoic acid signalling pathway during mESC-derived retinae formation, combined with experimental stimulation with retinoic acid, revealed that dynamic changes in retinoic acid levels are required for proper cone precursor maturation. Short supplementation at early stages in culture is optimal for cone differentiation in this system. Interestingly, the effects of retinoic acid on rod and cones differ, highlighting that relevant physiological conditions allow the balanced differentiation of various retinal cell types.

Chapter 5. Isolation and transplantation of mESC-derived cone photoreceptor precursors

5.1. Background

Retinal degenerations that lead to the death of photoreceptors, the sensory neurons responsible for detection of visual stimuli, are a leading cause of untreatable blindness. Since diseases of various etiologies all result in loss of photoreceptors, a common treatment strategy could be replacement of lost neurons by cell therapy (Brandl et al., 2015; Jayakody et al., 2015; Zhang et al., 2015). A promising strategy, identified by the Ali group, is the transplantation of photoreceptors to replace those lost. The group demonstrated that immature retinal cells, isolated from the early postnatal peak of rod genesis, migrated and integrated into the recipient photoreceptor layer of adult mice (MacLaren et al., 2006). Further investigation revealed that post-mitotic rod precursors, identified by an Nrl:GFP transgene, were largely responsible for this integration. These immature rod precursors showed increased integration capacity when isolated from early postnatal retina, between P3 and P9 (MacLaren et al., 2006; Pearson et al., 2012). Transplanted cells are proposed to migrate out of the subretinal cell mass, traverse the interphotoreceptor matrix and cross the outer limiting membrane to assume their final location in the recipient outer nuclear layer (MacLaren et al., 2006; Pearson et al., 2012; Warre-Cornish et al., 2014). In the recipient photoreceptor layer transplanted rods show extension of apical processes ending in outer segments and basal processes forming synaptic connections to the retinal interneurons (MacLaren et al., 2006; Pearson et al., 2012; Warre-Cornish et al., 2014), the morphological hallmarks of mature functional photoreceptors. Optimization of the isolation and delivery protocol enabled the rescue of useful vision in a model of stationery night blindness, the *Gnat1* knockout mouse. Animals transplanted with donor-derived rods showed dim light-evoked responses recorded from the visual cortex (V1), rescue of contrast sensitivity in low light measured by optokinetic head-tracking response and restored visually-guided behavior in a water maze-based test (Pearson et al., 2012). Collectively, these studies outlined a promising cell therapy strategy for retinal degeneration.

Whilst highly successful, this body of research also identified key obstacles in the recipient environment that limit the extent of cell replacement (Barber et al., 2013). In the degenerating retina Müller cells become activated extending processes forming a glial scar that creates a physical barrier to the passage of transplanted cells. These cells also secrete extracellular matrix components including chondroitin sulphate

proteoglycans (CSPGs), which are known to inhibit the extension of neurites (Friedlander et al., 1994). In some degenerative diseases the outer limiting membrane formed between Müller cells and photoreceptor inner segments can become compromised (Mehalow et al., 2003), which could facilitate migration of photoreceptors from the subretinal space. A study by Pearson and colleagues demonstrated that transplantation of rod precursors is feasible into a range of degeneration models, however, the number and morphology of integrating cells is dependent on the disease etiology, rather than its severity (Barber et al., 2013).

Apart from the limitations set by the host environment another consideration is the source of cells for transplantation. The advances described above were all made using cells isolated from retinae of developing mice. If this strategy was to be used in humans a renewable, scalable and ethically acceptable source of donor tissue is required. Hence the interest in deriving retinal tissue from embryonic stem cells, which are an expandable population that in theory could be directed to produce all cell types (Evans and Kaufman, 1981). Early studies on differentiation towards retinal fates focused primarily on stepwise induction of the neural rostral phenotype and obtaining the telencephalic progenitors followed by eye field induction (Ikeda et al., 2005; Osakada et al., 2008; Watanabe et al., 2005; West et al., 2012; Zhao et al., 2002). The first evidence of photoreceptor differentiation was obtained when neural progenitor differentiation cultures were supplemented with retinoic acid and basic fibroblast growth factor (bFGF) with subsequent co-culture with P1 retinae (Zhao et al., 2002). In subsequent studies efficient telencephalic differentiation was achieved in suspension culture of mESCs aggregates. Serum-free floating culture of embryoid bodies (SFEB) system combined with treatment with Wnt and Nodal antagonists (Dkk-1 and LeftyA, respectively) yielded a significant number of Bf1-positive telencephalic progenitors (Watanabe et al., 2005). Addition of serum and Activin-A pushed these cells towards Rax/Pax6-positive retinal progenitors, which through co-culture with retinal explants, differentiated into Crx-positive photoreceptor precursors. A small proportion of the Crx-positive cells developed further to express photoreceptor markers Rhodopsin and Recoverin. These were also found to be able to migrate into retinal explants cultured *in vitro* (Ikeda et al., 2005). This showed that recapitulation of the stepwise specification of stem cells into rostral neural progenitors with subsequent progression to retinal progenitors can yield cells showing markers of post-mitotic photoreceptor precursors. A seminal study from Sasai and colleagues went one step further and developed a differentiation protocol that not only mimicked the stepwise commitment to the retinal lineage but also managed to recapitulate three dimensional

tissue morphogenesis *in vitro* (Eiraku et al., 2011). In this differentiation protocol aggregates made using the SFEB method are supplemented with matrigel. This leads to formation of a continuous neuroepithelia. In appropriate media these become retinal neuroepithelia that spontaneously evaginate forming optic vesicles, which subsequently fold into bi-layered optic cups. All retinal cell types were found to be generated in a manner closely resembling *in vivo* retinogenesis (Eiraku et al., 2011). Adaptations of this protocol allowed generation of stage-specific rod precursors, which integrated following transplantation into adult and degenerate retinae in a manner very similar to cells derived from donor mice (Gonzalez-Cordero et al., 2013; Decembrini et al., 2014).

One of the final challenges faced by pre-clinical research into cell replacement strategies for the retina is cone photoreceptor transplantation. Most of our daily human activities like reading or driving are heavily dependent on high acuity and color vision, primarily mediated by cone cells. So far only a handful of studies have examined the possibility of cone cell transplantation. A study from the Ali group looked at the integration potential of photoreceptor precursors isolated from the Crx:GFP transgenic mouse line (Lakowski et al., 2010). Examination of transplants in which donor cells were isolated at embryonic stages, when cone cells constitute a large proportion of the donor population, revealed a small number of integrated cells that had the morphology and marker expression profile of cone cells. These integrated cones were not found in postnatal donor cell transplants, at which stage rod precursors are the predominant cell type in the donor population (Lakowski et al., 2010). Taking advantage of mouse genetics, Ader and colleagues isolated cells from *Nrl*-/- donor mice (Santos-Ferreira et al., 2015), which lack the transcription factor Nrl that is necessary for rod specification (Mears et al., 2001). In the absence of Nrl, photoreceptor precursors that would have developed into rods express blue cone opsin and other cone markers instead (Mears et al., 2001). Isolation and transplantation of this population demonstrated a developmental stage dependence, similar to that observed for rod precursor transplants, with a peak of integration capacity at P4 (Santos-Ferreira et al., 2015). These cone-like cells were able to drive light-evoked responses in retinal ganglion cells when transplanted into a mouse model lacking cone function (*Cpfl1*-/- retina). That study provided a proof-of-concept for daylight vision repair through cell replacement. However, thus far none of the studies have investigated the transplantation of a purified cone cell donor population generated from a renewable source.

5.2 Aims

Proof of concept studies using photoreceptor precursors derived from donor mice showed that integration of cone cells following transplantation is possible. However, due to the use of mixed rod and cone donor cell populations or genetically altered cone-like cells, the integration-competence of cone precursors that have developed normally has not been thoroughly investigated. In contrast to the rod cells, which were successfully differentiated from mESCs and transplanted into the adult retina (Decembrini et al., 2014; Gonzalez-Cordero et al., 2013), studies investigating cone transplantation used donor cells extracted from the developing mouse retina. Therefore the question of whether mESC retinal differentiation can provide a renewable source of integration-competent cones remains unresolved. Therefore the objectives of this study were to:

(1) determine if embryonic cone precursors generated from mESCs are able to integrate and mature following transplantation to the adult retina;
(2) determine the integration-competence and efficiency of mESC-derived cone precursors at stages comparable to postnatal retinal development;
(3) determine the effect the recipient retinal environment has on the efficiency of mESC-derived cone precursor cell integration.

5.3 Characterisation of an embryonic-equivalent photoreceptor precursor cell population using the Crx:GFP mESC line

Cone-rod homeodomain transcription factor (Crx) is an early marker of developing rod and cone photoreceptor cells, with expression maintained in the mature retina (Furukawa et al., 1997). A transgenic mouse line created with bacterial artificial chromosome (BAC) technology, with GFP inserted into the 5' untranslated region of the *Crx* gene (Muranishi et al., 2010; Samson et al., 2009), was used to isolate photoreceptor precursors for transplantation from embryonic retina. These populations, dominated by cone precursors, showed infrequent integration of cone cells following transplantation into the adult retina (Lakowski et al., 2010). Recently, an embryonic stem cell line was generated from the inner cell mass of isolated Crx:GFP mouse blastocysts and was found to closely follow the *in vivo* transgenic reporter expression pattern when subjected to suspension 3D retinal differentiation culture (Decembrini et al., 2014). To test whether this line could provide a donor cell population similar to the Crx:GFP-positive photoreceptors isolated from donor mice at embryonic stages, we examined Crx:GFP mESC line differentiated according to our differentiation protocol (please see Chapter 1 for details). Neuroepithelia formed around the embryoid

bodies in the first few days in culture and by day 9 optic vesicle structures had developed. For transplantation we decided to use aggregates at day 16 in culture, a stage similar to around E17.5 *in vivo*, when GFP-positive cells isolated from the mouse transgenic retina showed strong enrichment for cone-specific genes (Muranishi et al., 2010). Cone precursors constitute around 40% of GFP-positive cells in Crx:GFP mESC-derived retinae at this stage of culture (Decembrini et al., 2014). In our cultures, optic vesicles were clearly visible by light microscopy at this stage and showed green fluorescence restricted to these regions (Figure 5.1 a). Cryosections of these mESC-derived retinae showed numerous GFP-positive photoreceptor precursors in the apical part of the neuroblastic layer (Figure 5.1 b), consistent with the late embryonic developing Crx:GFP transgenic retina *in vivo* (Muranishi et al., 2010). A papain-based kit was used to dissociate the aggregates into a single cell suspension, from which GFP-positive cells were purified by FACS (Figure 5.1 c). Sorted GFP-positive cells showed strong enrichment for transcripts of cone-specific genes Thrb2, RXRγ and S opsin compared to the GFP-negative population (Figure 5.1 d), similar to the aforementioned observations *in vivo* (Muranishi et al., 2010). Together these data show that cultures of the Crx:GFP mESC line can provide a donor population of photoreceptor precursors that closely resembles that of the late embryonic retina *in vivo*.

5.4 Examination of mESC-derived cone precursor cell maturation and integration following transplantation of embryonic photoreceptor precursor cell populations to the adult retina

Our group previously demonstrated that Crx:GFP+ photoreceptors isolated at embryonic stages can yield integrated cone cells, following transplantation to the adult mouse retina (Lakowski et al., 2010). In order to determine whether mESC-derived embryonic cone precursors are able to integrate into the adult retina we dissociated the Crx:GFP mESC-derived aggregates at day 16 of culture. The resultant single cell suspension was purified by FACS (Figure 5.1 c) and $2x10^5$ GFP-positive cells were transplanted into the subretinal space of recipient adult wild-type mice, 10^5 cells into the superior and another 10^5 cells into the inferior hemisphere of the retina. Eyes injected with cells were harvested for histological examination three weeks after transplantation. In the transplanted eyes we observed GFP-positive subretinal masses of surviving cells as well as a relatively small number of integrated photoreceptors (Figure 5.3 a, quantified in b). We next examined the expression of cone markers in the cells surviving in the subretinal space following transplantation. Clear labelling for peanut agglutinin (PNA), a marker of extracellular matrix secreted by cone cells was

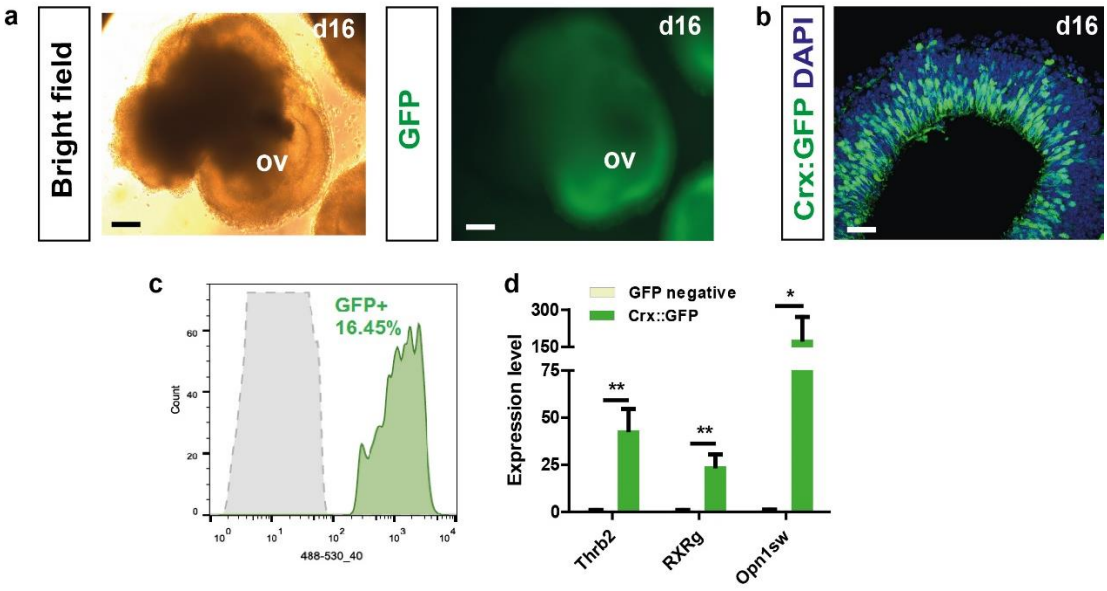

Figure 5.1. Isolation of early photoreceptor precursors differentiated from the Crx:GFP mESC line

(a) Bright field and green fluorescence images of aggregates differentiated from the Crx:GFP mESC line showing the formation of optic vesicles (ov) that contain GFP positive photoreceptor precursors in retinal neuroepithelia, at day 16 of differentiation; **(b)** immunohistochemistry demonstrating GFP expression in cryosectioned Crx:GFP mESC-derived retina at day 16 of culture; scale bar 150 µm in a, 20 µm in b **(c)** representative flow cytometry histogram showing GFP expression in isolated cells, percentage of GFP-positive cells indicated; **(d)** qPCR analysis of cone-specific gene expression in flow-sorted Crx:GFP-positive and –negative populations. Note high enrichment for cone-specific genes in the positive population at this timepoint.

found in the masses (Figure 5.2 a). Surviving early photoreceptors also matured in the adult environment to express two mouse colour opsins (M opsin in Figure 5.2 b and S opsin in 5.2 c). Expression of M opsin is particularly noteworthy since we have not observed this marker in culture (please refer to Chapter 1 for details).

Integrated Crx:GFP-positive cells were found located throughout the recipient photoreceptor layer and the majority showed typical morphology of mouse rod photoreceptors with a small soma, elongated inner segment and a basal process ending in a synaptic bouton-like structure (Figure 5.3 a and c). The number of integrated cells was markedly lower than that of Crx:GFP-positive photoreceptor precursors isolated from donor mice (Figure 5.3 b, an average of 181±39 cells versus around 500 cells), as was previously also found in mESC-derived rod precursor transplants (Decembrini et al., 2014; Gonzalez-Cordero et al., 2013). Importantly however, a small fraction (<1%) of the integrated cells stained positive for mature cone markers Cone α-Transducin (GNAT2) and PNA (Figure 5.3 d and e, respectively). These rare cells were found located towards the apical edge of the outer nuclear layer similar to the tissue location of endogenous cones. This is similar to what has been observed in the case of the donor-derived embryonic Crx:GFP-positive population, where less than 1% of integrated cells were cones (Lakowski et al., 2010). It is important to note however, that reliable detection of mature markers, the majority of which localise to outer segments, is difficult in cells integrated into more basal positions in the photoreceptor layer and therefore this observation regarding transplants of early mESC-derived photoreceptor precursors warrants further investigation. For instance, transgenic mouse knockout lines, in which cone-specific proteins are ablated could be used to identify wild-type transplanted cells through immunostaining for the missing protein analogously to the experiments performed for rod precursors in *Gnat1*$^{-/-}$ or *Rho*$^{-/-}$ lines (Barber et al., 2013; Gonzalez-Cordero et al., 2013; Pearson et al., 2012). However, at the time of the study such lines, with associated reliable staining protocols, were not available for cones in the group. In conclusion, the data presented here show that mESC differentiation cultures resemble the embryonic retina in their capacity to yield cone precursors capable of integrating into the adult retina. In addition, transplanted cone photoreceptor precursors developed within the adult retina and demonstrated mature cone marker expression, some of which were unseen *in vitro*.

5.5 Isolation of a purified population of cone precursors at a stage equivalent to the postnatal retina

Studies from our group demonstrated that integration of donor-derived rod precursors occurs within a specific time window, at which the cells are post-mitotic precursors

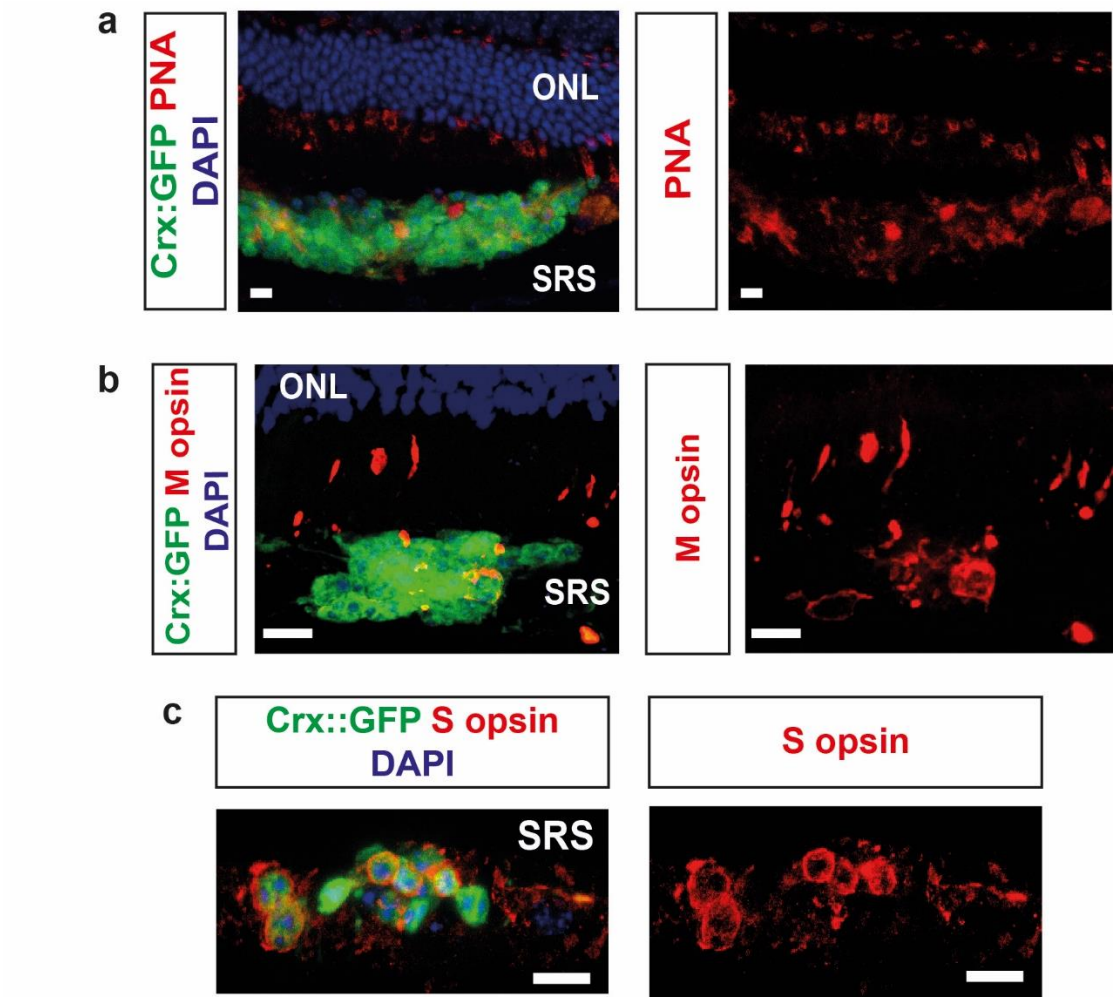

Figure 5.2. Expression of cone markers in subretinal cell masses of early Crx:GFP mESC-derived photoreceptor precursors transplanted into adult retina.

(a) PNA labelling (red) of GFP-positive cell mass (green) in the subretinal space (SRS) of a wild-type recipient. **(b)** Cluster of GFP-expressing transplanted cells showing immunolabeling for M opsin (red). **(c)** Transplanted GFP-positive photoreceptor precursors showing immunostaining for S opsin. Scale bar in all 10 µm. ONL – outer nuclear layer, SRS – subretinal space.

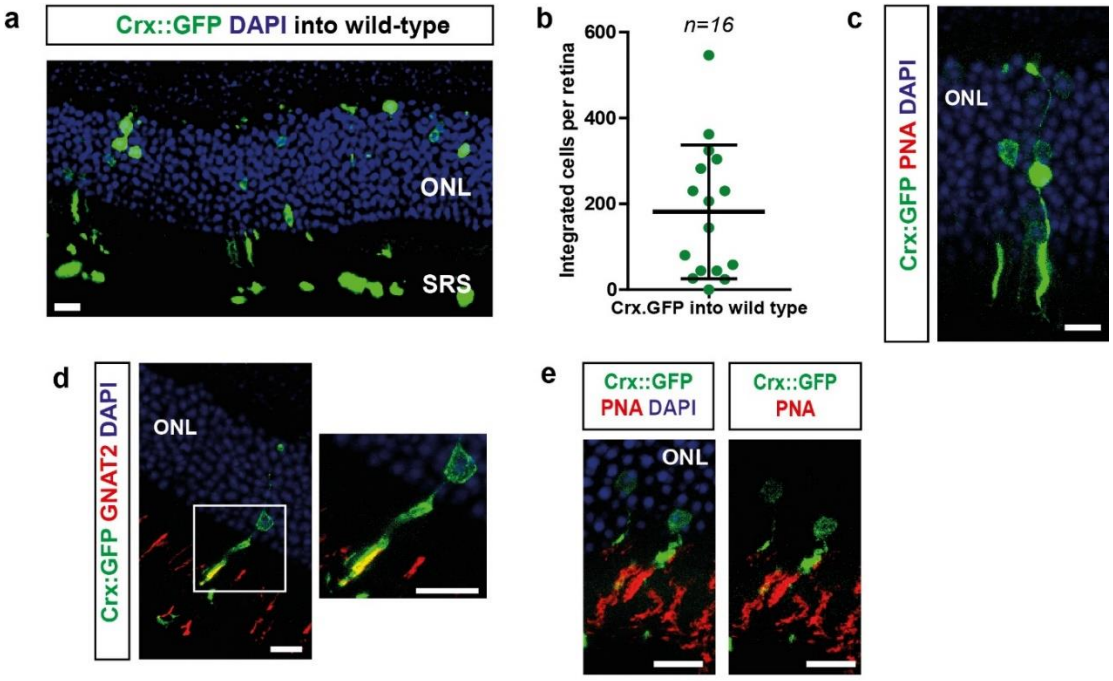

Figure 5.3. Early staged Crx:GFP-positive photoreceptor precursors integrate into the adult retina following transplantation with rare integrated cone cells

(a) Section of a transplanted retina showing an area of integration. **(b)** Quantification of the number of integrated cells per retina in the *n=16* eyes transplanted. Average ±SD marked. **(c)** Typical rod photoreceptor morphology shown by most of integrated cells. **(d)** Integrated cell showing immunoreactivity for cone transducin (GNAT2, in red) in the outer segment. **(e)** Integrated cell showing staining for PNA in the outer segment. Note that in both examples the cell nuclei are positioned at the apical aspect of the outer nuclear layer. Scale bar in all 10 µm. ONL – outer nuclear layer; SRS – subretinal space.

(MacLaren et al., 2006; Pearson et al., 2012). Neither transplanted retinal progenitors nor adult mature rod cells were found to yield integrated photoreceptors in any significant number (Jayakody et al., 2015; MacLaren et al., 2006). With respect to the post-mitotic rod precursors, their capacity to integrate following transplantation into adult retina appears to be most efficient between P3 and P9. Rod precursors isolated from embryonic retina integrate in relatively small numbers similar to the ones isolated beyond P10 (MacLaren et al., 2006). Accordingly, mESC-derived rod precursors were found to engraft most readily within an equivalent time window (Decembrini et al., 2014; Gonzalez-Cordero et al., 2013). A recent report using donor mice in which the transcriptional regulator *Nrl*, essential for rod genesis, was genetically inactivated demonstrated robust integration of the donor cone-like cells isolated from the postnatal retina of this mouse model, suggesting that a similar integration time window may exist for cone precursors (Santos-Ferreira et al., 2015). To interrogate whether, analogous to rod precursors, cone cells can show integration when transplanted from a postnatal donor population we utilized viral labelling to introduce a fluorescent reporter construct into cone precursors in culture. The 2.1 kb human red-green opsin promoter (Wang et al., 1992) driving GFP expression (ConeOpsin.GFP) packaged in an adeno-associated viral vector serotype 2/9 was found to result in strong and specific labelling of cone cells in the mature mouse retina following subretinal injection (Figure 5.4 a). Since the great majority of mouse cone cells express M opsin at least to some extent (Applebury et al., 2000), this vector enables tagging of most cone cells with a GFP reporter. To test whether this genetic element would be active in developing mESC-derived cone precursors *in vitro*, we infected differentiation cultures with the purified vector at day 20-22 (Figure 5.4 b), since beyond this stage little increase in the proportion of Trβ2-positive cells can be observed (please see Figure 1.4), suggesting that cone generation is reaching completion. Aggregates examined a week later showed strong expression of GFP in mESC-derived retinal neuroepithelia (Figure 5.4 c). Moreover, cryosectioning of infected aggregates revealed GFP-positive cells with elongated morphology characteristic of differentiating photoreceptor precursors (Figure 5.4 d). To determine whether these cells represent a population distinct from developing rod precursors, co-infection with a vector encoding rhodopsin promoter driving an RFP fluorescent reporter was performed. Histological examination of infected differentiation cultures showed numerous green or red fluorescent marker expressing cells in the mESC-derived neural retina (Figure 5.4 f). However, examination of a large number of infected cells (a total of 971) did not reveal any cells co-expressing both reporters (Figure 5.4 g). Dissociation of infected aggregates between days 26 and 30, a stage corresponding to P5-P10 *in vivo*, followed by flow cytometric analysis showed that a

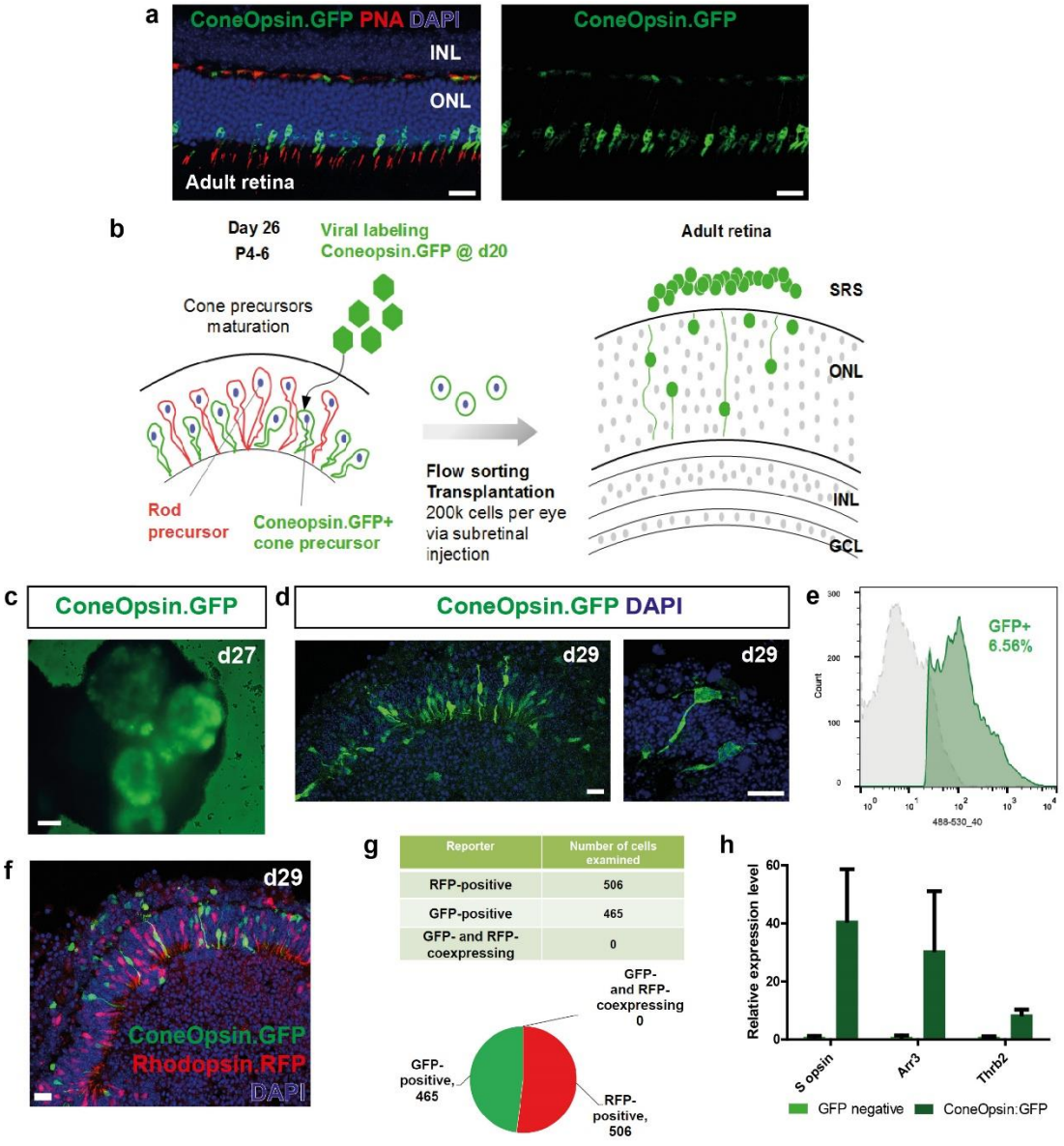

Figure 5.4. Labelling and isolation of mESC-derived cone precursors at stages equivalent to early postnatal development

(a) Expression of ConeOpsin.GFP reporter in cone photoreceptors of the adult mouse retina following subretinal injection of purified rAAV2/9 viral vector preparation. Section co-stained for PNA (red). Please note that GFP expression is restricted to apically located cone cells that exhibit characteristic morphology. Scale bar 20 µm. **(b)** Schematic representation of the protocol used for viral labelling of mESC-derived cone precursors. Viral vector was added to cultures at day 20. Between day 26 and day 30 cells were dissociated, purified by FACS and transplanted. **(c)** Expression of the ConeOpsin.GFP reporter in the embryoid body. The expression is restricted to the retinal neuroepithelium structures. Scale bar 150 µm. **(d)** Section of embryoid body aggregate at day 29 of differentiation infected with ConeOpsin.GFP viral vector at day 20 demonstrating photoreceptor morphology of reporter-expressing cells. Scale bar 10 µm. **(e)** Representative flow cytometry histogram of dissociated aggregates showing

ConeOpsin.GFP expression in a sub-population of cells. **(f)** Section of a differentiated embryoid body at day 29 co-infected with ConeOpsin.GFP (in green) and Rhodopsin.RFP (in red) viral vectors. Note that reporters are not co-expressed. Scale bar 10 µm. **(g)** Quantification of reporter expressing cells in 7 sections of different aggregates. No co-labelled cells were identified. **(h)** Samples of dissociated and FACS-purified ConeOpsin.GFP-positive and GFP-negative cells analysed by qPCR for expression of cone-specific genes S opsin, Cone Arrestin (Arrestin3) and Trβ2. High enrichment for cone-specific genes is shown in the GFP-positive versus the negative population.

yield of 5-15% of single live GFP-positive cells could be routinely achieved (Figure 5.4 e). These GFP-positive cells were purified and collected using FACS, with total RNA extracted from both the GFP-positive as well GFP-negative populations. Analysis of gene expression by qPCR in these two populations showed strong enrichment for cone-specific transcripts such as Arrestin3, S opsin and Trβ2 in the GFP-positive population (Figure 5.4 h). Collectively, these results show that the labelling of developing cone precursors by means of AAV viral vector-mediated delivery of a ConeOpsin.GFP reporter construct, allows for isolation of a large number of purified cone precursors at stages corresponding to the peak of rod precursor integration.

In our and other groups' experience a relatively high number of cells needs to be placed in the subretinal space to achieve optimal integration (reviewed in Jayakody et al., 2015). In the case of donor-derived rod precursors transplantation of $2x10^5$ of flow-sorted cells per retina gave the best outcome (Pearson et al., 2012). Similar numbers of mESC-derived rods were used to show their integration capacity (Decembrini et al., 2014; Gonzalez-Cordero et al., 2013). For the purpose of transplanting purified mESC-derived cone precursors we employed a papain-based dissociation kit, which gave good yields of viable retinal cells in a single cell suspension necessary for FACS. Using this dissociation method, ConeOpsin.GFP vector-infected aggregates yielded 5-15% GFP-positive cells of the single live cells obtained. Using a 24-well plate with each well containing around 12 aggregates cultured in suspension for dissociation, we could routinely obtain $5x10^5$-$1.5x10^6$ viable purified GFP-positive cells. A total of $2x10^5$ GFP-positive cells were transplanted as dual injections, with 10^5 cells injected into the superior and 10^5 cells injected into the inferior hemisphere of the retina, since injections into both hemispheres were shown to improve the outcome of rod precursor transplants (Pearson et al., 2012). This was found to be a reliable method of transplantation for cone photoreceptors as nearly all of the injected eyes contained surviving and integrated cells. This allowed a true assessment of the integration capacity of mESC-derived cone precursors.

5.6 Purified postnatal cone precursors transplanted into the adult retina survive, integrate and express mature cone markers

Eyes transplanted with a suspension of dissociated ConeOpsin.GFP-expressing cone precursors isolated between day 26 and day 30, approximately equivalent to P5-P10 *in vivo*, were examined for expression of cone markers using immunohistochemistry. As mentioned before, in the majority of transplanted eyes a subretinal cell mass was present (26 out of 29, 89.7%). These masses clearly stained for the cone markers PNA

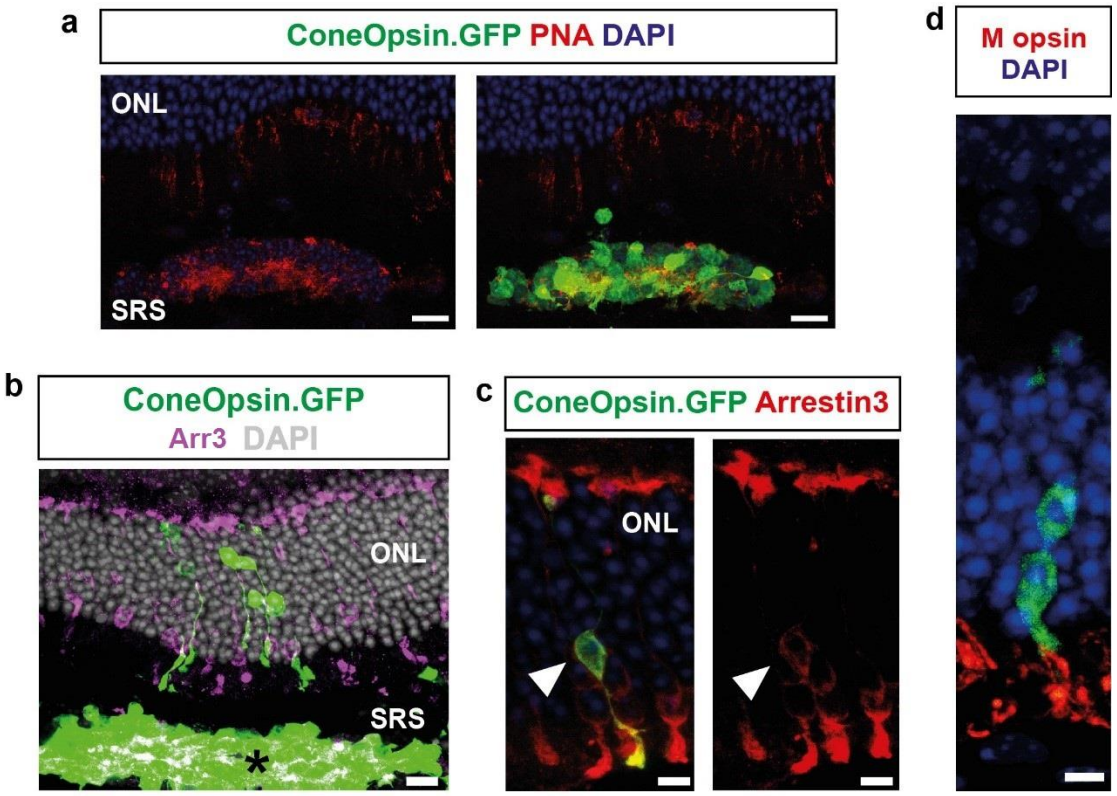

Figure 5.5. Cone precursors isolated from 3D mESC retinal differentiation cultures at a stage resembling early postnatal retina survive, integrate and express mature cone markers when transplanted into the adult mouse retina.

(a) Section showing a subretinal mass of surviving transplanted ConeOpsin.GFP-positive cells expressing the cone marker PNA (in red). Scale bar 20 µm. **(b)** Section showing the subretinal cell mass and integrated cells in the recipient ONL. Note expression of Cone Arrestin (Arrestin3) in the mass (white). Scale bar 10 µm. **(c)** Integrated cone cell immunostaining for Arrestin3 (in red). Arrow points to an integrated ConeOpsin.GFP-positive cell positive for Arrestin3. Scale bar 5 µm. **(d)** Integrated ConeOpsin.GFP-positive cells showing expression of M opsin in outer segments. Scale bar 5 µm. ONL – outer nuclear layer; SRS – subretinal space.

(Figure 5.5 a) as well as Arrestin3 (* in Figure 5.5 b). GFP+ cells were also found in the recipient outer nuclear layer where photoreceptors reside (Figure 5.5 b). These integrated cells were also examined for expression of cone markers. This showed that a proportion of the integrated cells matured to express Arrestin3 (Figure 5.5 c) and possessed outer segments positive for M opsin (Figure 5.5 d). To examine if the GFP-positive cells found following transplantation differentiated exclusively into cone photoreceptors, sections of the transplanted eyes were stained for the rod markers Rhodopsin and Rod α-Transducin (GNAT1). This analysis showed that subretinal masses of transplanted cones did not stain positive for Rhodopsin (Figure 5.6 a) nor did they show GNAT1 immunoreactivity (Figure 5.6 b). Likewise, in the *Nrl*$^{-/-}$ recipient, which lacks rod gene expression downstream of Nrl, GFP-positive cells did not show staining for GNAT1 (Figure 5.6 c). A small number of GFP-negative cells expressing GNAT1 was found, with very rare integrated ones showing rod-like morphology (arrows in Figure 5.6 c and higher power view). These occasional rod marker-expressing cells could come from rod precursor cell contamination of the sorted population (purity checks of populations sorted for transplantation routinely showed above 95% purity) or they could be a subset of cells that differentiated into rod photoreceptors and switched off the ConeOpsin.GFP reporter. Together these observations demonstrate that mESC-derived cone precursors isolated at postnatal stages are capable of integrating into the adult host photoreceptor layer and expressing mature cone markers, following subretinal transplantation.

5.7 Basal processes of integrated cone precursors contain synaptic proteins

Cone precursors transplanted at a stage equivalent to early postnatal retina, engrafted into the host photoreceptor layer and frequently demonstrated both apical as well as basal processes (Figure 5.6 a-c). Some of the basal processes were found within or in close proximity to the outer plexiform layer, where synapses between photoreceptors and interneurons are formed. To determine whether these processes show expression of proteins required for synaptic connectivity and transmission, immunohistochemistry was performed on sections of transplanted eyes for PNA, which marks the extracellular matrix surrounding the cone pedicle, ribbon synapse protein ribeye and synaptic vesicle marker synaptophysin. Larger basal extensions of integrated cells were found staining for PNA (Figure 5.7 a) as well as containing puncta of the structural component of the ribbon synapse ribeye (Figure 5.7 b). These extensions also stained positive for synaptophysin, a protein associated with synaptic vesicles. These observations suggest that integrated cells show basal processes ending with synaptic terminal-like

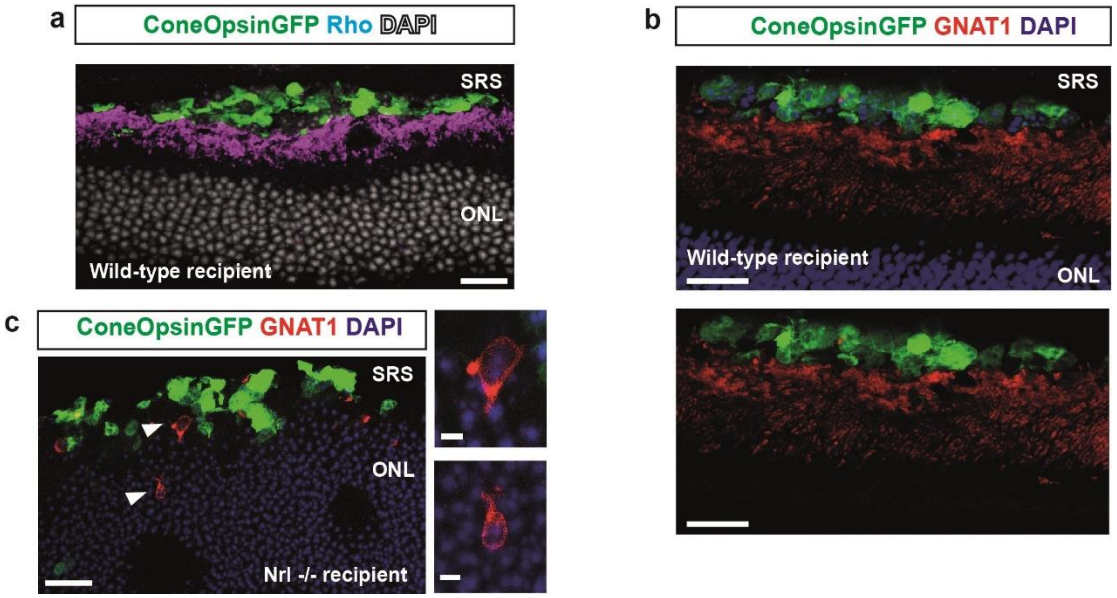

Figure 5.6. ConeOpsin.GFP-positive cells express cone but not rod markers following transplantation into the adult mouse retina.

(a) Section showing a mass of surviving transplanted ConeOpsin.GFP-positive cells in the subretinal space, negative for the rod marker Rhodopsin (magenta). **(b)** Subretinal GFP-positive cells do not show expression of Rod α-Transducin (GNAT1; red). **(c)** ConeOpsin.GFP cells transplanted into an *Nrl*$^{-/-}$ recipient do not show staining for GNAT1. A few GFP-negative cells express GNAT1, including one integrated cell (lower insert panel). Higher power view on the right. Scale bar 20 µm. ONL – outer nuclear layer; SRS – subretinal space.

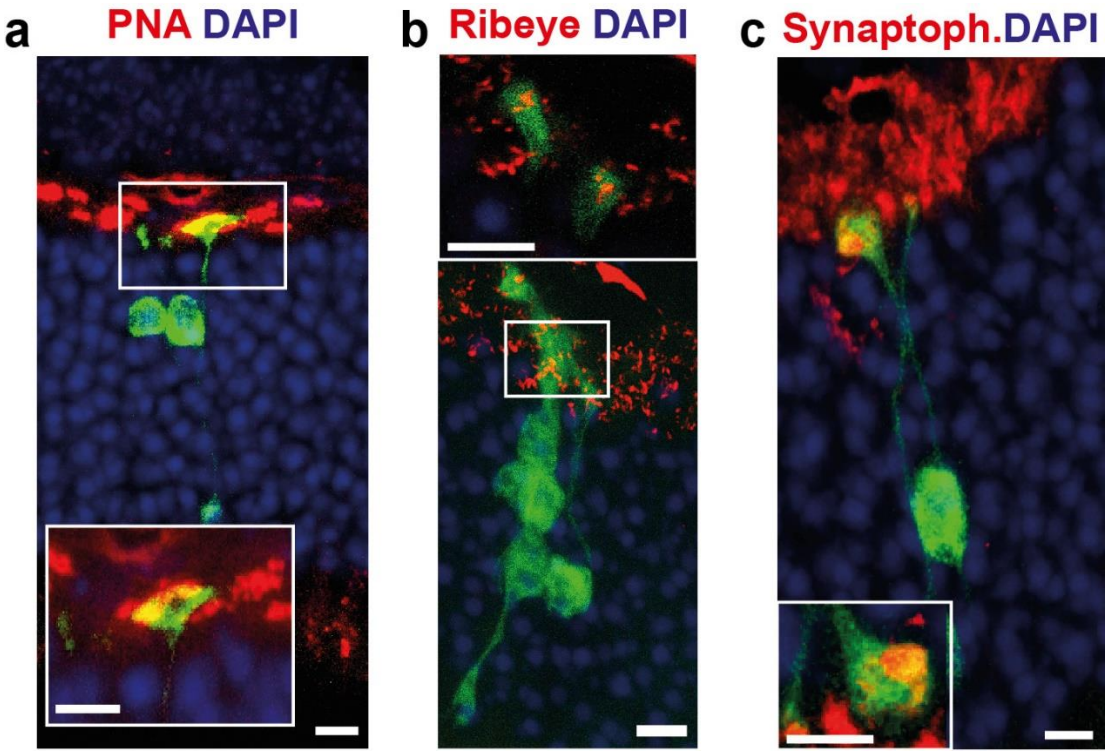

Figure 5.7. Integrated mESC-derived cone precursors extend basal processes positive for synaptic markers.

(a) Integrated ConeOpsin.GFP cell with a pedicle-like structure staining for PNA (in red) in a wild-type recipient. Scale bar 10 µm. **(b)** Cluster of GFP-positive integrated cells with basal neurites immunoreactive for ribeye (in red) in an *Nrl*$^{-/-}$ recipient retina. Scale bar 10 µm. **(c)** Synaptic terminal-like structure of an integrated cone co-localizing with synaptophysin (in red) in an *Nrl*$^{-/-}$ host retina. Nuclei stained with DAPI in all images (in blue). Scale bar 5 µm.

structures that contain structural components (ribeye, synaptophysin) associated with synaptic transmission as well as extracellular matrix associated with the cone synapse (PNA).

5.8 Cone precursor integration is enhanced in the rod-less retina of the *Nrl*$^{-/-}$ mouse

Previous studies from our group clearly demonstrated that the outcome of transplantation into wild-type and degenerate mouse retina is dependent not only on the donor population properties, but also on the features of the recipient retinal environment (Barber et al., 2013; Jayakody et al., 2015; Pearson et al., 2014). Little if anything is known about the impact of the host retinal environment on cone precursor integration. Transplantation of embryonic stage Crx:GFP photoreceptor precursors showed an elevated number of integrated cones in the cone-deficient retina of *Gucy2e*$^{-/-}$ mice, suggesting that a cone-depleted environment might be favourable to cone integration (Lakowski et al., 2010). However, the number of integrated cones in this study was very low and a mixed population of photoreceptors, although biased towards cones, was used. More recently, a study looking at the integration of cone-like cells derived from *Nrl*$^{-/-}$ mice showed a highly significant increase in the number of cells integrated into the *Nrl*$^{-/-}$ host compared to the wild-type recipient (Santos-Ferreira et al., 2015). Since integration into a cone-rich environment, such as the human macula is of interest from a clinical perspective, we performed experiments transplanting mESC-derived cone precursors into the *Nrl*$^{-/-}$ recipient animals. Subretinal cell masses were readily observed in all transplants into this mouse model (18 injected eyes) as well as integration of the transplanted cells. Interestingly, in the *Nrl*$^{-/-}$ recipients large numbers of cells were found to have migrated into the host outer nuclear layer in a columnar fashion (Figure 5.8 a and c). Quantification of the integrated cells showed a highly significant increase in the number of GFP-positive transplanted cone precursors found in the recipient photoreceptor layer following transplantation into *Nrl*$^{-/-}$ recipients, compared with wildtype mice (Figure 5.8 b; 1415 ±311 versus 466 ±86 in the wild-type; $p<0.0001$, Student's *t*-test). Closer examination of the clusters of integrated cells showed that they frequently formed a column integrating in between the columns of recipient photoreceptors (Figure 5.8 c) in a pattern resembling integration of rod precursors into models with disrupted outer limiting membrane (Barber et al., 2013; Pearson et al., 2010; West et al., 2008), the layer of tight junctions at the apical edge of the photoreceptor layer. Indeed deficits in outer limiting membrane integrity have been reported for the *Nrl*$^{-/-}$ mouse model (Mears et al., 2001). Together, these data demonstrate enhanced integration of mESC-derived cone precursors into a model of

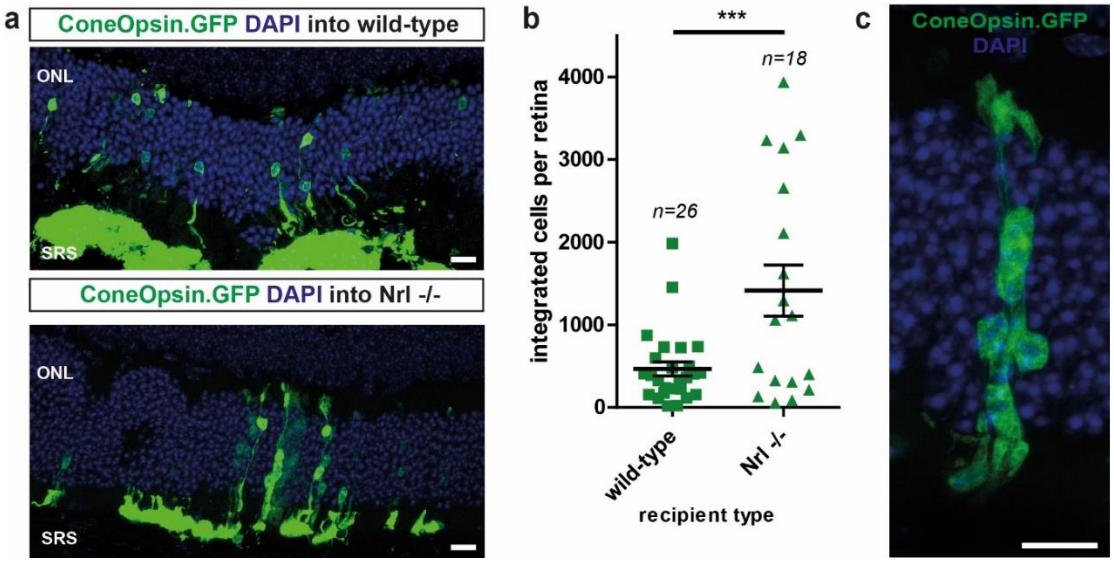

Figure 5.8. ConeOpsin.GFP-positive mESC-derived cone precursors integrate in higher numbers into the rod-less retina.

(a) Sections of wild-type (upper panel) and Nrl$^{-/-}$ recipients (lower panel) transplanted with ConeOpsin.GFP-expressing cells showing enhanced integration into the Nrl$^{-/-}$ host. ONL – outer nuclear layer; SRS – subretinal space. Scale bar 20 µm. **(b)** Quantification of the number of integrated cells in wild-type and Nrl$^{-/-}$ recipients. Note the significantly increased integration into Nrl$^{-/-}$ recipients (p<0.001 Student's t-test). **(c)** Cluster of integrated ConeOpsin.GFP-positive cells demonstrating columnar integration often observed in the Nrl$^{-/-}$ recipients. Scale bar 20 µm.

rod-less retina that could in part stem from compromised outer limiting membrane integrity.

5.9. Position and nuclear morphology of integrated cones within the host photoreceptor layer

Mouse cone photoreceptors are confined to the apical part of the photoreceptor layer and this position is a result of their migration to this location during postnatal development (Razafsky et al., 2012; Rich et al., 1997). Not only do the positions of cone and rod nuclei differ within the retina, their nuclear architecture also display different characteristics. Rod photoreceptors of nocturnal species such as mice show an unusual inverted chromatin architecture with a single condensed cluster of heterochromatin at the centre of the nucleus. Cone photoreceptors show typical nuclear morphology with several heterochromatin clumps called chromocenters (Solovei et al., 2009). To determine the positions and nuclear architecture of transplanted cone precursors we analysed sections of transplanted retinae with respect to the position of integrated cells within the outer nuclear layer and the morphology of their nucleus. As observed for integrated cone-like cells (Santos-Ferreira et al., 2015), many integrated cones were found scattered in between host rod cells in addition to the apical location characteristic of endogenous cones (Figure 5.9 a). The position of the integrated cells was counted as apical when their nucleus was within the first two rows of nuclei from the apical edge of the photoreceptor layer (Figure 5.9 a, arrowheads). Cells with nuclei located more basally were counted as 'dispersed' within the recipient photoreceptor layer (Figure 5.9 a). This quantification revealed that in the 15 transplanted retinae analysed 11.8%±9.2 of integrated nuclei were in the apical position, whereas the remaining 88.2%±9.2 were dispersed in more basal layers. Next, nuclear morphology of integrated cells was examined using confocal microscopy. Optical sections through the integrated nuclei were taken and analysed for the number of chromocenters present. Nuclei of precursors in the subretinal space typically showed three chromocenters in all transplants performed (Figure 5.9 c and d). However, the number of chromocenters in the integrated cells depended both on the type of donor population as well as on the recipient environment. Nearly all mESC-derived Crx.GFP precursors integrating into the wild-type recipient showed a single condensed nucleus (Figure 5.9 c and d) in accordance with most of the integrated cells being rods. Intriguingly, ConeOpsin.GFP-positive cells integrated into the wild-type recipient also showed a single chromocenter, whereas in the rod-less environment of the *Nrl*$^{-/-}$ retina these cells had typically at least two chromocenters (Figure 5.9 c and d). In conclusion, these results show that transplanted mESC-derived

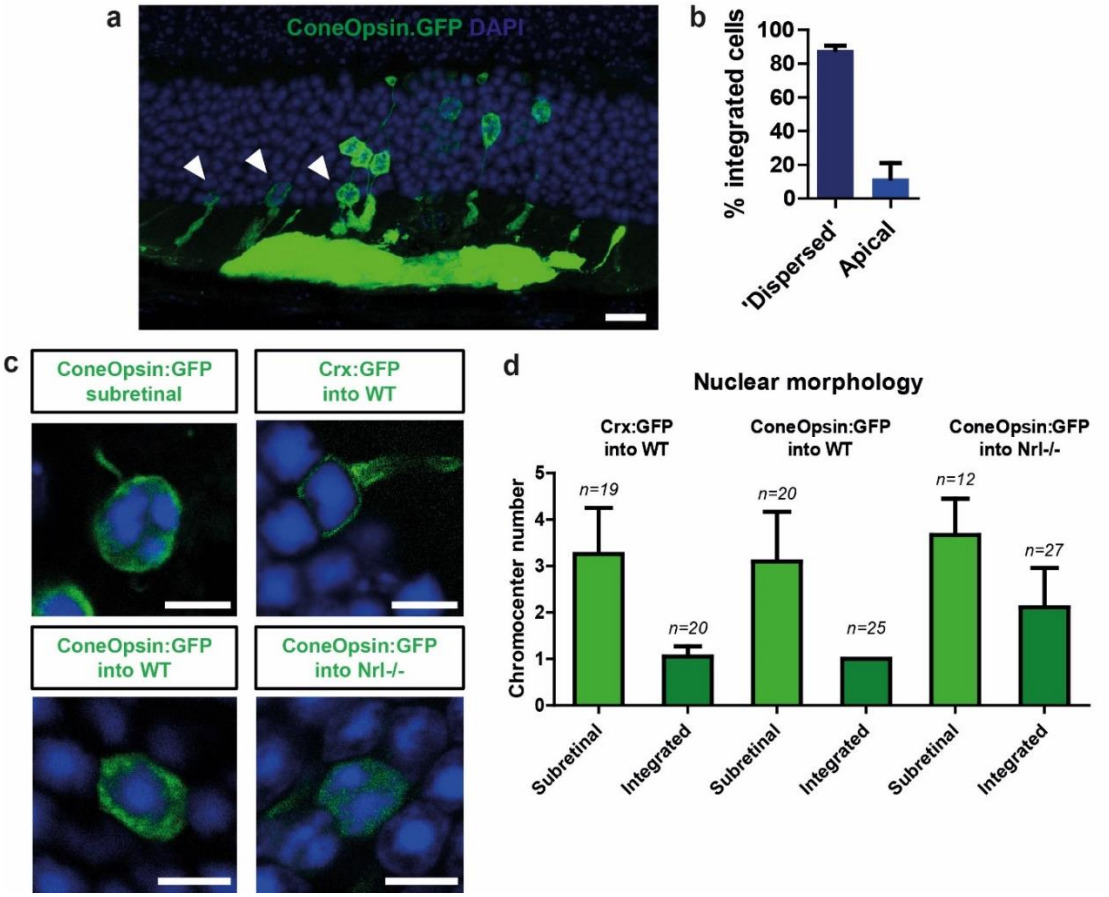

Figure 5.9. Cone precursors integrate throughout the host outer nuclear layer and the nuclear morphology of integrated cells depends on the donor cell type and the recipient environment.

(a) Section of a wild-type recipient transplanted with ConeOpsin.GFP-positive cells showing a region of integration. Note that GFP-positive cells integrate throughout the host photoreceptor layer. Arrowheads point to cells that assumed positions in the apical aspect of the outer nuclear layer. Scale bar 10 µm. **(b)** Quantification of integrated cell positions within the host photoreceptor layer. Cells were counted as 'apical' when within the two apical-most rows of photoreceptors. Cells in more basal locations were counted as 'dispersed'. Graph represents data from 15 transplanted eyes. Mean percentage ±SEM shown. **(c)** Representative examples of nuclear morphology of different populations following transplantation (DAPI in blue). Scale bar 5 µm. **(d)** Quantification of the number of chromocenters in the surviving transplanted cells. Please observe that cells in the subretinal space always exhibit around 3 chromocenters in their nucleus, whilst the number within integrated cells varies depending on the donor cell population and the recipient retina. Number of cells examined for each group noted above the bars.

cone precursors, similar to donor-derived cone-like cells, integrate throughout the host photoreceptor layer and display nuclear morphology analogous to the host environment.

5.10 Conclusions and discussion

Retinal degenerations that lead to the loss of photoreceptors are a leading cause of blindness in the developed world (Cruess et al., 2008; Owen et al., 2012; Rudnicka et al., 2015). Studies from both our and other groups (reviewed in Jayakody et al., 2015) have shown that replacing lost photoreceptors in a degenerate retina, by means of cell transplantation, is feasible and can restore visual responses driven by rods (Pearson et al., 2012). Due to the scarcity of the donor population in mice research looking at the transplantation of cone photoreceptor precursors has proved challenging and is not as advanced as that of rod precursors. However, taking advantage of mouse genetics, Ader and colleagues have shown that transplantation of cone-like cells from mice in which rod-determining transcription factor *Nrl* was genetically removed, led to levels of integration sufficient to observe light-evoked responses recorded from underlying ganglion cells in a retina lacking cone function (Santos-Ferreira et al., 2015). This demonstrates proof of concept that daylight vision repair is possible in mice. To date however, transplantation of a purified cone population derived from a renewable source has not been investigated. In recent years there has been tremendous progress in the use of stem cell technology to differentiate retinal cell types from pluripotent stem cells (Decembrini et al., 2014; Eiraku et al., 2011; Gonzalez-Cordero et al., 2013; Ikeda et al., 2005; Nakano et al., 2012; Osakada et al., 2008; Reichman et al., 2014; Zhong et al., 2014) that could provide a renewable and scalable source of cells for transplantation purposes. In particular a seminal study by the Sasai laboratory described a differentiation protocol showing retinal morphogenesis with optic vesicle and optic cup formation, very closely mimicking *in vivo* development (Eiraku et al., 2011). This advance in retinal differentiation methodology enabled the generation and transplantation of rod precursors, which were found to engraft into the host photoreceptor layer (Gonzalez-Cordero et al., 2013). In this chapter, we determined whether mESC-derived cone precursors, with properties resembling those of the developing retina, were capable of integrating into the adult host retina.

Crx is a transcription factor expressed in both rods and cones and essential for their proper differentiation, maturation and function (Furukawa et al., 1997). Examination of the genetic elements driving its expression *in vivo* enabled a mouse line, expressing a GFP reporter from the *Crx* locus, to be engineered using BAC technology (Muranishi et al., 2010; Samson et al., 2009). This reporter line was used in a transplantation

study, in which authors isolated GFP-expressing photoreceptor precursors at various stages of development (between E12.5 and P3) and observed infrequent integration of cone cells when the donor population was isolated from embryonic retina (E14.5-E17.5) (Lakowski et al., 2010). A Crx:GFP mESC line was generated from these mice by culturing the inner cell mass of transgenic mouse blastocysts (Decembrini et al., 2014). Moreover, rod photoreceptors differentiated from this line were shown to integrate when transplanted at the equivalent of postnatal stages (Decembrini et al., 2014). Here, we show that differentiation of this line according to our protocol (for details please refer to Chapter 1) allows us to recapitulate the competence of embryonic donor retina, to yield a very small number of integrated cone precursors, following subretinal transplantation. Similar to the Crx:GFP precursors isolated from transgenic mice at E17.5, GFP-positive cells isolated from day 16 of culture, a corresponding stage, showed strong enrichment for cone specific transcripts in comparison to the GFP-negative population. Following transplantation, these cells showed expression of cone markers in the subretinal cell masses as well as in rare integrated cells. These observations demonstrate that the capacity to engraft into the host adult retina is maintained in cone precursors generated by our 3D retinal differentiation system. However, it is worth noting that the number of integrated cells is much smaller in the mESC-derived transplants (less than 200 versus 500 on average), which suggests that either certain signals required for this behaviour are insufficient *in vitro* or that the preparation and purification of cells from this source is not optimal. Experiments improving the isolation and further in-depth quality assessment of both donor- and mESC-derived populations could help to address this question.

The study using Crx:GFP donor cells (Lakowski et al., 2010) as well as other studies from our and other groups (Decembrini et al., 2014; Gonzalez-Cordero et al., 2013; MacLaren et al., 2006; Pearson et al., 2012; Santos-Ferreira et al., 2015) showed that integration efficiency of photoreceptor precursors is dependent on the developmental stage of the donor population both in the case of cells isolated from donor mice as well as mESC-derived retinal tissue. This dependency is best studied for rod precursors, which show a peak of integration between P3-P9 (MacLaren et al., 2006; Pearson et al., 2012). Signals that determine this competency are currently unknown. One of the hypotheses put forward to explain this phenomenon is that enhanced integration capacity is correlated with the developmental stage at which photoreceptor nuclei position themselves within the maturing retina. Both cone and rod photoreceptors show migratory behaviour during the postnatal period prior to eye opening that occurs

approximately at P14 (Razafsky et al., 2012; Rich et al., 1997 and unpublished observations from the Ali laboratory). With respect to cone cells, their nucleus is positioned towards the apical edge of the outer nuclear layer just beneath the outer limiting membrane in the mature retina (Rich et al., 1997). During postnatal development, between P4 and P11, cone nuclei become scattered throughout the photoreceptor layer before assuming their mature position at the apical edge of the retina by P12 (Rich et al., 1997). In this study, we isolated mESC-derived cone precursors at developmental stages similar to this migratory phase and observed robust integration, with the number of integrated cone precursors (average of 466 integrated cells) comparable to that seen for mESC-derived rod precursors (Gonzalez-Cordero et al., 2013). These cells assumed positions scattered throughout the recipient photoreceptor layer, resembling the scattered locations of cone nuclei in the P4 to P11 retina, a stage similar to which they were isolated from, day 26-30 of differentiation culture. The developmental signals that trigger the movement of cone nuclei to their final locations are unknown at present. However, it appears that this positioning is dependent on Linkers of the Nucleoskeleton to the Cytoskeleton (LINC complexes), which span the nuclear envelope and connect it to the peripheral cytoskeleton (Razafsky et al., 2012). Regardless of the exact molecular mechanisms responsible for this migration, detailed histological analysis of postnatal rod precursor transplants revealed a stereotype sequence of morphologies adopted by integrating cells. Donor-derived rod precursors are proposed to migrate out of the subretinal cell mass, move through the interphotoreceptor matrix, arrive at close proximity of the outer limiting membrane, grow an apical process and translocate their nucleus through the outer limiting membrane, followed by growth of the basal process and basal migration of the nucleus into the host photoreceptor layer (Warre-Cornish et al., 2014). Morphologies very similar to those observed for rod precursor migration could also be observed in cone cell transplants, suggesting similarities in the mode of integration between these two cell types. The previous study, also suggested that migration in the apical direction within the host outer nuclear layer was unlikely to be occurring (Warre-Cornish et al., 2014). Therefore it seems that the adult retina might be devoid of signals required for appropriate localization of integrated cone nuclei, which could explain the scattered positions of integrated mESC-derived precursors presented here, as well as the same observation reported for transplanted cone-like cells from donor mice (Santos-Ferreira et al., 2015). Nevertheless, it is clear from the data presented in this chapter that the apparent integration of cone precursors is not limited to embryonic stages and that cone cells derived from mESC can integrate into the host adult retina,

when derived at stages equivalent to postnatal development, in a fashion similar to the integration of rod precursors.

An unusual location could be one explanation for the lower expression of mature markers in the integrated cells, as compared to the endogenous cone cells when examined by immunostaining (Figure 5.9). Moreover, examination of postnatal rod precursor transplants into mice lacking rod α-transducin (*Gnat1*$^{-/-}$, a model of stationery night blindness), one of the last phototransduction proteins to be expressed during the maturation of rods, showed delayed onset of expression in comparison with normal development, with only about half of the integrated cells being Gnat1-positive two weeks post transplantation. Only by 5-6 weeks had nearly all integrated rods switched on this marker (Warre-Cornish et al., 2014). A similar delayed onset of expression, relative to normal development, could provide an explanation for the weak cone arrestin staining observed in the integrated cone cells and that not all integrated cells were found to be positive for this marker at three weeks post-transplantation. Experiments examining the timecourse of cone marker expression following transplantation, including later timepoints, are needed to determine the temporal aspects of expression of mature cone markers following integration into the adult retina. Importantly, we haven't found expression of rod markers in transplanted cells that expressed ConeOpsin.GFP reporter in the subretinal space (Figure 5.6). Some degree of developmental plasticity has been reported in the developing retina with markers of rod and cone photoreceptors co-expressed in a small population of precursors at embryonic stages (Ng et al., 2011). This plasticity appears to be transient and restricted to the developing retina. Inducible deletion of rod-determining transcription factor *Nrl* showed that its genetic removal altered cell fate only at a specific time window, which is most likely restricted by acquisition of epigenetic marks stabilising the fate choice (Montana et al., 2013). Since we isolated cells from a developing retina and placed them in a mature environment, which could alter the course of their differentiation, examining expression of not only cone but also rod markers in the transplanted population was pertinent. The only cells that were found to express rod markers in the cone transplants did not show expression of the cone-specific reporter used and could result from impurities of the cell sort or switching off of reporter expression in a fraction of transplanted cells as a result of developmental plasticity.

Post-mitotic rod precursors transplanted into adult retina were found to form synaptic connections with retinal interneurons, bipolar and horizontal cells, and appeared morphologically very similar to those of endogenous host rod cells. Furthermore, these

connections were found to be functional, allowing transmission of visual signals into the V1 region of the visual cortex and mediating optokinetic head tracking responses and visually guided behaviour in a water maze test (Pearson et al., 2012). Transplanted cone-like cells also showed formation of terminals positive for pre-synaptic markers Bassoon and Synaptophysin, albeit their morphology was somewhat more reminiscent of rod synaptic connections. However, functional assessment using multi electrode arrays showed that these were functional synapses that passed visual stimuli on to interneurons and ganglion cells from which recordings were performed (Santos-Ferreira et al., 2015). In this study, we found that integrated cone precursors formed basal processes ending in synaptic terminal-like structures that stained positive for the synaptic vesicle marker synaptophysin and the structural component of the photoreceptor ribbon synapse ribeye (Figure 5.6). Additionally, co-localisation with PNA, which labels the extracellular matrix of the cone pedicle, was also found (Figure 5.6). The relatively low numbers of integrated cells did not allow us to perform functional assessments in this study and further optimisation to achieve higher levels of integration will be required to establish if the observed structures represent functional synapses. Examination of these synapse-like structures for the presence of additional components, characteristic of cone terminals (Nuhn and Fuerst, 2014), could also help to clarify how similar they are to host cone cell connections.

In order to integrate into the host retina, the transplanted photoreceptor precursors need to migrate out of the subretinal cell mass, cross the interphotoreceptor matrix and the outer limiting membrane to reach the outer nuclear layer and elaborate neurites forming outer segments and synaptic terminals (Pearson et al., 2014). The outcome of this process of integration is not only dependent on the developmental stage of the donor population, but also on the interaction of these cells with the recipient retinal environment. A study comparing integration of donor-derived rod precursors into six models of retinal degeneration demonstrated that these precursors could integrate even into severe degeneration models, but the number of integrated cells and their morphology were highly dependent on the etiology of the disease (Barber et al., 2013). Several critical features of the recipient environment that have an impact on integration efficiency were identified. In degenerating, retina Müller glial cells become activated and can form scar tissue, posing a physical barrier for integration. Activated müller glia can also produce extracellular matrix components that are deposited into the interphotoreceptor matrix and are known to inhibit axonal regeneration (Friedlander et al., 1994) and negatively affect integration (Pearson et al., 2010). The outer limiting membrane, which is formed between Müller cell processes and photoreceptor cells,

can become compromised in some retinal disease models (reviewed in Pearson et al., 2014). In this study, we found that the integration of cone precursors derived from mESCs is similarly affected by the host environment. Numbers of integrated cones were significantly higher in *Nrl*$^{-/-}$ animals and their nuclear morphology differed from that observed in transplants into wild-type mice. In addition, cells were observed integrating in columnar clusters in *Nrl*$^{-/-}$ retinas much more frequently than in wild-type recipients. All these differences can be explained by characteristics of the host environment. Firstly, the outer limiting membrane was found to be compromised in this mouse model (Mears et al., 2001). The outer limiting membrane might act as a physical barrier to the passage of transplanted cells from the interphotoreceptor matrix into the outer nuclear layer and it's reduced integrity has been shown to correlate with increased numbers of integrated cells (Barber et al., 2013; Pearson et al., 2010). Cells integrated in a column are often found to share their apical attachment at the level of outer limiting membrane. Therefore, small gaps or breaks in this structure are suggested to have allowed these cells to migrate inside forming a column (Warre-Cornish et al., 2014). Moreover, nuclear morphology of immature transplanted rods was also found to depend on the recipient environment. When cells isolated at early postnatal period were transplanted into age-matched recipients their nuclei showed slow maturation into a single central heterochromatin cluster with an average of 3 chromocenters still observed three weeks after transplantation (Warre-Cornish et al., 2014). However, the same donor cells placed into the adult retina underwent rapid condensation of chromatin over the course of integration, with a single chromocenter present as early as 48 hours post transplantation (Warre-Cornish et al., 2014). This is a very significant enhancement given that this process of nuclear maturation is only finished by around P28 *in vivo* (Solovei et al., 2009). The cone precursor transplants performed in this study showed a similar dependence on the host environment. Cone precursors isolated from mESC-derived retinae and transplanted into rod-dominant adult mouse eyes showed nuclear condensation unusual for this cell type. However, in the *Nrl*$^{-/-}$ rod-less retina the same donor population gave rise to integrated cells having more than two chromocenters much like typical cone cells. In all cases cells remaining in the subretinal space showed more than three chromocenters on average. In this way they differed from donor-derived rod precursor transplants, which tend to condense chromatin reducing the number of chromocenters even in the subretinal space (Warre-Cornish et al., 2014). The molecular mechanisms underlying the characteristic organization of the rod chromatin remain largely unknown. This feature is absent in genetic knockouts of key rod-determining transcription factors *Rorb* and *Nrl* (Jia et al., 2009; Mears et al., 2001). Loss of this characteristic also occurs when

two histone acetyltransferases p300 and CREB binding protein (CBP), which interact with photoreceptor transcription factor Crx, are genetically removed, suggesting that coupling of fate determining transcription factors with chromatin modifying enzymes is required (Hennig et al., 2013). Further insights into this regulation are needed to determine how central clustering of heterochromatin is triggered in transplanted cone and rod precursor nuclei, following transplantation into adult but not immature or rod-less retinae.

An alternative explanation for the observations regarding integrated cones position, cell soma and nuclear morphology could be that these cells arise from cell fusion between the subretinal cell mass and host photoreceptors. Many reports of transplanted stem cell *in vivo* differentiation and integration were later found to be in fact a result of fusion with the host tissue (Kemp et al., 2014). Typical cell fusion involves merging of two cells with their nuclei. The nuclei may remain as separate entities for many weeks if the process involves mature cells (Alvarez-Dolado et al., 2003). Cell fusion is fairly common when a stem cell is involved, however, it is very rare between two differentiated post-mitotic cells (Kemp et al., 2014). Indeed, subretinal transplantation of hematopoietic stem cells led to the observation of frequent cell fusion events with the host retina (Sanges et al., 2016). Studies transplanting photoreceptor precursors have addressed this issue using two experimental techniques (Bartsch et al., 2008; MacLaren et al., 2006). Firstly, donor animals were injected with BrdU to introduce permanent nuclear labeling of donor cells. When photoreceptor precursors from these animals were transplanted examples of BrdU+ cells in the host outer nuclear layer were found. These were rather infrequent, perhaps not surprisingly given that only a proportion of donor cells incorporated BrdU (MacLaren et al., 2006). Secondly, a combination of distinct fluorescent reporters expressed by donor and host cells were used to determine the merging of their cytoplasmic content. These analyses showed that a proportion of integrated cells showed clear presence of one but not the other reporter (Bartsch et al., 2008; MacLaren et al., 2006). Given the limitations of the two techniques, it will be of importance to further investigate the identity of these GFP+ cells. Fusion with host rod cells could explain the location of the GFP+ cells in cone transplants throughout the host outer nuclear layer rather than being confined to the apical most row of photoreceptors (Figure 5.9 a and b), which is a normal characteristic of wild-type mouse cones. Additionally, this would provide an explanation for the chromatin features resembling host tissue rather than donor cells with condensed chromatin observed in the GFP+ cells in the outer nuclear layer of wild-type mouse recipients, a

typical feature of rods rather than cones, and the multiple chromocenters present in *Nrl*$^{-/-}$ animals, in which nuclear condensation does not occur (Figure 5.9 c and d). Whilst cells containing two nuclei were never observed in photoreceptor precursor transplants most likely excluding typical nuclear fusion (MacLaren et al., 2006), less common mechanisms of cell fusion involving cytoplasm transfer cannot be ruled out at this point.

The ultimate goal of cell replacement therapy is to restore useful vision to a degenerate retina. Rod precursor transplantation studies proved that by identification of an optimal developmental stage of the donor population (MacLaren et al., 2006) and optimisation of delivery techniques it was possible to achieve restoration of visually guided behavior in a model of stationery night blindness (Pearson et al., 2012). Here, we examined integration of a mixed photoreceptor population with a proportion of cone precursors, isolated at stages corresponding to embryonic retina and purified cone precursors at a stage equivalent to the postnatal eye. The latter population showed higher integration potential demonstrating that cone precursors at postnatal stages are apparently capable of integration into the recipient photoreceptor layer with expression of mature markers. However, the number of integrated cells is relatively low. This is not surprising given the source of these cells. Rod precursors derived from mESCs showed only modest integration of around 500 cells, as compared with up to 30,000 cells achieved with the donor-derived rod precursors (Pearson et al., 2012). High levels of integration are needed for reliable assessment of their functionality. Around $3x10^4$ integrated rods are required for visually guided behavior under scotopic light conditions in a water maze-based test (Pearson et al., 2012). The number of functional cells required for reliable detection using an electroretinogram (ERG), which measures the electrical activity of photoreceptors and bipolar cells across the whole retina, is even higher with clear signals observed from ~$15x10^4$ but not ~$6x10^4$ functional cells (Pearson et al., 2012). For this reason, no data sets showing clear robust responses from transplanted cells have so far been obtained using this measure. Emergence of new technologies to assess the functionality of transplanted cells might facilitate determining the functionality of smaller numbers of integrated cells. Multi electrode arrays (MEA), that measure electrical activity of retinal ganglion cells placed in close proximity, allowed detection of light-evoked responses at high light intensities (photopic conditions) from transplanted cone-like cells, with an average integration efficiency of around 1000 cells. This might not be that surprising, given that the absolute number of cones in the rodent retina is quite small (around $2x10^5$). Even so, the number of integrated cells obtained with mESC-derived cone precursors in this study is still only a half of that (less than 500, versus over 1000) and therefore functional assessments were not

performed, in recognition that further streamlining of the transplantation procedure is necessary for those experiments to be successful.

In conclusion, the data sets presented in this chapter demonstrate that integration-competent cone precursors can be generated by 3D retinal differentiation culture of mESCs. This advance has enabled the purification of a cone precursor population at a postnatal stage of development, which has not been achieved using donor mice to date. Cone precursors isolated from mESC-derived retinae at early postnatal stages, similar to the optimal stage for rod precursor integration, were found to express mature cone markers and extend basal processes co-labeling for synaptic markers, following transplantation to the adult retina. Furthermore, integration of these cells is significantly enhanced when transplanted into a rod-less retina. These findings open new avenues for daylight vision repair studies providing a renewable source of donor cells.

IV. Significance and perspectives

IV. I. Modelling development using stem cell-derived organoids

Biological systems exhibit an astounding potential for self-organization, as an example a fertilized egg can give rise to a complex multicellular organism through a stereotypical sequence of progressive cell lineage restriction and specification. Developmental biologists have studied this remarkable self-organisation capacity for decades. In the early classical studies using embryonic chick tissues, organs were dissociated and re-aggregated *in vitro*. Results of these experiments show that cells of multicellular organisms spontaneously form clusters with similar properties to the organ they derive from. In the case of dissociated chick kidney for instance nearly complete renal development can be achieved in re-aggregated tissue (Weiss and Taylor, 1960). Two mechanisms appear to contribute to this phenomenon (Lancaster and Knoblich, 2014a). Firstly, cells with similar adhesive properties segregate into separate domains. Secondly, progenitor cells make spatially and temporally restricted cell fate decisions. An excellent example of the latter mechanism is the cell fate specification in the vertebrate retina (Livesey and Cepko, 2001). Neuroepithelial progenitors of the developing retina generate the neurons and glia forming three retinal laminae in an evolutionarily-conserved birth order and in a spatially-dependent manner (Bassett and Wallace, 2012; Cepko, 2014; Livesey and Cepko, 2001; Swaroop et al., 2010). Indeed, re-aggregation of chick retina older than E6 does not yield lamina formation (Vollmer and Layer, 1986), showing that apart from cell sorting out also sequential, spatially-restricted specification is key.

These fundamental mechanisms of organ development formed a basis for induction of organ formation from stem cells cultured *in vitro*. Advent of modern stem cell biology started with isolation from the blastocyst inner cell mass and establishment of *in vitro* culture of mouse embryonic stem cells by Evans and Martin in the early 1980s (Evans and Kaufman, 1981; Martin, 1981). These seminal studies showed that clusters of embryonic stem cells (termed embryoid bodies) differentiate into cells of the three germ layers following addition of exogenous factors such as serum (Evans and Kaufman, 1981; Martin, 1981). Injection of undifferentiated stem cells into immunologically compromised mice leads to formation of tumours called teratomas. Teratomas contain organised tissues including nervous tissue, gut, epidermis, bone as well as eyes (Sergi et al., 1999). Eyes formed in teratomas demonstrate latent self-organisation potential of embryonic stem cells to generate retinal tissue when an appropriate programme of development is initiated. Much effort has been devoted into directing differentiation of

pluripotent stem cells into retina formation (Eiraku et al., 2011; Ikeda et al., 2005; Osakada et al., 2008). Embryoid body aggregates can undergo initial development much like a pre-gastrulation embryo (Lancaster and Knoblich, 2014a), therefore presenting an appropriate starting material for retinal induction. Culture of embryoid bodies under low growth factor conditions with addition of Matrigel basement membrane components enabled formation *in vitro* of retinal neuroepithelia, which evaginated into an optic vesicle and undergone further morphogenesis into bi-layered optic cups (Eiraku et al., 2011).

In this study, we utilised this method to investigate the formation of a rare retinal neuron the cone photoreceptor as part of retinal tissue morphogenesis. During equivalents of embryonic retinal development *in vivo*, between day 12 and 20 in culture, we found expression of transcription factors Onecut1, Olig2 and Otx2 associated with retinal progenitors biased towards generation of cone precursors (Figure 1.1). This is followed from day 12 of differentiation by appearance of early cone precursors expressing the nuclear receptor Trβ2 (Figure 1.4), a direct transcriptional target of Onecut1 and Otx2 (Emerson et al., 2013). The proportion of neural retina cells that cone precursors constitute increases substantially from day 12 to around day 20, from when it remains at around 17% until at least day 26 in culture (Figure 1.4). Cone precursors develop further to express phototransduction-related proteins S opsin and Arrestin3 (Figure 1.5), recapitulating *in vivo* cone photoreceptor development. Therefore the temporal sequence of cone genesis in the mouse is reproduced by appropriate induction of a self-organisation programme in mESCs *in vitro*.

Having observed robust cone genesis with a proportion of cone precursors likely exceeding that of the developing retina (Figure 1.5), we also examined whether their development is modulated by signalling pathways relevant for *in vivo* photoreceptor differentiation (Chapters 2 and 4). We found that Notch signalling limits photoreceptor production in retinal progenitors as *in vivo* and its timely inhibition when Trβ2-expressing cone precursors rise in abundance leads to increased numbers of cone cells that further develop expressing mature markers S opsin and Arrestin3 (Chapter 2). The maturation process is influenced by levels of retinoic acid. Expression analysis of retinoic acid synthesis enzymes *Raldh1* and *Raldh3* suggest that this molecule is generated in high amounts early in retinogenesis *in vitro*, similarly to the neural retina within the developing mouse. Transcription of genes encoding these two enzymes diminishes at photoreceptor maturation stage and a corresponding decrease in the levels of retinoic acid is required for proper induction of both S opsin and Arrestin3, genes associated with cone maturation (Chapter 4). These observations demonstrate

that the differentiation of cone cells in retinae generated *in vitro* from mESCs is guided by developmentally-relevant signalling pathways.

An important limitation, observed in many pluripotent stem cell-derived organoids, is poor functional maturation of the tissue. Photoreceptors differentiated *in vitro* using this system do not spontaneously grow outer segment structures (Gonzalez-Cordero et al., 2013) nor do they show light sensitivity (Sasai laboratory, personal communication). However, these cells possess the potential for biogenesis of outer segments in this setting since overexpression of the members of a sensory organ-specific miRNA cluster miR-182 and miR-183 leads to extension of distal structures reminiscent of developing outer segments (Busskamp et al., 2014). Nevertheless, at late stages in culture mouse neural retina *in vitro* deteriorates losing lamination and forming rosettes (Decembrini et al., 2014; Gonzalez-Cordero et al., 2013 and Figure 1.5). Development of brain organoids was improved by the use of a spinning bioreactor through enhanced nutrient and oxygen delivery (Lancaster and Knoblich, 2014b; Lancaster et al., 2013). Similarly, high oxygen conditions seem to be more conductive for healthy differentiation of mouse retinal organoids (Decembrini et al., 2014). Notably though, long-term culture of human iPSC-derived optic cups resulted in formation of outer segment-like structures and detection of light-evoked responses (Zhong et al., 2014). In conclusion, pluripotent stem cells can be directed *in vitro* to reproduce the development of retina to an onset of functionality stage via induction of an intrinsic self-organisation potential.

IV.II. Retina as a model for study of cell lineage specification

Since the pioneering work of the Spanish neurobiologist Santiago Ramón y Cajal at the end of the 19th century histologically describing stereotypical morphologies and orderly laminar organisation of retinal neurons, the retina has been extensively used as a model system for studying neurogenesis (reviewed in Bassett and Wallace, 2012; Cepko, 2014; Livesey and Cepko, 2001; Swaroop et al., 2010). Several features of the retina facilitate its use in this type of studies. Firstly, retinal cells are organised into three distinct cellular layers with two synaptic layers in between. Secondly, a relatively small number of classes of retinal neurons and glia exhibit stereotypical tissue locations and morphologies and therefore the different cell types can be easily identified. Furthermore, the retina is an accessible part of the central nervous system and its function can be assessed by an array of standardized tests (Livesey and Cepko, 2001; Swaroop et al., 2010). Classical lineage tracing studies conducted in the 1980s using infection with retroviruses and intracellular tracers have shown that retinal progenitor cells are multipotent producing clones of varying size containing all retinal

cell types (reviewed in Cepko, 2014; Livesey and Cepko, 2001). However, retinal neurons are born in an evolutionary conserved order and as retinogenesis progresses the choice of progeny becomes restricted (reviewed in Bassett and Wallace, 2012; Cepko, 2014; Swaroop et al., 2010; Zagozewski et al., 2014). Several models of lineage commitment have been proposed to explain these observations, including early patterning of progenitors as well as involvement of extrinsic or stochastic mechanisms (please see Introduction for details; Cepko, 2014).

We investigated cone photoreceptor specification using a mESC-derived retinal organoid tissue culture model system. We observed a temporal sequence of commitment to the cone lineage mimicking the *in vivo* process with initial expression of transcription factors Onecut1, Otx2 and Olig2 which bias retinal progenitors to the generation of cone precursors, followed by increasing number of early post-mitotic cone cells expressing Trβ2 (transcriptional target of Onecut1 and Otx2; Chapter 1). As *in vivo*, commitment to the photoreceptor lineage is limited by Notch activity (Chapter 2). These cells subsequently showed further markers of cone specification such as S opsin and cone arrestin, expression of which is regulated by retinoic acid signalling (Chapter 4). Collectively, these observations demonstrate progressive differentiation towards the cone lineage resembling that occurring *in vivo*. They also highlight the utility of this tissue culture system for study of retinal cell fate specification in a simple and efficient manner *in vitro,* potentially allowing to reduce the use of laboratory animals for basic research.

Differentiation of photoreceptor cells is a complex process in which both intrinsic genetic factors as well as extrinsic signalling molecules participate in not fully understood ways (Cepko, 2014; Forrest and Swaroop, 2012; Swaroop et al., 2010). Derivation of retinal organoids from mESCs offers a simplified system to examine both soluble and genetic factors affecting retinal lineage specification. Soluble factors or pharmacological agents can be dissolved in the culture media and added to the organoids at specific stages of development. Here we show proof-of-concept for such use by determining the inhibitory effect of high concentrations of retinoic acid on cone precursor maturation (Chapter 4). Also, pharmacological inhibitors of Notch signalling DAPT and RO4929097 were used to establish the role of Notch activity in inducing non-photoreceptor cell fates and temporal restriction of cone genesis in culture to stages equivalent to pre-natal retina (Chapter 2). Actions of intrinsic regulators can be interrogated by overexpression/knockdown experiments using viral vectors targeting progenitors and/or post-mitotic photoreceptor cells. In this work we took advantage of the characteristics of lentiviral and AAV vectors in this context. Forced expression of

Onecut1 using a lentiviral vector at day 9, an early stage of retinal differentiation when majority of the cells in the mESC-derived retina are proliferating progenitors, resulted in the formation of relatively small clusters of transduced cells containing an increased proportion of horizontal cells. Post-mitotic photoreceptor precursors were transduced using AAV vectors. We determined that the ShH10 viral serotype obtained using a directed-evolution approach (Klimczak et al., 2009) infects mESC-derived retinal tissue more efficiently compared to 2/2, 2/5, 2/8, 2/8Y(733) or 2/9 serotypes (Chapter 3). Use of AAV vectors allowed to examine how the binary rod versus cone photoreceptor cell fate choice is dependent on the expression levels of the rod-determining transcription factors Nrl and Nr2e3, through the use of *Nrl* and *Nr2e3* knockdown constructs (Chapter 3). Significant reduction in expression of both of these transcriptional regulators did not lead to increased expression of *Thrb2* or *Rxrg*, genes associated with early post-mitotic cone precursors (Chapter 3). This suggests that induction of each of the photoreceptor cell fates occurs at a very early stage in their differentiation, possibly in the terminally dividing retinal progenitor cells as suggested by recent studies (Emerson et al., 2013; Hafler et al., 2012). Moreover, some level of plasticity was identified with increased expression of S opsin following *Nrl* and *Nr2e3* knockdown (Chapter 3). Taken together, these results demonstrate that various aspects of commitment to the photoreceptor lineage can be examined using synthetic mouse retinae derived from ESCs.

The findings presented in this work open new avenues for further study of cone photoreceptor differentiation. To date this was a very challenging task because cone cells constitute only a small fraction of photoreceptors in most mammals. For instance, insufficient quantities of starting material hindered detailed examination of the effects of soluble factors on cone development. We demonstrate that this limitation can be partially overcome by the use of mESCs retinal differentiation cultures as a convenient tissue culture model. As shown here, these cultures can provide valuable insights into the modulators of the lineage commitment and maturation of this type of neuron. Such investigations can also add to the broader question of how the diversity of functionally specialised neuron types is generated in the central nervous system.

IV.III. Understanding human retinal development

Concomitantly with the progress in development of organoid systems using mESCs also significant achievements have been made with hESCs and relatively recently generated human iPSCs (Cramer and MacLaren, 2013; Jayakody et al., 2015; Lancaster and Knoblich, 2014a). In particular, differentiation protocols for derivation of retinal tissues from hESCs and iPSCs have been established and optimised

(Kuwahara et al., 2015; Lamba et al., 2006; Meyer et al., 2009; Nakano et al., 2012; Osakada et al., 2008; Reichman et al., 2014; Zhong et al., 2014), so that advanced photoreceptor maturation with expression of multiple components of the phototransduction cascade, biogenesis of outer segments and onset of light sensitivity have been achieved (Zhong et al., 2014). Establishing such protocols, faithfully recapitulating *in vivo* retinal organogenesis, allows more in-depth study of human retinal development, to date limited by the short supply and often poor quality of human retinal tissue at revelant stages. Several aspects of the work presented in this dissertation could inform such future studies. Firstly, the function of retinoic acid as a temporal signalling molecule during retinal development in zebrafish and mice could extend to humans. Indeed there is already some indication that retinoic acid has stage-dependent effects on human photoreceptor differentiation (Zhong et al., 2014). More detailed analysis including examination of both rod and cone photoreceptor phenotypes might be informative for creating an appropriate environment for proper differentiation and maturation of human photoreceptors for use in disease modelling and cell transplantation. Also the function of the Notch signalling pathway appears to be evolutionarily conserved. The data suggesting cone photoreceptor enrichment following pharmacological Notch inhibition (Chapter 2) could prove useful for increasing or synchronising development of human cone precursors. Early observations using the human retinal organoid system suggest that application of the Notch signalling inhibitor DAPT could increase expression of certain cone markers in this context (Reichman et al., 2014). Moreover, from a translational research perspective, methodologies developed in this study could be informative for isolation and transplantation of hESC/hiPSC-derived cone precursors. Specifically, the 2.1 kb fragment of the human red-green cone opsin promoter (ConeOpsin.GFP in this study) can provide a suitable reporter for isolation of human cone precursors for subsequent study and transplantation. It could also facilitate identification of cell surface molecules characteristic of developing cone precursors. In addition, the dissociation protocol optimised for cone isolation from mouse retinal organoids should be easily adaptable for purification of human cone precursors. In conclusion, insights from the study of cone differentiation in the mouse retinal organoid system could inform the use of human retinal organoids to model development, disease and establish cell therapy approaches.

IV.IV. Prospects for cell therapy in treatment of retinal degenerations

Inherited and sporadic retinal degenerations constitute the main cause of blindness in developed countries (Cruess et al., 2008; Owen et al., 2012; Rudnicka et al., 2015). Diseases of various aetiologies converge on photoreceptor and/or RPE cell death as the common outcome at late stages (Owen et al., 2012; Rudnicka et al., 2015). Since these conditions severely impair life quality as well as being associated with a high economic burden (Cruess et al., 2008), there is significant interest in developing strategies to not only maintain but also improve vision in these pathologies. Less than two decades ago human embryonic stem cells were derived opening new opportunities for development of cell-based therapies (Thomson et al., 1998). These pluripotent cells potentially offer an inexhaustible source of donor cells that could be differentiated into desired tissues, providing that appropriate protocols are developed and validated for clinical use (Borooah et al., 2013; Jayakody et al., 2015). In ophthalmology, clinical translation has been so far achieved for RPE cells (Schwartz et al., 2012). In the first-in-man clinical trial of hESCs-derived cell therapy approach Lanza and colleagues aimed to assess the safety and tolerability of hESC-derived RPE cells injected subretinally in Stargardt's macular dystrophy and dry age-related macular degeneration (Schwartz et al., 2012). The investigators did not find any signs of teratoma formation, hyperproliferation, abnormal growth or immune rejection up to 4 months post-transplant. Structural evidence demonstrated cell attachment and persistence in one of the two subjects during the study period. Taken together, these results show promise that hESC-derived cells can be safely injected into adult human eyes without immediate major adverse effects.

Rapid developments in the field of RPE differentiation and transplantation are partially due to its nature as a flat monolayer of a single cell type facilitating differentiation and maintenance in common tissue culture systems. Photoreceptors develop in a much more complex three-dimensional tissue environment and appropriate morphogenesis is critical in recapitulating photoreceptor differentiation niche (Gonzalez-Cordero et al., 2013; West et al., 2012). Recent years, however, have seen major advances in 3D tissue culture systems (Marx, 2013) and protocols to differentiate organoids from pluripotent stem cell sources that show many features of native organs (Lancaster and Knoblich, 2014a). A major breakthrough in the eye field came with development of a protocol to derive optic cups in 3D culture of mESCs (Eiraku et al., 2011). Subsequently this led to the differentiation of light-responsive photoreceptors from human iPSCs (Zhong et al., 2014), paving the path towards clinical translation.

In this study, we closely examined differentiation of cone photoreceptors in such 3D organoid cultures. We observed near normal differentiation of cone precursors regulated by developmentally-relevant signalling pathways. The main differences observed between the *in vitro* and *in vivo* cone development are the lack of M opsin induction in mESC retinal differentiation and absence of outer segments (Chapter 4 and 1, respectively). This does not preclude the use of this system for transplantation studies since immature post-mitotic photoreceptor cells before the onset of outer segment biogenesis were found to functionally engraft (Gust and Reh, 2011; MacLaren et al., 2006; Pearson et al., 2012; Santos-Ferreira et al, 2015; Singh et al, 2013). Similarly, in the clinical trial of hESC-derived RPE cells immature lightly pigmented cells were selected for transplantation into patients (Schwartz et al., 2012).

Scarcity of cone cells in the donor mouse retina precluded proper examination of the transplantation potential of cone cells (Lakowski et al., 2010; Santos-Ferreira et al., 2015; Smiley et al., 2016). In this study we optimised methodologies for efficient isolation of cone precursors, which are abundant in mESC-derived retinae, in large quantities that allowed assessment of their transplantation potential into wild-type and cone-like cell-rich adult mouse retinae (Chapter 5). We observed high numbers of GFP-positive cells in the host outer nuclear following transplantation of cone precursors isolated at an equivalent of the second post-natal week *in vivo*, with numbers of "integrated" cells similar to those of mESC-derived rod cells (mean of 466 ±86 cells versus 420 ±98 cells per retina). This process was further enhanced in *Nrl*$^{-/-}$ model of rod-less retina (466 ±86 cells versus 1415 ±311 cells per retina). Cone precursors in this work were isolated at a stage when they naturally exhibit nuclear migration (Rich et al., 1997), which could have contributed to this relatively high efficiency. High numbers of GFP-positive cells found in recipient outer nuclear layer in the transplants from the postnatal-equivalent stages were in contrast to relatively low "integration" (mean of 182 ±39 cells per retina) of a mixed population enriched for cone precursors at day 16 of differentiation, corresponding to late embryonic retina (Chapter 5). This observation is in accordance with the published work using cells isolated from a donor mouse harbouring the same Crx:GFP reporter (Lakowski et al., 2010). Many more such cells were observed with donor-derived cone-like cells isolated at neonatal stages with numbers further increased in the *Nrl*$^{-/-}$ model (Santos-Ferreira et al., 2015). Hence, the behaviour of mESC-derived cone precursors in the context of transplantation appears to resemble that of donor-derived cell populations adding support to the conclusion that retinal differentiation of mESCs can provide a renewable, expandable and scalable source of cells for development of cell therapies for daylight

vision loss. Our results are an important step in pre-clinical research into development of such cell therapy. Transplantation of donor-derived rod photoreceptors was sufficiently effective to restore vision in a model of night blindness in mice (Pearson et al., 2012) and proof of concept for restoration of cone-mediated responses was provided using cone-like cells (Santos-Ferreira et al., 2015). Nevertheless, a robust source of cone cells, identified in this study, is key for further development of this strategy, since human vision is primarily dependent on cone cells.

Mechanisms responsible for retinal repair following transplantation of photoreceptor precursors are still poorly understood (Jayakody et al., 2015; Pearson, 2014). It is hypothesised that a fraction of the transplanted cells exhibits unusual migratory behaviour undergoing a stereotypical sequence of morphologies before attaining their final location (Warre-Cornish et al., 2014). Of note, photoreceptors during *in vivo* development do not show typical motility, but they do perform nuclear migration within the tissue (Rich et al., 1997). In our experiments we found that isolated cone precursors at equivalents of this migratory phase efficiently generate GFP-positive cells in the host photoreceptor layer in a manner and number similar to rod photoreceptor precursors at the same stage (Chapter 5). As in the case of donor-derived cones (Smiley et al., 2016) and cone-like cells (Santos-Ferreira et al., 2015) these were found scattered throughout the recipient photoreceptor layer rather than aligned at the apical edge as the host cones and showing rod-like morphologies (Chapter 5). In contrast to a recent report (Smiley et al., 2016) we did occasionally find expression of cone arrestin in these atypically localized cells (Chapter 5). The unusual morphology of the GFP-positive cells in the host outer nuclear raised concerns whether these really represent integration or could arise from fusion with recipient photoreceptors (Smiley et al., 2016). Nuclear fusion can be excluded in this context since cells with two nuclei were never observed in this study, previous studies by our group and studies by other groups and nuclear fusion is not reported to occur between two post-mitotic cells (Jayakody et al., 2015). Moreover, there is evidence that at least some integration events do occur in the form of BrdU-labelled donor cells present in the host outer nuclear layer (MacLaren et al., 2006). Furthermore, live imaging studies recently performed in the Ali group show evidence of migration from the cell mass into outer nuclear layer in explanted retinae (Pearson et al., 2016). Additional studies performed at the time of completion of this manuscript determined that in the rod precursor transplants the majority of GFP-positive cells observed in the recipient outer nuclear layer are a result of uptake of cellular components from the subretinal cell mass. Three techniques provided particularly strong evidence for this process. Firstly,

GFP-labelled cells were transplanted into dsRed-expressing hosts followed by analysis by flow cytometry. This showed that the great majority of GFP-positive cells isolated from the recipient retina were also dsRed-positive (Appendix A and Pearson et al., 2016). Secondly, male donor cells were transplanted and presence of the Y chromosome examined in the outer nuclear layer by fluorescent *in situ* hybridization. Most of the GFP-positive cells were found to lack the Y chromosome signal. Thirdly, donor cells expressing Cre recombinase were injected into transgenic mice harbouring a floxed tdTomato reporter cassette. Activation of the tdTomato reporter was observed in a large number of cells in the host photoreceptor layer in these experiments (Pearson et al, 2016). Together, these observations demonstrate transfer of protein from the subretinal rod precursor cell mass as a major mechanism generating cells previously thought to have migrated and integrated from the graft. Those results strongly suggest that an analogous process occurs following cone transplantation and current research in the Ali group is testing this hypothesis. Exosomes are small membrane-enveloped vesicles released from cells that can carry a variety of cellular components between different cell types including neurons (Kawikova and Askenase, 2015). Conceivably, exosomes could transfer material from the subretinal cell mass to the host photoreceptors, however, how only sparse, single cells could show their uptake is difficult to explain. Nevertheless, the biological mechanism of material transfer from the transplanted cells warrants further investigation.

Whilst discovery of material transfer from the rod precursor subretinal cell mass to the host photoreceptors necessitates re-interpretation of some observations regarding photoreceptor precursor transplantation into non-degenerative retina, cone precursors are clearly present in the subretinal space of nearly all transplanted animals where they express mature phototransduction-related proteins (Chapter 5). Highest priority for future work should therefore be given to cone precursor transplantation into models of severe retinal degeneration with associated extensive photoreceptor loss. Such environment better mimics potential clinical application in patients with advanced retinal degeneration. Promising results were observed with transplantation of donor-derived rods into *rd1* mice, a model of rapid and severe retinal degeneration. Rod precursors transplanted at a stage when nearly all host rods were lost not only matured but also showed signs of connectivity with host interneurons. In addition, modest improvements in vision-related behavioural tests were detected (Singh et al, 2013). Similarly, evidence of synapse formation with the recipient was observed following transplantation of mESC-derived retina sheets in the same animal model (Assawachananont et al, 2014). To conclude, regardless of the mechanism of cell

repair in the non-degenerative retina, photoreceptor replacement remains an attractive strategy to develop treatments for vision loss resulting from photoreceptor death.

In summary, we determined that cone precursor differentiation in mESC-derived retinae is efficient and follows typical sequence of marker expression. Differentiation of these cells is modulated by Notch and retinoic acid signalling pathways, which also regulate photoreceptor development *in vivo*. Cone precursors can be isolated from mESC-derived retinal tissue in quantities sufficient for analysis and transplantation. Following injection into the subretinal space of adult mouse recipients these cells survive and show behaviour mimicking that observed for donor-derived cones and cone-like cells. Therefore, we conclude that mESC retinal differentiation provides a robust, renewable source of cells for daylight vision restoration studies.

Appendix A

Assessment of cell fusion following transplantation of mESC-derived cone precursors into non-degenerative retina.

Studies aiming to establish the potential for photoreceptor cell replacement by transplantation of photoreceptor precursors examined cell grafts in a range of host environments including healthy wild-type mouse retina or genetic models of degeneration with varying degree of cell loss (Barber et al., 2013; Barnea-Cramer et al., 2016; Lakowski et al., 2010; MacLaren et al., 2006; Pearson et al., 2012; Singh et al., 2013). Whilst the initial future application of photoreceptor transplantation would likely involve placing the cells in severely degenerated retinae of patients with end-stage disease, where photoreceptor loss is extensive (Cramer and MacLaren, 2013; Reh, 2016), transplantation into adult retina without any degeneration was treated as proof of concept for cell replacement in a non-neurogenic environment, also lacking the secondary changes associated with photoreceptor cell degeneration such as gliosis or deposition of extracellular matrix proteins (Pearson et al., 2014). Strikingly, in transplants into healthy adult mouse retina distinct cells apparently expressing the fluorescent reporter labelling the donor cells and showing mature photoreceptor morphology were observed in the host outer nuclear layer. These cells presented all key features of fully developed photoreceptor cells including centrally condensed heterochomatin in the nucleus, outer segments and synaptic terminals indistinguishable from the surrounding recipient cells (Gonzalez-Cordero et al., 2013; MacLaren et al., 2006; Pearson et al., 2012; see also Chapter 5). The well-developed mature features of these cells contrasted with compromised morphology with limited distal outer segment-like structures formation in a severe retinal degeneration model using dissociated cells (Singh et al., 2013). It was believed that these cells had arisen from migration of transplanted precursors from the subretinal cell mass into the host outer nuclear layer. Examination of cell morphology in various degeneration models suggested that morphological features of host cells were assumed (Barber et al., 2013). More surprisingly however, transplantation of dissociated cone and cone-like cells resulted in GFP reporter-marked cells in the recipient outer nuclear layer with the morphology of rod rather than cone photoreceptors (Santos-Ferreira et al., 2015; Smiley et al., 2016) raising the question whether these cells truly result from migration of transplanted precursors or could arise from cytoplasmic fusion with the graft.

To determine and quantify the occurrence of cytoplasmic component transfer into the recipient photoreceptor layer following mESC-derived cone precursor transplantation

flow cytometry analysis was employed. Three weeks post-transplant, DsRed transgenic recipient mouse retinae (ubiquitously expressing red fluorescent protein) transplanted with ConeOpsin.GFP-labelled mESC-derived cone precursors were dissected out, the subretinal cell mass carefully removed and the recipient neural retina tissue dissociated into single cell suspension followed with analysis by flow cytometry (Figure A1 A). Given that the host cells are marked with expression of a red fluorescent protein and the donor cells are labelled with a green fluorescent protein presence of cells positive for both fluorescent reporters would indicate transfer of cellular material from the donor cell mass into recipient photoreceptor cells. As controls for the experiment retinae of wild-type and transgenic DsRed mice that did not receive the transplant and the donor ConeOpsin.GFP-transduced retinal organoids were used. Dissociated cell suspensions from all sources were stained with DRAQ7 dye to distinguish live cells. Based on light scatter properties single live cells were selected for analysis. In such subpopulations no green or red fluorescence was present in wild-type retina (Figure A1 B), whereas clear red fluorescence was detected in DsRed transgenic tissue (Figure A1 C). Neither of those tissues showed GFP fluorescence signal (Figure A1 B,C). As expected, suspensions of donor organoids (Figure A1 D) and dissected transplanted retinae (Figure A1 E; N=2 independent transplants, n=12 retinae) showed GFP positive populations. The number of GFP+ cells in transplanted retinae was low, consistent with previous quantification using sectioned tissue (Chapter 5; Figure 5.8). Strikingly, nearly all of the GFP+ cells were also DsRed+ (99.4% ±1.0%, n=12 retinae, N=2 independent transplants). Only a very small proportion (total of 0.6% ±1.0%) exhibited the GFP signal alone. These results demonstrate that the overwhelming majority of GFP+ cells observed in the host outer nuclear layer following mESC-derived cone precursor transplantation into a non-degenerative retina are a result of uptake of cellular components from the cell graft.

Cell fusion is a phenomenon frequently observed in stem cell transplantation (Kemp et al., 2014). Occurrence of classical nuclear fusion is extremely rare when two post-mitotic cells are involved (Alvarez-Dolado et al., 2003). Consistently, cells with double nuclei were not observed in this or other related studies (Pearson et al., 2016). Since photoreceptors used in this and most other studies are post-mitotic committed precursors fusion in this context is an unexpected phenomenon. To drive the reported improvements in visual function the mechanism involved needs to be efficient, allowing sustained transfer of protein and/or RNA, so that recipient photoreceptors receive substantial quantities of the protein/RNA for which they are genetically deficient

(Pearson et al., 2012). This process must occur between both rods and cones, but not other related neurons, since only transplantation of post-mitotic photoreceptors results in appearance of reporter-positive cells in the host outer nuclear layer (MacLaren et al., 2006; Santos-Ferreira et al., 2015; Smiley et al., 2016). The nature of the material transfer can only be a matter of speculation, but involvement of extracellular vesicles or formation of nanotubes are considered most plausible hypotheses at present.

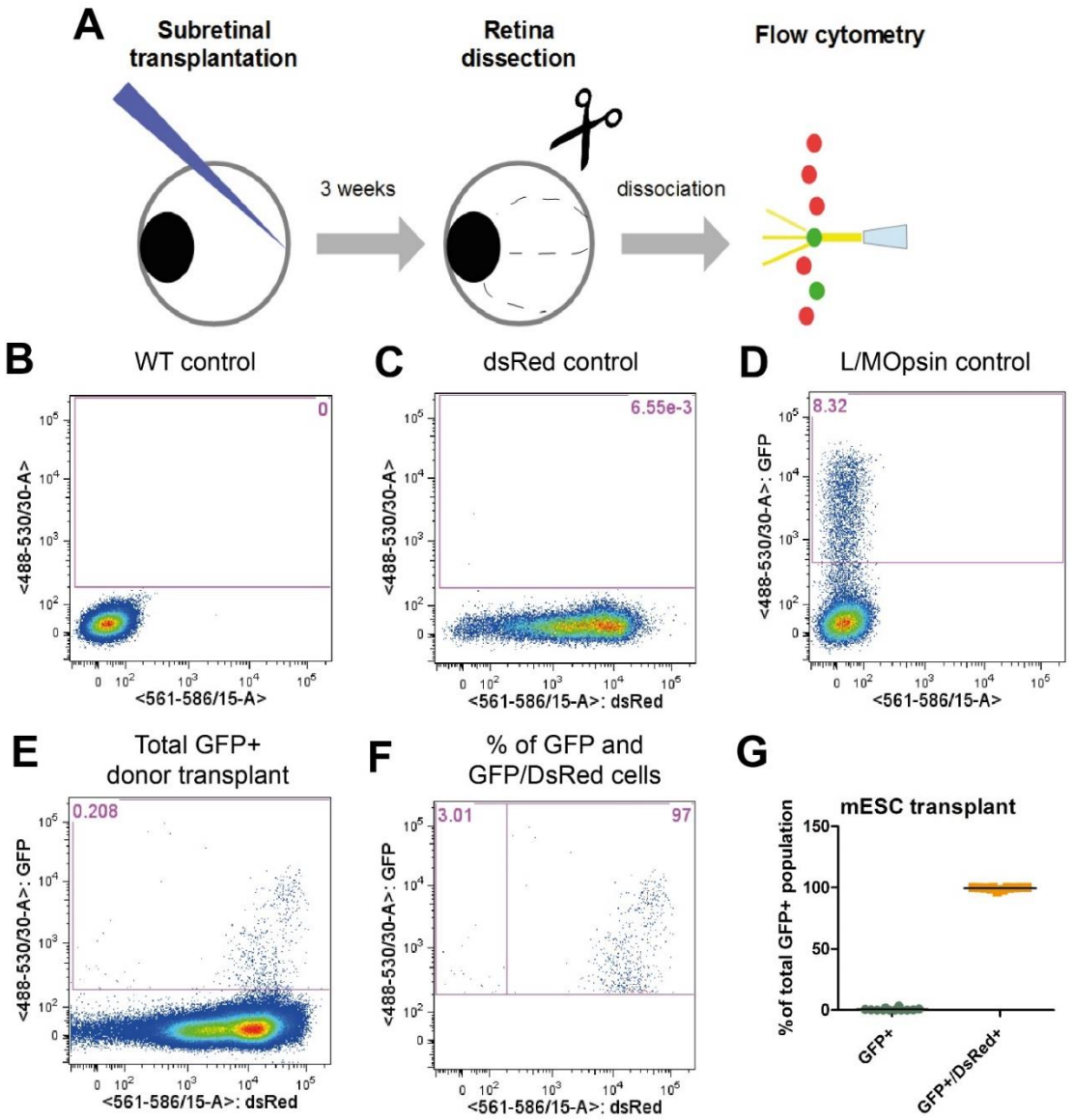

Figure A1. Assessment of cellular material transfer from transplanted mESC-derived cone precursors into host retina of dsRed transgenic recipient mice.

(**A**) Schematic representation of the experimental approach. (**B**) Representative scatter plot graph of dissociated control wild-type retina without any red or green fluorescent signal. (**C**) Example of uninjected dsRed sample showing a red-fluorescent population. (**D**) Dissociated donor retinal organoids transduced with the ConeOpsin.GFP vector. Note the GFP+ population expressing the vector-encoded reporter. (**E**) Representative sample of transplanted retina harvested three weeks post cell injection. A small number of cells shows GFP signal. (**F**) Gating for GFP-only and GFP+dsRed+ populations. (**G**) Quantification of the percentage of GFP-only and GFP and dsRed double positive cells amongst the total GFP+ cells. N=2 independent transplants, n=12 retinae.

Appendix B

Transplantation of mESC-derived cone precursors into the *Aipl1*$^{-/-}$ mouse model of rapid and severe retinal degeneration.

The majority of studies investigating photoreceptor transplantation used either healthy wild type mouse recipients or models in which photoreceptors are dysfunctional, but survive (Barber et al., 2013; Gonzalez-Cordero et al., 2013; Lakowski et al., 2010; MacLaren et al., 2006; Santos-Ferreira et al., 2015). A study from the Ali group examined transplantation into several models of retinal degeneration varying in their etiology and severity (Barber et al., 2013). Interestingly, transplanted photoreceptor precursors survived even when the loss of host photoreceptors was extensive. Therefore, photoreceptor precursor transplantation could offer a potential future treatment for retinal degenerations of different etiologies and, importantly, including very severely degenerated retinae. This is of importance since the initial application of photoreceptor transplantation would likely be in the very degenerated retinae of end-stage retinal disease patients, where photoreceptor loss is extensive precluding other forms of treatment (Cramer and MacLaren, 2013; Reh, 2016). Transplantation of dissociated photoreceptor precursors into the *rd1* mouse model of rapid and severe retinal degeneration demonstrated survival, signs of maturation and potential connection to the host interneurons (Singh et al., 2013). However, the organisation of the graft and morphology of individual transplanted photoreceptors was poor, contrasting with relatively well structured regions found in retina sheet transplants (Assawachananont et al., 2014; Shirai et al., 2016). Transplantation of cone precursors into a model of advanced retinal degeneration has not been performed to date. Hence, the possibility of treating central vision loss using this approach remains unexplored.

In order to determine the feasibility of cone photoreceptor cell replacement in a severely degenerated retina, we performed transplants into the *Aipl1*$^{-/-}$ recipient mice. Mutations in the human *AIPL1* gene, encoding aryl hydrocarbon receptor interacting protein like 1, underlie Leber congenital amaurosis (LCA), the most severe inherited retinal dystrophy in humans. Consistent with the patient phenotype, *Aipl1* knockout mice show very rapid loss of photoreceptors from the second week of age (Kolandaivelu et al., 2014; Ramamurthy et al., 2004). *Aipl1*$^{-/-}$ recipients from 8 weeks of age were injected with purified ConeOpsin.GFP+ mESC-derived cone precursors, 10^5 cells into the superior and another 10^5 into the inferior hemisphere. Injected eyes were collected and examined 3 weeks post-transplantation. ConeOpsin.GFP+ cells were found surviving in all injected eyes (9 out of 9, Figure B1 A). The cell suspension

spread considerably overlaying the remaining host interneurons (Figure B1 A,B; PKCα+ recipient bipolar cells stained in red). Near the injection site the transplanted cells were found in clusters, in which they showed apico-basally polarized morphologies, whilst further displaced cells extended their neurites more horizontally (Figure B1 A,B). Müller glia, performing support functions for the photoreceptors, become activated in retinal degenerations, in some types of disease forming a glial scar that may prevent donor/host interactions (Pearson et al., 2014). Glial fibrillary acidic protein (GFAP) is expressed in activated Müller glia. Strong GFAP immunostaining signal was detected in basal processes of Müller cells in the *Aipl1*$^{-/-}$ retinae (Figure B1. C). Notably at the interface between the graft and the host tissues focal extensions of Müller glia processes into the cone photoreceptor graft could be observed (Figure B1 C), suggesting that normal interactions between these two cell types might be restored.

Next, the *in vivo* maturation and potential connectivity of the transplanted cones were examined. A number of phototransduction-related proteins including M opsin, Gnat2 and Cngb3 were detected in the grafted cone photoreceptor precursors using immunostaining (Figure B2. A-C). Moreover, formation of distal processes, staining for the outer segment protein Peripherin2 and directed towards the host RPE cells, was observed (Figure B2. D). Furthermore, the transplanted cells extended basal neurites in the direction of recipient horizontal interneurons (Figure B2. E). These neurites immunolabelled for the structural component of the sensory neuron synapses ribeye (Figure B2.F) as well as synaptic vesicle-associated protein synaptophysin (Figure B2. G). Collectively, these data demonstrate the potential for survival and maturation of transplanted dissociated cone precursors in a severely diseased retina.

Transplantation of purified cone and cone-like precursors have only been so far performed in either healthy wild-type retina or genetic models without extensive photoreceptor loss. Since most GFP-labelled cells in the recipient outer nuclear layer following transplantation into mice with an intact retina are a result of uptake of cellular components from the subretinal photoreceptor graft, the morphology and marker expression the transplanted cone cells in prior studies most likely is that of host rods that have engaged in cytoplasmic cell fusion/ material transfer with the graft. Therefore, this is the first examination of the true cone precursor morphology and marker expression following subretinal transplantation of a purified cell suspension into a severely degenerated retina. The observation of phototransduction components expression, potential formation of outer segment bud-like structures combined with extension of basal neurites contacting host interneurons and showing presence of

synaptic proteins is clearly encouraging. These features suggest that restoring some degree of light sensitivity to the recipient retina using these cells might be possible. Whilst future studies will need to determine the potential functionality of the grafted cones, this work represents the first steps towards the aim of cone cell replacement.

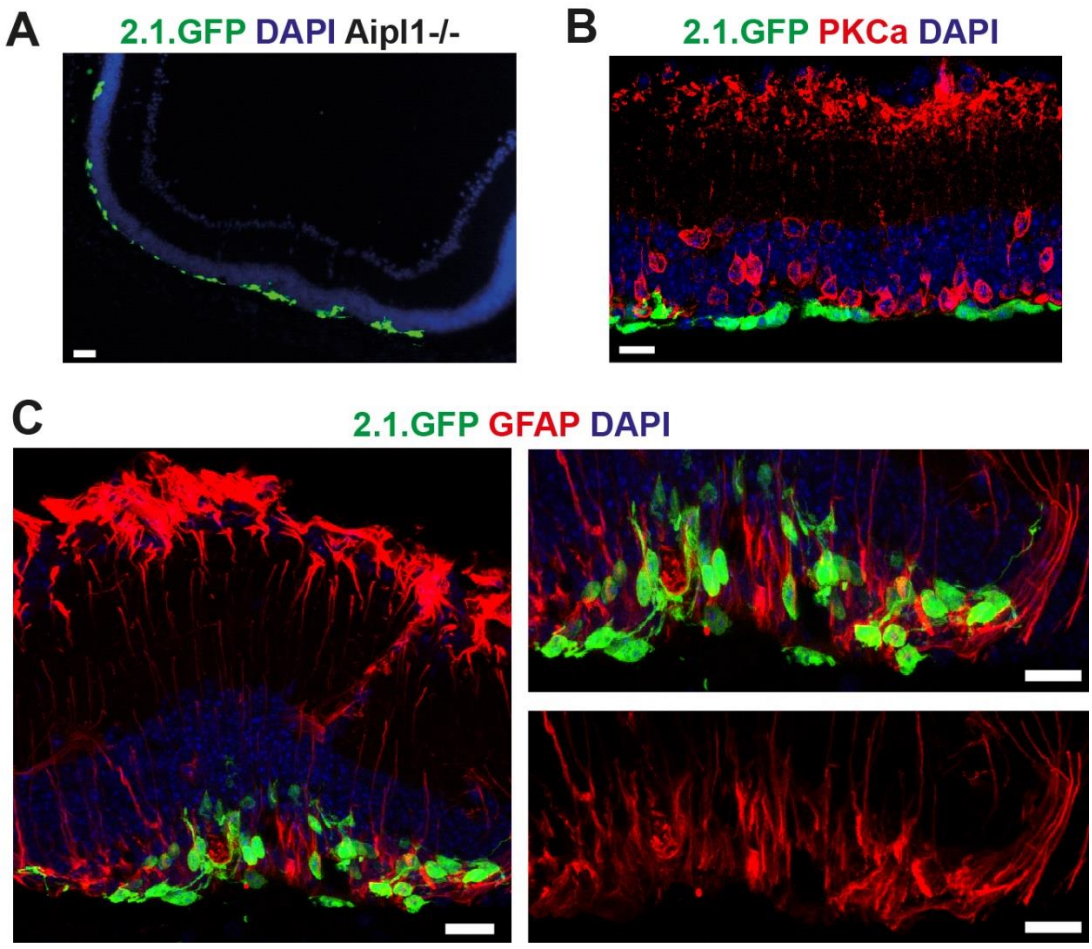

Figure B1. Transplantation of mESC-derived cone precursors into the *Aipl1*$^{-/-}$ of advanced retinal degeneration.

(A) ConeOpsin.GFP-labelled mESC-derived cone precursors are found surviving spread across a large area of recipient retina. Scale bar 20 µm. **(B)** Immunostaining for the bipolar cell marker PKCα shows the GFP+ cells overlaying host interneurons. **(C)** Antibody staining for activated Müller glia marker GFAP demonstrates close interaction between transplanted cone precursors and host Müller cells. Scale bars in (B) and (C) 10 µm.

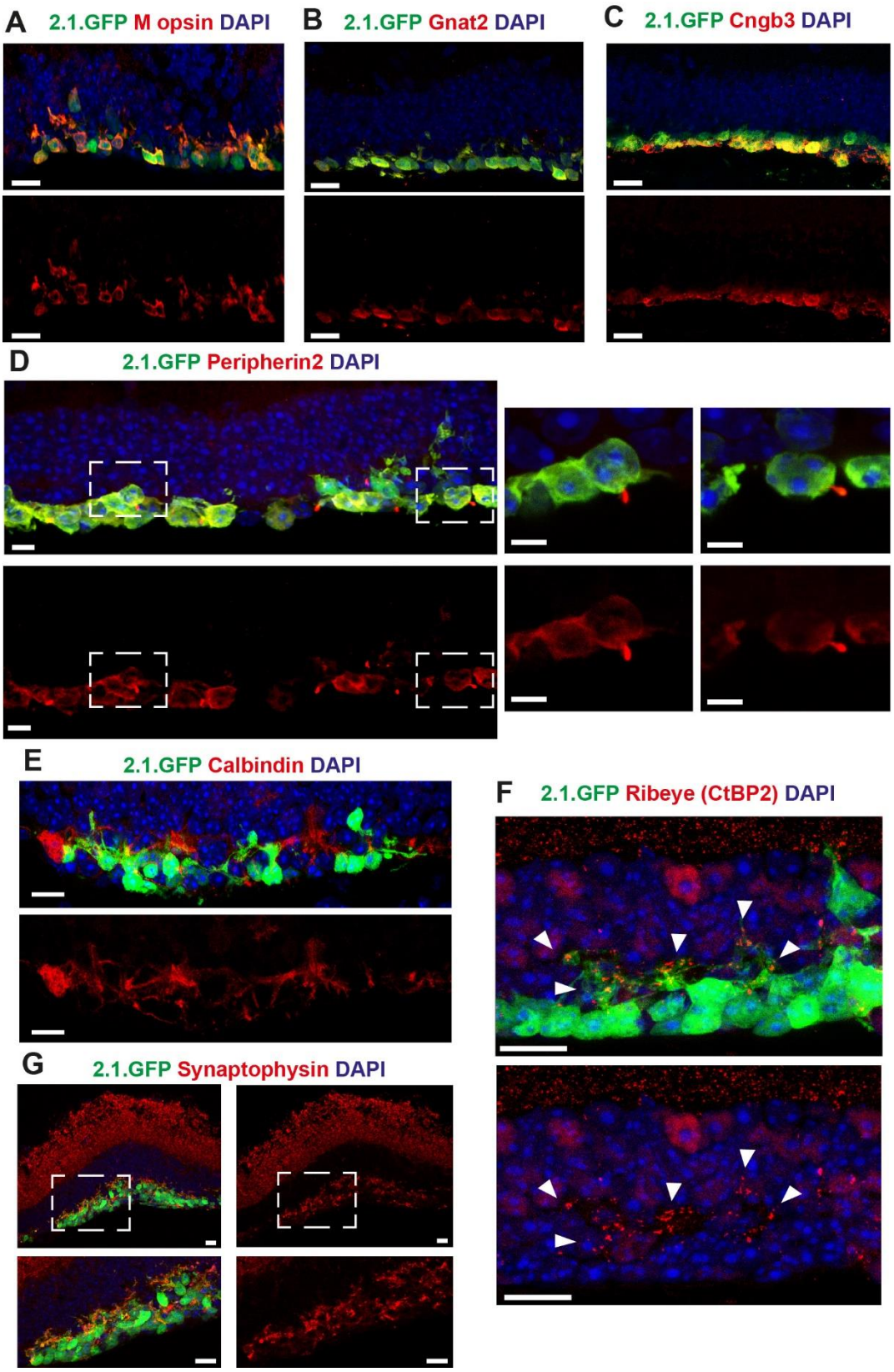

Figure B2. Maturation of transplanted mESC-derived cone precursors in the *Aipl1*$^{-/-}$ retina.

(A-C) Immunostaining for cone-specific phototransduction-related proteins M opsin (A), Gnat2 (B) and Cngb3 (C) in the transplanted ConeOpsin.GFP+ cones. **(D)** Peripherin2 staining accumulated in distal processes formed by transplanted cones.

Right panels show a higher resolution image of selected regions. **(E)** ConeOpsin.GFP+ cells are found in close proximity of calbindin+ host horizontal cell dendrites. **(F,G)** Antibody staining for synaptic proteins ribeye (CtBP2; F) synaptophysin (G) expressed by transplanted ConeOpsin.GFP+ cells. Scale bar 5 µm in (F) 10 µm in all other images. INL – inner nuclear layer.

Literature:

Aasen, T., Raya, A., Barrero, M.J., Garreta, E., Consiglio, A., Gonzalez, F., Vassena, R., Bilić, J., Pekarik, V., Tiscornia, G., et al. (2008). Efficient and rapid generation of induced pluripotent stem cells from human keratinocytes. Nat. Biotechnol. *26*, 1276–1284.

Abu-Abed, S., MacLean, G., Fraulob, V., Chambon, P., Petkovich, M., and Dollé, P. (2002). Differential expression of the retinoic acid-metabolizing enzymes CYP26A1 and CYP26B1 during murine organogenesis. Mech. Dev. *110*, 173–177.

Akhmedov, N.B., Piriev, N.I., Chang, B., Rapoport, A.L., Hawes, N.L., Nishina, P.M., Nusinowitz, S., Heckenlively, J.R., Roderick, T.H., Kozak, C.A., et al. (2000). A deletion in a photoreceptor-specific nuclear receptor mRNA causes retinal degeneration in the rd7 mouse. Proc. Natl. Acad. Sci. U. S. A. *97*, 5551–5556.

Akimoto, M., Cheng, H., Zhu, D., Brzezinski, J.A., Khanna, R., Filippova, E., Oh, E.C.T., Jing, Y., Linares, J.-L., Brooks, M., et al. (2006). Targeting of GFP to newborn rods by Nrl promoter and temporal expression profiling of flow-sorted photoreceptors. Proc. Natl. Acad. Sci. U. S. A. *103*, 3890–3895.

Alexiades, M.R., and Cepko, C. (1996). Quantitative analysis of proliferation and cell cycle length during development of the rat retina. Dev. Dyn. Off. Publ. Am. Assoc. Anat. *205*, 293–307.

Alfano, G., Conte, I., Caramico, T., Avellino, R., Arno, B., Pizzo, M.T., Tanimoto, N., Beck, S.C., Huber, G., Dolle, P., et al. (2011). Vax2 regulates retinoic acid distribution and cone opsin expression in the vertebrate eye. Development *138*, 261–271.

Alvarez-Dolado, M., Pardal, R., Garcia-Verdugo, J.M., Fike, J.R., Lee, H.O., Pfeffer, K., Lois, C., Morrison, S.J., and Alvarez-Buylla, A. (2003). Fusion of bone-marrow-derived cells with Purkinje neurons, cardiomyocytes and hepatocytes. Nature *425*, 968–973.

Amato, M.A., Arnault, E., and Perron, M. (2004). Retinal stem cells in vertebrates: parallels and divergences. Int. J. Dev. Biol. *48*, 993–1001.

Aoto, J., Nam, C.I., Poon, M.M., Ting, P., and Chen, L. (2008). Synaptic Signaling by All-Trans Retinoic Acid in Homeostatic Synaptic Plasticity. Neuron *60*, 308–320.

Applebury, M.L., Antoch, M.P., Baxter, L.C., Chun, L.L.Y., Falk, J.D., Farhangfar, F., Kage, K., Krzystolik, M.G., Lyass, L.A., and Robbins, J.T. (2000). The murine cone photoreceptor: a single cone type expresses both S and M opsins with retinal spatial patterning. Neuron *27*, 513–523.

Assawachananont, J., Mandai, M., Okamoto, S., Yamada, C., Eiraku, M., Yonemura, S., Sasai, Y., and Takahashi, M. (2014). Transplantation of embryonic and induced pluripotent stem cell-derived 3D retinal sheets into retinal degenerative mice. Stem Cell Rep. *2*, 662–674.

Asteriti, S., Grillner, S., and Cangiano, L. (2015). A Cambrian origin for vertebrate rods. eLife *4*.

Bain, G., Kitchens, D., Yao, M., Huettner, J.E., and Gottlieb, D.I. (1995). Embryonic stem cells express neuronal properties in vitro. Dev. Biol. *168*, 342–357.

Bainbridge, J.W.B., Smith, A.J., Barker, S.S., Robbie, S., Henderson, R., Balaggan, K., Viswanathan, A., Holder, G.E., Stockman, A., Tyler, N., et al. (2008). Effect of gene therapy on visual function in Leber's congenital amaurosis. N. Engl. J. Med. *358*, 2231–2239.

Barber, A.C., Hippert, C., Duran, Y., West, E.L., Bainbridge, J.W.B., Warre-Cornish, K., Luhmann, U.F.O., Lakowski, J., Sowden, J.C., Ali, R.R., et al. (2013). Repair of the degenerate retina by photoreceptor transplantation. Proc. Natl. Acad. Sci. *110*, 354–359.

Barbosa-Sabanero, K., Hoffmann, A., Judge, C., Lightcap, N., Tsonis, P.A., and Del Rio-Tsonis, K. (2012). Lens and retina regeneration: new perspectives from model organisms. Biochem. J. *447*, 321–334.

Bartsch, U., Oriyakhel, W., Kenna, P.F., Linke, S., Richard, G., Petrowitz, B., Humphries, P., Farrar, G.J., and Ader, M. (2008). Retinal cells integrate into the outer nuclear layer and differentiate into mature photoreceptors after subretinal transplantation into adult mice. Exp. Eye Res. *86*, 691–700.

Bassett, E.A., and Wallace, V.A. (2012). Cell fate determination in the vertebrate retina. Trends Neurosci. *35*, 565–573.

Beby, F., and Lamonerie, T. (2013). The homeobox gene Otx2 in development and disease. Exp. Eye Res. *111*, 9–16.

Behesti, H., Holt, J.K.L., and Sowden, J.C. (2006). The level of BMP4 signaling is critical for the regulation of distinct T-box gene expression domains and growth along the dorso-ventral axis of the optic cup. BMC Dev. Biol. *6*, 62.

Bernardos, R.L., Barthel, L.K., Meyers, J.R., and Raymond, P.A. (2007). Late-Stage Neuronal Progenitors in the Retina Are Radial Muller Glia That Function as Retinal Stem Cells. J. Neurosci. *27*, 7028–7040.

Bhatia, B., Singhal, S., Lawrence, J.M., Khaw, P.T., and Limb, G.A. (2009). Distribution of Müller stem cells within the neural retina: Evidence for the existence of a ciliary margin-like zone in the adult human eye. Exp. Eye Res. *89*, 373–382.

Bok, D. (1993). The retinal pigment epithelium: a versatile partner in vision. J. Cell Sci. Suppl. *17*, 189–195.

Borooah, S., Phillips, M.J., Bilican, B., Wright, A.F., Wilmut, I., Chandran, S., Gamm, D., and Dhillon, B. (2013). Using human induced pluripotent stem cells to treat retinal disease. Prog. Retin. Eye Res. *37*, 163–181.

Brandl, C., Grassmann, F., Riolfi, J., and Weber, B.H.F. (2015). Tapping Stem Cells to Target AMD: Challenges and Prospects. J. Clin. Med. *4*, 282–303.

Breuninger, T., Puller, C., Haverkamp, S., and Euler, T. (2011). Chromatic bipolar cell pathways in the mouse retina. J. Neurosci. Off. J. Soc. Neurosci. *31*, 6504–6517.

Brooks, M.J., Rajasimha, H.K., Roger, J.E., and Swaroop, A. (2011). Next-generation sequencing facilitates quantitative analysis of wild-type and Nrl(-/-) retinal transcriptomes. Mol. Vis. *17*, 3034–3054.

Brzezinski, J.A., Kim, E.J., Johnson, J.E., and Reh, T.A. (2011). Ascl1 expression defines a subpopulation of lineage-restricted progenitors in the mammalian retina. Dev. Camb. Engl. *138*, 3519–3531.

Buganim, Y., Itskovich, E., Hu, Y.-C., Cheng, A.W., Ganz, K., Sarkar, S., Fu, D., Welstead, G.G., Page, D.C., and Jaenisch, R. (2012). Direct reprogramming of fibroblasts into embryonic Sertoli-like cells by defined factors. Cell Stem Cell *11*, 373–386.

Busskamp, V., Krol, J., Nelidova, D., Daum, J., Szikra, T., Tsuda, B., Jüttner, J., Farrow, K., Scherf, B.G., Alvarez, C.P.P., et al. (2014). miRNAs 182 and 183 are necessary to maintain adult cone photoreceptor outer segments and visual function. Neuron *83*, 586–600.

Campbell, I.C., Coudrillier, B., and Ross Ethier, C. (2014). Biomechanics of the posterior eye: a critical role in health and disease. J. Biomech. Eng. *136*, 021005.

Carl, M., Loosli, F., and Wittbrodt, J. (2002). Six3 inactivation reveals its essential role for the formation and patterning of the vertebrate eye. Dev. Camb. Engl. *129*, 4057–4063.

Carpenter, M.K., and Rao, M.S. (2015). Concise review: making and using clinically compliant pluripotent stem cell lines. Stem Cells Transl. Med. *4*, 381–388.

Caspi, A., Dorn, J.D., McClure, K.H., Humayun, M.S., Greenberg, R.J., and McMahon, M.J. (2009). Feasibility study of a retinal prosthesis: spatial vision with a 16-electrode implant. Arch. Ophthalmol. Chic. Ill 1960 *127*, 398–401.

Cepko, C. (2014). Intrinsically different retinal progenitor cells produce specific types of progeny. Nat. Rev. Neurosci.

Chen, J., Rattner, A., and Nathans, J. (2006). Effects of L1 retrotransposon insertion on transcript processing, localization and accumulation: lessons from the retinal degeneration 7 mouse and implications for the genomic ecology of L1 elements. Hum. Mol. Genet. *15*, 2146–2156.

Cheng, H., Aleman, T.S., Cideciyan, A.V., Khanna, R., Jacobson, S.G., and Swaroop, A. (2006). In vivo function of the orphan nuclear receptor NR2E3 in establishing photoreceptor identity during mammalian retinal development. Hum. Mol. Genet. *15*, 2588–2602.

Chiang, C., Litingtung, Y., Lee, E., Young, K.E., Corden, J.L., Westphal, H., and Beachy, P.A. (1996). Cyclopia and defective axial patterning in mice lacking Sonic hedgehog gene function. Nature *383*, 407–413.

Chow, R.L., and Lang, R.A. (2001). Early eye development in vertebrates. Annu. Rev. Cell Dev. Biol. *17*, 255–296.

Chow, L., Levine, E.M., and Reh, T.A. (1998). The nuclear receptor transcription factor, retinoid-related orphan receptor beta, regulates retinal progenitor proliferation. Mech. Dev. *77*, 149–164.

Chow, R.L., Altmann, C.R., Lang, R.A., and Hemmati-Brivanlou, A. (1999). Pax6 induces ectopic eyes in a vertebrate. Dev. Camb. Engl. *126*, 4213–4222.

Chuang, J.-Z., Zhao, Y., and Sung, C.-H. (2007). SARA-Regulated Vesicular Targeting Underlies Formation of the Light-Sensing Organelle in Mammalian Rods. Cell *130*, 535–547.

Corbo, J.C., and Cepko, C.L. (2005). A hybrid photoreceptor expressing both rod and cone genes in a mouse model of enhanced S-cone syndrome. PLoS Genet. *1*, e11.

Cramer, A.O., and MacLaren, R.E. (2013). Translating induced pluripotent stem cells from bench to bedside: application to retinal diseases. Curr. Gene Ther. *13*, 139–151.

Croteau, W., Davey, J.C., Galton, V.A., and St Germain, D.L. (1996). Cloning of the mammalian type II iodothyronine deiodinase. A selenoprotein differentially expressed and regulated in human and rat brain and other tissues. J. Clin. Invest. *98*, 405–417.

Cruess, A.F., Zlateva, G., Xu, X., Soubrane, G., Pauleikhoff, D., Lotery, A., Mones, J., Buggage, R., Schaefer, C., Knight, T., et al. (2008). Economic burden of bilateral neovascular age-related macular degeneration: multi-country observational study. PharmacoEconomics *26*, 57–73.

Das, B.C., Thapa, P., Karki, R., Das, S., Mahapatra, S., Liu, T.-C., Torregroza, I., Wallace, D.P., Kambhampati, S., Van Veldhuizen, P., et al. (2014). Retinoic acid signaling pathways in development and diseases. Bioorg. Med. Chem. *22*, 673–683.

De Kloe, G.E., and De Strooper, B. (2014). Small molecules that inhibit Notch signaling. Methods Mol. Biol. Clifton NJ *1187*, 311–322.

Decembrini, S., Koch, U., Radtke, F., Moulin, A., and Arsenijevic, Y. (2014). Derivation of Traceable and Transplantable Photoreceptors from Mouse Embryonic Stem Cells. Stem Cell Rep. *2*, 853–865.

Del Debbio, C.B., Balasubramanian, S., Parameswaran, S., Chaudhuri, A., Qiu, F., and Ahmad, I. (2010). Notch and Wnt Signaling Mediated Rod Photoreceptor Regeneration by Müller Cells in Adult Mammalian Retina. PLoS ONE *5*, e12425.

DelMonte, D.W., and Kim, T. (2011). Anatomy and physiology of the cornea. J. Cataract Refract. Surg. *37*, 588–598.

Dyer, M.A., and Cepko, C.L. (2000). Control of Müller glial cell proliferation and activation following retinal injury. Nat. Neurosci. *3*, 873–880.

Eiraku, M., Takata, N., Ishibashi, H., Kawada, M., Sakakura, E., Okuda, S., Sekiguchi, K., Adachi, T., and Sasai, Y. (2011). Self-organizing optic-cup morphogenesis in three-dimensional culture. Nature *472*, 51–56.

Eiraku, M., Adachi, T., and Sasai, Y. (2012). Relaxation-expansion model for self-driven retinal morphogenesis: a hypothesis from the perspective of biosystems dynamics at the multi-cellular level. BioEssays News Rev. Mol. Cell. Dev. Biol. *34*, 17–25.

Emerson, M.M., Surzenko, N., Goetz, J.J., Trimarchi, J., and Cepko, C.L. (2013). Otx2 and Onecut1 Promote the Fates of Cone Photoreceptors and Horizontal Cells and Repress Rod Photoreceptors. Dev. Cell *26*, 59–72.

Engelhardt, M., Wachs, F.-P., Couillard-Despres, S., and Aigner, L. (2004). The neurogenic competence of progenitors from the postnatal rat retina in vitro. Exp. Eye Res. *78*, 1025–1036.

Evans, M.J., and Kaufman, M.H. (1981). Establishment in culture of pluripotential cells from mouse embryos. Nature *292*, 154–156.

Felix, N.J., Suri, A., Salter-Cid, L., Nadler, S.G., Gujrathi, S., Corbo, M., and Aranda, R. (2010). Targeting lymphocyte co-stimulation: from bench to bedside. Autoimmunity *43*, 514–525.

Fisher, S.K., Erickson, P.A., Lewis, G.P., and Anderson, D.H. (1991). Intraretinal proliferation induced by retinal detachment. Invest. Ophthalmol. Vis. Sci. *32*, 1739–1748.

Forrest, D., and Swaroop, A. (2012). Minireview: the role of nuclear receptors in photoreceptor differentiation and disease. Mol. Endocrinol. Baltim. Md *26*, 905–915.

Freund, C.L., Wang, Q.L., Chen, S., Muskat, B.L., Wiles, C.D., Sheffield, V.C., Jacobson, S.G., McInnes, R.R., Zack, D.J., and Stone, E.M. (1998). De novo mutations in the CRX homeobox gene associated with Leber congenital amaurosis. Nat. Genet. *18*, 311–312.

Friedlander, D.R., Milev, P., Karthikeyan, L., Margolis, R.K., Margolis, R.U., and Grumet, M. (1994). The neuronal chondroitin sulfate proteoglycan neurocan binds to the neural cell adhesion molecules Ng-CAM/L1/NILE and N-CAM, and inhibits neuronal adhesion and neurite outgrowth. J. Cell Biol. *125*, 669–680.

Fu, Y., Liu, H., Ng, L., Kim, J.-W., Hao, H., Swaroop, A., and Forrest, D. (2014). Feedback induction of a photoreceptor-specific isoform of retinoid-related orphan nuclear receptor β by the rod transcription factor NRL. J. Biol. Chem. *289*, 32469–32480.

Fuhrmann, S. (2010). Eye morphogenesis and patterning of the optic vesicle. Curr. Top. Dev. Biol. *93*, 61–84.

Fuhrmann, S., Levine, E.M., and Reh, T.A. (2000). Extraocular mesenchyme patterns the optic vesicle during early eye development in the embryonic chick. Dev. Camb. Engl. *127*, 4599–4609.

Furukawa, T., Morrow, E.M., and Cepko, C.L. (1997). Crx, a novel otx-like homeobox gene, shows photoreceptor-specific expression and regulates photoreceptor differentiation. Cell *91*, 531–541.

Gal, A., Li, Y., Thompson, D.A., Weir, J., Orth, U., Jacobson, S.G., Apfelstedt-Sylla, E., and Vollrath, D. (2000). Mutations in MERTK, the human orthologue of the RCS rat retinal dystrophy gene, cause retinitis pigmentosa. Nat. Genet. *26*, 270–271.

Geng, X., Speirs, C., Lagutin, O., Inbal, A., Liu, W., Solnica-Krezel, L., Jeong, Y., Epstein, D.J., and Oliver, G. (2008). Haploinsufficiency of Six3 fails to activate Sonic hedgehog expression in the ventral forebrain and causes holoprosencephaly. Dev. Cell *15*, 236–247.

Georgiadis, A., Tschernutter, M., Bainbridge, J.W.B., Robbie, S.J., McIntosh, J., Nathwani, A.C., Smith, A.J., and Ali, R.R. (2010). AAV-mediated knockdown of peripherin-2 in vivo using miRNA-based hairpins. Gene Ther. *17*, 486–493.

Ghosh, F., Juliusson, B., ArnéR, K., and Ehinger, B. (1999). Partial and Full-Thickness Neuroretinal Transplants. Exp. Eye Res. *68*, 67–74.

Giorgetti, A., Montserrat, N., Aasen, T., Gonzalez, F., Rodríguez-Pizà, I., Vassena, R., Raya, A., Boué, S., Barrero, M.J., Corbella, B.A., et al. (2009). Generation of induced pluripotent stem cells from human cord blood using OCT4 and SOX2. Cell Stem Cell *5*, 353–357.

Glaser, T., Jepeal, L., Edwards, J.G., Young, S.R., Favor, J., and Maas, R.L. (1994). PAX6 gene dosage effect in a family with congenital cataracts, aniridia, anophthalmia and central nervous system defects. Nat. Genet. *7*, 463–471.

Gomes, F.L.A.F., Zhang, G., Carbonell, F., Correa, J.A., Harris, W.A., Simons, B.D., and Cayouette, M. (2011). Reconstruction of rat retinal progenitor cell lineages in vitro reveals a surprising degree of stochasticity in cell fate decisions. Dev. Camb. Engl. *138*, 227–235.

Gonzalez-Cordero, A., West, E.L., Pearson, R.A., Duran, Y., Carvalho, L.S., Chu, C.J., Naeem, A., Blackford, S.J.I., Georgiadis, A., Lakowski, J., et al. (2013). Photoreceptor precursors derived from three-dimensional embryonic stem cell cultures integrate and mature within adult degenerate retina. Nat. Biotechnol. *31*, 741–747.

Gust, J., and Reh, T.A. (2011). Adult donor rod photoreceptors integrate into the mature mouse retina. Invest. Ophthalmol. Vis. Sci. *52*, 5266–5272.

Hafler, B.P., Surzenko, N., Beier, K.T., Punzo, C., Trimarchi, J.M., Kong, J.H., and Cepko, C.L. (2012). Transcription factor Olig2 defines subpopulations of retinal progenitor cells biased toward specific cell fates. Proc. Natl. Acad. Sci. *109*, 7882–7887.

Haider, N.B., Jacobson, S.G., Cideciyan, A.V., Swiderski, R., Streb, L.M., Searby, C., Beck, G., Hockey, R., Hanna, D.B., Gorman, S., et al. (2000). Mutation of a nuclear receptor gene, NR2E3, causes enhanced S cone syndrome, a disorder of retinal cell fate. Nat. Genet. *24*, 127–131.

Hendrickson, A., Bumsted-O'Brien, K., Natoli, R., Ramamurthy, V., Possin, D., and Provis, J. (2008). Rod photoreceptor differentiation in fetal and infant human retina. Exp. Eye Res. *87*, 415–426.

Hennig, A.K., Peng, G.-H., and Chen, S. (2008). Regulation of photoreceptor gene expression by Crx-associated transcription factor network. Brain Res. *1192*, 114–133.

Hennig, A.K., Peng, G.-H., and Chen, S. (2013). Transcription coactivators p300 and CBP are necessary for photoreceptor-specific chromatin organization and gene expression. PloS One *8*, e69721.

Hiler, D., Chen, X., Hazen, J., Kupriyanov, S., Carroll, P.A., Qu, C., Xu, B., Johnson, D., Griffiths, L., Frase, S., et al. (2015). Quantification of Retinogenesis in 3D Cultures Reveals Epigenetic Memory and Higher Efficiency in iPSCs Derived from Rod Photoreceptors. Cell Stem Cell *17*, 101–115.

Hoon, M., Okawa, H., Della Santina, L., and Wong, R.O.L. (2014). Functional architecture of the retina: development and disease. Prog. Retin. Eye Res. *42*, 44–84.

Hu, Q., Friedrich, A.M., Johnson, L.V., and Clegg, D.O. (2010). Memory in induced pluripotent stem cells: reprogrammed human retinal-pigmented epithelial cells show tendency for spontaneous redifferentiation. Stem Cells Dayt. Ohio *28*, 1981–1991.

Huang, S.A. (2005). Physiology and pathophysiology of type 3 deiodinase in humans. Thyroid Off. J. Am. Thyroid Assoc. *15*, 875–881.

Huang, P., Chandra, V., and Rastinejad, F. (2014). Retinoic acid actions through mammalian nuclear receptors. Chem. Rev. *114*, 233–254.

Hyatt, G.A., and Dowling, J.E. (1997). Retinoic acid. A key molecule for eye and photoreceptor development. Invest. Ophthalmol. Vis. Sci. *38*, 1471–1475.

Hyatt, G.A., Schmitt, E.A., Marsh-Armstrong, N.R., and Dowling, J.E. (1992). Retinoic acid-induced duplication of the zebrafish retina. Proc. Natl. Acad. Sci. U. S. A. *89*, 8293–8297.

Hyatt, G.A., Schmitt, E.A., Fadool, J.M., and Dowling, J.E. (1996). Retinoic acid alters photoreceptor development in vivo. Proc. Natl. Acad. Sci. *93*, 13298–13303.

Ichijo, H. (2004). Proteoglycans as cues for axonal guidance in formation of retinotectal or retinocollicular projections. Mol. Neurobiol. *30*, 23–33.

Ikeda, H., Osakada, F., Watanabe, K., Mizuseki, K., Haraguchi, T., Miyoshi, H., Kamiya, D., Honda, Y., Sasai, N., Yoshimura, N., et al. (2005). Generation of Rx+/Pax6+ neural retinal precursors from embryonic stem cells. Proc. Natl. Acad. Sci. U. S. A. *102*, 11331–11336.

Inatani, M., and Tanihara, H. (2002). Proteoglycans in retina. Prog. Retin. Eye Res. *21*, 429–447.

Inatani, M., Tanihara, H., Oohira, A., Otori, Y., Nishida, A., Honjo, M., Kido, N., and Honda, Y. (2000). Neuroglycan C, a neural tissue-specific transmembrane chondroitin sulfate proteoglycan, in retinal neural network formation. Invest. Ophthalmol. Vis. Sci. *41*, 4338–4346.

Jadhav, A.P. (2006). Notch 1 inhibits photoreceptor production in the developing mammalian retina. Development *133*, 913–923.

Janesick, A., Wu, S.C., and Blumberg, B. (2015). Retinoic acid signaling and neuronal differentiation. Cell. Mol. Life Sci. CMLS *72*, 1559–1576.

Jayakody, S.A., Gonzalez-Cordero, A., Ali, R.R., and Pearson, R.A. (2015). Cellular strategies for retinal repair by photoreceptor replacement. Prog. Retin. Eye Res. *46*, 31–66.

Jeon, C.J., Strettoi, E., and Masland, R.H. (1998). The major cell populations of the mouse retina. J. Neurosci. Off. J. Soc. Neurosci. *18*, 8936–8946.

Jia, L., Oh, E.C.T., Ng, L., Srinivas, M., Brooks, M., Swaroop, A., and Forrest, D. (2009). Retinoid-related orphan nuclear receptor RORbeta is an early-acting factor in rod photoreceptor development. Proc. Natl. Acad. Sci. U. S. A. *106*, 17534–17539.

Jian, Q., Xu, H., Xie, H., Tian, C., Zhao, T., and Yin, Z. (2009). Activation of retinal stem cells in the proliferating marginal region of RCS rats during development of retinitis pigmentosa. Neurosci. Lett. *465*, 41–44.

Jiang, L.Q., and Streilein, J.W. (1991). Immune responses elicited by transplantation and tissue-restricted antigens expressed on retinal tissues implanted subconjunctivally. Transplantation *52*, 513–519.

Jones, I., Ng, L., Liu, H., and Forrest, D. (2007). An Intron Control Region Differentially Regulates Expression of Thyroid Hormone Receptor β2 in the Cochlea, Pituitary, and Cone Photoreceptors. Mol. Endocrinol. *21*, 1108–1119.

Kaludov, N., Handelman, B., and Chiorini, J.A. (2002). Scalable purification of adeno-associated virus type 2, 4, or 5 using ion-exchange chromatography. Hum. Gene Ther. *13*, 1235–1243.

Kastner, P., Grondona, J.M., Mark, M., Gansmuller, A., LeMeur, M., Decimo, D., Vonesch, J.L., Dollé, P., and Chambon, P. (1994). Genetic analysis of RXR alpha developmental function: convergence of RXR and RAR signaling pathways in heart and eye morphogenesis. Cell *78*, 987–1003.

Kawasaki, H., Mizuseki, K., Nishikawa, S., Kaneko, S., Kuwana, Y., Nakanishi, S., Nishikawa, S.I., and Sasai, Y. (2000). Induction of midbrain dopaminergic neurons from ES cells by stromal cell-derived inducing activity. Neuron *28*, 31–40.

Kawikova, I., and Askenase, P.W. (2015). Diagnostic and therapeutic potentials of exosomes in CNS diseases. Brain Res. *1617*, 63–71.

Kelley, M.W., Turner, J.K., and Reh, T.A. (1994). Retinoic acid promotes differentiation of photoreceptors in vitro. Dev. Camb. Engl. *120*, 2091–2102.

Kelley, M.W., Turner, J.K., and Reh, T.A. (1995). Ligands of steroid/thyroid receptors induce cone photoreceptors in vertebrate retina. Dev. Camb. Engl. *121*, 3777–3785.

Kemp, K., Wilkins, A., and Scolding, N. (2014). Cell fusion in the brain: two cells forward, one cell back. Acta Neuropathol. (Berl.) *128*, 629–638.

Kiecker, C., and Niehrs, C. (2001). A morphogen gradient of Wnt/beta-catenin signalling regulates anteroposterior neural patterning in Xenopus. Dev. Camb. Engl. *128*, 4189–4201.

Kim, S.U. (2007). Genetically engineered human neural stem cells for brain repair in neurological diseases. Brain Dev. *29*, 193–201.

Kim, H.-T., and Kim, J.W. (2012). Compartmentalization of vertebrate optic neuroephithelium: external cues and transcription factors. Mol. Cells *33*, 317–324.

Kim, J., Wu, H.-H., Lander, A.D., Lyons, K.M., Matzuk, M.M., and Calof, A.L. (2005). GDF11 controls the timing of progenitor cell competence in developing retina. Science *308*, 1927–1930.

Kim, J.-W., Yang, H.-J., Oel, A.P., Brooks, M.J., Jia, L., Plachetzki, D.C., Li, W., Allison, W.T., and Swaroop, A. (2016). Recruitment of Rod Photoreceptors from Short-Wavelength-Sensitive Cones during the Evolution of Nocturnal Vision in Mammals. Dev. Cell *37*, 520–532.

Kim, K., Doi, A., Wen, B., Ng, K., Zhao, R., Cahan, P., Kim, J., Aryee, M.J., Ji, H., Ehrlich, L.I.R., et al. (2010). Epigenetic memory in induced pluripotent stem cells. Nature *467*, 285–290.

Klassen, H., Warfvinge, K., Schwartz, P.H., Kiilgaard, J.F., Shamie, N., Jiang, C., Samuel, M., Scherfig, E., Prather, R.S., and Young, M.J. (2008). Isolation of progenitor cells from GFP-transgenic pigs and transplantation to the retina of allorecipients. Cloning Stem Cells *10*, 391–402.

Klassen, H.J., Ng, T.F., Kurimoto, Y., Kirov, I., Shatos, M., Coffey, P., and Young, M.J. (2004). Multipotent retinal progenitors express developmental markers, differentiate into retinal neurons, and preserve light-mediated behavior. Invest. Ophthalmol. Vis. Sci. *45*, 4167–4173.

Klimczak, R.R., Koerber, J.T., Dalkara, D., Flannery, J.G., and Schaffer, D.V. (2009). A Novel Adeno-Associated Viral Variant for Efficient and Selective Intravitreal Transduction of Rat Müller Cells. PLoS ONE *4*, e7467.

Kobayashi, M., Takezawa, S., Hara, K., Yu, R.T., Umesono, Y., Agata, K., Taniwaki, M., Yasuda, K., and Umesono, K. (1999). Identification of a photoreceptor cell-specific nuclear receptor. Proc. Natl. Acad. Sci. U. S. A. *96*, 4814–4819.

Kruse, S.W., Suino-Powell, K., Zhou, X.E., Kretschman, J.E., Reynolds, R., Vonrhein, C., Xu, Y., Wang, L., Tsai, S.Y., Tsai, M.-J., et al. (2008). Identification of COUP-TFII orphan nuclear receptor as a retinoic acid-activated receptor. PLoS Biol. *6*, e227.

Kurosawa, H. (2007). Methods for inducing embryoid body formation: in vitro differentiation system of embryonic stem cells. J. Biosci. Bioeng. *103*, 389–398.

Kuwahara, A., Ozone, C., Nakano, T., Saito, K., Eiraku, M., and Sasai, Y. (2015). Generation of a ciliary margin-like stem cell niche from self-organizing human retinal tissue. Nat. Commun. *6*, 6286.

Lai, C.M., Lai, Y.K.Y., and Rakoczy, P.E. (2002). Adenovirus and adeno-associated virus vectors. DNA Cell Biol. *21*, 895–913.

Lakowski, J., Baron, M., Bainbridge, J., Barber, A.C., Pearson, R.A., Ali, R.R., and Sowden, J.C. (2010). Cone and rod photoreceptor transplantation in models of the childhood retinopathy Leber congenital amaurosis using flow-sorted Crx-positive donor cells. Hum. Mol. Genet. *19*, 4545–4559.

Lamb, T.D. (2009). Evolution of vertebrate retinal photoreception. Philos. Trans. R. Soc. Lond. B. Biol. Sci. *364*, 2911–2924.

Lamb, T.D. (2013). Evolution of phototransduction, vertebrate photoreceptors and retina. Prog. Retin. Eye Res. *36*, 52–119.

Lamba, D.A., Karl, M.O., Ware, C.B., and Reh, T.A. (2006). Efficient generation of retinal progenitor cells from human embryonic stem cells. Proc. Natl. Acad. Sci. U. S. A. *103*, 12769–12774.

Lamba, D.A., Gust, J., and Reh, T.A. (2009). Transplantation of human embryonic stem cell-derived photoreceptors restores some visual function in Crx-deficient mice. Cell Stem Cell *4*, 73–79.

Lancaster, M.A., and Knoblich, J.A. (2014a). Organogenesis in a dish: modeling development and disease using organoid technologies. Science *345*, 1247125.

Lancaster, M.A., and Knoblich, J.A. (2014b). Generation of cerebral organoids from human pluripotent stem cells. Nat. Protoc. *9*, 2329–2340.

Lancaster, M.A., Renner, M., Martin, C.-A., Wenzel, D., Bicknell, L.S., Hurles, M.E., Homfray, T., Penninger, J.M., Jackson, A.P., and Knoblich, J.A. (2013). Cerebral organoids model human brain development and microcephaly. Nature *501*, 373–379.

Larhammar, D., Nordström, K., and Larsson, T.A. (2009). Evolution of vertebrate rod and cone phototransduction genes. Philos. Trans. R. Soc. Lond. B. Biol. Sci. *364*, 2867–2880.

LaVail, M.M. (1973). KINETICS OF ROD OUTER SEGMENT RENEWAL IN THE DEVELOPING MOUSE RETINA. J. Cell Biol. *58*, 650–661.

LaVail, M.M. (1983). Outer segment disc shedding and phagocytosis in the outer retina. Trans. Ophthalmol. Soc. U. K. *103 (Pt 4)*, 397–404.

Lee, S.H., Lumelsky, N., Studer, L., Auerbach, J.M., and McKay, R.D. (2000). Efficient generation of midbrain and hindbrain neurons from mouse embryonic stem cells. Nat. Biotechnol. *18*, 675–679.

Lewis, J. (1996). Neurogenic genes and vertebrate neurogenesis. Curr. Opin. Neurobiol. *6*, 3–10.

Lewis, G.P., and Fisher, S.K. (2003). Up-regulation of glial fibrillary acidic protein in response to retinal injury: its potential role in glial remodeling and a comparison to vimentin expression. Int. Rev. Cytol. *230*, 263–290.

Lindsell, C.E., Boulter, J., diSibio, G., Gossler, A., and Weinmaster, G. (1996). Expression patterns of Jagged, Delta1, Notch1, Notch2, and Notch3 genes identify ligand-receptor pairs that may function in neural development. Mol. Cell. Neurosci. *8*, 14–27.

Liu, I.S., Chen, J.D., Ploder, L., Vidgen, D., van der Kooy, D., Kalnins, V.I., and McInnes, R.R. (1994). Developmental expression of a novel murine homeobox gene (Chx10): evidence for roles in determination of the neuroretina and inner nuclear layer. Neuron *13*, 377–393.

Liu, W., Lagutin, O., Swindell, E., Jamrich, M., and Oliver, G. (2010). Neuroretina specification in mouse embryos requires Six3-mediated suppression of Wnt8b in the anterior neural plate. J. Clin. Invest. *120*, 3568–3577.

Livesey, F.J., and Cepko, C.L. (2001). Vertebrate neural cell-fate determination: lessons from the retina. Nat. Rev. Neurosci. *2*, 109–118.

Livesey, F.J., Furukawa, T., Steffen, M.A., Church, G.M., and Cepko, C.L. (2000). Microarray analysis of the transcriptional network controlled by the photoreceptor homeobox gene Crx. Curr. Biol. CB *10*, 301–310.

Loh, Y.-H., Agarwal, S., Park, I.-H., Urbach, A., Huo, H., Heffner, G.C., Kim, K., Miller, J.D., Ng, K., and Daley, G.Q. (2009). Generation of induced pluripotent stem cells from human blood. Blood *113*, 5476–5479.

Lu, A., Ng, L., Ma, M., Kefas, B., Davies, T.F., Hernandez, A., Chan, C.-C., and Forrest, D. (2009). Retarded developmental expression and patterning of retinal cone opsins in hypothyroid mice. Endocrinology *150*, 1536–1544.

Lukáts, A., Szabó, A., Röhlich, P., Vígh, B., and Szél, A. (2005). Photopigment coexpression in mammals: comparative and developmental aspects. Histol. Histopathol. *20*, 551–574.

Ma, N., and Streilein, J.W. (1998). Contribution of microglia as passenger leukocytes to the fate of intraocular neuronal retinal grafts. Invest. Ophthalmol. Vis. Sci. *39*, 2384–2393.

Ma, H., Thapa, A., Morris, L., Redmond, T.M., Baehr, W., and Ding, X.-Q. (2014). Suppressing thyroid hormone signaling preserves cone photoreceptors in mouse models of retinal degeneration. Proc. Natl. Acad. Sci. U. S. A. *111*, 3602–3607.

MacLaren, R.E., Pearson, R.A., MacNeil, A., Douglas, R.H., Salt, T.E., Akimoto, M., Swaroop, A., Sowden, J.C., and Ali, R.R. (2006). Retinal repair by transplantation of photoreceptor precursors. Nature *444*, 203–207.

Maeda, A., and Palczewski, K. (2013). Retinal degeneration in animal models with a defective visual cycle. Drug Discov. Today Dis. Models *10*, e163–e172.

Maguire, A.M., Simonelli, F., Pierce, E.A., Pugh, E.N., Mingozzi, F., Bennicelli, J., Banfi, S., Marshall, K.A., Testa, F., Surace, E.M., et al. (2008). Safety and efficacy of gene transfer for Leber's congenital amaurosis. N. Engl. J. Med. *358*, 2240–2248.

Marc, R.E., Jones, B.W., Watt, C.B., and Strettoi, E. (2003). Neural remodeling in retinal degeneration. Prog. Retin. Eye Res. *22*, 607–655.

Marquardt, T., Ashery-Padan, R., Andrejewski, N., Scardigli, R., Guillemot, F., and Gruss, P. (2001). Pax6 is required for the multipotent state of retinal progenitor cells. Cell *105*, 43–55.

Marsh-Armstrong, N., McCaffery, P., Gilbert, W., Dowling, J.E., and Dräger, U.C. (1994). Retinoic acid is necessary for development of the ventral retina in zebrafish. Proc. Natl. Acad. Sci. U. S. A. *91*, 7286–7290.

Martin, G.R. (1981). Isolation of a pluripotent cell line from early mouse embryos cultured in medium conditioned by teratocarcinoma stem cells. Proc. Natl. Acad. Sci. U. S. A. *78*, 7634–7638.

Martinez Arias, A., Zecchini, V., and Brennan, K. (2002). CSL-independent Notch signalling: a checkpoint in cell fate decisions during development? Curr. Opin. Genet. Dev. *12*, 524–533.

Marx, V. (2013). Cell culture: A better brew. Nature *496*, 253–258.

Mathers, P.H., Grinberg, A., Mahon, K.A., and Jamrich, M. (1997). The Rx homeobox gene is essential for vertebrate eye development. Nature *387*, 603–607.

Matsuo, I., Kuratani, S., Kimura, C., Takeda, N., and Aizawa, S. (1995). Mouse Otx2 functions in the formation and patterning of rostral head. Genes Dev. *9*, 2646–2658.

Matsushima, D., Heavner, W., and Pevny, L.H. (2011). Combinatorial regulation of optic cup progenitor cell fate by SOX2 and PAX6. Dev. Camb. Engl. *138*, 443–454.

Matthews, G., and Fuchs, P. (2010). The diverse roles of ribbon synapses in sensory neurotransmission. Nat. Rev. Neurosci. *11*, 812–822.

McCaffery, P., Wagner, E., O'Neil, J., Petkovich, M., and Dräger, U.C. (1999). Dorsal and ventral retinal territories defined by retinoic acid synthesis, break-down and nuclear receptor expression. Mech. Dev. *82*, 119–130.

McCaffrery, P., Posch, K.C., Napoli, J.L., Gudas, L., and Dräger, U.C. (1993). Changing patterns of the retinoic acid system in the developing retina. Dev. Biol. *158*, 390–399.

McLaren, D.S. (1999). Vitamin A deficiency disorders. J. Indian Med. Assoc. *97*, 320–323.

Mears, A.J., Kondo, M., Swain, P.K., Takada, Y., Bush, R.A., Saunders, T.L., Sieving, P.A., and Swaroop, A. (2001). Nrl is required for rod photoreceptor development. Nat. Genet. *29*, 447–452.

Mehalow, A.K., Kameya, S., Smith, R.S., Hawes, N.L., Denegre, J.M., Young, J.A., Bechtold, L., Haider, N.B., Tepass, U., Heckenlively, J.R., et al. (2003). CRB1 is essential for external limiting membrane integrity and photoreceptor morphogenesis in the mammalian retina. Hum. Mol. Genet. *12*, 2179–2189.

de Melo, J., Peng, G.-H., Chen, S., and Blackshaw, S. (2011). The Spalt family transcription factor Sall3 regulates the development of cone photoreceptors and retinal horizontal interneurons. Dev. Camb. Engl. *138*, 2325–2336.

Mercer, A.J., and Thoreson, W.B. (2011). The dynamic architecture of photoreceptor ribbon synapses: Cytoskeletal, extracellular matrix, and intramembrane proteins. Vis. Neurosci. *28*, 453–471.

Meuleman, J., van de Pavert, S.A., and Wijnholds, J. (2004). Crumbs homologue 1 in polarity and blindness. Biochem. Soc. Trans. *32*, 828–830.

Meyer, J.S., Shearer, R.L., Capowski, E.E., Wright, L.S., Wallace, K.A., McMillan, E.L., Zhang, S.-C., and Gamm, D.M. (2009). Modeling early retinal development with human embryonic and induced pluripotent stem cells. Proc. Natl. Acad. Sci. U. S. A. *106*, 16698–16703.

Mic, F.A., Molotkov, A., Fan, X., Cuenca, A.E., and Duester, G. (2000). RALDH3, a retinaldehyde dehydrogenase that generates retinoic acid, is expressed in the ventral retina, otic vesicle and olfactory pit during mouse development. Mech. Dev. *97*, 227–230.

Milam, A.H., Rose, L., Cideciyan, A.V., Barakat, M.R., Tang, W.-X., Gupta, N., Aleman, T.S., Wright, A.F., Stone, E.M., Sheffield, V.C., et al. (2002). The nuclear receptor NR2E3 plays a role in human retinal photoreceptor differentiation and degeneration. Proc. Natl. Acad. Sci. U. S. A. *99*, 473–478.

Mizeracka, K., DeMaso, C.R., and Cepko, C.L. (2013). Notch1 is required in newly postmitotic cells to inhibit the rod photoreceptor fate. Development *140*, 3188–3197.

Montana, C.L., Kolesnikov, A.V., Shen, S.Q., Myers, C.A., Kefalov, V.J., and Corbo, J.C. (2013). Reprogramming of adult rod photoreceptors prevents retinal degeneration. Proc. Natl. Acad. Sci. U. S. A. *110*, 1732–1737.

Mori, M., Ghyselinck, N.B., Chambon, P., and Mark, M. (2001). Systematic immunolocalization of retinoid receptors in developing and adult mouse eyes. Invest. Ophthalmol. Vis. Sci. *42*, 1312–1318.

Morshedian, A., and Fain, G.L. (2015). Single-Photon Sensitivity of Lamprey Rods with Cone-like Outer Segments. Curr. Biol. *25*, 484–487.

Muranishi, Y., Sato, S., Inoue, T., Ueno, S., Koyasu, T., Kondo, M., and Furukawa, T. (2010). Gene expression analysis of embryonic photoreceptor precursor cells using BAC-Crx-EGFP transgenic mouse. Biochem. Biophys. Res. Commun. *392*, 317–322.

Mustafi, D., Engel, A.H., and Palczewski, K. (2009). Structure of cone photoreceptors. Prog. Retin. Eye Res. *28*, 289–302.

Nakano, T., Ando, S., Takata, N., Kawada, M., Muguruma, K., Sekiguchi, K., Saito, K., Yonemura, S., Eiraku, M., and Sasai, Y. (2012). Self-formation of optic cups and storable stratified neural retina from human ESCs. Cell Stem Cell *10*, 771–785.

Nasonkin, I.O., Merbs, S.L., Lazo, K., Oliver, V.F., Brooks, M., Patel, K., Enke, R.A., Nellissery, J., Jamrich, M., Le, Y.Z., et al. (2013). Conditional knockdown of DNA methyltransferase 1 reveals a key role of retinal pigment epithelium integrity in photoreceptor outer segment morphogenesis. Dev. Camb. Engl. *140*, 1330–1341.

Nelson, B.R., Hartman, B.H., Georgi, S.A., Lan, M.S., and Reh, T.A. (2007). Transient inactivation of Notch signaling synchronizes differentiation of neural progenitor cells. Dev. Biol. *304*, 479–498.

Ng, L., Hurley, J.B., Dierks, B., Srinivas, M., Saltó, C., Vennström, B., Reh, T.A., and Forrest, D. (2001). A thyroid hormone receptor that is required for the development of green cone photoreceptors. Nat. Genet. *27*, 94–98.

Ng, L., Ma, M., Curran, T., and Forrest, D. (2009). Developmental expression of thyroid hormone receptor β2 protein in cone photoreceptors in the mouse: NeuroReport *20*, 627–631.

Ng, L., Lyubarsky, A., Nikonov, S.S., Ma, M., Srinivas, M., Kefas, B., St Germain, D.L., Hernandez, A., Pugh, E.N., and Forrest, D. (2010). Type 3 deiodinase, a thyroid-hormone-inactivating enzyme, controls survival and maturation of cone photoreceptors. J. Neurosci. Off. J. Soc. Neurosci. *30*, 3347–3357.

Ng, L., Lu, A., Swaroop, A., Sharlin, D.S., Swaroop, A., and Forrest, D. (2011). Two transcription factors can direct three photoreceptor outcomes from rod precursor cells in mouse retinal development. J. Neurosci. Off. J. Soc. Neurosci. *31*, 11118–11125.

Nickell, S., Park, P.S.-H., Baumeister, W., and Palczewski, K. (2007). Three-dimensional architecture of murine rod outer segments determined by cryoelectron tomography. J. Cell Biol. *177*, 917–925.

Nickerson, P.E.B., Emsley, J.G., Myers, T., and Clarke, D.B. (2007). Proliferation and Expression of Progenitor and Mature Retinal Phenotypes in the Adult Mammalian

Ciliary Body after Retinal Ganglion Cell Injury. Investig. Opthalmology Vis. Sci. *48*, 5266.

Nieuwkoop, P.D., and Others (1952). Activation and organization of the central nervous system in amphibians. Part I. Induction and activation. J. Exp. Zool. *120*, 1–31.

Nishida, A., Furukawa, A., Koike, C., Tano, Y., Aizawa, S., Matsuo, I., and Furukawa, T. (2003). Otx2 homeobox gene controls retinal photoreceptor cell fate and pineal gland development. Nat. Neurosci. *6*, 1255–1263.

Nuhn, J.S., and Fuerst, P.G. (2014). Developmental localization of adhesion and scaffolding proteins at the cone synapse. Gene Expr. Patterns GEP *16*, 36–50.

O'Brien, K.M.B., Schulte, D., and Hendrickson, A.E. (2003). Expression of photoreceptor-associated molecules during human fetal eye development. Mol. Vis. *9*, 401–409.

Oh, E.C.T., Khan, N., Novelli, E., Khanna, H., Strettoi, E., and Swaroop, A. (2007). Transformation of cone precursors to functional rod photoreceptors by bZIP transcription factor NRL. Proc. Natl. Acad. Sci. U. S. A. *104*, 1679–1684.

Ohsawa, R., and Kageyama, R. (2008). Regulation of retinal cell fate specification by multiple transcription factors. Brain Res. *1192*, 90–98.

Okita, K., Ichisaka, T., and Yamanaka, S. (2007). Generation of germline-competent induced pluripotent stem cells. Nature *448*, 313–317.

Ooto, S., Akagi, T., Kageyama, R., Akita, J., Mandai, M., Honda, Y., and Takahashi, M. (2004). Potential for neural regeneration after neurotoxic injury in the adult mammalian retina. Proc. Natl. Acad. Sci. *101*, 13654–13659.

Osakada, F., Ikeda, H., Mandai, M., Wataya, T., Watanabe, K., Yoshimura, N., Akaike, A., Akaike, A., Sasai, Y., and Takahashi, M. (2008). Toward the generation of rod and cone photoreceptors from mouse, monkey and human embryonic stem cells. Nat. Biotechnol. *26*, 215–224.

Owen, C.G., Jarrar, Z., Wormald, R., Cook, D.G., Fletcher, A.E., and Rudnicka, A.R. (2012). The estimated prevalence and incidence of late stage age related macular degeneration in the UK. Br. J. Ophthalmol. *96*, 752–756.

Palczewski, K. (2012). Chemistry and Biology of Vision. J. Biol. Chem. *287*, 1612–1619.

Parker, R., Wang, J.-S., Kefalov, V.J., and Crouch, R.K. (2011). Interphotoreceptor Retinoid-Binding Protein as the Physiologically Relevant Carrier of 11-cis-Retinol in the Cone Visual Cycle. J. Neurosci. *31*, 4714–4719.

Pearson, R.A. (2014). Advances in repairing the degenerate retina by rod photoreceptor transplantation. Biotechnol. Adv. *32*, 485–491.

Pearson, R.A., Barber, A.C., West, E.L., MacLaren, R.E., Duran, Y., Bainbridge, J.W., Sowden, J.C., and Ali, R.R. (2010). Targeted disruption of outer limiting membrane junctional proteins (Crb1 and ZO-1) increases integration of transplanted

photoreceptor precursors into the adult wild-type and degenerating retina. Cell Transplant. *19*, 487–503.

Pearson, R.A., Barber, A.C., Rizzi, M., Hippert, C., Xue, T., West, E.L., Duran, Y., Smith, A.J., Chuang, J.Z., Azam, S.A., et al. (2012). Restoration of vision after transplantation of photoreceptors. Nature *485*, 99–103.

Pearson, R.A., Hippert, C., Graca, A.B., and Barber, A.C. (2014). Photoreceptor replacement therapy: Challenges presented by the diseased recipient retinal environment. Vis. Neurosci. *31*, 333–344.

Peng, G.-H., Ahmad, O., Ahmad, F., Liu, J., and Chen, S. (2005). The photoreceptor-specific nuclear receptor Nr2e3 interacts with Crx and exerts opposing effects on the transcription of rod versus cone genes. Hum. Mol. Genet. *14*, 747–764.

Pittack, C., Grunwald, G.B., and Reh, T.A. (1997). Fibroblast growth factors are necessary for neural retina but not pigmented epithelium differentiation in chick embryos. Dev. Camb. Engl. *124*, 805–816.

Porter, F.D., Drago, J., Xu, Y., Cheema, S.S., Wassif, C., Huang, S.P., Lee, E., Grinberg, A., Massalas, J.S., Bodine, D., et al. (1997). Lhx2, a LIM homeobox gene, is required for eye, forebrain, and definitive erythrocyte development. Dev. Camb. Engl. *124*, 2935–2944.

Qiu, G., Seiler, M.J., Mui, C., Arai, S., Aramant, R.B., de Juan, E., and Sadda, S. (2005). Photoreceptor differentiation and integration of retinal progenitor cells transplanted into transgenic rats. Exp. Eye Res. *80*, 515–525.

Razafsky, D., Blecher, N., Markov, A., Stewart-Hutchinson, P.J., and Hodzic, D. (2012). LINC Complexes Mediate the Positioning of Cone Photoreceptor Nuclei in Mouse Retina. PLoS ONE *7*, e47180.

Reh, T.A. (2016). Photoreceptor Transplantation in Late Stage Retinal Degeneration. Invest. Ophthalmol. Vis. Sci. *57*, ORSFg1-7.

Reh, T.A., and Pittack, C. (1995). Transdifferentiation and retinal regeneration. Semin. Cell Biol. *6*, 137–142.

Reichman, S., Terray, A., Slembrouck, A., Nanteau, C., Orieux, G., Habeler, W., Nandrot, E.F., Sahel, J.-A., Monville, C., and Goureau, O. (2014). From confluent human iPS cells to self-forming neural retina and retinal pigmented epithelium. Proc. Natl. Acad. Sci. U. S. A. *111*, 8518–8523.

Rembold, M., Loosli, F., Adams, R.J., and Wittbrodt, J. (2006). Individual cell migration serves as the driving force for optic vesicle evagination. Science *313*, 1130–1134.

Rich, K.A., Zhan, Y., and Blanks, J.C. (1997). Migration and synaptogenesis of cone photoreceptors in the developing mouse retina. J. Comp. Neurol. *388*, 47–63.

Richard-Parpaillon, L., Héligon, C., Chesnel, F., Boujard, D., and Philpott, A. (2002). The IGF pathway regulates head formation by inhibiting Wnt signaling in Xenopus. Dev. Biol. *244*, 407–417.

Riesenberg, A.N., Liu, Z., Kopan, R., and Brown, N.L. (2009). Rbpj cell autonomous regulation of retinal ganglion cell and cone photoreceptor fates in the mouse retina. J. Neurosci. Off. J. Soc. Neurosci. *29*, 12865–12877.

Roberts, M.R., Hendrickson, A., McGuire, C.R., and Reh, T.A. (2005). Retinoid X receptor (gamma) is necessary to establish the S-opsin gradient in cone photoreceptors of the developing mouse retina. Invest. Ophthalmol. Vis. Sci. *46*, 2897–2904.

Roberts, M.R., Srinivas, M., Forrest, D., Morreale de Escobar, G., and Reh, T.A. (2006). Making the gradient: thyroid hormone regulates cone opsin expression in the developing mouse retina. Proc. Natl. Acad. Sci. U. S. A. *103*, 6218–6223.

Rompani, S.B., and Cepko, C.L. (2008). Retinal progenitor cells can produce restricted subsets of horizontal cells. Proc. Natl. Acad. Sci. U. S. A. *105*, 192–197.

Roosing, S., Thiadens, A.A.H.J., Hoyng, C.B., Klaver, C.C.W., den Hollander, A.I., and Cremers, F.P.M. (2014). Causes and consequences of inherited cone disorders. Prog. Retin. Eye Res. *42*, 1–26.

Rowan, S., Chen, C.-M.A., Young, T.L., Fisher, D.E., and Cepko, C.L. (2004). Transdifferentiation of the retina into pigmented cells in ocular retardation mice defines a new function of the homeodomain gene Chx10. Dev. Camb. Engl. *131*, 5139–5152.

Rudnicka, A.R., Kapetanakis, V.V., Jarrar, Z., Wathern, A.K., Wormald, R., Fletcher, A.E., Cook, D.G., and Owen, C.G. (2015). Incidence of Late-Stage Age-Related Macular Degeneration in American Whites: Systematic Review and Meta-analysis. Am. J. Ophthalmol. *160*, 85–93.e3.

Sakaguchi, D.S., Van Hoffelen, S.J., Grozdanic, S.D., Kwon, Y.H., Kardon, R.H., and Young, M.J. (2005). Neural progenitor cell transplants into the developing and mature central nervous system. Ann. N. Y. Acad. Sci. *1049*, 118–134.

Sakai, Y., Luo, T., McCaffery, P., Hamada, H., and Dräger, U.C. (2004). CYP26A1 and CYP26C1 cooperate in degrading retinoic acid within the equatorial retina during later eye development. Dev. Biol. *276*, 143–157.

Sam, T.N., Xiao, J., Roehrich, H., Low, W.C., and Gregerson, D.S. (2006). Engrafted neural progenitor cells express a tissue-restricted reporter gene associated with differentiated retinal photoreceptor cells. Cell Transplant. *15*, 147–160.

Samson, M., Emerson, M.M., and Cepko, C.L. (2009). Robust marking of photoreceptor cells and pinealocytes with several reporters under control of the *Crx* gene. Dev. Dyn. *238*, 3218–3225.

Sanges, D., Simonte, G., Di Vicino, U., Romo, N., Pinilla, I., Nicolás, M., and Cosma, M.P. (2016). Reprogramming Müller glia via in vivo cell fusion regenerates murine photoreceptors. J. Clin. Invest. *126*, 3104–3116.

Santos-Ferreira, T., Postel, K., Stutzki, H., Kurth, T., Zeck, G., and Ader, M. (2015). Daylight Vision Repair by Cell Transplantation: Daylight Vision Repair by Cell Transplantation. STEM CELLS *33*, 79–90.

Sasagawa, S., Takabatake, T., Takabatake, Y., Muramatsu, T., and Takeshima, K. (2002). Axes establishment during eye morphogenesis in Xenopus by coordinate and antagonistic actions of BMP4, Shh, and RA. Genes. N. Y. N 2000 *33*, 86–96.

Satoh, S., Tang, K., Iida, A., Inoue, M., Kodama, T., Tsai, S.Y., Tsai, M.-J., Furuta, Y., and Watanabe, S. (2009). The spatial patterning of mouse cone opsin expression is regulated by bone morphogenetic protein signaling through downstream effector COUP-TF nuclear receptors. J. Neurosci. Off. J. Soc. Neurosci. *29*, 12401–12411.

Schneider, C.A., Rasband, W.S., and Eliceiri, K.W. (2012). NIH Image to ImageJ: 25 years of image analysis. Nat. Methods *9*, 671–675.

Schwartz, S.D., Hubschman, J.-P., Heilwell, G., Franco-Cardenas, V., Pan, C.K., Ostrick, R.M., Mickunas, E., Gay, R., Klimanskaya, I., and Lanza, R. (2012). Embryonic stem cell trials for macular degeneration: a preliminary report. Lancet Lond. Engl. *379*, 713–720.

Sedmak, T., and Wolfrum, U. (2010). Intraflagellar transport molecules in ciliary and nonciliary cells of the retina. J. Cell Biol. *189*, 171–186.

Seiler, M.J., and Aramant, R.B. (2012). Cell replacement and visual restoration by retinal sheet transplants. Prog. Retin. Eye Res. *31*, 661–687.

Sergi, C., Ehemann, V., Beedgen, B., Linderkamp, O., and Otto, H.F. (1999). Huge fetal sacrococcygeal teratoma with a completely formed eye and intratumoral DNA ploidy heterogeneity. Pediatr. Dev. Pathol. Off. J. Soc. Pediatr. Pathol. Paediatr. Pathol. Soc. *2*, 50–57.

Shibusawa, N., Hashimoto, K., Nikrodhanond, A.A., Liberman, M.C., Applebury, M.L., Liao, X.H., Robbins, J.T., Refetoff, S., Cohen, R.N., and Wondisford, F.E. (2003). Thyroid hormone action in the absence of thyroid hormone receptor DNA-binding in vivo. J. Clin. Invest. *112*, 588–597.

Silver, I.., Deas, J., and Erecińska, M. (1997). Ion homeostasis in brain cells: differences in intracellular ion responses to energy limitation between cultured neurons and glial cells. Neuroscience *78*, 589–601.

Singh, M.S., Charbel Issa, P., Butler, R., Martin, C., Lipinski, D.M., Sekaran, S., Barnard, A.R., and MacLaren, R.E. (2013). Reversal of end-stage retinal degeneration and restoration of visual function by photoreceptor transplantation. Proc. Natl. Acad. Sci. U. S. A. *110*, 1101–1106.

Smiley, S., Nickerson, P.E., Comanita, L., Daftarian, N., El-Sehemy, A., Tsai, E.L.S., Matan-Lithwick, S., Yan, K., Thurig, S., Touahri, Y., et al. (2016). Establishment of a cone photoreceptor transplantation platform based on a novel cone-GFP reporter mouse line. Sci. Rep. *6*, 22867.

Smith, W.C., and Harland, R.M. (1991). Injected Xwnt-8 RNA acts early in Xenopus embryos to promote formation of a vegetal dorsalizing center. Cell *67*, 753–765.

Solovei, I., Kreysing, M., Lanctôt, C., Kösem, S., Peichl, L., Cremer, T., Guck, J., and Joffe, B. (2009). Nuclear Architecture of Rod Photoreceptor Cells Adapts to Vision in Mammalian Evolution. Cell *137*, 356–368.

Sommer, A., and Vyas, K.S. (2012). A global clinical view on vitamin A and carotenoids. Am. J. Clin. Nutr. *96*, 1204S–6S.

Song, M.J., and Bharti, K. (2015). Looking into the future: Using induced pluripotent stem cells to build two and three dimensional ocular tissue for cell therapy and disease modeling. Brain Res.

Srinivas, M., Ng, L., Liu, H., Jia, L., and Forrest, D. (2006). Activation of the blue opsin gene in cone photoreceptor development by retinoid-related orphan receptor beta. Mol. Endocrinol. Baltim. Md *20*, 1728–1741.

Stehlin-Gaon, C., Willmann, D., Zeyer, D., Sanglier, S., Van Dorsselaer, A., Renaud, J.-P., Moras, D., and Schüle, R. (2003). All-trans retinoic acid is a ligand for the orphan nuclear receptor ROR beta. Nat. Struct. Biol. *10*, 820–825.

Stevens, C.B., Cameron, D.A., and Stenkamp, D.L. (2011). Plasticity of photoreceptor-generating retinal progenitors revealed by prolonged retinoic acid exposure. BMC Dev. Biol. *11*, 51.

Stone, J. (1999). Mechanisms of photoreceptor death and survival in mammalian retina. Prog. Retin. Eye Res. *18*, 689–735.

Sun, Y., Williams, A., Waisbourd, M., Iacovitti, L., and Katz, L.J. (2015). Stem cell therapy for glaucoma: science or snake oil? Surv. Ophthalmol. *60*, 93–105.

Sung, C.-H., and Chuang, J.-Z. (2010). The cell biology of vision. J. Cell Biol. *190*, 953–963.

Sung, C.-H., and Tai, A.W. (1999). Rhodopsin Trafficking and its Role in Retinal Dystrophies. In International Review of Cytology, (Elsevier), pp. 215–267.

Suzuki, S.C., Bleckert, A., Williams, P.R., Takechi, M., Kawamura, S., and Wong, R.O.L. (2013). Cone photoreceptor types in zebrafish are generated by symmetric terminal divisions of dedicated precursors. Proc. Natl. Acad. Sci. U. S. A. *110*, 15109–15114.

Swaroop, A., Xu, J.Z., Pawar, H., Jackson, A., Skolnick, C., and Agarwal, N. (1992). A conserved retina-specific gene encodes a basic motif/leucine zipper domain. Proc. Natl. Acad. Sci. U. S. A. *89*, 266–270.

Swaroop, A., Kim, D., and Forrest, D. (2010). Transcriptional regulation of photoreceptor development and homeostasis in the mammalian retina. Nat. Rev. Neurosci. *11*, 563–576.

Takahashi, K., Tanabe, K., Ohnuki, M., Narita, M., Ichisaka, T., Tomoda, K., and Yamanaka, S. (2007). Induction of pluripotent stem cells from adult human fibroblasts by defined factors. Cell *131*, 861–872.

Take-uchi, M., Clarke, J.D.W., and Wilson, S.W. (2003). Hedgehog signalling maintains the optic stalk-retinal interface through the regulation of Vax gene activity. Dev. Camb. Engl. *130*, 955–968.

Taranova, O.V., Magness, S.T., Fagan, B.M., Wu, Y., Surzenko, N., Hutton, S.R., and Pevny, L.H. (2006). SOX2 is a dose-dependent regulator of retinal neural progenitor competence. Genes Dev. *20*, 1187–1202.

Thomson, J.A., Itskovitz-Eldor, J., Shapiro, S.S., Waknitz, M.A., Swiergiel, J.J., Marshall, V.S., and Jones, J.M. (1998). Embryonic stem cell lines derived from human blastocysts. Science *282*, 1145–1147.

Trimarchi, J.M., Stadler, M.B., and Cepko, C.L. (2008). Individual retinal progenitor cells display extensive heterogeneity of gene expression. PloS One *3*, e1588.

Tucker, B.A., Park, I.-H., Qi, S.D., Klassen, H.J., Jiang, C., Yao, J., Redenti, S., Daley, G.Q., and Young, M.J. (2011). Transplantation of adult mouse iPS cell-derived photoreceptor precursors restores retinal structure and function in degenerative mice. PloS One *6*, e18992.

Vollmer, G., and Layer, P.G. (1986). Reaggregation of chick retinal and mixtures of retinal and pigment epithelial cells: the degree of laminar organization is dependent on age. Neurosci. Lett. *63*, 91–95.

Wallace, V.A., and Jensen, A.M. (1999). IBMX, taurine and 9-cis retinoic acid all act to accelerate rhodopsin expression in postmitotic cells. Exp. Eye Res. *69*, 617–627.

Wang, J.-S., and Kefalov, V.J. (2011). The Cone-specific visual cycle. Prog. Retin. Eye Res. *30*, 115–128.

Wang, Y., and Xie, T. (2014). Extracellular, stem cells and regenerative ophthalmology. J. Glaucoma *23*, S30-33.

Wang, S., Sengel, C., Emerson, M.M., and Cepko, C.L. (2014). A gene regulatory network controls the binary fate decision of rod and bipolar cells in the vertebrate retina. Dev. Cell *30*, 513–527.

Wang, Y., Macke, J.P., Merbs, S.L., Zack, D.J., Klaunberg, B., Bennett, J., Gearhart, J., and Nathans, J. (1992). A locus control region adjacent to the human red and green visual pigment genes. Neuron *9*, 429–440.

Warkany, J., and Schraffenberger, E. (1946). Congenital malformations induced in rats by maternal vitamin A deficiency; defects of the eye. Arch. Ophthalmol. Chic. Ill 1929 *35*, 150–169.

Warre-Cornish, K., Barber, A.C., Sowden, J.C., Ali, R.R., and Pearson, R.A. (2014). Migration, integration and maturation of photoreceptor precursors following transplantation in the mouse retina. Stem Cells Dev. *23*, 941–954.

Watanabe, T., and Raff, M.C. (1990). Rod photoreceptor development in vitro: intrinsic properties of proliferating neuroepithelial cells change as development proceeds in the rat retina. Neuron *4*, 461–467.

Watanabe, T., and Raff, M.C. (1992). Diffusible rod-promoting signals in the developing rat retina. Dev. Camb. Engl. *114*, 899–906.

Watanabe, K., Kamiya, D., Nishiyama, A., Katayama, T., Nozaki, S., Kawasaki, H., Watanabe, Y., Mizuseki, K., and Sasai, Y. (2005). Directed differentiation of telencephalic precursors from embryonic stem cells. Nat. Neurosci. *8*, 288–296.

Watanabe, S., Sanuki, R., Ueno, S., Koyasu, T., Hasegawa, T., and Furukawa, T. (2013). Tropisms of AAV for subretinal delivery to the neonatal mouse retina and its

application for in vivo rescue of developmental photoreceptor disorders. PloS One *8*, e54146.

Weiss, P., and Taylor, A.C. (1960). RECONSTITUTION OF COMPLETE ORGANS FROM SINGLE-CELL SUSPENSIONS OF CHICK EMBRYOS IN ADVANCED STAGES OF DIFFERENTIATION. Proc. Natl. Acad. Sci. U. S. A. *46*, 1177–1185.

Wenkel, H., and Streilein, J.W. (1998). Analysis of immune deviation elicited by antigens injected into the subretinal space. Invest. Ophthalmol. Vis. Sci. *39*, 1823–1834.

Wernig, M., Meissner, A., Foreman, R., Brambrink, T., Ku, M., Hochedlinger, K., Bernstein, B.E., and Jaenisch, R. (2007). In vitro reprogramming of fibroblasts into a pluripotent ES-cell-like state. Nature *448*, 318–324.

West, E.L., Pearson, R.A., Tschernutter, M., Sowden, J.C., MacLaren, R.E., and Ali, R.R. (2008). Pharmacological disruption of the outer limiting membrane leads to increased retinal integration of transplanted photoreceptor precursors. Exp. Eye Res. *86*, 601–611.

West, E.L., Pearson, R.A., Barker, S.E., Luhmann, U.F.O., Maclaren, R.E., Barber, A.C., Duran, Y., Smith, A.J., Sowden, J.C., and Ali, R.R. (2010). Long-term survival of photoreceptors transplanted into the adult murine neural retina requires immune modulation. Stem Cells Dayt. Ohio *28*, 1997–2007.

West, E.L., Gonzalez-Cordero, A., Hippert, C., Osakada, F., Martinez-Barbera, J.P., Pearson, R.A., Sowden, J.C., Takahashi, M., and Ali, R.R. (2012). Defining the Integration Capacity of Embryonic Stem Cell-Derived Photoreceptor Precursors. STEM CELLS *30*, 1424–1435.

Westenskow, P., Piccolo, S., and Fuhrmann, S. (2009). Beta-catenin controls differentiation of the retinal pigment epithelium in the mouse optic cup by regulating Mitf and Otx2 expression. Dev. Camb. Engl. *136*, 2505–2510.

Wichterle, H., Lieberam, I., Porter, J.A., and Jessell, T.M. (2002). Directed differentiation of embryonic stem cells into motor neurons. Cell *110*, 385–397.

Wilbanks, G.A., and Streilein, J.W. (1990). Characterization of suppressor cells in anterior chamber-associated immune deviation (ACAID) induced by soluble antigen. Evidence of two functionally and phenotypically distinct T-suppressor cell populations. Immunology *71*, 383–389.

Xiang, M. (2013). Intrinsic control of mammalian retinogenesis. Cell. Mol. Life Sci. CMLS *70*, 2519–2532.

Xiao, M., and Hendrickson, A. (2000). Spatial and temporal expression of short, long/medium, or both opsins in human fetal cones. J. Comp. Neurol. *425*, 545–559.

Yang, P., Seiler, M.J., Aramant, R.B., and Whittemore, S.R. (2002). In vitro isolation and expansion of human retinal progenitor cells. Exp. Neurol. *177*, 326–331.

Yaron, O. (2006). Notch1 functions to suppress cone-photoreceptor fate specification in the developing mouse retina. Development *133*, 1367–1378.

Yin, X., Mead, B.E., Safaee, H., Langer, R., Karp, J.M., and Levy, O. (2016). Engineering Stem Cell Organoids. Cell Stem Cell *18*, 25–38.

Ying, Q.-L., Stavridis, M., Griffiths, D., Li, M., and Smith, A. (2003). Conversion of embryonic stem cells into neuroectodermal precursors in adherent monoculture. Nat. Biotechnol. *21*, 183–186.

Young, R.W. (1967). THE RENEWAL OF PHOTORECEPTOR CELL OUTER SEGMENTS. J. Cell Biol. *33*, 61–72.

Young, R.W. (1968). THE RENEWAL OF PROTEIN IN RETINAL RODS AND CONES. J. Cell Biol. *39*, 169–184.

Young, M.J., Ray, J., Whiteley, S.J., Klassen, H., and Gage, F.H. (2000). Neuronal differentiation and morphological integration of hippocampal progenitor cells transplanted to the retina of immature and mature dystrophic rats. Mol. Cell. Neurosci. *16*, 197–205.

Yun, S., Saijoh, Y., Hirokawa, K.E., Kopinke, D., Murtaugh, L.C., Monuki, E.S., and Levine, E.M. (2009). Lhx2 links the intrinsic and extrinsic factors that control optic cup formation. Dev. Camb. Engl. *136*, 3895–3906.

Zagozewski, J.L., Zhang, Q., and Eisenstat, D.D. (2014). Genetic regulation of vertebrate eye development. Clin. Genet. *86*, 453–460.

Zhang, J.-X., Wang, N.-L., and Lu, Q.-J. (2015). Development of gene and stem cell therapy for ocular neurodegeneration. Int. J. Ophthalmol. *8*, 622–630.

Zhao, S., Hung, F.C., Colvin, J.S., White, A., Dai, W., Lovicu, F.J., Ornitz, D.M., and Overbeek, P.A. (2001). Patterning the optic neuroepithelium by FGF signaling and Ras activation. Dev. Camb. Engl. *128*, 5051–5060.

Zhao, T., Zhang, Z.-N., Rong, Z., and Xu, Y. (2011). Immunogenicity of induced pluripotent stem cells. Nature *474*, 212–215.

Zhao, X., Liu, J., and Ahmad, I. (2002). Differentiation of embryonic stem cells into retinal neurons. Biochem. Biophys. Res. Commun. *297*, 177–184.

Zhao, X., Das, A.V., Soto-Leon, F., and Ahmad, I. (2005). Growth factor-responsive progenitors in the postnatal mammalian retina. Dev. Dyn. *232*, 349–358.

Zhong, X., Gutierrez, C., Xue, T., Hampton, C., Vergara, M.N., Cao, L.-H., Peters, A., Park, T.S., Zambidis, E.T., Meyer, J.S., et al. (2014). Generation of three-dimensional retinal tissue with functional photoreceptors from human iPSCs. Nat. Commun. *5*, 4047.

Zhou, Y., Tanzie, C., Yan, Z., Chen, S., Duncan, M., Gaudenz, K., Li, H., Seidel, C., Lewis, B., Moran, A., et al. (2013). Notch2 regulates BMP signaling and epithelial morphogenesis in the ciliary body of the mouse eye. Proc. Natl. Acad. Sci. U. S. A. *110*, 8966–8971.

Zuber, M.E., Gestri, G., Viczian, A.S., Barsacchi, G., and Harris, W.A. (2003). Specification of the vertebrate eye by a network of eye field transcription factors. Dev. Camb. Engl. *130*, 5155–5167.

Abbreviations:

AAA – alpha-aminoadipic acid

AAV – adeno-associated virus

bHLH – basic helix loop helix transcription factor

BMP – bone morphogenetic protein

BrdU – Bromodeoxyuridine

BSA – bovine serum albumin

cGMP – cyclic guanosine monophosphate

CNS – central nervous system

CMV – cytomegalovirus

COUP-TF – chicken ovalbumin upstream promoter-transcription factor

Crx – cone-rod homeobox transcription factor

CRALBP – cellular retinal binding protein

CSPG – chondroitin sulfate proteoglycan

DAPI - 4',6-diamidino-2-phenylindole

DAPT - N-[N-(3,5-Difluorophenacetyl)-L-alanyl]-S-phenylglycine t-butyl ester

DMSO - dimethylsulphoxide

DNA - deoxyribonucleic acid

EB – embryoid body

EdU – 5-ethynyl-2'-deoxyuridine

ECM – extracellular matrix

EGF – epidermal growth factor

ERG – electroretinogram

ESC – embryonic stem cell

FACS – fluorescence-activated cell sorting

FGF – fibroblast growth factor

FBS – foetal bovine serum

GABA - γ-aminobutyric acid

GCL – ganglion cell layer

GDF11 – growth and differentiation factor

GDP - guanosine diphosphate

GFAP – glial acidic fibrillary protein

GFP – green fluorescent protein

GFR – growth factor-reduced

GNAT1 – rod α tranducin

GNAT2 – cone α tranducin

GTP - guanosine triphosphate

hESC – human embryonic stem cell

IGF – insulin-like growth factor

INL – inner nuclear layer

IPL – inner plexiform layer

iPSC – induced pluripotent stem cell

IRBP – interphotoreceptor retinoid-binding protein

IRES – internal ribosome entry site

IS – inner segment

ITR – inverted terminal repeat

KSR – knockout serum replacement

LIF – leukaemia inhibitory factor

LRAT - lecithin:retinol acyltransferase

MACS – magnetic-activated cell sorting

MEA – multi electrode array

MOI – multiplicity of infection

mESC – mouse embryonic stem cell

Nrl – neural retina leucine zipper protein

NADP – nicotinamide adenine dinucleotide phosphate

NADPH – reduced form of nicotinamide adenine dinucleotide phosphate

OLM – outer limiting membrane

ONL – outer nuclear layer

OPL – outer plexiform layer

OS – outer segment

PBS – phosphate buffered saline

PCR – polymerase chain reaction

PDE – phosphodiesterase

PEI – polyethylenimine

PFA – paraformaldehyde

PNA – peanut agglutinin

qPCR – quantitative polymerase chain reaction

rAAV- recombinant adeno-associated viral vector

RA – retinoic acid

RAR – retinoic acid receptor

RARE – retinoic acid responsive element

RGC – retinal ganglion cell

RFP –red fluorescent protein

RMM – retinal maturation medium

RNA – ribonucleic acid

ROR – retinoid orphan receptor

RPC – retinal progenitor cell

RPE – retinal pigmented epithelium

RPE65 - Retinal Pigment Epithelium-Specific Protein 65kDa

RXRγ – retinoid X receptor isoform γ

RT-PCR – reverse transcription-PCR

SARA – Smad anchor for receptor activation

SD – standard deviation

SEM – standard error of the mean

SFEB – serum-free floating culture of embryoid body-like aggregates

Shh – sonic hedgehog protein

SRS – subretinal space

STRA6 – stimulated by retinoic acid 6

T3 – triiodothyronine

T4 - thyroxine

TGFβ – transforming growth factor β

Trβ2 – thyroid hormone receptor β2

WPRE – woodchuck hepatitis virus posttranscriptional regulatory element

WT – wild-type